Michel Deza, Michel Petitjean,
Krassimir Markov (eds.)

Mathematics of Distances and Applications

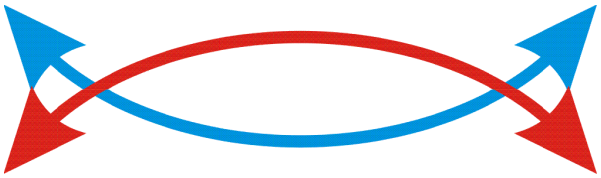

I T H E A
SOFIA
2012

Michel Deza, Michel Petitjean, Krassimir Markov (eds.)

Mathematics of Distances and Applications

ITHEA®

ISBN 978-954-16-0063-4 (printed);

ISBN 978-954-16-0064-1 (online)

ITHEA IBS ISC No.: 25

Sofia, Bulgaria, 2012

First edition

Printed in Bulgaria

Recommended for publication by The Scientific Council of the Institute of Information Theories and Applications FOI ITHEA

The papers accepted and presented at the International Conference "Mathematics of Distances and Applications", July 02-05, 2012, Varna, Bulgaria, are published in this book.

The concept of distance is basic to human experience. In everyday life it usually means some degree of closeness of two physical objects or ideas, i.e., length, time interval, gap, rank difference, coolness or remoteness, while the term metric is often used as a standard for a measurement. Except for the last two topics, the mathematical meaning of those terms, which is an abstraction of measurement, is considered. Distance metrics and distances have now become an essential tool in many areas of Mathematics and its applications including Geometry, Probability, Statistics, Coding/Graph Theory, Clustering, Data Analysis, Pattern Recognition, Networks, Engineering, Computer Graphics/Vision, Astronomy, Cosmology, Molecular Biology, and many other areas of science. Devising the most suitable distance metrics and similarities, to quantify the proximity between objects, has become a standard task for many researchers. Especially intense ongoing search for such distances occurs, for example, in Computational Biology, Image Analysis, Speech Recognition, and Information Retrieval.

For experts in the field of mathematics, information technologies as well as for practical users.

IOI-978954/16/00634/25/1 (printed); IOI-978954/16/00641/25/1 (online)

ISBN: 978-954-16-0063-4 (printed)
ISBN: 978-954-16-0064-1 (online)

C\o Jusautor, Sofia, 2012

Foreword

This book consist of papers presented at the MDA 2012 International Conference on

"Mathematics of Distances and Applications"

held at Varna, Bulgaria, July 2-5, 2012.

http://www.foibg.com/conf/ITA2012/2012mda.htm

Several sessions were organized:

- Geometric complexity in aperiodic order, chaired by Michael Baake and Uwe Grimm
- Distances in probability, statistics and data analysis, chaired by Ernst Gabidulin
- Distances in behavioral, life, and physical sciences, chaired by Ehtibar Dzhafarov and Michel Petitjean
- Discrete geometry, combinatorics, and distances, chaired by Norman Johnson and Asia Weiss
- Distances in graphs, chaired by Egon Schulte
- Coding theory, chaired by Nina Pilipchuk

Although a wide diversity of distances related topics were considered, the set of papers consists of approximatively equal two parts with mostly theoretical and mostly applied papers, even if the division is approximative also. The papers were submitted to an anonymous peer review process. The managing of this process was done with the session organizers and with the kind help of the members of the Programme Committee: Tetsuo Asano, Michael Baake, Stefan Dodunekov, Ehtibar Dzhafarov, Ernst Gabidulin, Uwe Grimm, Vladimir Gurvich, Sandi Klavzar, Jacobus Koolen, Svetlozar Rachev, Egon Schulte, Sergey Shpectorov, Kokichi Sugihara, Koen Vanhoof, Cedric Villani.

We are very grateful to the following organizers: ITHEA International Scientific Society, Institute of Information Theories and Applications FOI ITHEA (Bulgaria), Institute of Mathematics and Informatics, BAS (Bulgaria).

We are highly thankful to our general sponsor FOI Bulgaria for supporting the MDA 2012 Conference.

Michel Deza (France)
Michel Petitjean (France)
Krassimir Markov (Bulgaria)

Table of contents

Part 1: Theoretical Aspects of Mathematics of Distances

Table of contents

Part 2: Applications of Mathematics of Distances

PART 1

Theoretical Aspects of

Mathematics of Distances

DIFFERENTIAL GEOMETRY DERIVED FROM DIVERGENCE FUNCTIONS: INFORMATION GEOMETRY APPROACH

Shun-ichi Amari

Abstract: *We study differential-geometrical structure of an information manifold equipped with a divergence function. A divergence function generates a Riemannian metric and furthermore it provides a symmetric third-order tensor, when the divergence is asymmetric. This induces a pair of affine connections dually coupled to each other with respect to the Riemannian metric. This is the arising emerged from information geometry. When a manifold is dually flat (it may be curved in the sense of the Levi-Civita connection), we have a canonical divergence and a pair of convex functions from which the original dual geometry is reconstructed. The generalized Pythagorean theorem and projection theorem hold in such a manifold. This structure has lots of applications in information sciences including statistics, machine learning, optimization, computer vision and Tsallis statistical mechanics. The present article reviews the structure of information geometry and its relation to the divergence function. We further consider the conformal structure given rise to by the generalized statistical model in relation to the power law.*

Keywords: *divergence, information geometry, dual affine connection, Bregman divergence, generalized Pythagorean theorem*

ACM Classification Keywords*: G.3 PROBABILITY AND STATISTICS*

MSC*:* 52, 53, 60

Introduction

A divergence function $D[P : Q]$ between two points P and Q in a manifold M plays a fundamental role in many engineering problems, including information theory, statistics, machine learning, computer vision, optimization and brain science. It has dimension of the square of distance but is not in general symmetric with respect to P and Q. The present article surveys the differential-geometric structure generated by a divergence function [Vos, 1991], [Amari and Nagaoka, 2000], [Eguchi, 1983], [Amari and Cichocki, 2010]. When it is symmetric, it gives a Riemannian metric and the Levi-Civita affine connection follows as was studied by [Rao, 1945]. However, when it is asymmetric, we have a third-order symmetric tensor, which gives a pair of affine connections dually coupled to each other with respect to the Riemannian metric. These are the central structure of information geometry [Amari and Nagaoka, 2000] which studies an invariant structure of a manifold of probability distributions [Amari, 1985].

Many asymmetric divergence functions are used in application of information theory. For example, the Kullback-Leibler divergence, which is frequently used in statistics, information theory and others, is a typical example of asymmetric divergence. We study the geometrical structure arising from by an asymmetric divergence. It consists of a Riemannian metric which is symmetric positive-definite second-order tensor and a symmetric third-order tensor which vanishes in the symmetric case. A pair of affine connections is defined by using the two tensors. The Levi-Civita connection is the average of the two connections. They are not metric connections but are dually coupled with respect to the Riemannian metric in the sense that the parallel transports of a vector by the two affine connections keep their inner product invariant with respect to the Riemannian metric. The duality can be expressed in terms of the related covariant derivatives. See [Amari and Nagaoka, 2000] for details.

When a Riemann-Christoffel curvature vanishes with respect to one affine connection, it vanishes automatically with respect to the dual affine connection. We have a dually flat manifold in this case, even though the Riemannian

curvature with respect to the Levi-Civita connection does not vanish in general. A dually flat Riemannian manifold has nice properties such as the generalized Pythagorean theorem and projection theorem. Moreover, when a manifold is dually flat, we have two convex functions from which a canonical divergence is uniquely determined. The canonical divergence generates the original dually flat Riemannian structure. Euclidean space is a special example of the dually flat manifold which has a symmetric divergence given by the square of the Euclidean distance.

A dually flat manifold has two affine coordinate systems related to the two flat affine connections. They are connected by the Legendre transformation of the two convex functions. The canonical divergence is given as the Bregman divergence [Bregman, 1967]. The Legendre structure has a geometrical foundation in the framework of the dually flat geometry.

What is the natural divergence function to be introduced in a manifold? We study this question in the case of a manifold of probability distributions. We impose an invariant criterion such that the geometry is invariant under bijective transformations of random variables [Chentsov, 1982], [Picard, 1992] (more generally invariant by using sufficient statistics). Then, the Kullback-Leibler divergence is given as the unique canonical divergence. We further extend our notions to the manifold of positive measures [Amari, 2009]. We have invariant structure [Chentsov, 1982; Amari, 1985] and non-invariant flat structure [Amari and Ohara, 2011] which is related to the Tsallis entropy
[Tsallis, 2009].

We finally study the structure of deformed exponential family [Naudts, 2011] which includes the Tsallis q-structure [Tsallis, 2009]. We can introduce a dually flat geometry in this manifold, which is not invariant in general. We prove that the invariant structure is limited to the α- or q-geometry, which gives non-flat dual geometry. However, we can define a dually flat structure in the q-family which is not invariant, extending the geometry. We prove that the q- or α-structure is unique in the sense that the flat geometry is given by a conformal transformation of the invariant geometry [Amari and Ohara, 2011], [Amari, Ohara and Matsuzoe, 2012].

We do not mention applications of dual geometry, which are now hot topics of research in many fields.
See, e.g., [Banerjee et al., 2005], [Ikeda, Tanaka and Amari, 2004], [Takenouchi et al., 2008],
[Boissonnat, Nielsen and Nock, 2010], [Vemuri et al., 2011], [Liu et al, 2010], [Amari, 2009] and [Cichocki et al., 2009].

Divergence Function and Differential Geometry

Let us consider a manifold M homeomorphic to $\boldsymbol{R}^n$. We use a coordinate system in M and denote the coordinates of a point P by $\boldsymbol{x} = (x_1, \cdots, x_n)$. We consider a function $D[P : Q]$ of two points P and Q in M, which is written as $D[\boldsymbol{x} : \boldsymbol{y}]$ by using the coordinates $\boldsymbol{x}$ and $\boldsymbol{y}$ of P and Q.

Definition: A function $D[P : Q]$ is called a divergence, when the following conditions are satisfied
[Amari and Cichocki, 2010]:

1) $D[\boldsymbol{x} : \boldsymbol{y}] \geq 0$ with equality when and only when $\boldsymbol{x} = \boldsymbol{y}$.

2) $D[\boldsymbol{x} : \boldsymbol{y}]$ is differentiable and the Hessian with respect to $\boldsymbol{x}$ at $\boldsymbol{y} = \boldsymbol{x}$ is positive definite.

It should be noted that $D[\boldsymbol{x} : \boldsymbol{y}]$ is not necessarily symmetric with respect to $\boldsymbol{x}$ and $\boldsymbol{y}$. Hence, it is not a distance. The triangular inequality does not hold either. It has dimension of the square of distance as will be seen below (cf. [Chen, Chen and Rao, 2008]).

Given a divergence function D, for infinitesimally close two points $\boldsymbol{x}$ and $\boldsymbol{y} = \boldsymbol{x} + d\boldsymbol{x}$, we have by Taylor expansion

$$D\left[\boldsymbol{x} : \boldsymbol{x} + d\boldsymbol{x}\right] = \sum g_{ij}(\boldsymbol{x}) dx^i dx^j + O\left(|d\boldsymbol{x}|^3\right), \tag{1}$$

where

$$g_{ij}(\boldsymbol{x}) = \frac{\partial^2}{\partial x_i \partial x_j} D\left[\boldsymbol{x} : \boldsymbol{y}\right] \big|_{\boldsymbol{y}=\boldsymbol{x}} . \tag{2}$$

Since g_{ij} is a positive-definite matrix, it gives a Riemannian metric derived from the divergence. For the sake of notational convenience, we introduce the following abbreviation by using the partial differential operator (natural basis of the tangent space),

$$\partial_i = \frac{\partial}{\partial x_i} \tag{3}$$

and define, for a number of operators $\partial_i, \partial_j, \partial_k$, etc.,

$$D\left[\partial_i \partial_j : \partial_k ; \boldsymbol{x}\right] = \frac{\partial^3}{\partial x_i \partial x_j \partial y_k} D[\boldsymbol{x} : \boldsymbol{y}] \big|_{\boldsymbol{y}=\boldsymbol{x}} . \tag{4}$$

Here, the operators in the left part of D operate on $\boldsymbol{x}$, while those on the right operate on $\boldsymbol{y}$, and finally the result is evaluated at $\boldsymbol{y} = \boldsymbol{x}$. Then, we have, for example,

$$D\left[\partial_i : \cdot ; \boldsymbol{x}\right] = \frac{\partial}{\partial x_i} D[\boldsymbol{x} : \boldsymbol{y}]_{|\boldsymbol{y}=\boldsymbol{x}} = 0 \tag{5}$$

$$D\left[\cdot : \partial_j ; \boldsymbol{x}\right] = \frac{\partial}{\partial y_j} D[\boldsymbol{x} : \boldsymbol{y}]_{\boldsymbol{y}=\boldsymbol{x}} = 0 \tag{6}$$

$$g_{ij} = D\left[\partial_i \partial_j : \cdot ; \boldsymbol{x}\right] = D\left[\cdot : \partial_i \partial_j ; \boldsymbol{x}\right] = -D\left[\partial_i : \partial_j ; \boldsymbol{x}\right]. \tag{7}$$

The above properties are proved as follow. When $\boldsymbol{y} - \boldsymbol{x}$ is small, we have from (1)

$$D[\boldsymbol{x} : \boldsymbol{y}] = \sum g_{ij}(\boldsymbol{x}) \left(x_1 - y_i\right) \left(x_j - y_j\right) + O\left(|\boldsymbol{x} - \boldsymbol{y}|^3\right). \tag{8}$$

By differentiating this with respect to x_i and/or y_j, and then putting $\boldsymbol{y} = \boldsymbol{x}$, we have (5), (6), (7).

We can easily prove that g_{ij} is a tensor.

Define

$$T_{ijk}(\boldsymbol{x}) = D\left[\partial_k : \partial_i \partial_j ; \boldsymbol{x}\right] - D\left[\partial_i \partial_j : \partial_k ; \boldsymbol{x}\right]. \tag{9}$$

We can prove that T_{ijk} is a tensor symmetric with respect to the three indices[Eguchi, 1983]. When $D[\boldsymbol{x} : \boldsymbol{y}]$ is symmetric, i.e., $D[\boldsymbol{x} : \boldsymbol{y}] = D[\boldsymbol{y} : \boldsymbol{x}]$,

$$T_{ijk} = 0. \tag{10}$$

A manifold M having a divergence function is equipped with two quantities g_{ij} and T_{ijk} derived from it. We write it as $\{M, g_{ij}, T_{ijk}\}$. Obviously the inner product of ∂_i and ∂_j is $\langle \partial_i, \partial_j \rangle = g_{ij}$.

We introduce affine connections in manifold M equipped with metric g_{ij} and cubic form T_{ijk}, that is, $\{M, g_{ij}, T_{ijk}\}$. When g_{ij} is given, the Levi-Civita or Riemannian connection is given by the Christoffel symbol

$$\Gamma^0_{ijk}(\boldsymbol{x}) = [i, j; k] = \frac{1}{2} \left(\partial_i g_{jk} + \partial_j g_{ik} - \partial_k g_{ij}\right). \tag{11}$$

This is a symmetric connection (torsion-free) and the related covariant derivative ∇^0 in the direction ∂_i satisfies

$$\nabla^0_{\partial_i} \langle \partial_j, \partial_k \rangle = \nabla^0_{\partial_i} g_{jk} = 0. \tag{12}$$

When a cubic tensor T_{ijk} is given in addition to g_{jk}, we define the α-connection [Amari and Nagaoka, 2000] by

$$\Gamma^{\alpha}_{ijk}(\boldsymbol{x}) = \Gamma^{0}_{ijk} - \frac{\alpha}{2} T_{ijk}, \tag{13}$$

where α is a real scalar parameter. The α-covariant derivative ∇^{α} is characterized by

$$\nabla^{\alpha}_{\partial i} g_{jk} = \frac{\alpha}{2} T_{ijk}. \tag{14}$$

The Levi-Civita connection is a special case of α-connection because it is given by $\alpha = 0$. When $\alpha = 1$, we call the 1-connection simply the (primal) connection and when $\alpha = -1$, the dual connection, respectively, derived from the divergence. The duality will be explained in the next section.

Dual connections with respect to Riemannian metric

We search for geometrical structure of manifold $\{M, g_{ij}, T_{ijk}\}$. Two affine connections Γ_{ijk} and Γ^{*}_{ijk} (or their covariant derivatives ∇ and ∇^{*}) in M are said to be dual with respect to Riemannian metric g_{ij}, when the following relation holds for three vector fields A, B and C

$$A\langle B, C\rangle = \langle \nabla_A B, C\rangle + \langle B, \nabla^{*}_A C\rangle, \tag{15}$$

where

$$\langle B, C\rangle = \sum g_{ij} B^i C^j \tag{16}$$

is the inner product of B and C, and A is the directional derivative operator, $\sum A^i \partial_i$, where $A = \sum A^i \partial_i$, $B = \sum B^i \partial_i$ and $C = \sum C^i \partial_i$. The following theorem is known [Amari, 1985], [Amari and Nagaoka, 2000].

Theorem 1. The α-connection and $-\alpha$-connection are dual with respect to the Riemannian metric g_{ij}.

Dually flat manifold

Manifold $\{M, g_{ij}, T_{ijk}\}$ derived from a divergence function is equipped with a Riemannian metric and two dual affine connections. Hence, we may represent it by $\{M, g, \nabla, \nabla^{*}\}$ in terms of metric $g = (g_{ij})$ and two dual affine connections (covariant derivatives) ∇ and ∇^{*}. Manifold M is in general curved, having non-zero Riemann-Christoffel curvature.

We prove that, when the Riemann-Christoffel curvature vanishes for the primal connection ∇, the Riemann-Christoffel curvature of the dual connection ∇^{*} vanishes automatically. But the Riemann-Christoffel curvature of the Levi-Civita connection does not vanish in general. A manifold $\{M, g, \nabla, \nabla^{*}\}$ is said to be dually flat, when the curvatures for ∇ and ∇^{*} vanish.

Theorem 2. When the primal curvature vanishes, the dual curvature vanishes at the same time.

Proof. Let $\prod$ and $\prod^{*}$ be parallel transport operators of a vector due to ∇ and ∇^{*}, respectively. The duality implies, in terms of the parallel transports, that

$$\langle A, B\rangle_P = \langle \prod A, \overset{*}{\prod} B\rangle_Q, \tag{17}$$

when two vectors A and B are transported from point P to Q along a curve connecting P and Q by the two parallel transports $\prod$ and $\prod^{*}$. Let us consider a loop c starting from P and ending at Q. Then, when the primal curvature vanishes, we have

$$\prod_c A = A \tag{18}$$

for any A. This implies

$$\prod_c^* B = B \tag{19}$$

for any B. This proves that the curvature vanishes for the dual connection.

When M is dually flat, the following properties hold. See [Amari and Nagaoka, 2000] for mathematical details.

Theorem 3. Let $\{M, g, \nabla, \nabla^*\}$ be a dually flat manifold. Then, the following holds.

1) There are two affine coordinate systems $\boldsymbol{\theta} = \left(\theta^1, \cdots, \theta^n\right)$ and $\boldsymbol{\eta} = (\eta_1, \cdots, \eta_n)$ in which the coefficients of the primal and dual connections vanish, respectively,

$$\Gamma_{ijk}(\boldsymbol{\theta}) = 0, \quad \Gamma^{*ijk}(\boldsymbol{\eta}) = 0. \tag{20}$$

We denote the components of $\boldsymbol{\theta}$ by θ^i using the upper index (contravariant) and those of $\boldsymbol{\eta}$ by η_i using the lower index (covariant) because of the duality. The two affine coordinates are unique up to affine transformations.

2) There exist two potential functions $\psi(\boldsymbol{\theta})$ and $\varphi(\boldsymbol{\eta})$ which are convex.

3) The Riemannian metric is given by the Hessian of the potential functions in the respective coordinate systems,

$$g_{ij}(\boldsymbol{\theta}) = \partial_i \partial_j \psi(\boldsymbol{\theta}), \quad \partial_i = \frac{\partial}{\partial \theta^i}, \tag{21}$$

$$g^{ij}(\boldsymbol{\eta}) = \partial^i \partial^j \varphi(\boldsymbol{\eta}), \quad \partial^i = \frac{\partial}{\partial \eta_i}. \tag{22}$$

Here, g_{ij} and g^{ij} are inverse matrices,

$$\sum g_{ij} g^{jk} = \delta_i^k, \tag{23}$$

where $\left(\delta_i^k\right)$is the identity matrix and the cubic tensor T is given by

$$T_{ijk}(\boldsymbol{\theta}) = \partial_i \partial_j \partial_k \psi(\boldsymbol{\theta}), \quad T^{ijk}(\boldsymbol{\eta}) = \partial^i \partial^j \partial^k \varphi(\boldsymbol{\eta}). \tag{24}$$

4) There exists a canonical divergence $D\left[\boldsymbol{\theta} : \boldsymbol{\theta}'\right]$, which is unique up to a scalar constant and is defined by

$$D\left[\boldsymbol{\theta} : \boldsymbol{\theta}'\right] = \psi(\boldsymbol{\theta}) + \varphi\left(\boldsymbol{\eta}'\right) - \sum \theta^i \eta_i'. \tag{25}$$

The geometrical structure, the Riemannian metric and the dual affine connections ∇ and ∇^*, derived from this divergence is the same as that of the original $\{M, g, T\}$.

5) A primal geodesic is linear in the $\boldsymbol{\theta}$ coordinate system and the dual geodesic is linear in the $\boldsymbol{\eta}$ coordinate system, so that they are given, respectively, by

$$\boldsymbol{\theta}(t) = t\boldsymbol{a} + \boldsymbol{c}, \quad \boldsymbol{\eta}(t) = t\boldsymbol{b} + \boldsymbol{c}', \tag{26}$$

where $\boldsymbol{a}$, $\boldsymbol{b}$, $\boldsymbol{c}$, $\boldsymbol{c}'$ are constant vectors.

Convex function and Legendre duality

A dually flat manifold M has two convex functions $\psi(\boldsymbol{\theta})$ and $\varphi(\boldsymbol{\eta})$. Given a convex function $\psi(\boldsymbol{\theta})$ of $\boldsymbol{\theta}$ in M, the Legendre transformation from $\boldsymbol{\theta}$ to $\boldsymbol{\eta}$ is

$$\eta_i = \partial_i \psi(\boldsymbol{\theta}). \tag{27}$$

There exists a dual potential $\varphi(\boldsymbol{\eta})$ which is convex with respect to $\boldsymbol{\eta}$ and the inverse transformation is given by

$$\theta^i = \partial^i \varphi(\boldsymbol{\eta}). \tag{28}$$

The two potential functions can be chosen to satisfy

$$\psi(\boldsymbol{\theta}) + \varphi(\boldsymbol{\eta}) - \sum \theta^i \eta_i = 0. \tag{29}$$

This gives the coordinate transformation between the primal affine coordinates $\boldsymbol{\theta}$ and the dual affine coordinates $\boldsymbol{\eta}$ on a dually flat manifold M.

We can define the canonical divergence between two points $\boldsymbol{\theta}$ and $\boldsymbol{\theta}'$ (or $\boldsymbol{\eta}$ and $\boldsymbol{\eta}'$) by using the potential function.

$$D\left[\boldsymbol{\theta} : \boldsymbol{\theta}'\right] = \psi(\boldsymbol{\theta}) - \psi\left(\boldsymbol{\theta}'\right) - \sum \partial_i \psi\left(\boldsymbol{\theta}'\right)\left(\theta^i - \theta'^i\right). \tag{30}$$

This is known as the Bregman divergence [Bregman, 1967] and is written in the dual form as

$$D\left[\boldsymbol{\theta} : \boldsymbol{\theta}'\right] = \psi(\boldsymbol{\theta}) + \varphi\left(\boldsymbol{\eta}'\right) - \sum \theta^i \eta'_i. \tag{31}$$

When a convex function $\psi(\boldsymbol{\theta})$ is given on M, a dually flat structure is constructed on M and conversely a dually flat M possesses an affine coordinate system $\boldsymbol{\theta}$, a convex potential $\psi(\boldsymbol{\theta})$ and the canonical divergence $D\left[\boldsymbol{\theta} : \boldsymbol{\theta}'\right]$.

Generalized Pythagorean theorem and projection theorem in flat M

The generalized Pythagorean theorem holds in a dually flat manifold M. Let P, Q, and R be three points in M.

Theorem 4. When the primal geodesic connecting Q and R is orthogonal in the sense of Riemannian metric g to the dual geodesic connecting P and Q, then

$$D\left[P : Q\right] + D[Q : R] = D[P : R] \tag{32}$$

and when the dual geodesic connecting Q and R is orthogonal to the geodesic connecting P and Q, then

$$D[Q : P] + D[R : Q] = D[R : P]. \tag{33}$$

The generalized Pythagorean theorem is a natural extension of that in a Euclidean space. Indeed, a Euclidean space is a special case of the dually flat manifold, where $T_{ijk} = 0$. In such a case, a primal geodesic and a dual geodesic are the same because the two coordinate systems $\boldsymbol{\theta}$ and $\boldsymbol{\eta}$ are the same, and g_{ij} reduces to δ_{ij} (identity matrix) in this coordinate system. The potential functions are written as

$$\psi(\boldsymbol{\theta}) = \varphi(\boldsymbol{\eta}) = \frac{1}{2}\sum \left(\theta^i\right)^2 = \frac{1}{2}\sum \left(\eta_i\right)^2 \tag{34}$$

and the divergence is

$$D\left[\boldsymbol{\theta} : \boldsymbol{\theta}'\right] = \frac{1}{2}\sum \left(\theta^i - \theta'^i\right)^2. \tag{35}$$

Therefore, theorem 4 is a natural extension of the Pythagorean theorem.

The projection theorem is a direct consequence of the Pythagorean theorem, which has many applications in real problems. See, e.g., [Boissonnat, Nielsen and Nock, 2010], [Takenouchi et al., 2008], [Ikeda, Tanaka and Amari, 2004], [Amari et al., 2003], etc.

Theorem 5. Let S be a submanifold in a dually flat manifold M. Given a point P, the point $\hat{P} \in S$ that is closest to P in the sense of minimizing divergences $D[P:Q]$, $Q \in S$ is called the geodesic projection of P to S. The dual geodesic projection $\hat{P}^*$ of P to S is the point that minimize $D[Q:P]$, $Q \in S$. The geodesic projection $\hat{P}$ (dual geodesic projection $\hat{P}^*$) is given by the point that satisfies the following: The geodesic (dual geodesic) connecting P and $\hat{P}$ (P and $\hat{P}^*$) is orthogonal to S.

Invariant divergence in the manifold of probability distributions

Let us consider a manifold of probability distributions. We consider the discrete case where random variable x takes values on finite set $X = \{1, 2, \cdots, n\}$. Then the set of all the probability distributions

$$S_n = \{p(x)\} \tag{36}$$

forms an $(n-1)$-dimensional manifold, called the probability $(n-1)$-simplex. We may write

$$p_i = \text{Prob}\{x = i\}. \tag{37}$$

Then the probability simplex is specified by $\boldsymbol{p} = (p_i)$, where

$$\sum p_i = 1, \quad p_i > 0. \tag{38}$$

We introduce a divergence $D[\boldsymbol{p}:\boldsymbol{q}]$ between two distributions $\boldsymbol{p}$ and $\boldsymbol{q} \in S_n$ that satisfies the following invariance criterion [Chentsov, 1982], [Csiszar, 1991]. For this purpose, we partition X into disjoint subsets $X_1, \cdots, X_m$,

$$X = \{X_1, \cdots, X_m\}, \quad \cup X_i = X, \quad X_i \cap X_j = \phi. \tag{39}$$

Then, the partition naturally induces a reduced probability distribution $\bar{\boldsymbol{p}}$ on $\bar{X} = \{X_1, \cdots, X_m\}$ such that

$$\bar{p}_i = \sum_{j \in X_i} p_j. \tag{40}$$

This is a coarse graining of observation of x such that we do not know x but know the subclass X_i to which x belongs, so that there is loss of information. A loss is expressed in terms of the divergence as follows.

Invariance Criterion: A divergence is said to be monotone when

$$D[\boldsymbol{p}:\boldsymbol{q}] \geq D[\bar{\boldsymbol{p}}:\bar{\boldsymbol{q}}] \tag{41}$$

holds for any partition of X. Moreover, it is said to be invariant, when

$$D[\boldsymbol{p}:\boldsymbol{q}] = D[\bar{\boldsymbol{p}}:\bar{\boldsymbol{q}}] \tag{42}$$

holds, if and only if the conditional probabilities of x conditioned on any X_i are equal for both $\boldsymbol{p}$ and $\boldsymbol{q}$,

$$p(x|X_i) = q(x|X_i), \quad i = 1, \cdots, m \tag{43}$$

or

$$p_i = c_j q_i, \quad i \in X_j \tag{44}$$

for constant c_j.

A divergence is said to be decomposable, when it is written as

$$D[\boldsymbol{p}:\boldsymbol{q}] = \sum d(p_i, q_i) \tag{45}$$

for some function d. The following theorem is known [Amari, 2009], [Amari and Nagaoka, 2000].

Theorem 6. The invariant divergence that gives dually flat structure is unique in S_n and is given by the Kullback-Leibler (KL) divergence.

$$KL\left[\boldsymbol{p}:\boldsymbol{q}\right]=\sum p_i\log\frac{p_i}{q_i}. \tag{46}$$

Theorem 7. The invariant Riemannian metric of S_n is given by the Fisher information matrix,

$$g_{ij}(\boldsymbol{p})=\sum_x p(x)\frac{\partial\log p(x)}{\partial p_i}\frac{\partial\log p(x)}{\partial p_j},\quad i,j=1,\cdots,n-1. \tag{47}$$

The invariant third-order tensor is given by

$$T_{ijk}(\boldsymbol{p})=\sum_x p(x)\frac{\partial\log p(x)}{\partial p_i}\frac{\partial\log p(x)}{\partial p_j}\frac{\partial\log p(x)}{\partial p_k}. \tag{48}$$

Theorem 8. S_n is a dually flat manifold and the $\boldsymbol{\theta}$ coordinates are

$$\theta^i=\log\frac{p_i}{p_n},\quad i=1,\cdots,n-1 \tag{49}$$

the dual $\boldsymbol{\eta}$ coordinates are

$$\eta_i=p_i,\quad i=1,\cdots,n-1, \tag{50}$$

the potential function is

$$\psi(\boldsymbol{\theta})=\log\left\{1+\sum\exp\left(\theta^i\right)\right\}, \tag{51}$$

which is the cumulant generating function, the dual potential function is

$$\varphi(\boldsymbol{\eta})=\sum\eta_i\log\eta_i+\left(1-\sum\eta_i\right)\log\left(1-\sum\eta_i\right), \tag{52}$$

which is the negative of Shannon entropy, and the canonical divergence is the KL divergence.

Information geometry is applied to statistical inference, in particular to higher-order asymptotic theory of statistical inference [Amari, 1985]. For example, consider a statistical model $M=\{p(x,\boldsymbol{u})\}\subset S_n$ specified by parameter $\boldsymbol{u}=(u_1,\cdots,u_m)$, where m is smaller than n. When x is observed N times, the observation defines the empirical distribution $\hat{\boldsymbol{p}}$,

$$\hat{p}_i=\frac{1}{N}\sharp\left\{x=i\right\}. \tag{53}$$

The maximum likelihood estimator $\hat{\boldsymbol{u}}$ is given by the geodesic projection of $\hat{\boldsymbol{p}}$ to the statistical model $M=\{p(x,\boldsymbol{u})\}$ in S_n. The error of estimation is evaluated by the Fisher information (Cramér-Rao theorem and by the embedding curvature of M in S_n). Information geometry can also be applied to semiparametric statistical inference, where a theory of estimating functions is established [Amari and Kawanabe, 1997]. We use a fiber-bundle-like structure in this case, when x is a continuous variable and the manifold is infinite-dimensional. However, we should be careful for mathematical difficulties in generalizing the above theory of the discrete case to an infinite-dimensional case. There are lots of applications of information geometry to optimization, machine learning, computer vision and neural networks.

Divergence introduced in the space of positive measures

Let us consider the set $\boldsymbol{R}_+^n$ of positive measures on X, where $m(x)$ gives a measure of $x\in X$. By introducing the delta function $\delta_i(x)$,

$$\delta_i(x)=\begin{cases}1, & x=i\\ 0, & \text{otherwise},\end{cases} \tag{54}$$

we can write

$$m(x, \boldsymbol{z}) = \sum z_i \delta_i(x), \tag{55}$$

where $z_i > 0$. $\boldsymbol{R}_n^+$ is a manifold where $\boldsymbol{z}$ is a coordinate system. The probability simplex S_n is its submanifold satisfying

$$\sum z_i = 1. \tag{56}$$

Let $u(z)$ and $v(z)$ be two differentiable and monotonically increasing functions satisfying

$$u(0) = v(0) = 0. \tag{57}$$

Define two coordinate systems $\boldsymbol{\theta}$ and $\boldsymbol{\eta}$ by

$$\theta^i = u(z_i), \tag{58}$$
$$\eta_i = v(z_i), \tag{59}$$

which are non-linear rescalings of z_i. We introduce the dually flat structure to $\boldsymbol{R}_+^n$ such that $\boldsymbol{\theta}$ and $\boldsymbol{\eta}$ are dually flat affine coordinate systems. The structure is called the (u, v)-structure, since it is defined by using two functions u and v. Note that the dual invariant affine coordinates $\boldsymbol{\theta}$ and $\boldsymbol{\eta}$ of (49) and (50) in S_n are given by

$$u(z) = \log z, \tag{60}$$
$$v(z) = z, \tag{61}$$

within the constraint of (56). The following theorem is given by [Amari, Ohara and Matsuzoe, 2012].

Theorem 9. The potential functions of the (u, v)-structure are given by

$$\psi(\boldsymbol{\theta}) = \sum \int d\theta_i \int \frac{v'\left\{u^{-1}(\theta_i)\right\}}{u'\left\{u^{-1}(\theta_i)\right\}} d\theta_i, \tag{62}$$
$$\varphi(\boldsymbol{\eta}) = \sum \int d\eta_i \int \frac{u'\left\{v^{-1}(\eta_i)\right\}}{v'\left\{v^{-1}(\eta_i)\right\}} d\eta_i. \tag{63}$$

Proof. Since the two coordinates are connected by Legendre transformations

$$\eta_i = \frac{\partial \psi(\boldsymbol{\theta})}{\partial \theta^i}, \quad \theta^i = \frac{\partial \varphi(\boldsymbol{\eta})}{\partial \eta_i}, \tag{64}$$

by integrating them, we have (62) and (63).

Theorem 10. The (u, v)-structure of $\boldsymbol{R}_n^+$ gives a Riemannian metric

$$g_{ij}(\boldsymbol{\theta}) = \partial_i \partial_j \psi(\boldsymbol{\theta}) \delta_{ij}, \tag{65}$$

and a cubic tensor

$$T_{ijk}(\boldsymbol{\theta}) = \partial_i \partial_j \partial_k \psi(\boldsymbol{\theta}) \delta_{ijk} \tag{66}$$

which includes only diagonal components since δ_{ij} and δ_{ijk} are 1 when $i = j$ and $i = j = k$, respectively, and 0 otherwise. The metric is Euclidean so that the curvature due to the Levi-Civita connection vanishes.

There are lots of applications of the (u, v)-divergences, in particular in the following form. The (u, v)-structure gives a dually flat affine structure to the Euclidean manifold $\boldsymbol{R}_n^+$ by rescaling the axes. We give examples of (u, v)-structures. See [Cichocki, Cruces and Amari, 2011].

1. Logarithmic structure

When

$$u(z) = \log z, \quad v(z) = z, \tag{67}$$

we have

$$\theta^i = \log z_i, \quad \eta_i = z_i \tag{68}$$

so that

$$m(x, \boldsymbol{z}) = \exp\left\{\sum \theta^i \delta_i(x)\right\}. \tag{69}$$

The potential functions are

$$\psi(\boldsymbol{\theta}) = \sum e^{\theta_i}, \quad \varphi(\boldsymbol{\eta}) = \sum \eta_i \log \eta_i - \sum \eta_i \tag{70}$$

and the canonical divergence is

$$D\left[\boldsymbol{z} : \boldsymbol{z}'\right] = \sum \left(z_i - z_i' + z_i \log \frac{z_i}{z_i'}\right), \tag{71}$$

which is the generalized KL divergence. The probability simplex S_n is the linear subspace given by

$$\sum \eta_i = 1 \tag{72}$$

and therefore is also dually flat. This gives the invariant structure satisfying the invariance criterion.

2. (α, β)**-structure** [Cichocki, Cruces and Amari, 2011]

Define

$$u(z) = z^\alpha, \quad v(z) = z^\beta \tag{73}$$

for two real parameters α and β. Then

$$\theta^i = (z_i)^\alpha, \quad \eta_i = (z_i)^\beta \tag{74}$$

and the potential functions are

$$\psi(\boldsymbol{\theta}) = \frac{\alpha}{\alpha+\beta} \sum \left(\theta^i\right)^{\frac{\alpha+\beta}{\alpha}}, \quad \varphi(\boldsymbol{\eta}) = \frac{\beta}{\alpha+\beta} \sum \left(\eta_i\right)^{\frac{\alpha+\beta}{\beta}}. \tag{75}$$

The divergence, named the (α, β)-divergence, is given by

$$D_{\alpha,\beta}\left[\boldsymbol{z} : \boldsymbol{z}'\right] = \sum \left\{\frac{\alpha}{\alpha+\beta}(z_i)^{\alpha+\beta} + \frac{\beta}{\alpha+\beta}\left(z_i'\right)^{\alpha+\beta} - (z_i)^\alpha \left(z_i'\right)^\beta\right\}. \tag{76}$$

The probability simplex S_n is a subspace, but the derived structure is neither invariant nor dually flat in general.

It should be remarked that, taking limit $\alpha \to 0$ carefully and putting $\beta = 1$, we have

$$\theta^i = \log z^i, \quad \eta_i = z_i. \tag{77}$$

Hence, $(0, 1)$-structure is the logarithmic structure.

3. α**-structure (**q**-structure)** [Amari and Nagaoka, 2000; Amari, 2007]

When $\alpha + \beta = 1$, we replace α by $1 - q = (1 - \tilde{\alpha})/2$ and β by $q = (1 + \tilde{\alpha})/2$, having

$$u(z) = z^{\frac{1-\tilde{\alpha}}{2}} = z^{1-q}, \quad v(z) = z^{\frac{1+\tilde{\alpha}}{2}} = z^q. \tag{78}$$

The structure is called the $\tilde{\alpha}$-structure or q-structure, where $\tilde{\alpha} = 1 - 2q$. We simply replace $\tilde{\alpha}$ by α, omitting $\tilde{}$. The α-structure is used in information geometry, but the same structure is used in non-extensive statistical mechanics by [Tsallis, 2009] and others under the name of q-entropy, etc.

Theorem 11. The $\alpha(q)$-affine coordinates are given by

$$\theta^i = (z_i)^{\frac{1-\alpha}{2}} = (z_i)^{1-q}, \ ; \ \eta_i = (z_i)^{\frac{1+\alpha}{2}} = (z_i)^q \tag{79}$$

with potential functions

$$\psi(\boldsymbol{\theta}) = \frac{1-\alpha}{2}\sum (\theta_i)^{\frac{2}{1-\alpha}} = \frac{1-\alpha}{2}\sum z_i \ ; \tag{80}$$

$$\varphi(\boldsymbol{\eta}) = \frac{1+\alpha}{2}\sum (\eta_i)^{\frac{2}{1+\alpha}} = \frac{1+\alpha}{2}\sum z_i. \tag{81}$$

The α-divergence is defined by

$$D_\alpha\left[\boldsymbol{z}:\boldsymbol{z}'\right] = \sum\left\{\frac{1-\alpha}{2}z_i + \frac{1+\alpha}{2}z_i - (z_i)^{\frac{1-\alpha}{2}}(z_i)^{\frac{1+\alpha}{2}}\right\}. \tag{82}$$

The α-structure introduced in the probability simplex S_n is not dually flat. However, the α-divergence is given in S_n by

$$D_\alpha\left[\boldsymbol{p}:\boldsymbol{p}'\right] = \sum\left\{1-(p_i)^{\frac{1-\alpha}{2}}\left(p_i'\right)^{\frac{1+\alpha}{2}}\right\}. \tag{83}$$

This is an invariant divergence. We extend the invariance principle to be applicable to $\boldsymbol{R}_+^n$. Then we have the following theorem [Amari, 2009].

Theorem 12. The α-divergence is the unique class of invariant divergence that gives dually flat structure to $\boldsymbol{R}_+^n$.

q exponential family and deformed exponential family

An exponential family S of probability distributions is a statistical model defined by

$$S = \left\{p(\boldsymbol{x},\boldsymbol{\theta}) = \exp\left[\sum\theta^i x_i - \psi(\boldsymbol{\theta})\right]\right\}, \tag{84}$$

where $\boldsymbol{x}$ is a vector random variable and $\boldsymbol{\theta} = \left(\theta^i\right)$ is called the natural parameters to specify a distribution. The invariant geometry introduced in S is dually flat, where $\boldsymbol{\theta}$ is the affine coordinate system, $\psi(\boldsymbol{\theta})$ is the potential function and the dual affine coordinates are given by

$$\eta_i = \partial_i\psi(\boldsymbol{\theta}) = \int x_i p(\boldsymbol{x},\boldsymbol{\theta})d\boldsymbol{x}. \tag{85}$$

This is called the expectation parameter. The dual potential is the negative entropy,

$$\varphi(\boldsymbol{\eta}) = \int p(\boldsymbol{x},\boldsymbol{\theta})\log p(\boldsymbol{x},\boldsymbol{\theta})d\boldsymbol{x}. \tag{86}$$

Instead of the logarithm, we introduce the q-logarithm (see [Tsallis, 2009], [Naudts, 2011]) defined by

$$\log_q z = \frac{1}{1-q}\left(z^{1-q}-1\right). \tag{87}$$

Then, a family of probability distributions of the form

$$\log_q p(\boldsymbol{x},\boldsymbol{\theta}) = \sum\theta^i x_i - \psi(\boldsymbol{\theta}) \tag{88}$$

is called a q-exponential family.

More generally, we define χ-logarithm [Naudts, 2011] by

$$\log_\chi(z) = \int_1^z \frac{1}{\chi(t)} dt, \tag{89}$$

where $\chi(t)$ is a monotonically increasing positive function. When

$$\chi(t) = t, \tag{90}$$

this gives the logarithm and when

$$\chi(t) = t^q, \tag{91}$$

this gives the q-logarithm.

The inverse function of the χ-logarithm is the χ-exponential given by

$$\exp_\chi(z) = 1 + \int_0^z \lambda(t) dt \tag{92}$$

where $\lambda(t)$ is related to χ by

$$\lambda\left(\log_\chi z\right) = \chi(z). \tag{93}$$

A family of probability distributions is called a χ-exponential family or χ-family in short when they are written as

$$p(\boldsymbol{x}, \boldsymbol{\theta}) = \chi\left\{\sum \theta^i x_i - \psi_\chi(\boldsymbol{\theta})\right\}. \tag{94}$$

with respect to dominating measure $\mu(\boldsymbol{x})$. The potential function $\psi_\chi(\boldsymbol{\theta})$ is determined from the normalization condition

$$\int p(\boldsymbol{x}, \boldsymbol{\theta}) d\mu(\boldsymbol{x}) = 1. \tag{95}$$

We may call $\psi_\chi(\boldsymbol{\theta})$ the χ-free energy. We can prove that it is a convex function [Amari, Ohara and Matsuzoe, 2012].

The probability simplex S_n is a χ-exponential family for any χ, since any distribution $p(x)$ on X is written as

$$\log_\chi p(x) = \sum_{i=1}^{n-1} \theta^i \delta_i(x) + \log_\chi\left(1 - \sum p_i\right), \tag{96}$$

where

$$\theta^i = \log_\chi p_i - \log_\chi p_n \tag{97}$$

$$x_i = \delta_i(x), \quad i = 1, \cdots, n-1. \tag{98}$$

We can introduce the geometrical structure (the metric and dual affine connections) from the invariance principle for any χ-family. However, except for exponential families and mixture families, the induced structure is not dually flat (except for the 1-dimensional case where the curvature always vanishes).

Instead, we can introduce a dually flat χ-structure to a χ-family, which in general is different from the invariant structure. In particular, the probability simplex S_n has χ-dually flat structure for any χ, which is different from the invariant structure in general.

By using the χ-free energy or χ-potential function $\psi_\chi(\boldsymbol{\theta})$, we define the χ-metric and χ-cubic tensor by

$$g_{ij}^\chi = \partial_i \partial_j \psi_\chi(\boldsymbol{\theta}), \tag{99}$$

$$T_{ijk}^\chi = \partial_i \partial_j \partial_k \psi_\chi(\boldsymbol{\theta}). \tag{100}$$

They give a dually flat geometrical structure. The dual affine coordinates are given by

$$\eta_i = \partial_i \psi_\chi(\boldsymbol{\theta}). \tag{101}$$

The dual potential function in S_n is given by

$$\varphi(\boldsymbol{\eta}) = \frac{1}{h_\chi} \sum u' \left\{ v\left(p_i\right) \right\} v\left(p_i\right). \tag{102}$$

In the case of the q-family in S_n, we have

$$\varphi_q(\boldsymbol{\eta}) = \frac{1}{1-q} \left(\frac{1}{h_q} - 1 \right). \tag{103}$$

Therefore, it is natural to define the q-entropy by

$$H_q(\boldsymbol{p}) = \frac{1}{h_q(\boldsymbol{p})} \tag{104}$$

up to a scale and constant. This is different from the Tsallis q-entropy defined by

$$H_{\text{Tsallis}} = -h_q(\boldsymbol{p}). \tag{105}$$

From the geometrical point of view, our definition of the q-entropy is natural.

We finally study how the χ-metric is related to the invariant Fisher metric in S_n [Amari and Ohara, 2011]. The following is an interesting observation, connecting q-geometry and conformal geometry [Kurose, 1994]. When a metric g_{ij} is changed to

$$\tilde{g}_{ij}(\boldsymbol{p}) = \sigma(\boldsymbol{p}) g_{ij}(\boldsymbol{p}), \tag{106}$$

where $\sigma(\boldsymbol{p})$ is a positive scalar function in a Riemannian manifold, the transformation is said to be conformal. In the case of $\{M, g, T\}$, a conformal transformation changes T_{ijk} as

$$\tilde{T}_{ijk}(\boldsymbol{p}) = \sigma(\boldsymbol{p}) T_{ijk} + \left(\partial_i \sigma\right) g_{jk} + \left(\partial_j \sigma\right) g_{ik} + \left(\partial_k \sigma\right) g_{ij}. \tag{107}$$

Theorem 13. The q-geometry is the unique class of probability distributions that is conformally connected to the invariant geometry with Fisher information metric. The conformal factor is given by

$$\sigma(\boldsymbol{p}) = \frac{1}{h_q(\boldsymbol{p})}. \tag{108}$$

Conclusion

We have reviewed the current status of information geometry which emerged from the study of invariant geometrical structure of the manifold of probability distributions. The structure is related to the divergence function and hence is regarded as the geometry of divergence. It consists of a Riemannian metric together with a pair of dual affine connections. A dually flat Riemannian manifold is of particular interest in applications. We have given its mathematical structure and showed that it gives the canonical divergence in the form of the Bregman divergence and vice versa.

We also show the invariance principle to be applied to the manifold of probability distributions. The Kullback-Leibler divergence is its canonical divergence. We also show various types of divergence functions which give the dually

flat structure. The Tsallis entropy and the deformed exponential family arising from it are studied in detail. We have proved that the q-structure is the unique class that is derived from conformal transformation of the invariant geometry having the Fisher information metric.

It is natural to use the geometry derived from the invariance principle, when we study statistical inference. However, the invariance geometry is given by α-geometry including a free parameter α. We usually treat the case of $\alpha = \pm 1$. The $\alpha = 0$ case reduces to the Riemannian geometry. There are interesting applications using other α [Matsuyama, 2002]. The invariance principle is applicable only to a manifold of probability distributions. Hence, we can construct a dually flat geometry in many problems such as vision and machine learning, when a convex function is used. This widens the applicability of information geometry.

Finally, we point out its extension. The extension to the infinite-dimensional function space is studied by [Cena and Pistone, 2007]. Its extension to Finsler geometry and Wasserstein geometry is also expected in future.

Bibliography

[Amari, 1985] S. Amari. Differential-Geometrical Methods in Statistics. Springer Lecture Notes in Statistics, 28, 1985

[Amari, 2007] S. Amari. Integration of Stochastic Models by Minimizing α-Divergence. Neural Computation, 19, 10, 2780–2796, 2007.

[Amari, 2009] S. Amari. α-divergence is unique, belonging to both f-divergence and Bregman divergence classes. IEEE Transactions on Information Theory, 55, 11, 4925–4931, 2009.

[Amari and Cichocki, 2010] S. Amari and A. Cichocki. Information geometry of divergence functions. Bulletin of the polish academy of sciences technical sciences, 58, 1, 183–195, 2010.

[Amari and Kawanabe, 1997] S. Amari and M. Kawanabe. Information geometry of estimating functions in semi-parametric statistical models. Bernoulli, 3, 29–54, 1997.

[Amari and Nagaoka, 2000] S. Amari and H. Nagaoka. Methods of Information Geometry. Translations of Mathematical Monographs, 191, Oxford University Press, 2000.

[Amari et al., 2003] S. Amari, H. Nakahara, S. Wu and Y. Sakai. Synchronous Firing and Higher-Order Interactions in Neuron Pool. Neural Computation, 15, 127–142, 2003.

[Amari and Ohara, 2011] S. Amari and A. Ohara. Geometry of q-exponential family of probability distributions. Entropy, 13, 1170–1185; doi:10.3390/e13061170, 2011.

[Amari, Ohara and Matsuzoe, 2012] S. Amari, A. Ohara and H. Matsuzoe. Geometry of deformed exponential families: Invariant, dually-flat and conformal geometries. Physica A, accepted for publication.

[Banerjee et al., 2005] A. Banerjee, S. Merugu, I. S. Dhillon and J. Gosh. Clustering with Bregman divergences. J. Machine Learning Research, 6, 1705–1749, 2005.

[Boissonnat, Nielsen and Nock, 2010] J.-D. Boissonnat, F. Nielsen and R. Nock. Bregman Voronoi diagrams. Discrete and Computational Geometry, 44, 281–307, 2010.

[Bregman, 1967] L. M. Bregman. The relaxation method of finding the common point of convex sets and its application to the solution of problems in convex programming. USSR Computational Mathematics and Physics, 7, 200–217, 1967.

[Cena and Pistone, 2007] A. Cena and G. Pistone. Exponential statistical manifold. Annals of Institute of Statist. Math., 59, 27–56, 2007.

[Chen, Chen and Rao, 2008] P. Chen, Y. Chen and M. Rao. Metrics defined by Bregman divergences: Part 2. Commun. Math. Sci., 6, 927–948, 2008.

[Chentsov, 1982] N. N. Chentsov. Statistical Decision Rules and Optimal Inference. AMS Translation Series, 1982.

[Cichocki, Cruces and Amari, 2011] A. Cichocki, S. Cruces and S. Amari. Generalized Alpha-Beta Divergences and Their Application to Robust Nonnegative Matrix Factorization. Entropy, 13, 134–170, 2011.

[Cichocki et al., 2009] A. Cichocki, R. Zdunek, A. H. Phan and S. Amari. Nonnegative Matrix and Tensor Factorizations. John Wiley and Sons, U.K., 2009.

[Csiszar, 1991] I. Csiszar. Why least squares and maximum entropy? An axiomatic approach to inference for linear inverse problems. Annals of Statistics, 19, 2032–2066, 1991.

[Eguchi, 1983] S. Eguchi. Second-order efficiency of minimum contrast estimators in a curved exponential family. Annals of Statistics, 11, 793–803, 1983.

[Ikeda, Tanaka and Amari, 2004] S. Ikeda, T. Tanaka and S. Amari. Information Geometry of Turbo and Low-Density Parity-Check Codes. IEEE Transactions on Information Theory, 50, 6, 1097–1114, 2004.

[Kurose, 1994] T. Kurose. On the divergence of 1-conformally flat statistical manifold. Tohoku Math. J., 46, 427–433, 1994.

[Liu et al, 2010] M. Liu, B. C. Vemuri, S. Amari and F. Nielsen. Total Bregman divergence and its applications to shape retrieval. IEEE CVPR, 3463–3468, 2010.

[Matsuyama, 2002] Y. Matsuyama. The α-EM algorithm: Surrogate likelihood maximization using αlogarithmic information measure. IEEE Trans. Information Theory, 49, 672–706, 2002.

[Naudts, 2011] J. Naudts. Generalized Thermostatistics, Springer, 2011.

[Picard, 1992] D. Picard. Statistical morphisms and related invariance properties. Annals of the Institute of Statistical Mathematics, 44, 45–61, 1992.

[Rao, 1945] C. R. Rao. Information and accuracy attainable in the estimation of statistical parameters. Bulletin of Calcutta Mathematical Society, 37, 81–91, 1945.

[Takenouchi et al., 2008] T. Takenouchi, S. Eguchi, N. Murata and T. Kanamori. Robust boosting algorithm against mislabeling in multi-class problems. Neural Computation, 20, 6, 1596–1630, 2008

[Tsallis, 2009] C. Tsallis. Introduction to Non-Extensive Statistical Mechanics: Approaching a Complex World. Springer, 2009.

[Vemuri et al., 2011] B. C. Vemuri, M. Lie, S. Amari and F. Nielsen. Total Bregman divergence and its applications to DTI analysis. IEEE Trans. on Medical Imaging, 30, 475–483, 2011.

[Vos, 1991] P. W. Vos. Geometry of f-divergence. Annals of the Institute of Statistical Mathematics, 43, 515–537, 1991.

Authors' Information

Shun-ichi Amari *- Senior Advisor, RIKEN Brain Science Institute, Hirosawa 2-1, Wako-shi, Saitama 351-0198, Japan; e-mail: amari@brain.riken.jp*
Major Fields of Scientific Research: Information geometry, mathematical neuroscience, machine learning, statistics

CLASSIFICATION RESULTS FOR $(v, k, 1)$ CYCLIC DIFFERENCE FAMILIES WITH SMALL PARAMETERS

Tsonka Baicheva and Svetlana Topalova

Abstract: *Classifications of $(v, k, 1)$ cyclic difference families (CDFs) by other authors are known for $k = 3$ and $v \leq 57$, $k = 4$ and $v \leq 64$, $k = 5$ and $v \leq 65$, $k = 6$ and $v = 91$ and $k = 7$ and $v = 91$. In this work we construct all inequivalent $(v, k, 1)$ CDFs (respectively all multiplier inequivalent cyclic 2-$(v, k, 1)$ designs) with $k \leq 11$ and some small v by a computer search and an algorithm similar to the one applied for the classification of optimal orthogonal codes in our previous works. We obtain the same number of inequivalent CDFs for all the parameters, for which previous classification results are known. The new parameters covered by our software for $k \leq 7$ are $(61, 3, 1)$, $(73, 4, 1)$, $(76, 4, 1)$, $(81, 5, 1)$, and $(85, 5, 1)$ CDFs.*

Keywords*: cyclic difference set, Steiner triple system, optical orthogonal code*

ACM Classification Keywords*: Algorithms*

MSC*: 05B05, 05B07, 05B10*

Introduction

Definition 1. *Let $\mathbf{B}$ be a subset of an additive group G. We denote by $\Delta\mathbf{B}$ the list of all possible differences $b - b'$ with (b, b') an ordered pair of distinct elements of $\mathbf{B}$. More generally, if $\mathbf{F} = \{B_1, B_2, \ldots, B_n\}$ is a collection of subsets of G, then the list of differences from $\mathbf{F}$, denoted by $\Delta\mathbf{F}$, is the multiset obtained by joining $\Delta B_1, \ldots, \Delta B_n$. $\mathbf{F}$ is said to be a $(\mathbf{v}, \mathbf{k}, \mathbf{1})$* **difference family (DF)** *if G has order v, every B_i is of size $k \geq 3$, and $\Delta\mathbf{F}$ covers every non-zero element of G exactly once. If further, $G = Z_v$, then this difference family is said to be* **cyclic (CDF)**.

For general background on difference families we refer to [Abel, 1996] and [Beth, Jungnickel, Lenz, 1999]. Complete sets of CDFs are of interest in their own right, as well as for applications in the construction of other types of combinatorial structures. There are known applications to one-factorizations of complete graphs and to cyclically resolvable cyclic Steiner triple systems [Fuji-Hara, Miao, Shinohara, 2002], as well as to constructions of regular LDPC codes [Fujisawa, Sakata, 2005]. Very efficient constructions of new optimal perfect secrecy systems that are onefold secure against spoofing are obtained via CDF [Huber, 2012]. Optimal frequency-hopping sequences can also be constructed from $(v, k, 1)$ CDFs.

01 Related combinatorial structures

Differences can be considered as a measure of distance. That is why CDFs correspond to several different combinatorial structures, for which a distance condition is defined by means of scalar product, or Hamming distance. A very suitable example are the two different definitions that authors very often give for (v, k, λ) optical orthogonal codes (OOCs).

Definition 2. *A (v,k,λ) optical orthogonal code $\mathcal{C}$ is a collection of $\{0,1\}$ sequences of length v and Hamming weight k such that:*

$$\sum_{i=0}^{v-1} x(i)x(i+j) \leq \lambda,\ 1 \leq j \leq v-1 \tag{1}$$

$$\sum_{i=0}^{v-1} x(i)y(i+j) \leq \lambda,\ 0 \leq j \leq v-1 \tag{2}$$

for all pairs of distinct sequences $x, y \in \mathcal{C}$. The same definition holds for a (v,k,λ) binary cyclically permutable constant weight (CPCW) code.

Definition 3. *A (v,k,λ) optical orthogonal code (OOC) can be defined as a collection $\mathcal{C} = \{C_1, \ldots, C_s\}$ of k-subsets (codeword-sets) of Z_v such that any two distinct translates of a codeword-set and any two translates of two distinct codeword-sets share at most λ elements:*

$$|C_i \cap (C_i + t)| \leq \lambda,\ 1 \leq i \leq s,\ 1 \leq t \leq v-1 \tag{3}$$

$$|C_i \cap (C_j + t)| \leq \lambda,\ 1 \leq i < j \leq s,\ 0 \leq t \leq v-1. \tag{4}$$

And if $(v,k,1)$ OOCs are considered, the latter definition is usually replaced by the following one.

Definition 4. *A $(v,k,1)$ optical orthogonal code (OOC) may be viewed as a set of k-subsets of Z_v whose list of differences has no repeated elements.*

A $(v,k,1)$ OOC is *optimal* when its size reaches the upper bound $\left\lfloor \frac{(v-1)}{k(k-1)} \right\rfloor$. If its size is exactly equal to $\frac{(v-1)}{k(k-1)}$, the code is *perfect* because its list of differences covers all nonzero elements of Z_v. A perfect $(v,k,1)$ OOC forms a $(v,k,1)$ CDF.

Next we supply definitions of other combinatorial structures related to difference families.

Definition 5. *Let $V = \{P_i\}_{i=1}^{v}$ be a finite set of points, and $\mathcal{B} = \{B_j\}_{j=1}^{b}$ a finite collection of k-element subsets of V, called blocks. $D = (V, \mathcal{B})$ is a design with parameters t-(v,k,λ) if any t-subset of V is contained in exactly λ blocks of $\mathcal{B}$.*

A t-(v,k,λ) design is *cyclic* if it has an automorphism permuting its points in one cycle.

Definition 6. *An (n,w,d) binary constant weight code (CWC) of length n, weight w and minimal distance d is a collection of binary vectors of length n (codewords), which have exactly w nonzero positions and the Hamming distance between any two codewords is at least d. A CWC is cyclic if the cyclic shift of each codeword is a codeword too. A cyclic CWC corresponds to an $(n,w,w-d/2)$ CPCW code.*

A $(v,k,1)$ CDF can be obtained from any optimal perfect $(v,k,1)$ CPCW code (optimal perfect $(v,k,1)$ OOC), and from any optimal cyclic binary CWC with weight k and minimal distance $2(k-1)$. CDFs with $v \equiv k\ (mod\, k(k-1))$ do not correspond to CPCW codes (OOCs) and cyclic binary CWCs.

There is a one-to-one correspondence between $(v,k,1)$ CDFs and cyclic 2-$(v,k,1)$ designs. An example illustrating the relations between difference families and other combinatorial structures is presented in Figure 1.

02 Equivalence

The aim of our work is classification of CDFs. That is why we have to know when two CDFs are equivalent.

Figure 1: Relations of cyclic difference families
a) - Perfect $(13, 3, 1)$ OOC and $(13, 3, 1)$ CDF

codeword-sets(sets)	differences
{0,1,4}	1 3 4 9 10 12
{0,2,8}	2 5 6 7 8 11

b) - Related cyclic 2-(13,3,1) design and cyclic (13,3,4) CWC

0	1 0 0 0 0 0 0 0 0 1 0 0 1	1 0 0 0 0 1 0 0 0 0 0 1 0
1	1 1 0 0 0 0 0 0 0 0 1 0 0	0 1 0 0 0 0 1 0 0 0 0 0 1
2	0 1 1 0 0 0 0 0 0 0 0 1 0	1 0 1 0 0 0 0 1 0 0 0 0 0
3	0 0 1 1 0 0 0 0 0 0 0 0 1	0 1 0 1 0 0 0 0 1 0 0 0 0
4	1 0 0 1 1 0 0 0 0 0 0 0 0	0 0 1 0 1 0 0 0 0 1 0 0 0
5	0 1 0 0 1 1 0 0 0 0 0 0 0	0 0 0 1 0 1 0 0 0 0 1 0 0
6	0 0 1 0 0 1 1 0 0 0 0 0 0	0 0 0 0 1 0 1 0 0 0 0 1 0
7	0 0 0 1 0 0 1 1 0 0 0 0 0	0 0 0 0 0 1 0 1 0 0 0 0 1
8	0 0 0 0 1 0 0 1 1 0 0 0 0	1 0 0 0 0 0 1 0 1 0 0 0 0
9	0 0 0 0 0 1 0 0 1 1 0 0 0	0 1 0 0 0 0 0 1 0 1 0 0 0
10	0 0 0 0 0 0 1 0 0 1 1 0 0	0 0 1 0 0 0 0 0 1 0 1 0 0
11	0 0 0 0 0 0 0 1 0 0 1 1 0	0 0 0 1 0 0 0 0 0 1 0 1 0
12	0 0 0 0 0 0 0 0 1 0 0 1 1	0 0 0 0 1 0 0 0 0 0 1 0 1

Definition 7. *Two difference families* $\mathbf{F} = \{B_1, B_2, \ldots, B_n\}$ *and* $\mathbf{F}' = \{B'_1, B'_2, \ldots, B'_n\}$ *over a group* G *are equivalent if there is an automorphism* α *of* G *such that for each* $i = 1, 2, \ldots, n$ *there exists* B'_j *which is a translate of* $\alpha(B_i)$.

We are also interested in the equivalence definitions for the related to the CDFs combinatorial objects, because classifying CDFs we classify them too.

Definition 8. *Two* 2-(v, k, λ) *designs* D *and* D' *are isomorphic if there exists a permutation of the points which maps each block of* D *to a block of* D'.

Definition 9. *Two* (v, k, λ) *CPCW codes* C *and* C' *are isomorphic if there exists a permutation of* Z_v*, which maps the collection of translates of each block of* C *to the collection of translates of a block of* C'.

Multiplier equivalence is defined for cyclic combinatorial objects.

Definition 10. *Two* (v, k, λ) *CPCW codes (OOCs) are multiplier equivalent if they can be obtained from one another by an automorphism of* Z_v *and replacement of blocks by some of their translates.*

Definition 11. *Two cyclic* 2-(v, k, λ) *designs* D *and* D' *are multiplier equivalent if there exists an automorphism of* Z_v *which maps each block of* D *to a block of* D'.

Two cyclic designs can be isomorphic, but multiplier inequivalent. The same holds for two CPCW codes.

The number of multiplier inequivalent perfect optimal 2-$(v, k, 1)$ CPCW codes (OOCs) is the same as the number of the inequivalent 2-$(v, k, 1)$ CDFs.

The number of inequivalent $(v, k, 1)$ CDFs is the same as the number of multiplier inequivalent cyclic 2-$(v, k, 1)$ designs, and vice versa.

03 Existence Results

The known existence results for CDFs with $k = 3, 4, 5, 6, 7$ can be summarized as follows:

Theorem 1. *A $(v, k, 1)$ CDF can exist for $v \equiv 1, k \ (mod\ k(k-1))$.*

Theorem 2. *[Dinitz, Shalaby, 2002] There exists a $(v, 3, 1)$ difference family for every $v \equiv 1, 3 \ (mod\ 6)$ except $v = 9$.*

Theorem 3. *([Bose 1939],[Buratti, 1995],[Buratti, 1997],[Colbourn, Dinitz (eds.), 1996],[Lidl, Niederreiter, 1983])*

1. For any prime power $q \equiv 1 \ (mod\ 12)$ there exists a $(q, 4, 1)$ difference family in GF(q).

2. For any prime power $q \equiv 1 \ (mod\ 20)$ there exists a $(q, 5, 1)$ difference family in GF(q).

Theorem 4. *([Abel, Burati, 2004],[Abel, Costa, Finizio, 2004])*

1. A $(12t + 1, 4, 1)$ differnce family exists for $1 \leq t \leq 50$ except for $t = 2$.

2. A $(20t + 1, 5, 1)$ differnce family exists for $1 \leq t \leq 50$ except possibly for $t = 16, 25, 31, 34, 40, 45$.

Theorem 5. *([Chen, Zhu, 1998]) There exists a $(q, 6, 1)$ DF for any prime power $q \equiv 1 \ (mod\ 30)$ with one exception of $q = 61$.*

Theorem 6. *([Chen, Wei, Zhu, 2002]) There exists a $(q, 7, 1)$ DF for any prime power $q \equiv 1 \ (mod\ 42)$ except for $q = 43$, posibly for $q = 127, 211, 31^6$, and primes $q \in [261239791, 1.236597.10^{13}]$ such that $(-3)^{\frac{(q-1)}{14}} = 1$ in GF(q).*

04 On the classification problem

The classification and the public accessibility of the classified CDFs with small parameters is of particular interest, because it can help to choose, among CDFs with the same parameters, the one which is most suitable for some application (for optical code-division multiple-access channels for instance), or the one which is most suitable to serve as ingredient in some recursive construction of CDFs with higher parameters.

Classifications of cyclic difference families by other authors are known for $k = 3$ and $v \leq 57$ [Colbourn, Rosa, 1999], $k = 4$ and $v \leq 64$ [Colbourn, Mathon, 1980], $k = 5$ and $v \leq 65$ [Colbourn, Mathon, 1980], $k = 6$ and $v = 91$ [Colbourn, 1981], [Janko, Tonchev, 1991] and $k = 7$ and $v = 91$ [Bhat-Nayak, Kane, Kocay, Stanton, 1983]. In this work we construct all inequivalent cyclic difference families with $k \leq 11$ and some small v.

Construction method

We use a modification of our algorithm for classification of optimal $(v, k, 1)$ OOCs [Baicheva, Topalova, 2011].

We classify the $(v, k, 1)$ CDFs up to equivalence by back-track search with minimality test on the partial solutions [Kaski, Östergård, 2006, section 7.1.2]. Without loss of generality we can assume that $b_1 < b_2 < \cdots < b_s$ for each set $\mathbf{B} = \{b_1, b_2, \ldots, b_s\}$. We first arrange all possibilities for the sets B_i with respect to a lexicographic order defined on them. If a set $B_i \in \mathbf{F}$ is replaced by one of its translates, we obtain an equivalent CDF. That is why we can assume that each set of $\mathbf{F}$ is lexicographically smaller than its translates. This means that $b_1 = 0$ and when we say that B_1 is mapped to B_2 by the permutation φ, we mean that B_2 is the smallest translate of $\varphi(B_1)$.

Let $\varphi_0, \varphi_1, \ldots, \varphi_{m-1}$ be the automorphisms of Z_v, where φ_0 is the identity. We construct an array of all sets $\mathbf{B}$ of k elements of Z_v which might become sets of $\mathbf{F}$, i.e. they are smaller than all their translates and $\Delta\mathbf{B}$ does not contain repeated differences. We find them in lexicographic order. To each constructed set we apply the permutations $\varphi_i, i = 1, 2, \ldots, m-1$. If some of them maps it to a smaller set, we do not add the current set since it is already somewhere in the array. If we add the current set to the array, we also add after it the $m-1$ sets to which it is mapped by $\varphi_1, \varphi_2, \ldots, \varphi_{m-1}$.

Most of the sets of a CDF have $v-1$ translates. If $v \equiv k \ (mod\ k(k-1))$ one of the sets has v/k translates and is equal to $\{0, v/k, 2v/k, \ldots, (k-1)v/k\}$, so we first add this set to the CDF. We then apply back-track search to choose the sets with $v-1$ translates from the upper list of all possibilities for them. The above described ordering

of all the possible sets allows repeated sets in the array, but makes the minimality test of the partial solutions very fast. By the minimality test we check if the current solution can be mapped to a lexicographically smaller one by the automorphisms of Z_v and reject it if so.

In this way we classify the CDFs up to multiplier equivalence. We use our own software written in C++.

Classification results

CDFs correspond to the perfect optimal OOCs which we have classified in our papers on optimal OOCs with parameters $(v, 4, 1)$ [Baicheva, Topalova, 2011], $(v, 5, 1)$ [Baicheva, Topalova, 2012a] and $(v, 3, 1)$ [Baicheva, Topalova, 2012b]. Therefore, in these papers new results about CDFs are obtained too. In the present paper we repeat all previous results on CDFs (ours and of other authors) and add some new ones, which we obtain by the above described construction method. We find the same number of inequivalent CDFs for all the parameters, for which previous classification results are known. To the results of other authors for $k \leq 7$ we add classifications of $(61, 3, 1)$, $(73, 4, 1)$, $(76, 4, 1)$, $(81, 5, 1)$ and $(85, 5, 1)$ CDFs. A summary is presented in Table 1.

Since previous classification results have been obtained by different authors for the different parameters, we think that collecting them together is of particular interest. We believe that both Table 1 and the files with all the inequivalent difference sets (available from the authors) will be very useful for applications and to people who will go on with research in this field.

Table 1: Inequivalent cyclic (v,k,1) difference families (Multiplier inequivalent cyclic 2-(v,k,1) designs)

v	k	CDFs
7	3	1
9	3	0
13	3	1
15	3	2
19	3	4
21	3	7
25	3	12
27	3	8
31	3	80
33	3	84
37	3	820
39	3	798
43	3	9508
45	3	11616
49	3	157340
51	3	139828
55	3	3027456
57	3	2353310
61	3	42373196

v	k	CDFs
13	4	1
16	4	0
25	4	0
28	4	0
37	4	2
40	4	10
49	4	224
52	4	206
61	4	18132
64	4	12048
73	4	1426986
76	4	1113024
21	5	1
25	5	0
41	5	1
45	5	0
61	5	10
65	5	2
81	5	528

v	k	CDFs
85	5	170
31	6	1
36	6	0
61	6	0
66	6	0
91	6	4
96	6	0
43	7	0
49	7	0
85	7	0
91	7	2
57	8	1
64	8	0
73	9	1
81	9	0
91	10	1
100	10	0
111	11	0
121	11	0

Bibliography

[Shannon, 1949] C.E.Shannon. The Mathematical theory of communication. In: The Mathematical Theory of Communication. Ed. C.E.Shannon and W.Weaver. University of Illinois Press, Urbana, 1949.

[Abel, 1996] R.J.R. Abel, *Difference families*, in: C.J. Colbourn, J.H. Dinitz (Eds.), The CRC Handbook of Combinatorial Designs, CRC Press, Boca Raton, FL, 1996, pp. 270Ű-287.

[Beth, Jungnickel, Lenz, 1999] T. Beth, D. Jungnickel, H. Lenz, *Design Theory*, Cambridge University Press, Cambridge (1999).

[Fuji-Hara, Miao, Shinohara, 2002] R. Fuji-Hara, Y. Miao and S. Shinohara, Complete Sets of Disjoint Difference Families and their Applications, *Journal of Statistical Planning and Inference*, Volume 106, Issues 1Ű2, 1 August 2002, pp. 87 Ű 103.

[Fujisawa, Sakata, 2005] Fujisawa, M., Sakata, S., A class of quasi-cyclic regular LDPC codes from cyclic difference families with girth 8 , *Proceedings International Symposium on Information Theory*, 4-9 Sept. 2005, pp. 2290 - 2294.

[Huber, 2012] M. Huber, Perfect Secrecy Systems Immune to Spoofing Attacks, arXiv:1205.4874v1.

[Dinitz, Shalaby, 2002] H.J. Dinitz, N. Shalaby, Block disjoint difference families for Steiner tripple systems: $v \equiv 3 \ (mod \ 6)$, *J. Stat. Plann. Infer.*, 106, 2002, pp. 77 - 86.

[Bose 1939] 3. R. C. Bose, On the construction of balanced incomplete block designs, *Ann. Eugenics*, Vol. 9, 1939, pp. 353 - 399.

[Buratti, 1995] M. Buratti, Constructions for $(q, k, 1)$ difference families with q a prime power and $k = 4, 5$, *Discrete Mathematics*, Vol. 138, 1995, pp. 169 - 175.

[Buratti, 1997] M. Buratti, From a $(G, k, 1)$ difference family to a $(C_k \oplus G, k, 1)$ difference family, *Designs, Codes and Cryptography*, Vol. 11, 1997, pp. 5 - 9.

[Colbourn, Dinitz (eds.), 1996] C. J. Colbourn and J. H. Dinitz (eds.), *The CRC Handbook of Combinatorial Designs*, CRC Press, New York, 1996.

[Lidl, Niederreiter, 1983] R. Lidl and H. Niederreiter, *Finite fields, Encyclopedia of Mathematics and Its Applications*, Vol. 20, Cambridge University Press, Cambridge, 1983.

[Abel, Burati, 2004] R.J.R. Abel, M. Burati, Some progress on $(v, 4, 1)$ diffrence families and optical orthogonal codes, *J. Combin Theory* A, 106, 2004, pp. 59 - 75.

[Abel, Costa, Finizio, 2004] R.J.R. Abel, S. Costa, N.j. Finizio, Directed-ordered whist tournaments and $(v, 5, 1)$ difference families: Existence results and some new classes of Z-cyclic solutions, *Discrete Appl. Math.*, 143, 2004, pp. 43 - 53.

[Chen, Zhu, 1998] K. Chen, L. Zhu, Existence of $(q, 6, 1)$ difference families with q a prime power, *Designs, Codes and Cryptography*, 15, 1998, pp. 167 - 173.

[Chen, Wei, Zhu, 2002] K. Chen,R. Wei, L. Zhu, Existence of $(q, 7, 1)$ difference families with q a prime power, *Journal of Combinatorial Designs*, 10, Issue 2, 2002, pp. 126 - 138.

[Colbourn, Rosa, 1999] C. J. Colbourn, and A. Rosa, *Triple systems*, Oxford University Press, Oxford, 1999.

[Baicheva, Topalova, 2011] T. Baicheva and S. Topalova, Classification of optimal (v,4,1) binary cyclically permutable constant weight codes and cyclic S(2,4,v) designs with $v \leq 76$, *Problems of Information Transmission*, vol. 47(3), 2011, pp. 224 - 231.

[Colbourn, Mathon, 1980] Colbourn M.J., Mathon R.A., On cyclic Steiner 2-designs, *Ann. Discrete Math.*, vol. 7, 1980, pp. 215 - 253.

[Colbourn, 1981] C. J. Colbourn, On cyclic Steiner systems S(2,6,91), *Abstracts Amer. Math. Soc.*, 2, 1981.

[Janko, Tonchev, 1991] Z. Janko, V. D. Tonchev, Cyclic 2-(91, 6, 1) designs with multiplier automorphisms, *Discrete Mathematics*, Volume 97, Issues 1Ű3, 1991, pp. 265 - 268.

[Bhat-Nayak, Kane, Kocay, Stanton, 1983] V. N. Bhat-Nayak, V. D. Kane, W. L. Kocay, R. G. Stanton, Settling some BIBD conjectures, *Ars Combin.*, 16, 1983, pp. 229 - 234.

[Kaski, Östergård, 2006] P. Kaski, P. Östergård, *Classification algorithms for codes and designs*, Springer, Berlin, 2006.

[Baicheva, Topalova, 2012a] T. Baicheva and S. Topalova, Optimal optical orthogonal codes of weight 5 and small lengths, International Conference on Applications of Computer Algebra, Sofia, Bulgaria, 2012.

[Baicheva, Topalova, 2012b] T. Baicheva and S. Topalova, Optimal $(v, 3, 1)$ binary cyclically permutable constant weight codes with small v, *Proc. of the International Workshop on Algebraic and Combinatorial Coding Theory*, Pomorie, Bulgaria, 2012, pp. 41 - 46.

Authors' Information

Tsonka Stefanova Baicheva *- associate professor, Institute of Mathematics and Informatics Bulgarian Academy of Sciences, P.O.Box 323, 5000 V. Tarnovo, Bulgaria*
e-mail: tsonka@math.bas.bg

Svetlana Todorova Topalova *- associate professor, Institute of Mathematics and Informatics Bulgarian Academy of Sciences, P.O.Box 323, 5000 V. Tarnovo, Bulgaria*
e-mail: svetlana@math.bas.bg

LOGARITHMIC DISTANCES IN GRAPHS

Pavel Chebotarev

Abstract: *The walk distances in graphs are defined as the result of appropriate transformations of the $\sum_{k=0}^{\infty}(tA)^k$ proximity measures, where A is the weighted adjacency matrix of a graph and t is a sufficiently small positive parameter. The walk distances are graph-geodetic; moreover, they converge to the shortest path distance and to the so-called long walk distance as the parameter t approaches its limiting values. Furthermore, the logarithmic forest distances which are known to generalize the resistance distance and the shortest path distance are a specific subclass of walk distances. On the other hand, the long walk distance is equal to the resistance distance in a transformed graph.*

Keywords: *graph distances, walk distances, logarithmic forest distances, transitional measure, Laplacian matrix, resistance distance, network*

ACM Classification Keywords*: G.2.2 Graph Theory – Network problems; E.1 Data Structures – Graphs and networks; C.2.1 Network Architecture and Design – Network topology*

MSC*: 05C12, 05C50, 15B48*

The classical distances for graph vertices are the well-known shortest path distance, the resistance distance, which is proportional to the commute time distance, and the square root version of the resistance distance. The latter two distances were first studied by Gerald Subak-Sharpe in the 60s. Recently, a need for a wider variety of graph distances has been strongly felt (see [Deza and Deza, 2009; von Luxburg, Radl, and Hein, 2011; Tang, 2010; Estrada, 2011] among many others).

Recall the well-known fact that the shortest path distance and the resistance distance coincide on each tree. In particular, for every path, the resistance distance between every two adjacent vertices is one, as well as the shortest path distance. However, in some applications two central adjacent vertices in a path may be considered as being *closer* to each other than two peripheral adjacent vertices are as there are more walks (of length 3, 5, etc.) connecting two central vertices. Such a "gravitational" property holds for the forest distances we studied since 1995. In some other applications, a terminal vertex in a path can be considered as being closer to its neighbor than two central adjacent vertices are. For example, if someone has a single friend, then this friendship is often stronger than that between persons having more friends. This heuristic is supported by the logarithmic forest distances [Chebotarev, 2011].

In [Chebotarev, 2011a], a general framework was proposed for constructing graph-geodetic metrics (a distance $d(i,j)$ for graph vertices is graph-geodetic whenever $d(i,j)+d(j,k)=d(i,k)$ if and only if every path connecting i and k visits j). Namely, it has been shown that if a matrix $S=(s_{ij})$ produces a strictly positive transitional measure on a graph G (i.e., $s_{ij}\,s_{jk}\le s_{ik}\,s_{jj}$ for all vertices i, j, and k, while $s_{ij}\,s_{jk}=s_{ik}\,s_{jj}$ if and only if every path from i to k visits j), then the logarithmic transformation $h_{ij}=\ln s_{ij}$ and the inverse covariance mapping $d_{ij}=h_{ii}+h_{jj}-h_{ij}-h_{ji}$ convert S into the matrix of a graph-geodetic distance. In the case of digraphs, five transitional measures were found in [Chebotarev, 2011a], namely, the "connection reliability", the "path accessibility" with a sufficiently small parameter, the "walk accessibility", and two versions of the "forest accessibility".

Earlier, the inverse covariance mapping has been applied to the matrices of walk weights $\sum_{k=0}^{\infty}(tA)^k$, where A is the adjacency matrix of a graph. This leads to distances whenever the positive parameter t is sufficiently small. However, these distances are not graph-geodetic and some of their properties are quite exotic.

In the present paper, we study the graph-geodetic *walk distances*, which involves the logarithmic transformation. The walk distances are expressed in terms of commute cycles and via block matrix operations. Two limiting cases

of walk distances are investigated: the short walk distance coincides with the classical shortest path distance, while the long walk distance is original. Furthermore, modified walk distances (the "e-walk distances") are considered which generalize the classical *weighted* shortest path distance. It is shown that adding "balancing loops" converts the logarithmic forest distances into a subclass of walk distances. This implies, in particular, that the resistance distance is also a limiting walk distance. Finally, several graph metrics are compared on simple examples.

Bibliography

[Chebotarev, 2011] P. Chebotarev, A class of graph-geodetic distances generalizing the shortest-path and the resistance distances, Discrete Appl. Math. 159 (2011) 295–302.

[Chebotarev, 2011a] P. Chebotarev, The graph bottleneck identity, Adv. in Appl. Math. 47 (2011) 403–413.

[Chebotarev, 2012] P. Chebotarev, The walk distances in graphs, Discrete Appl. Math., 160 (2012) 1484–1500.

[Deza and Deza, 2009] M. Deza, E. Deza, Encyclopedia of Distances, Springer, Berlin–Heidelberg, 2009.

[Estrada, 2011] E. Estrada, The Structure of Complex Networks: Theory and Applications, Oxford Univ. Press, Oxford, 2011.

[Tang, 2010] M. Tang, Graph Metrics and Dimension Reduction, Ph.D. Thesis, School of Informatics and Computing, Indiana University, Bloomington, IN, 2010.

[von Luxburg, Radl, and Hein, 2011] U. von Luxburg, A. Radl, M. Hein, Getting lost in space: Large sample analysis of the resistance distance, in: NIPS 2010, Twenty-Fourth Annual Conference on Neural Information Processing Systems, Curran, Red Hook, New York, 2011, pp. 2622–2630.

Authors' Information

Pavel Chebotarev *- Institute of Control Sciences of the Russian Academy of Sciences, Leading researcher, 65 Profsoyuznaya Street, Moscow, 117997, Russia; e-mail: upi@ipu.ru*
Major Fields of Scientific Research: Graph theory, Matrix analysis, Decision making, Social dynamics

CONES OF WEIGHTED QUASIMETRICS, WEIGHTED QUASIHYPERMETRICS AND OF ORIENTED CUTS

Michel Deza, Vyacheslav P. Grishukhin, Elena Deza

Abstract: *We show that the cone of weighted n-point quasi-metrics $WQMet_n$, the cone of weighted quasi-hypermetrics $WHyp_n$ and the cone of oriented cuts $OCut_n$ are projections along an extreme ray of the metric cone Met_{n+1}, of the hypermetric cone Hyp_{n+1} and of the cut cone Cut_{n+1}, respectively. This projection is such that if one knows all faces of an original cone then one knows all faces of the projected cone.*

Keywords: *distance, metrics, hypermetrics, cut metrics, quasi-metrics.*

MSC*: 52B12, 51F99, 90C57*

1 Introduction

Oriented (or directed) distances are encountered very often, for example, these are one-way transport routes, a river with quick flow and so on.

The notions of directed distances, quasi-metrics and oriented cuts are generalizations of the notions of distances, metrics and cuts, which are central objects in graph theory and combinatorial optimization.

Quasi-metrics are used in semantics of computations (see, for example, [Se97]) and in computational geometry (see, for example, [AACMP97]). Oriented distances have been used already by Hausdorff in 1914, see [Ha14].

In [CMM06], an example of directed metric derived from a metric is given. Let d be a metric on a set $V \cup \{0\}$, where 0 is a distinguished point. Then a quasi-metric q on the set V is given as

$$q_{ij} = d_{ij} + d_{i0} - d_{j0}.$$

This quasi-metric belongs to a special important subclass of quasi-metrics, namely, to a class of *weighted quasi-metrics*. We show in this paper that *any* weighted quasi-metric is obtained from a metric by this method.

All semi-metrics on a set of cardinality n form a metric cone Met_n. There are two important sub-cones of Met_n, namely, the cone Hyp_n of hypermetrics, and the cone Cut_n of ℓ_1-metrics. These three cones form the following nested family $Cut_n \subseteq Hyp_n \subseteq Met_n$, see [DL97].

In this paper we introduce a special space Q_n, called a space of weighted quasi-metrics. We define in this space a cone $WQMet_n$. Elements of this cone satisfy triangle and non-negativity inequalities. Among extreme rays of the cone $WQMet_n$ there are rays spanned by ocut vectors, i.e. incidence vectors of oriented cuts.

We define in the space Q_n a cone $OCut_n$ of oriented cuts as the cone hull of ocut vectors. Elements of the cone $OCut_n$ are weighted quasi-ℓ-metrics.

Let metrics of the cone Met_{n+1} are defined on the set $V \cup \{0\}$. The cut-cone Cut_{n+1} of ℓ_1-metrics on this set is a cone hull of cut-metrics $\delta(S)$ for all $S \subset V \cup \{0\}$. The cut-metrics $\delta(S)$ are extreme rays of all the three cones Met_{n+1}, Hyp_{n+1} and Cut_{n+1}. In particular, $\delta(\{0\}) = \delta(V)$ is an extreme ray of these three cones.

In this paper, it is shown that the cones $WQMet_n$ and $OCut_n$ are projections of the corresponding cones Met_{n+1} and Cut_{n+1} along the extreme ray $\delta(V)$. We define a cone $WQHyp_n$ of weighted quasi-hypermetrics as projection along $\delta(V)$ of the cone Hyp_{n+1}. So, we obtain a nested family $OCut_n \subseteq WQHyp_n \subseteq WQMet_n$.

Weighted quasi-metrics and other generalizations of metrics are studied, for example, in [DD10] and [DDV11]. The cone and the polytope of oriented cuts are considered in [AM11].

2 Spaces $\mathbb{R}^E$ and $\mathbb{R}^{E^{\mathcal{O}}}$

Let V be a set of cardinality $|V| = n$. Let E and $E^{\mathcal{O}}$ be sets of all unordered (ij) and ordered ij pairs of elements $i, j \in V$. Consider two Euclidean spaces $\mathbb{R}^E$ and $\mathbb{R}^{E^{\mathcal{O}}}$ of vectors $d \in \mathbb{R}^E$ and $g \in \mathbb{R}^{E^{\mathcal{O}}}$ with coordinates $d_{(ij)}$ and g_{ij}, where $(ij) \in E$ and $ij \in E^{\mathcal{O}}$, respectively. Obviously, dimensions of the spaces $\mathbb{R}^E$ and $\mathbb{R}^{E^{\mathcal{O}}}_s$ are $|E| = \frac{n(n-1)}{2}$ and $|E^{\mathcal{O}}| = n(n-1)$, respectively.

Denote by $(d, t) = \sum_{(ij)\in E} d_{(ij)} t_{(ij)}$ scalar product of vectors $d, t \in \mathbb{R}^E$. Similarly $(f, g) = \sum_{ij\in E^{\mathcal{O}}} f_{ij} g_{ij}$ denote scalar product of vectors $f, g \in \mathbb{R}^{E^{\mathcal{O}}}$.

Let $\{e_{(ij)} : (ij) \in E\}$ and $\{e_{ij} : ij \in E^{\mathcal{O}}\}$ be orthonormal bases of $\mathbb{R}^E$ and $\mathbb{R}^{E^{\mathcal{O}}}$, respectively. Then, for $f \in \mathbb{R}^E$ and $q \in \mathbb{R}^{E^{\mathcal{O}}}$, we have

$$(e_{(ij)}, f) = f_{(ij)} \text{ and } (e_{ij}, q) = q_{ij}.$$

For $f \in \mathbb{R}^{E^{\mathcal{O}}}$, define $f^* \in \mathbb{R}^{E^{\mathcal{O}}}$ as follows

$$f^*_{ij} = f_{ji} \text{ for all } ij \in E^{\mathcal{O}}.$$

Call a vector g *symmetric* if $g^* = g$, and *antisymmetric* if $g^* = -g$. Each vector $g \in \mathbb{R}^{E^{\mathcal{O}}}$ can be decompose into *symmetric* g^s and *antisymmetric* g^a parts as follows:

$$g^s = \frac{1}{2}(g + g^*),\ g^a = \frac{1}{2}(g - g^*),\ g = g^s + g^a.$$

Let $\mathbb{R}^{E^{\mathcal{O}}}_s$ and $\mathbb{R}^{E^{\mathcal{O}}}_a$ be subspaces of symmetric and antisymmetric vectors, respectively. Note that the spaces $\mathbb{R}^{E^{\mathcal{O}}}_s$ and $\mathbb{R}^{E^{\mathcal{O}}}_a$ are mutually orthogonal. In fact, for $p \in \mathbb{R}^{E^{\mathcal{O}}}_s$ and $f \in \mathbb{R}^{E^{\mathcal{O}}}_a$, we have

$$(p, f) = \sum_{ij\in E^{\mathcal{O}}} p_{ij} f_{ij} = \sum_{(ij)\in E} (p_{ij} f_{ij} + p_{ji} f_{ji}) = \sum_{(ij)\in E} (p_{ij} f_{ij} - p_{ij} f_{ij}) = 0.$$

Hence

$$\mathbb{R}^{E^{\mathcal{O}}} = \mathbb{R}^{E^{\mathcal{O}}}_s \oplus \mathbb{R}^{E^{\mathcal{O}}}_a,$$

where $\oplus$ is direct sum.

Obviously, there is an isomorphism φ between the spaces $\mathbb{R}^E$ and $\mathbb{R}^{E^{\mathcal{O}}}_s$. Let $d \in \mathbb{R}^E$ have coordinates $d_{(ij)}$. Then we set

$$d^{\mathcal{O}} = \varphi(d) \in \mathbb{R}^{E^{\mathcal{O}}}_s \text{ such that } d^{\mathcal{O}}_{ij} = d^{\mathcal{O}}_{ji} = d_{(ij)}.$$

In particular,

$$\varphi(e_{(ij)}) = e_{ij} + e_{ji}.$$

The map φ is invertible. In fact, for $q \in \mathbb{R}^{E^{\mathcal{O}}}_s$, we have $\varphi^{-1}(q) = d \in \mathbb{R}^E$ such that $d_{(ij)} = q_{ij} = q_{ji}$. The isomorphism φ will be useful in what follows.

3 Space of weights Q^w_n

One can consider the sets E and $E^{\mathcal{O}}$ as sets of edges (ij) and arcs ij of an unordered and ordered complete graphs K_n and $K^{\mathcal{O}}_n$ on the vertex set V, respectively. The graph $K^{\mathcal{O}}_n$ has two arcs ij and ji between each pair of vertices $i, j \in V$.

It is convenient to consider vectors $g \in \mathbb{R}^{E^{\mathcal{O}}}$ as functions on the set of arcs $E^{\mathcal{O}}$ of the graph $K^{\mathcal{O}}_n$. So, the decomposition $\mathbb{R}^{E^{\mathcal{O}}} = \mathbb{R}^{E^{\mathcal{O}}}_s \oplus \mathbb{R}^{E^{\mathcal{O}}}_a$ is a decomposition of the space of all functions on arcs in $E^{\mathcal{O}}$ onto the spaces of symmetric and antisymmetric functions.

Besides, there is an important direct decomposition of the space $\mathbb{R}_a^{E^{\mathcal{O}}}$ of antisymmetric functions onto two subspaces. In theory of electric networks these spaces are called spaces of *tensions* and *flows* (see also [Aig79]).

The tension space relates to *potentials* (or *weights*) w_i given on vertices $i \in V$ of the graph $K_n^{\mathcal{O}}$. The corresponding antisymmetric function g^w is determined as

$$g_{ij}^w = w_i - w_j.$$

It is called *tension* on the arc ij. Obviously, $g_{ji}^w = w_j - w_i = -g_{ij}^w$. Denote by Q_n^w the subspace of $\mathbb{R}^{E^{\mathcal{O}}}$ generated by all tensions on arcs $ij \in E^{\mathcal{O}}$. We call Q_n^w by a *space of weights*.

Each tension function g^w is represented as weighted sum of *elementary potential* functions $p(k)$ for $k \in V$ as follows

$$g^w = \sum_{k \in V} w_k p(k),$$

where

$$p(k) = \sum_{j \in V - \{k\}} (e_{kj} - e_{jk}), \text{ for all } k \in V, \tag{1}$$

are basic functions that generate the space of weights Q_n^w. Hence values of the basic functions $p(k)$ on arcs are as follows

$$p_{ij}(k) = \begin{cases} 1 & \text{if } i = k \\ -1 & \text{if } j = k \\ 0 & \text{otherwise.} \end{cases} \tag{2}$$

We obtain

$$g_{ij}^w = \sum_{k \in V} w_k p_{ij}(k) = w_i - w_j.$$

It is easy to verify that

$$p^2(k) = (p(k), p(k)) = 2(n-1),\ (p(k), p(l)) = -2 \text{ for all } k, l \in V, k \neq l,\ \sum_{k \in V} p(k) = 0.$$

Hence there are only $n-1$ independent functions $q(k)$ that generate the space Q_n^w.

Weighted quasimetrics lie in the space $\mathbb{R}_s^{E^{\mathcal{O}}} \oplus Q_n^w$ that we denote as Q_n. Direct complements of Q_n^w in $\mathbb{R}_a^{E^{\mathcal{O}}}$ and Q_n in $\mathbb{R}^{E^{\mathcal{O}}}$ is a space Q_n^c of *circuits* (or *flows*).

4 Space of circuits Q_n^c

The space of circuits (or space of flows) is generated by characteristic vectors of oriented circuits in the graph $K_n^{\mathcal{O}}$. Arcs of $K_n^{\mathcal{O}}$ are ordered pairs ij of vertices $i, j \in V$. The arc ij is oriented from the vertex i to the vertex j. Recall that $K_n^{\mathcal{O}}$ has both the arcs ij and ji for each pair of vertices $i, j \in V$.

Let $G_s \subseteq K_n$ be an undirected subgraph with a set of edges $E(G_s) \subseteq E$. We relate to the undirected graph G_s a directed graph $G \subseteq K_n^{\mathcal{O}}$ with the arc set $E^{\mathcal{O}}(G) \subseteq E^{\mathcal{O}}$ as follows. An arc ij belongs to G, i.e. $ij \in E^{\mathcal{O}}(G)$, if and only if $(ij) = (ji) \in E(G)$. This definition implies that the arc ji belongs to G also, i.e. $ji \in E^{\mathcal{O}}(G)$.

Let C_s be a circuit in the graph K_n. The circuit C_s is determined by a sequence of distinct vertices $i_k \in V$, where $1 \leq k \leq p$ and p is the length of C_s. Edges of C_s are unordered pairs (i_k, i_{k+1}), where indices are taken modulo p. By above definition, an *oriented bicircuit* C of the graph $K_n^{\mathcal{O}}$ relates to to the circuit C_s. Arcs of C are ordered pairs $i_k i_{k+1}$ and $i_{k+1} i_k$, where indices are taken modulo p. Take an orientation of C. Denote by $-C$ the *opposite* circuit with opposite orientation. Denote an arc of C *direct* or *opposite* if its direction coincides with or is opposite to the given orientation of C, respectively. Let C^+ and C^- be subcircuits of C consisting of direct and opposite arcs, respectively.

The following vector f^C is the characteristic vector of the bicircuit C:

$$f^C_{ij} = \begin{cases} 1 & \text{if } ij \in C^+, \\ -1 & \text{if } ij \in C^-, \\ 0 & \text{otherwise.} \end{cases}$$

Note that $f^{-C} = (f^C)^* = -f^C$, and $f^C \in \mathbb{R}_a^{E^{\mathcal{O}}}$.

Denote by Q_n^c the space linearly generated by circuit vectors f^C for all bicircuits C of the graph $K_n^{\mathcal{O}}$. It is well known that characteristic vectors of *fundamental* circuits form a basis of Q_n^c. Fundamental circuits are defined as follows.

Let T be a spanning tree of the graph K_n. Since T is spanning, its vertex set $V(T)$ is the set of all vertices of K_n, i.e. $V(T) = V$. Let $E(T) \subset E$ be the set of edges of T. Then any edge $e = (ij) \notin E(T)$ closes a unique path in T between vertices i and j into a circuit C_s^e. This circuit C_s^e is called *fundamental*. Call corresponding oriented bicircuit C^e also *fundamental*.

There are $|E - E(T)| = \frac{n(n-1)}{2} - (n-1)$ fundamental circuits. Hence

$$\dim Q_n^c = \frac{n(n-1)}{2} - (n-1), \text{ and } \dim Q_n + \dim Q_n^c = n(n-1) = \dim \mathbb{R}^{E^{\mathcal{O}}}.$$

This implies that Q_n^c is an orthogonal complement of Q_n^w in $\mathbb{R}_a^{\mathcal{O}}$ and Q_n in $\mathbb{R}^{E^{\mathcal{O}}}$, i.e.

$$\mathbb{R}_a^{E^{\mathcal{O}}} = Q_n^w \oplus Q_n^c \text{ and } \mathbb{R}^{E^{\mathcal{O}}} = Q_n \oplus Q_n^c = \mathbb{R}^{E_s^{\mathcal{O}}} \oplus Q_n^w \oplus Q_n^c.$$

5 Cut and ocut vector set-functions

The space Q_n is generated also by vectors of oriented cuts, which we define in this section.

Each subset $S \subseteq V$ determines cuts of the graphs K_n and $K_n^{\mathcal{O}}$ that are subsets of edges and arcs of these graphs.

A $cut(S) \subset E$ is a subset of edges (ij) of K_n such that $(ij) \in cut(S)$ if and only if $|\{i,j\} \cap S| = 1$.

A $cut^{\mathcal{O}}(S) \subset E^{\mathcal{O}}$ is a subset of arcs ij of $K_n^{\mathcal{O}}$ such that $ij \in cut^{\mathcal{O}}(S)$ if and only if $|\{i,j\} \cap S| = 1$. So, if $ij \in cut^{\mathcal{O}}(S)$, then $ji \in cut^{\mathcal{O}}(S)$ also.

An *oriented cut* is a subset $ocut(S) \subset E^{\mathcal{O}}$ of arcs ij of $K_n^{\mathcal{O}}$ such that $ij \in ocut(S)$ if and only if $i \in S$ and $j \notin S$.

We relate to these three types of cuts characteristic vectors $\delta(S) \in \mathbb{R}^E$, $\delta^{\mathcal{O}}(S) \in \mathbb{R}_s^{E^{\mathcal{O}}}$, $p(S) \in \mathbb{R}_a^{E^{\mathcal{O}}}$ and $c(S) \in \mathbb{R}^{E^{\mathcal{O}}}$ as follows.

For $cut(S)$, we set

$$\delta(S) = \sum_{i \in S, j \in \overline{S}} e_{(ij)}, \text{ such that } \delta_{(ij)}(S) = \begin{cases} 1 & \text{if } |\{i,j\} \cap S| = 1 \\ 0 & \text{otherwise,} \end{cases}$$

where $\overline{S} = V - S$. For $cut^{\mathcal{O}}(S)$, we set

$$\delta^{\mathcal{O}}(S) = \varphi(\delta(S)) = \sum_{i \in S, j \in \overline{S}} (e_{ij} + e_{ji}) \text{ and } p(S) = \sum_{i \in S, j \in \overline{S}} (e_{ij} - e_{ji}).$$

Hence

$$\delta^{\mathcal{O}}_{ij}(S) = \begin{cases} 1 & \text{if } |\{i,j\} \cap S| = 1 \\ 0 & \text{otherwise.} \end{cases} \quad \text{and } p_{ij}(S) = \begin{cases} 1 & \text{if } i \in S, j \notin S \\ -1 & \text{if } j \in S, i \notin S \\ 0 & \text{otherwise.} \end{cases}$$

Note that, for one-element sets $S = \{k\}$, the function $p(\{k\})$ is $p(k)$ of section 2. It is easy to see that

$$(\delta^{\mathcal{O}}(S), p(T)) = 0 \text{ for any } S, T \subseteq V.$$

For the oriented cut $ocut(S)$, we set

$$c(S) = \sum_{i \in S, j \in \overline{S}} e_{ij}.$$

Hence

$$c_{ij}(S) = \begin{cases} 1 & \text{if } i \in S, j \notin S \\ 0 & \text{otherwise.} \end{cases}$$

Obviously, it holds $c(\emptyset) = c(V) = \mathbf{0}$, where $\mathbf{0} \in \mathbb{R}^{E^{\mathcal{O}}}$ is a vector whose all coordinates are equal zero. We have the following equalities

$$c^*(S) = c(\overline{S}),\ c(S) + c(\overline{S}) = \delta^{\mathcal{O}}(S),\ c(S) - c(\overline{S}) = p(S) \text{ and } c(S) = \frac{1}{2}(\delta^{\mathcal{O}}(S) + p(S)). \quad (3)$$

Besides, we have

$$c^s(S) = \frac{1}{2}\delta^{\mathcal{O}}(S),\ c^a(S) = \frac{1}{2}p(S).$$

Recall that a set-function $f(S)$ on all $S \subseteq V$, is called *submodular* if, for any $S, T \subseteq V$, the following *submodular inequality* holds

$$f(S) + f(T) - (f(S \cap T) + f(S \cup T)) \geq 0.$$

It is well known that the vector set-function $\delta \in \mathbb{R}^E$ is submodular (see, for example, [Aig79]). The above isomorphism φ of the spaces $\mathbb{R}^E$ and $\mathbb{R}_s^{E^{\mathcal{O}}}$ implies that the vector set-function $\delta^{\mathcal{O}} = \varphi(\delta) \in \mathbb{R}_s^{E^{\mathcal{O}}}$ is submodular also.

A set-function $f(S)$ is called *modular* if, for any $S, T \subseteq V$, the above submodular inequality holds as equality. This equality is called *modular equality*. It is well known (and can be easily verified) that antisymmetric vector set-function $f^a(S)$ is modular for any oriented graph G. Hence our antisymmetric vector set-function $q(S) \in \mathbb{R}_a^{E^{\mathcal{O}}}$ for the oriented complete graph $K_n^{\mathcal{O}}$ is modular also.

Note that the set of all submodular set functons on a set V forms a cone in the space $\mathbb{R}^{2^V}$. Therefore the last equality in (3) implies that the vector set-function $c(S) \in \mathbb{R}^{E^{\mathcal{O}}}$ is submodular.

The modularity of the antisymmetric vector set-function $q(S)$ is important for what follows. It is well-known (see, for example, [Bir67]) (and it can be easily verified using modular equality) that any modular set-function $m(S)$ is completely determined by its values on the empty set and on all one-element sets. Hence a modular set-function $m(S)$ has the following form

$$m(S) = m_0 + \sum_{i \in S} m_i,$$

where $m_0 = m(\emptyset)$ and $m_i = m(\{i\}) - m(\emptyset)$. For brevity, we set $f(\{i\}) = f(i)$ for any set function $f(S)$. Since $p(\emptyset) = p(V) = 0$, we have

$$p(S) = \sum_{k \in S} p(k),\ S \subseteq V, \text{ and } p(V) = \sum_{k \in V} p(k) = 0. \quad (4)$$

Using equations (3) and (4), we obtain

$$c(S) = \frac{1}{2}(\delta^{\mathcal{O}}(S) + \sum_{k \in S} p(k)). \quad (5)$$

Now we show that ocut vectors $c(S)$ for all $S \subseteq V$ linearly generate the space $Q_n \subseteq \mathbb{R}^{E^{\mathcal{O}}}$. The space generated by $c(S)$ consists of the following vectors

$$c = \sum_{S \subseteq V} \alpha_S c(S), \text{ where } \alpha_S \in \mathbb{R}.$$

Recall that $c(S) = \frac{1}{2}(\delta^{\mathcal{O}}(S) + p(S))$. Hence we have

$$c = \frac{1}{2}\sum_{S\subset V}\alpha_S(\delta^{\mathcal{O}}(S) + p(S)) = \frac{1}{2}\sum_{S\subset V}\alpha_S\delta^{\mathcal{O}}(S) + \frac{1}{2}\sum_{S\subset V}\alpha_S p(S) = \frac{1}{2}(d^{\mathcal{O}} + p),$$

where $d^{\mathcal{O}} = \varphi(d)$ for $d = \sum_{S\subseteq V}\alpha_S\delta(S)$. For a vector p we have

$$p = \sum_{S\subset V}\alpha_S p(S) = \sum_{S\subset V}\alpha_S\sum_{k\in S}p(k) = \sum_{k\in V}w_k p(k), \text{ where } w_k = \sum_{V\supset S\ni k}\alpha_S.$$

Since $p_{ij} = \sum_{k\in V}w_k p_{ij}(k) = w_i - w_j$, we have

$$c_{ij} = \frac{1}{2}(d^{\mathcal{O}}_{ij} + w_i - w_j). \tag{6}$$

It is well-known (see, for example, [DL97]) that the vectors $\delta(S) \in \mathbb{R}^E$ for all $S \subseteq V$ linearly generate the full space $\mathbb{R}^E$. Hence the vectors $\delta^{\mathcal{O}}(S) \in \mathbb{R}^{E^{\mathcal{O}}}_s$ for all $S \subseteq V$ linearly generate the full space $\mathbb{R}^{E^{\mathcal{O}}}_s$.

According to (5), antisymmetric parts of vectors $c(S)$ generate the space Q^w_n. This implies that the space $Q_n = \mathbb{R}^{E^{\mathcal{O}}}_s \oplus Q^w_n$ is generated by $c(S)$ for all $S \subset V$.

6 Properties of the space Q_n

Let $x \in Q_n$ and let f^C be the characteristic vector of a bicircuit C. Since f^C is orthogonal to Q_n, we have $(x, f^C) = \sum_{ij\in C}f^C_{ij}x_{ij} = 0$. This equality implies that each point $x \in Q_n$ satisfies the following equalities

$$\sum_{ij\in C^+}x_{ij} = \sum_{ij\in C^-}x_{ij}$$

for any bicircuits C.

Let $K_{1,n-1} \subset K_n$ be a spanning star of K_n consisting of all $n-1$ edges incident to a vertex of K_n. Let this vertex be 1. Each edge of $K_n - K_{1,n-1}$ has the form (ij), where $i \neq 1 \neq j$. The edge (ij) closes a fundamental triangle with edges $(1i), (1j), (ij)$. The corresponding bitriangle $T(1ij)$ generates the equality

$$x_{1i} + x_{ij} + x_{j1} = x_{i1} + x_{1j} + x_{ji}.$$

These inequalities were derived by another way in [AM11]. They correspond to fundamental bi-triangles $T(1ij)$, for all $i, j \in V - \{1\}$, and are all $\frac{n(n-1)}{2} - (n-1)$ independent equalities determining the space, where the Q_n lies.

Above coordinates x_{ij} of a vector $x \in Q_n$ are given in the orthonormal basis $\{e_{ij} : ij \in E^{\mathcal{O}}\}$. But, for what follows, it is more convenient to consider vectors $q \in Q_n$ in another basis. Recall that $\mathbb{R}^{E^{\mathcal{O}}}_s = \varphi(\mathbb{R}^E)$. Let, for $(ij) \in E$, $\varphi(e_{(ij)}) = e_{ij} + e_{ji} \in \mathbb{R}^{E^{\mathcal{O}}}_s$ be basic vectors of the subspace $\mathbb{R}^{E^{\mathcal{O}}}_s \subset Q_n$. Let $p(i) \in Q^w_n, i \in V$, be basic vectors (defined in (1)) of the space $Q^w_n \subset Q_n$. Then, for $q \in Q_n$, we set

$$q = q^s + q^a, \text{ where } q^s = \sum_{(ij)\in E}q_{(ij)}\varphi(e_{(ij)}),\ q^a = \sum_{i\in V}w_i p(i).$$

Now, we obtain an important expression for the scalar product (g, q) of vectors $g, q \in Q_n$. Recall that $(\varphi(e_{(ij)}), p(k)) = ((e_{ij} + e_{ji}), p(k)) = 0$ for all $(ij) \in E$ and all $k \in V$. Hence $(g^s, q^a) = (g^a, q^s) = 0$, and we have

$$(g, q) = (g^s, q^s) + (g^a, q^a).$$

Besides, we have

$$((e_{ij} + e_{ji}), (e_{kl} + e_{lk})) = 0 \text{ if } (ij) \neq (kl),\ (e_{ij} + e_{ji})^2 = 2,$$

and (see Section 3)

$$(p(i),p(j)) = -2 \text{ if } i \neq j,\ (p(i))^2 = 2(n-1).$$

Let $v_i, w_i, i \in V$, be weights of the vector g, q, respectively. Then we have

$$(g,q) = 2\sum_{(ij)\in E} g_{(ij)}q_{(ij)} + 2(n-1)\sum_{i\in V} v_iw_i - 2\sum_{i\neq j\in V} v_iw_j.$$

For the last sum, we have

$$\sum_{i\neq j\in V} v_iw_j = (\sum_{i\in V} v_i)(\sum_{i\in V} w_i) - \sum_{i\in V} v_iw_i.$$

Since weights are defined up to an additive scalar, we can choose weights v_i such that $\sum_{i\in V} v_i = 0$. Then the last sum in the product (g,q) is equal to $-\sum_{i\in V} v_iw_i$. Finally we obtain that the sum of antisymmetric parts is equal to $2n\sum_{i\in V} v_iw_i$. So, for the product of two vectors $g, q \in Q_n$ we have the following expression

$$(g,q) = (g^s,q^s) + (g^a,q^a) = 2(\sum_{(ij)\in E} g_{(ij)}q_{(ij)} + n\sum_{i\in V} v_iw_i) \text{ if } \sum_{i\in V} v_i = 0 \text{ or } \sum_{i\in V} w_i = 0.$$

In what follows, we consider inequalities $(g,q) \geq 0$. We can delete the multiple 2, and rewrite such inequality as follows

$$\sum_{(ij)\in E} g_{(ij)}q_{(ij)} + n\sum_{i\in V} v_iw_i \geq 0, \tag{7}$$

where $\sum_{i\in V} v_i = 0$.

Below we consider some cones in the space Q_n. Since the space Q_n is orthogonal to the space of circuits Q_n^c, each facet vector of a cone in Q_n is defined up to a vector of the space Q_n^c. Of course each vector $g' \in \mathbb{R}^{E^{\mathcal{O}}}$ can be decomposed as $g' = g + g^c$, where $g \in Q_n$ and $g^c \in Q_n^c$. Call the vector $g \in Q_n$ *canonical representative* of the vector g'. Usually we will use canonical facet vectors. But sometimes not canonical representatives of a facet vector are useful.

Cones C that will be considered are invariant under the operation $q \to q^*$, defined in Section 2. In other words, $C^* = C$. This operation changes signs of weights:

$$q_{ij} = q_{(ij)} + w_i - w_j \to q_{(ij)} + w_j - w_i = q_{(ij)} - w_i + w_j.$$

Let $(g,q) \geq 0$ be an inequality determining a facet F of a cone $C \subset Q_n$. Since $C = C^*$, the cone C has with the facet F also a facet F^*. The facet F^* is determined by the inequality $(g^*,q) \geq 0$.

7 Projections of cones Con_{n+1}

Recall that $Q_n = \mathbb{R}_s^{E^{\mathcal{O}}} \oplus Q_n^w$, $\mathbb{R}_s^{E^{\mathcal{O}}} = \varphi(\mathbb{R}^E)$ and $\dim Q_n = \frac{n(n+1)}{2} - 1$.

Let $0 \notin V$ be an additional point. Then the set of unordered pairs (ij) for $i,j \in V \cup \{0\}$ is $E \cup E_0$, where $E_0 = \{(0i) : i \in V\}$. Obviously, $\mathbb{R}^{E\cup E_0} = \mathbb{R}^E \oplus \mathbb{R}^{E_0}$ and $\dim \mathbb{R}^{E\cup E_0} = \frac{n(n+1)}{2}$.

The space $\mathbb{R}^{E\cup E_0}$ contains the following three important cones: the cone Met_{n+1} of semi-metrics, the cone Hyp_{n+1} of hyper-semi-metrics and the cone Cut_{n+1} of ℓ_1-semi-metrics, all on the set $V \cup \{0\}$. Denote by Con_{n+1} any of these cones.

Recall that a semi-metric $d = \{d_{(ij)}\}$ is called *metric* if $d_{(ij)} \neq 0$ for all $(ij) \in E$. For brevity sake, in what follows, we call elements of the cones Con_{n+1} by metrics (or hypermetrics, ℓ_1-metrics), assuming that they can be semi-metrics.

Note that if $d \in Con_{n+1}$ is a metric on the set $V \cup \{0\}$, then a restriction d^V of d on the set V is a point of the cone $Con_n = Con_{n+1} \cap \mathbb{R}^E$ of metrics on the set V. In other words, we can suppose that $Con_n \subset Con_{n+1}$.

The cones Met_{n+1}, Hyp_{n+1} and Cut_{n+1} contain the cut vectors $\delta(S)$ that span extreme rays for all $S \subset V \cup \{0\}$. Denote by l_0 the extreme ray spanned by the cut vector $\delta(V) = \delta(\{0\})$. Consider a projection $\pi(\mathbb{R}^{E \cup E_0})$ of the space $\mathbb{R}^{E \cup E_0}$ along the ray l_0 onto a subspace of $\mathbb{R}^{E \cup E_0}$ that is orthogonal to $\delta(V)$. This projection is such that $\pi(\mathbb{R}^E) = \mathbb{R}^E$ and $\pi(\mathbb{R}^{E \cup E_0}) = \mathbb{R}^E \oplus \pi(\mathbb{R}^{E_0})$.

Note that $\delta(V) \in \mathbb{R}^{E_0}$, since, by Section 5, $\delta(V) = \sum_{i \in V} e_{(0i)}$. For simplicity sake, define the following vector

$$e_0 = \delta(\{0\}) = \delta(V) = \sum_{i \in V} e_{(0i)}.$$

Recall that the vector e_0 spans the extreme ray l_0. Obviously, the space $\mathbb{R}^E$ is orthogonal to l_0, and therefore $\pi(\mathbb{R}^E) = \mathbb{R}^E$.

Let $x \in \mathbb{R}^{E \cup E_0}$. We decompose this point as follows

$$x = x^V + x^0,$$

where $x^V = \sum_{(ij) \in E} x_{(ij)} e_{(ij)} \in \mathbb{R}^E$ and $x^0 = \sum_{i \in V} x_{(0i)} e_{(0i)} \in \mathbb{R}^{E_0}$. The projection π works on basic vectors as follows:

$$\pi(e_{(ij)}) = e_{(ij)} \text{ for } (ij) \in E, \text{ and } \pi(e_{(0i)}) = e_{(0i)} - \frac{1}{n} e_0 \text{ for } i \in V.$$

So, we have

$$\pi(x) = \pi(x^V) + \pi(x^0) = \sum_{(ij) \in E} x_{(ij)} e_{(ij)} + \sum_{i \in V} x_{(0i)} (e_{(0i)} - \frac{1}{n} e_0). \tag{8}$$

It is useful to note that the projection π transforms the positive orthant of the space $\mathbb{R}^{E_0}$ onto the whole space $\pi(\mathbb{R}^{E_0})$.

Now we describe how faces of a cone in the space $\mathbb{R}^{E \cup E_0}$ are projected along one of its extreme rays.

Let l be an extreme ray and F be a face of a cone in $\mathbb{R}^{E \cup E_0}$. Let π be the projection along l. Let $\dim F$ be dimension of the face F. Then the following equality holds

$$\dim \pi(F) = \dim F - \dim(F \cap l). \tag{9}$$

Let $g \in \mathbb{R}^{E \cup E_0}$ be a facet vector of a facet G, and e be a vector spanning the line l. Then $\dim(G \cap l) = 1$ if $(g, e) = 0$, and $\dim(G \cap l) = 0$ if $(g, e) \neq 0$.

Theorem 1. *Let G be a face of the cone $\pi(Con_{n+1})$. Then $G = \pi(F)$, where F is a face of Con_{n+1} such that there is a facet of Con_{n+1}, containing both F and the extreme ray l_0 spanned by $e_0 = \delta(V)$.*

In particular, G is a facet of $\pi(Con_{n+1})$ if and only if $G = \pi(F)$, where F is a facet of Con_{n+1} containing the extreme ray l_0. Similarly, l' is an extreme ray of $\pi(Con_{n+1})$ if and only if $l' = \pi(l)$, where l is an extreme ray of Con_{n+1} lying in a facet of Con_{n+1} that contains l_0.

Proof. Let $\mathcal{F}$ be a set of all facets of the cone Con_{n+1}. Then $\cup_{F \in \mathcal{F}} \pi(F)$ is a covering of the projection $\pi(Con_{n+1})$. By (9), in this covering, if $l_0 \subseteq F \in \mathcal{F}$, then $\pi(F)$ is a facet of $\pi(Con_{n+1})$. If $l_0 \not\subset F$, then there is a one-to-one correspondence between points of F and $\pi(F)$. Hence $\dim \pi(F) = n$, and $\pi(F)$ cannot be a facet of $\pi(Con_{n+1})$, since $\pi(F)$ fills an n-dimensional part of the cone $\pi(Con_{n+1})$.

If F' is a face of Con_{n+1}, then $\pi(F')$ is a face of the above covering. If F' belongs only to facets $F \in \mathcal{F}$ such that $l_0 \not\subset F$, then $\pi(F')$ lies inside of $\pi(Con_{n+1})$. In this case, it is not a face of $\pi(Con_{n+1})$. This implies that $\pi(F')$ is a face of $\pi(Con_{n+1})$ if and only if $F' \subseteq F$, where F is a facet of Con_{n+1} such that $l_0 \subset F$. Suppose that dimension of F' is $n-1$, and $l_0 \not\subset F'$. Then $\dim \pi(F') = n-1$. If F' is contained in a facet F of Con_{n+1} such that $l_0 \subset F$, then $\pi(F') = \pi(F)$. Hence $\pi(F')$ is a facet of the cone $\pi(Con_{n+1})$ that coincides with the facet $\pi(F)$.

Now, the assertions of Theorem about facets and extreme rays of $\pi(Con_{n+1})$ follow. □

Theorem 1 describes all faces of the cone $\pi(Con_{n+1})$ if one knows all faces of the cone Con_{n+1}.

Recall that we consider $Con_n = Con_{n+1} \cap \mathbb{R}^E$ as a sub-cone of Con_{n+1}, and therefore $\pi(Con_n) \subset \pi(Con_{n+1})$. Since $\pi(\mathbb{R}^E) = \mathbb{R}^E$, we have $\pi(Con_n) = Con_n$. Let $(f, x) \geq$ be a facet-defining inequality of a facet F of the cone Con_{n+1}. Since $Con_{n+1} \subset \mathbb{R}^E \oplus \mathbb{R}^{E_0}$, we represent vectors $f, x \in \mathbb{R}^{E \cup E_0}$ as $f = f^V + f^0, x = x^V + x^0$, where $f^V, x^V \in \mathbb{R}^E$ and $f^0, x^0 \in \mathbb{R}^{E_0}$. Hence the above facet-defining inequality can be rewritten as

$$(f, x) = (f^V, x^V) + (f^0, x^0) \geq 0.$$

It turns out that the cone Con_{n+1} has always a facet F whose facet vector $f = f^V + f^0$ is such that $f^0 = 0$. Since f^V is orthogonal to $\mathbb{R}^{E_0}$, the hyperplane $(f^V, x) = (f^V, x^V) = 0$ supporting the facet F contains the whole space $\mathbb{R}^{E_0}$. The equality $(f^V, x^V) = 0$ defines a facet $F^V = F \cap \mathbb{R}^E$ of the cone Con_n.

Definition. A facet F of the cone Con_{n+1} with a facet vector $f = f^V + f^0$ is called *zero-lifting* of a facet F^V of Con_n if $f^0 = 0$ and $F \cap \mathbb{R}^E = F^V$.

Similarly, a facet $\pi(F)$ of the cone $\pi(Con_{n+1})$ with a facet vector f is called zero-lifting of F^V if $f = f^V$ and $\pi(F) \cap \mathbb{R}^E = F^V$.

It is well-known, see, for example, [DL97], that each facet F^V with facet vector f^V of the cone Con_n can be zero-lifted up to a facet F of Con_{n+1} with the same facet vector f^V.

Proposition 1. *Let a facet F of Con_{n+1} be zero-lifting of a facet F^V of Con_n. Then $\pi(F)$ is a facet of $\pi(Con_{n+1})$ that is also zero-lifting of F^V.*

Proof. Recall that the hyperplane $\{x \in \mathbb{R}^{E \cup E_0} : (f^V, x) = 0\}$ supporting the facet F contains the whole space $\mathbb{R}^{E_0}$. Hence the facet F contains the extreme ray l_0 spanned by the vector $e_0 \in \mathbb{R}^{E_0}$. By Theorem 1, $\pi(F)$ is a facet of $\pi(Con_{n+1})$. The facet vector of $\pi(F)$ can be written as $f = f^V + f'$, where $f^V \in \mathbb{R}^E$ and $f' \in \pi(\mathbb{R}^{E_0})$. Since the hyperplane supporting the facet $\pi(F)$ is given by the equality $(f^V, x) = 0$ for $x \in \pi(\mathbb{R}^{E \cup E_0})$, we have $f' = 0$. Besides, obviously, $\pi(F) \cap \mathbb{R}^E = F^V$. Hence $\pi(F)$ is zero-lifting of F^V. □

8 Cones $\psi(Con_{n+1})$

Note that basic vectors of the space $\mathbb{R}^{E \cup E_0}$ are $e_{(ij)}$ for $(ij) \in E$ and $e_{(0i)}$ for $(0i) \in E_0$. Since $\pi(e_0) = \sum_{i \in V} \pi(e_{(0i)}) = 0$, we have dim$\pi(\mathbb{R}^{E_0}) = n - 1 =dimQ_n^w$. Recall that $\pi(\mathbb{R}^E) = \mathbb{R}^E$. Hence there is a one-to-one bijection χ between the spaces $\pi(\mathbb{R}^{E \cup E_0})$ and Q_n.

We define this bijection $\chi : \pi(\mathbb{R}^{E \cup E_0}) \to Q_n$ as follows

$$\chi(\mathbb{R}^E) = \varphi(\mathbb{R}^E) = \mathbb{R}_s^{E^{\mathcal{O}}}, \text{ and } \chi(\pi(\mathbb{R}^{E_0})) = Q_n^w,$$

where

$$\chi(e_{(ij)}) = \varphi(e_{(ij)}) = e_{ij} + e_{ji}, \text{ and } \chi(\pi(e_{(0i)})) = \chi(e_{(0i)} - \frac{1}{n} e_0) = p(i),$$

where $p(i)$ is defined in (1).

Note that $(e_{ij} + e_{ji})^2 = 2 = 2e_{(ij)}^2$ and

$$(p(i), p(j)) = -2 = 2n((e_{(0i)} - \frac{1}{n} e_0), (e_{(0j)} - \frac{1}{n} e_0)),\ p^2(i) = 2(n-1) = 2n(e_{(0i)} - \frac{1}{n} e_0)^2.$$

Roughly speaking, the map χ is a composition of homotheties that extends vectors $e_{(ij)}$ and $e_{(0i)} - \frac{1}{n} e_0$ up to vectors $e_{ij} + e_{ji}$ and $p(i)$ by the multiples $\sqrt{2}$ and $\sqrt{2n}$, respectively.

Setting $\psi = \chi \circ \pi$, we obtain a map $\psi : \mathbb{R}^{E \cup E_0} \to Q_n$ such that

$$\psi(e_{(ij)}) = e_{ij} + e_{ji} \text{ for } (ij) \in E,\ \psi(e_{(0i)}) = p(i) \text{ for } i \in V. \tag{10}$$

Now we show how a point $x = x^V + x^0 \in \mathbb{R}^{E\cup E_0}$ is transformed into a point $q = \psi(x) = \chi(\pi(x)) \in Q_n$. We have $\pi(x) = x^V + \pi(x^0)$, where, according to (8), $x^V = \sum_{(ij)\in E} x_{(ij)}e_{(ij)} \in \pi(\mathbb{R}^E) = \mathbb{R}^E$ and $\pi(x^0) = \sum_{i\in V} x_{(0i)}(e_{(0i)} - \frac{1}{n}e_0) \in \pi(\mathbb{R}^{E_0})$. Obviously, $\chi(x^V + \pi(x^0)) = \chi(x^V) + \chi(\pi(x^0))$, and

$$\psi(x^V) = \chi(x^V) = \sum_{(ij)\in E} x_{(ij)}(e_{ij} + e_{ji}) = \varphi(x^V) = q^s \text{ and } \chi(\pi(x^0)) = \sum_{i\in V} x_{(0i)}p(i) = q^a.$$

Recall that $q^s = \sum_{(ij)\in E} q_{(ij)}(e_{ij} + e_{ji})$ and $q^a = \sum_{i\in V} w_i p(i)$. Hence

$$q_{(ij)} = x_{(ij)},\ (ij) \in E, \text{ and } w_i = x_{(0i)},\ i \in V. \tag{11}$$

Let $f \in \mathbb{R}^{E\cup E_0}$ be a facet vector of a facet F of the cone Con_{n+1}, $f = f^V + f^0 = \sum_{(ij)\in E} f_{(ij)}e_{(ij)} + \sum_{i\in V} f_{(0i)}e_{(0i)}$.

Let $(f, x) \geq 0$ be the inequality determining the facet F. The inequality $(f, x) \geq 0$ takes on the set $V \cup \{0\}$ the following form

$$(f, x) = \sum_{(ij)\in E} f_{(ij)}x_{(ij)} + \sum_{i\in V} f_{(0i)}x_{(0i)} \geq 0.$$

Since $x_{(ij)} = q_{(ij)}, x_{(0i)} = w_i$, we can rewrite this inequality as follows

$$(f, q) = (f^V, q^s) + (f^0, q^a) \equiv \sum_{(ij)\in E} f_{(ij)}q_{(ij)} + \sum_{i\in V} f_{(0i)}w_i \geq 0. \tag{12}$$

Comparing the inequality (12) with (7), we see that a canonical form of the facet vector f is $f = f^s + f^a$, where

$$f^s_{ij} = f_{(ij)}, \text{ for } (ij) \in E,\ f^a_{ij} = v_i - v_j \text{ where } v_i = \frac{1}{n}f_{(0i)},\ i \in V. \tag{13}$$

Theorem 2. *Let F be a facet of the cone Con_{n+1}. Then $\psi(F)$ is a facet of the cone $\psi(Con_{n+1})$ if and only if the facet F contains the extreme ray l_0 spanned by the vector e_0.*

Let $l \neq l_0$ be an extreme ray of Con_{n+1}. Then $\psi(l)$ is an extreme ray of $\psi(Con_{n+1})$ if and only if the ray l belongs to a facet containing the extreme ray l_0.

Proof. By Theorem 1, the projection π transforms the facet F of Con_{n+1} into a facet of $\pi(Con_{n+1})$ if and only if $l_0 \subset F$. By the same Theorem, the projection $\pi(l)$ is an extreme ray of $\pi(Con_{n+1})$ if and only if l belongs to a facet containing the extreme ray l_0.

Recall that the map χ is a bijection between the spaces $\mathbb{R}^{E\cup E_0}$ and Q_n. This implies the assertion of this Theorem for the map $\psi = \chi \circ \pi$. □

By Theorem 2, the map ψ transforms the facet F in a facet of the cone $\psi(Con_{n+1})$ only if F contains the extreme ray l_0, i.e. only if the equality $(f, e_0) = 0$ holds. Hence the facet vector f should satisfy the equality $\sum_{i\in V} f_{(0i)} = 0$.

The inequalities (12) give all facet-defining inequalities of the cone $\psi(Con_{n+1})$ from known facet-defining inequalities of the cone Con_{n+1}.

So, we have the following algorithm for to find a list of facets of the cone $\psi(Con_{n+1})$ from a known list $\mathcal{L}$ of facet vectors of the cone Con_{n+1}.

Step 1. Take a facet vector $f = \{f_{(ij)} : (ij) \in E \cup E_0\} \in \mathcal{L}$ of the cone Con_{n+1}, and delete it from $\mathcal{L}$. Find a point $i \in V \cup \{0\}$ such that $\sum_{k\in V\cup\{0\}} f_{(ik)} = 0$. Go to Step 2.

Step 2. If such a point i does not exist, go to Step 1. Otherwise, make a permutation $i \to 0, 0 \to i$, and go to step 3.

Step 3. By formula (13) form a facet vector of the cone $\psi(Con_{n+1})$ from the facet vector f of the cone Con_{n+1}. If $\mathcal{L}$ is not empty, go to Step 1. Otherwise, end.

A proof of Proposition 2 below will be given later for each of the cones Met_{n+1}, Hyp_{n+1} and Cut_{n+1} separately.

Proposition 2. *Let F be a facet of Con_{n+1} with facet vector $f = f^V + f^0$ such that $(f^0, e_0) = 0$. Then Con_{n+1} has also a facet F^* with facet vector $f^* = f^V - f^0$.*

Proposition 2 implies the following important fact.

Proposition 3. *For $q = q^s + q^a \in \psi(Con_{n+1})$, the map $q = q^s + q^a \to q^* = q^s - q^a$ preserves the cone $\psi(Con_{n+1})$, i.e.*

$$(\psi(Con_{n+1}))^* = \psi(Con_{n+1}).$$

Proof. Let F be a facet of Con_{n+1} with facet vector f. By Proposition 2, if $\psi(F)$ is a facet of $\psi(Con_{n+1})$, then F^* is a facet of Con_{n+1} with facet vector f^*. Let $q \in \psi(Con_{n+1})$. Then q satisfies as the inequality $(f, q) = (f^V, q^s) + (f^0, q^a) \geq 0$ (see (12)) so the inequality $(f^*, q) = (f^V, q^s) - (f^0, q^a) \geq 0$. But it is easy to see that $(f, q) = (f^*, q^*)$ and $(f^*, q) = (f, q^*)$. This implies that $q^* \in \psi(Con_{n+1})$. □

Call a facet G of the cone $\psi(Con_{n+1})$ *symmetric* if $q \in F$ implies $q^* \in F$. Call a facet of $\psi(Con_{n+1})$ *asymmetric* if it is not symmetric.

The assertion of the following Proposition 4 is implied by the equality $(\psi(Con_{n+1}))^* = \psi(Con_{n+1})$.

Proposition 4. *Let $g \in Q_n$ be a facet vector of an asymmetric facet G of the cone $\psi(Con_{n+1})$, and let $G^* = \{q^* : q \in G\}$. Then G^* is a facet of $\psi(Con_{n+1})$, and g^* is its facet vector.*

Recall that Con_{n+1} has facets, that are zero-lifting of facets of Con_n. Call a facet G of the cone $\psi(Con_{n+1})$ *zero-lifting* of a facet F^V of Con_n if $G = \psi(F)$, where F is a facet of Con_{n+1} which is zero-lifting of F^V.

Proposition 5. *Let $g \in Q_n$ be a facet vector of a facet G of the cone $\psi(Con_{n+1})$. Then the following assertions are equivalent:*

(i) $g = g^*$;

(ii) the facet G is symmetric;

(iii) $G = \psi(F)$, where F is a facet of Con_{n+1} which is zero-lifting of a facet F^V of Con_n.

(iv) G is a zero-lifting of a facet F^V of Con_n.

Proof. (i)⇒(ii). If $g = g^*$, then $g = g^s$. Hence $q \in G$ implies $(g, q) = (g^s, q) = (g^s, q^s) = (g, q^*) = 0$. This means that $q^* \in G$, i.e. G is symmetric.

(ii)⇒(i). By Proposition 3, the map $q \to q^*$ is an automorphism of $\psi(Con_{n+1})$. This map transforms a facet G with facet vector g into a facet G^* with facet vector g^*. If G is symmetric, then $G^* = G$, and therefore $g^* = g$.

(iii)⇒(i). Let $f = f^V + f^0$ be a facet vector of a facet F of Con_{n+1} such that $f^0 = 0$. Then the facet F is zero-lifting of the facet $F^V = F \cap \mathbb{R}^E$ of the cone Con_n. In this case, f^V is also a facet vector of the facet $G = \psi(F)$ of $\psi(Con_{n+1})$. Obviously, $(f^V)^* = f^V$.

(iii)⇒(iv). This implication is implied by definition of zero-lifting of a facet of the cone $\psi(Con_{n+1})$.

(iv)⇒(i). The map χ induces a bijection between $\pi(F)$ and $\psi(F)$. Since $\pi(F)$ is zero-lifting of F^V, the facet vector of $\pi(F)$ belongs to $\mathbb{R}^E$. This implies that the facet vector g of $\psi(F)$ belongs to $\mathbb{R}_s^{E^{\mathcal{O}}}$, i.e. $g^* = g$. □

The symmetry group of Con_{n+1} is the symmetric group Σ_{n+1} of permutations of indices (see [DL97]). The group Σ_n is a subgroup of the symmetry group of the cone $\psi(Con_{n+1})$. The full symmetry group of $\psi(Con_{n+1})$ is $\Sigma_n \times \Sigma_2$, where Σ_2 corresponds to the map $q \to q^*$ for $q \in \psi(Con_{n+1})$. By Proposition 4, the set of facets of $\psi(Con_{n+1})$ is partitioned into pairs G, G^*. But it turns out that there are pairs such that $G^* = \sigma(G)$, where $\sigma \in \Sigma_n$.

9 Projections of hypermetric facets

The metric cone Met_{n+1}, the hypermetric cone Hyp_{n+1} and the cut cone Cut_{n+1} lying in the space $\mathbb{R}^{E\cup E_0}$ have an important class of *hypermetric* facets, that contains the class of *triangular* facets.

Let b_i, $i \in V$, be integers such that $\sum_{i\in V} b_i = \mu$, where $\mu = 0$ or $\mu = 1$. Usually these integers are denoted as a sequence $(b_1, b_2, ..., b_n)$, where $b_i \geq b_{i+1}$. If, for some i, we have $b_i = b_{i+1} = ... = b_{i+m-1}$, then the sequence is shortened as $(b_1, ..., b_i^m, b_{i+m}, ..., b_n)$.

One relates to this sequence the following inequality of type $b = (b_1, ..., b_n)$

$$(f(b), x) = -\sum_{i,j\in V} b_i b_j x_{(ij)} \geq 0,$$

where $x = \{x_{(ij)}\} \in \mathbb{R}^E$ and the vector $f(b) \in \mathbb{R}^E$ has coordinates $f(b)_{(ij)} = -b_i b_j$. This inequality is called of *negative* or *hypermetric* type if in the sum $\sum_{i\in V} b_i = \mu$ we have $\mu = 0$ or $\mu = 1$, respectively.

The set of hypermetric inequalities on the set $V \cup \{0\}$ determines a hypermetric cone Hyp_{n+1}. There are infinitely many hypermetric inequalities for metrics on $V \cup \{0\}$. But it is proved in [DL97], that only finite number of these inequalities determines facets of Hyp_{n+1}. Since triangle inequalities are inequalities $(f(b), x) \geq 0$ of type $b = (1^2, 0^{n-3}, -1)$, the hypermetric cone Hyp_{n+1} is contained in Met_{n+1}, i.e. $Hyp_{n+1} \subseteq Met_{n+1}$ with equality for $n = 2$.

The hypermetric inequality $(f(b), x) \geq 0$ takes the following form on the set $V \cup \{0\}$.

$$-\sum_{i,j\in V\cup\{0\}} b_i b_j x_{(ij)} = -\sum_{(ij)\in E} b_i b_j x_{(ij)} - \sum_{i\in V} b_0 b_i x_{(0i)} \geq 0. \tag{14}$$

If we decompose the vector $f(b)$ as $f(b) = f^V(b) + f^0(b)$, then $f^V(b)_{(ij)} = -b_i b_j$, $(ij) \in E$, and $f^0(b)_{(0i)} = -b_0 b_i$, $i \in V$.

Let, for $S \subseteq V$, the equality $\sum_{i\in S} b_i = 0$ hold. Denote by b^S a sequence such that $b_i^S = -b_i$ if $i \in S$ and $b_i^S = b_i$ if $i \notin S$. The sequence b^S is called *switching* of b by the set S.

The hypermetric cone Hyp_{n+1} has the following property (see [DL97]). If an inequality $(f(b), x) \geq 0$ defines a facet and $\sum_{i\in S} b_i = 0$ for some $S \subseteq V \cup \{0\}$, then the inequality $(f(b^S), x) \geq 0$ defines a facet, too.

Proof of Proposition 2 for Hyp_{n+1}.

Consider the inequality (14), where $(f^0(b), e_0) = -\sum_{i\in V} b_0 b_i = 0$. Then $\sum_{i\in V} b_i = 0$. Hence the cone Hyp_{n+1} has similar inequality for b^V, where $b_i^V = -b_i$ for all $i \in V$. Hence if one of these inequalities defines a facet so does another. Obviously, $f^0(b^V) = -f^0(b)$. Hence these facets satisfy the assertion of Proposition 2. □

Theorem 3. *Let $(f(b), x) \geq 0$ define a hypermetric facet of a cone in the space $\mathbb{R}^{E\cup E_0}$. Then the map ψ transforms it either in a hypemetric facet if $b_0 = 0$ or in a distortion of a facet of negative type if $b_0 = 1$. Otherwise, the projection is not a facet.*

Proof. By Section 8, the map ψ transforms the hypermetric inequality (14) for $x \in \mathbb{R}^{E\cup E_0}$ into the following inequality

$$-\sum_{(ij)\in E} b_i b_j q_{(ij)} - b_0 \sum_{i\in V} b_i w_i \geq 0$$

for $q = \sum_{(ij)\in E} q_{(ij)} \varphi(e_{(ij)}) + \sum_{i\in V} w_i q(i) \in Q_n$.

Since $f(b)$ determines a hypermetric inequality, we have $b_0 = 1 - \sum_{i\in V} b_i = 1 - \mu$. So, the above inequality takes the form

$$\sum_{(ij)\in E} b_i b_j q_{(ij)} \leq (\mu - 1) \sum_{i\in V} b_i w_i.$$

By Theorem 1, this facet is projected by the map ψ into a facet if and only if $(f(b), e_0) = 0$, where $e_0 = \sum_{i\in V} e_{(0i)}$. We have

$$(f(b), e_0) = \sum_{i\in V} f(b)_{(0i)} = -\sum_{i\in V} b_0 b_i = -b_0 \mu = (\mu - 1)\mu.$$

This implies that the hypermetric facet-defining inequality $(f(b), x) \geq 0$ is transformed into a facet-defining inequality if and only if either $\mu = 0$ and then $b_0 = 1$ or $\mu = 1$ and then $b_0 = 0$. So, we have

if $\mu = 1$ and $b_0 = 0$, then the above inequality is a usual hypermetric inequality in the space $\psi(\mathbb{R}^E) = \varphi(\mathbb{R}^E) = \mathbb{R}_s^{E^{\mathcal{O}}}$;

if $\mu = 0$ and $b_0 = 1$, then the above inequality is the following distortion of an inequality of negative type

$$-\sum_{(ij)\in E} b_i b_j q_{(ij)} - \sum_{i\in V} b_i w_i \geq 0, \text{ where } \sum_{i\in V} b_i = 0. \tag{15}$$

□

Comparing (7) with the inequality (15), we see that a canonical facet vector $g(b)$ of a facet of $\psi(Hyp_{n+1})$ has the form $g(b) = g^s(b) + g^a(b)$, where $g_{ij}(b) = g_{(ij)}(b) + v_i - v_j$, and

$$g_{(ij)}(b) = -b_i b_j, \; v_i = -\frac{1}{n} b_i \text{ for all } i \in V.$$

Define a cone of weighted quasi-hyper-metrics $WQHyp_n = \psi(Hyp_{n+1})$ We can apply Proposition 3, in order to obtain the following assertion.

Proposition 6. *The map $q \to q^*$ preserves the cone $WQHyp_n$, i.e.*

$$(WQHyp_n)^* = WQHyp_n.$$

In other words, if $q \in WQHyp_n$ has weights $w_i, i \in V$, then the cone $WQHyp_n$ has a point q^* with weights $-w_i, i \in V$. □

10 Generalizations of metrics

The metric cone Met_{n+1} is defined in the space $\mathbb{R}^{E\cup E_0}$. It has an extreme ray which is spanned by the vector $e_0 = \sum_{i\in V} e_{(0i)} \in \mathbb{R}^{E_0}$. Facets of Met_{n+1} are defined by the following set of triangle inequalities, where $d \in Met_{n+1}$.

Triangle inequalities of the sub-cone Met_n that define facets of Met_{n+1} that are zero-lifting and contain e_0:

$$d_{(ik)} + d_{(kj)} - d_{(ij)} \geq 0, \text{ for } i, j, k \in V. \tag{16}$$

Triangle inequalities defining facets that are not zero-lifting and contain the extreme ray l_0 spanned by the vector e_0:

$$d_{(ij)} + d_{(j0)} - d_{(i0)} \geq 0 \text{ and } d_{(ij)} + d_{(i0)} - d_{(j0)} \geq 0, \text{ for } i, j \in V. \tag{17}$$

Triangle inequalities defining facets that do not contain the extreme ray l_0 and do not define facets of Met_n.

$$d_{(i0)} + d_{(j0)} - d_{(ij)} \geq 0, \text{ for } i, j \in V. \tag{18}$$

One can say that the cone $Met_n \in \mathbb{R}^{E_0}$ is lifted into the space $\mathbb{R}^{E\cup E_0}$ using restrictions (17) and (18). Note that the inequalities (17) and (18) imply the following inequalities of non-negativity

$$d_{(i0)} \geq 0, \text{ for } i \in V. \tag{19}$$

A cone defined by inequalities (16) and (19) is called by cone $WMet_n$ of *weighted* metrics (d, w), where $d \in Met_n$ and $w_i = d_{(0i)}$ for $i \in V$ are *weights*.

If weights $w_i = d_{(0i)}$ satisfy also the inequalities (17) additionally to the inequalities (19), then the weighted metrics (d, w) form a cone $dWMet_n$ of *down-weighted* metrics. If metrics have weights that satisfy the inequalities (19) and (18), then these metrics are called *up-weighted* metrics. Detail see in [DD10], [DDV11].

Above defined generalizations of metrics are functions on unordered pairs $(ij) \in E \cup E_0$. Generalizations of metrics as functions on ordered pairs $ij \in E^{\mathcal{O}}$ are called *quasi-metrics*.

The cone $QMet_n$ of quasi-metrics is defined in the space $\mathbb{R}^{E^{\mathcal{O}}}$ by non-negativity inequalities $q_{ij} \geq 0$ for all $ij \in E^{\mathcal{O}}$, and by triangle inequalities $q_{ij} + q_{jk} - q_{ik} \geq 0$ for all ordered triples ijk for each $q \in QMet_n$. Below we consider in $QMet_n$ a sub-cone $WQMet_n$ of weighted quasi-metrics.

11 Cone of weighted quasi-metrics

We call a quasi-metric q *weighted* if it belongs to the subspace $Q_n \subset \mathbb{R}^{E^{\mathcal{O}}}$. So, we define

$$WQMet_n = QMet_n \cap Q_n.$$

A *quasi-metric* q is called *weightable* if there are weights $w_i \geq 0$ for all $i \in V$ such that the following equalities hold

$$q_{ij} + w_i = q_{ji} + w_j$$

for all $i, j \in V$, $i \neq j$. Since $q_{ij} = q^s_{ij} + q^a_{ij}$, we have $q_{ij} + w_i = q^s_{ij} + q^a_{ij} + w_i = q^s_{ji} + q^a_{ji} + w_j$, i.e. $q^a_{ij} - q^a_{ji} = 2q^a_{ij} = w_j - w_i$, what means that, up to multiple $\frac{1}{2}$ and sign, the antisymmetric part of q_{ij} is $w_i - w_j$. So, weightable quasi-metrics are weighted.

Note that weights of a weighted quasi-metric are defined up to an additive constant. So, if we take weights non-positive, we obtain a weightable quasi-metric. Hence, sets of weightable and weighted quasi-metrics coincide.

By definition of the cone $WQMet_n$ and by symmetry of this cone, the triangle inequality $q_{ij} + q_{jk} - q_{ik} \geq 0$ and non-negativity inequality $q_{ij} \geq 0$ determine facets of the cone $WQMet_n$. Facet vectors of these facets are

$$t_{ijk} = e_{ij} + e_{jk} - e_{ik} \text{ and } e_{ij},$$

respectively. It is not difficult to verify that $t_{ijk}, e_{ij} \notin Q_n$. Hence these facet vectors are not canonical. Below, we give canonical representatives of these facet vectors.

Let $T(ijk) \subseteq K^{\mathcal{O}}_n$ be a triangle of $K^{\mathcal{O}}_n$ with direct arcs ij, jk, ki and opposite arcs ji, kj, ik. Hence

$$f^{T(ijk)} = (e_{ij} + e_{jk} + e_{ki}) - (e_{ji} + e_{kj} + e_{ik}).$$

Proposition 7. *Canonical representatives of facet vectors t_{ijk} and e_{ij} are*

$$t_{ijk} + t^*_{ijk} = t_{ijk} + t_{kji}, \text{ and } g(ij) = (e_{ij} + e_{ji}) + \frac{1}{n}(p(i) - p(j)),$$

respectively.

Proof. We have $t_{ijk} - f^{T(ijk)} = e_{ji} + e_{kj} - e_{ki} = t_{kji} = t^*_{ijk}$. This implies that the facet vectors t_{ijk} and t_{kji} determine the same facet, and the vector $t_{ijk} + t_{kji} \in \mathbb{R}^{E^{\mathcal{O}}}_s$ is a canonical representative of facet vectors of this facet. We obtain the first assertion of Proposition.

Consider now the facet vector e_{ij}. It is more convenient to take the doubled vector $2e_{ij}$. We show that the vector

$$g(ij) = 2e_{ij} - \frac{1}{n} \sum_{k \in V - \{i,j\}} f^{T(ijk)}.$$

is a canonical representative of the facet vector $2e_{ij}$. It is sufficient to show that $g(ij) \in Q_n$, i.e. $g_{kl}(ij) = g^s_{kl}(ij) + w_k - w_l$. In fact, we have $g_{ij}(ij) = 2 - \frac{n-2}{n} = 1 + \frac{2}{n}$, $g_{ji}(ij) = \frac{n-2}{n} = 1 - \frac{2}{n}$, $g_{ik}(ij) = -g_{ki}(ij) = \frac{1}{n}$, $g_{jk}(ij) = -g_{kj}(ij) = -\frac{1}{n}$, $g_{kk'}(ij) = 0$. Hence we have

$$g^s(ij) = e_{ij} + e_{ji},\ w_i = -w_j = \frac{1}{n},\ \text{and } w_k = 0 \text{ for all } k \in V - \{i, j\}.$$

These equalities imply the second assertion of Proposition. □

Let τ_{ijk} be a facet vector of a facet of Met_n determined by the inequality $d_{(ij)} + d_{(jk)} - d_{(ik)} \geq 0$. Then $t_{ijk} + t_{kji} = \varphi(\tau_{ijk})$, where the map $\varphi : \mathbb{R}^E \to \mathbb{R}^{E^{\mathcal{O}}}_s$ is defined in Section 2. Obviously, a triangular facet is symmetric.

Recall that $q_{ij} = q_{(ij)} + w_i - w_j$ if $q \in WQMet_n$. Let $i, j, k \in V$. It is not difficult to verify that the following equalities hold:

$$q^s_{ij} + q^s_{jk} - q^s_{ik} = q_{ij} + q_{jk} - q_{ij} \geq 0. \tag{20}$$

Since $q^s_{ij} = q^s_{ji} = q_{(ij)}$, these inequalities show that the symmetric part q^s of the vector $q \in WQMet_n$ is a semi-metric. Hence if $w_i = w$ for all $i \in V$, then the quasi-semi-metric $q = q^s$ itself is a semi-metric. This implies that the cone $WQMet_n$ contains the semi-metric cone Met_n. Moreover, $Met_n = WQMet_n \cap \mathbb{R}^{E^{\mathcal{O}}}_s$.

Now we show explicitly how the map ψ transforms the cones Met_{n+1} and $dWMet_n$ into the cone $WQMet_n$.

Theorem 4. *The following equalities hold*

$$\psi(Met_{n+1}) = \psi(dWMet_n) = WQMet_n \text{ and } WQMet^*_n = WQMet_n.$$

Proof. All facets of the metric cone Met_{n+1} of metrics on the set $V \cup \{0\}$ are given by triangular inequalities $d_{(ij)} + d_{(ik)} - d_{(kj)} \geq 0$. They are hypermetric inequalities $(g(b), d) \geq 0$, where b has only three non-zero values $b_j = b_k = 1$ and $b_i = -1$ for some triple $\{ijk\} \subseteq V \cup \{0\}$. By Theorem 3, the map ψ transforms this facet into a hypermetric facet, i.e. into a triangular facets of the cone $\psi(Met_{n+1})$ if and only if $b_0 = 0$, i.e. if $0 \notin \{ijk\}$. If $0 \in \{ijk\}$, then, by the same theorem, the equality $b_0 = 1$ should be satisfied. This implies $0 \in \{jk\}$. In this case the facet defining inequality has the form (15), that in the case $k = 0$, is

$$q_{(ij)} + w_i - w_j \geq 0.$$

This inequality is the non-negativity inequality $q_{ij} \geq 0$.

If $b_i = 1, b_j = -1$ and $k = 0$, the inequality $d_{(ij)} + d_{j0)} - d_{(0i)} \geq 0$ is transformed into inequality

$$q_{(ij)} + w_j - w_i \geq 0, \text{ i.e. } q^*_{ij} \geq 0.$$

This inequality and inequalities (20) imply the last equality of this Theorem.

The inequalities (18) define facets F of Met_{n+1} and $dWMet_n$ that do not contain the extreme ray l_0. Hence, by Theorem 3, $\psi(F)$ are not facets of $WQMet_n$. But, recall that the cone $dWMet_n$ contains all facet of Met_{n+1} excluding facets defined by the inequalities (18). Instead of these facets, the cone $dWMet_n$ has facets G_i defined by the non-negativity equalities (19) with facet vectors $e_{(0i)}$ for all $i \in V$. Obviously all these facets do not contain the extreme ray l_0. Hence, by Theorem 2, $\psi(G_i)$ is not a facet of $\psi(dWMet_n)$. Hence we have also the equality $WQMet_n = \psi(dWMet_n)$. □

Remark. Facet vectors of facets of Met_{n+1} that contain the extreme ray l_0 spanned by the vector e_0 are $\tau_{ijk} = \tau^V_{ijk}$, $\tau_{ij0} = \tau^V + \tau^0$ and $\tau_{ji0} = \tau^V - \tau^0$, where $\tau^V = e_{(ij)}$ and $\tau^0 = e_{(j0)} - e_{(i0)}$. Hence Proposition 2 is true for Met_{n+1}, and we can apply Proposition 3 in order to obtain the equality $WQMet^*_n = WQMet_n$ of Theorem 4.

12 The cone Cut_{n+1}

The cut vectors $\delta(S) \in \mathbb{R}^{E \cup E_0}$ for all $S \subseteq V \cup \{0\}$ span all extreme rays of the cut cone $Cut_{n+1} \subset \mathbb{R}^{E \cup E_0}$. In

other words, Cut_{n+1} is the conic hull of all cut vectors. Since the cone Cut_{n+1} is full dimensional, its dimension is dimension of the space $\mathbb{R}^{E\cup E_0}$ that is $\frac{n(n+1)}{2}$.

Recall that $\delta(S) = \delta(V \cup \{0\} - S)$. Hence we can consider only S such that $S \subseteq V$, i.e. $0 \notin S$. Moreover, by Section 5,

$$\delta(S) = \sum_{i\in S, j\notin S} e_{(ij)} = \sum_{i\in S, j\in V-S} e_{(ij)} + \sum_{i\in S} e_{(0i)} = \delta^V(S) + \sum_{i\in S} e_{(0i)}, \tag{21}$$

where $\delta^V(S)$ is restriction of $\delta(S)$ on the space $\mathbb{R}^E = \psi(\mathbb{R}^E)$. Note that

$$\delta(V) = \delta(\{0\}) = \sum_{i\in V} e_{(0i)} = e_0.$$

Consider a facet F of Cut_{n+1}. Let f be facet vector of F. Set

$$R(F) = \{S \subseteq V : (f, \delta(S)) = 0\}.$$

For $S \in R(F)$, the vector $\delta(S)$ is called *root* of the facet F. By (21), for $S \in R(F)$, we have

$$(f, \delta(S)) = (f, \delta^V(S)) + \sum_{i\in S} f_{(0i)} = 0. \tag{22}$$

We represent each facet vector of Cut_{n+1} as $f = f^V + f^0$, where $f^V \in \mathbb{R}^E$ and $f^0 \in \mathbb{R}^{E_0}$.

The set of facets of the cone Cut_{n+1} is partitioned onto equivalence classes by *switchings* (see [DL97]). For each $S, T \subset V \cup \{0\}$, the switching by the set T transforms the cut vector $\delta(S)$ into the vector $\delta(S\Delta T)$, where Δ is symmetric difference, i.e. $S\Delta T = S\cup T - S\cap T$. It is proved in [DL97] that if $T \in R(F)$, then $\{\delta(S\Delta T) : S \in R(F)\}$ is the set of roots of the switched facet $F^{\delta(T)}$ of Cut_{n+1}. Hence $R(F^{\delta(T)}) = \{S\Delta T : S \in R(F)\}$.

Let F be a facet of Cut_{n+1}. Then F contains the vector $e_0 = \delta(V)$ if and only if $V \in R(F)$. Hence Lemma 1 below is an extended reformulation of Proposition 2.

Lemma 1. *Let F be a facet of Cut_{n+1} such that $V \in R(F)$. Let $f = f^V + f^0$ be facet vector of F. Then the vector $f^* = f^V - f^0$ is facet vector of switching $F^{\delta(V)}$ of the facet F, and $V \in R(F^{\delta(V)})$.*

Proof. Since $V \in R(F)$, $F^{\delta(V)}$ is a facet of Cut_{n+1}. Since $S\Delta V = V - S = \overline{S}$, for $S \subseteq V$, we have

$$R(F^{\delta(V)}) = \{\overline{S} : S \in R(F)\}.$$

Since $\emptyset \in R(F)$, the set $\emptyset\Delta V = V \in R(F^{\delta(V)})$. Now, using (22), for $S \in R(F^{\delta(V)})$, we have

$$(f^*, \delta(S)) = ((f^V - f^0), \delta(S)) = (f^V, \delta^V(S)) - \sum_{i\in S} f_{(0i)}.$$

Note that $\delta^V(\overline{S}) = \delta^V(S)$, and, since $V \in R(F)$, $\delta(V) = \delta(\{0\})$, we have $(f, \delta(V)) = \sum_{i\in V} f_{(0i)} = 0$. Hence $\sum_{i\in\overline{S}} f_{(0i)} = -\sum_{i\in S} f_{(0i)}$. It is easy to see, that $(f^*, \delta(S)) = (f, \delta(\overline{S}))$. Since $S \in R(F^{\delta(V)})$ if and only if $\overline{S} \in R(F)$, we see that f^* is a facet vector of $F^{\delta(V)}$. □

The set of facets of Cut_{n+1} is partitioned into orbits under action of the permutation group Σ_{n+1}. But some permutation non-equivalent facets are equivalent under switchings. We say that two facets F, F' of Cut_{n+1} belong to the same *type* if there are $\sigma \in \Sigma_{n+1}$ and $T \subseteq V$ such that $\sigma(F') = F^{\delta(T)}$.

13 Cone $OCut_n$

Denote by $OCut_n \subset \mathbb{R}^{E^{\mathcal{O}}}$ the cone whose extreme rays are spanned by ocut vectors $c(S)$ for all $S \subset V$, $S \neq \emptyset, V$. In other words, let

$$OCut_n = \{c \in Q_n : c = \sum_{S\subset V} \alpha_S c(S),\ \alpha_S \geq 0\}.$$

Coordinates c_{ij} of a vector $c \in OCut_n$ are given in (6), where $w_i \geq 0$ for all $i \in V$. Hence $OCut_n \subset Q_n$. Recall that

$$c(S) = \frac{1}{2}(\delta^{\mathcal{O}}(S) + \sum_{i \in S} p(i)), \tag{23}$$

where $\delta^{\mathcal{O}}(S) = \varphi(\delta^V(S))$. Note that $\delta^{\mathcal{O}}(\overline{S}) = \delta^{\mathcal{O}}(S)$ and $p(\overline{S}) = -p(S)$, where $\overline{S} = V - S$.
Denote by $Cut_n^{\mathcal{O}} = \varphi(Cut_n)$ the cone generated by $\delta^{\mathcal{O}}(S)$ for all $S \subset V$. The vectors $\delta^{\mathcal{O}}(S)$ for all $S \subset V$, $S \neq \emptyset, V$, are all extreme rays of the cone $Cut_n^{\mathcal{O}}$ that we identify with Cut_n embedded into the space $\mathbb{R}^{E^{\mathcal{O}}}$.

Lemma 2. *For $S \subseteq V$, the following equality holds*

$$\psi(\delta(S)) = 2c(S).$$

Proof. According to Section 8, $\psi(\delta^V(S)) = \varphi(\delta^V(S)) = \delta^{\mathcal{O}}(S)$. Besides, $\psi(e_{(0i)}) = p(i)$ for all $i \in V$. Hence, using (21), we obtain

$$\psi(\delta(S)) = \psi(\delta^V(S)) + \sum_{i \in S} \psi(e_{(0i)}) = \varphi(\delta^V(S)) + \sum_{i \in S} p(i) = \delta^{\mathcal{O}}(S) + p(S).$$

Recall that $\psi(\delta(V)) = \psi(e_0) = \mathbf{0}$ and $c(V) = 0$. Hence, according to (23), we obtain

$$\psi(\delta(S)) = 2c(S), \text{ for all } S \subseteq V.$$

Lemma is proved. □

Theorem 5. *The following equalities hold*

$$\psi(Cut_{n+1}) = OCut_n \text{ and } OCut_n^* = OCut_n.$$

Proof. Recall that the conic hull of vectors $\delta(S)$ for all $S \subseteq V$ is Cut_{n+1}. The conic hull of vectors $c(S)$ for all $S \subset V$ is the cone $OCut_n$. Since $\psi(\delta(V)) = c(V) = \mathbf{0}$, the first result follows.
The equality $OCut_n^* = OCut_n$ is implied by the equalities $c^*(S) = c(\overline{S})$ for all $S \subseteq V$.
By Lemma 1, the equality $OCut_n^* = OCut_n$ is a special case $Con_{n+1} = Cut_{n+1}$ of Proposition 3. □

14 Facets of $OCut_n$

Lemma 3. *Let F be a facet of Cut_{n+1}. Then $\psi(F)$ is a facet of $OCut_n$ if and only if $V \in R(F)$.*

Proof. By Theorem 2, $\psi(F)$ is a facet of $OCut_n$ if and only if $e_0 = \delta(V) \subset F$, i.e. if and only if $V \in R(F)$. □

For a facet G of $OCut_n$ with facet vector g, we set

$$R(G) = \{S \subseteq V : (g, c(S)) = 0\}$$

and call the vector $c(S)$ for $S \in R(G)$ by *root* of the facet G.
Note that $\delta(\emptyset) = \mathbf{0}$ and $c(\emptyset) = c(V) = \mathbf{0}$. Hence $\emptyset \in R(F)$ and $\emptyset \in R(G)$ for all facet F of Cut_{n+1} and all facets G of $OCut_n$. The roots $\delta(\emptyset) = \mathbf{0}$ and $c(\emptyset) = c(V) = \mathbf{0}$ are called *trivial* roots.

Proposition 8. *For a facet F of Cut_{n+1}, let $G = \psi(F)$ be a facet of $OCut_n$. Then the following equality holds*

$$R(G) = R(F).$$

Remark. We give two proofs of this equality. Both are useful.

First proof. According to Section 8, the map ψ transforms an inequality $(f,x)\geq 0$ defining a facet of Cut_{n+1} into the inequality (12) defining the facet $G=\psi(F)$ of $OCut_n$. Recall the the inequality (12) relates to the representation of vectors $q\in Q_n$ in the basis $\{\varphi(e_{ij}),p(i)\}$, i.e. $q=\sum_{(ij)\in E}q_{(ij)}\varphi(e_{(ij)})+\sum_{i\in V}w_ip(i)$. Let $q=c(S)$ for $S\in R(G)$. Then, according to (23), we have $q_{(ij)}=\frac{1}{2}\delta^V_{(ij)}(S)$, $w_i=\frac{1}{2}$ for $i\in S$ and $w_i=0$ for $i\in\overline{S}$. Hence, omitting the multiple $\frac{1}{2}$, the inequality in (12) gives the following equality

$$\sum_{(ij)\in E}f_{(ij)}\delta^V_{(ij)}(S)+\sum_{i\in S}f_{(0i)}=0$$

which coincides with (22). This implies the assertion of this Proposition.

Second proof. By Theorem 2, $\psi(l)$ is an extreme ray of $\psi(F)$ if and only if l is an extreme ray of F and $l\neq l_0$. Since l is spanned by $\delta(S)$ for some $S\in R(F)$ and $\psi(l)$ is spanned by $\psi(\delta(S))=c(S)$, we have $R(G)=\{S\subset V:S\in R(F)\}$. Since $c(V)=\mathbf{0}$, we can suppose that $V\in R(G)$, and then $R(G)=R(F)$. □

Remark. Note that $\delta(V)=\delta(\{0\})=e_0\neq\mathbf{0}$ is a non-trivial root of F, i.e. $V\in R(F)$. But $c(V)=\psi(\delta(V))=\mathbf{0}$ is a trivial root of $R(G)$.

Recall that, for a subset $T\subseteq V$, we set $\overline{T}=V-T$. Note that $\overline{T}=V\Delta T$ and $\overline{T}\neq V\cup\{0\}-T$.

Lemma 4. *Let F be a facet of Cut_{n+1}, and $T\in R(F)$. Then the image $\psi(F^{\delta(T)})$ of the switched facet $F^{\delta(T)}$ is a facet of $OCut_n$ if and only if $\overline{T}\in R(F)$.*

Proof. By Lemma 3, $\psi(F^{\delta(T)})$ is a facet of $OCut_n$ if and only if $V\in R(F^{\delta(T)})$, i.e. if and only if $V\Delta T=\overline{T}\in R(F)$. □

For a facet G of $OCut_n$, define $G^{\delta(T)}$ as the conic hull of $c(S\Delta T)$ for all $S\in R(G)$. Since each facet G of $OCut_n$ is $\psi(F)$ for some facet F of Cut_{n+1}, Lemma 4 and Proposition 8 imply the following assertion.

Theorem 6. *Let G be a facet of $OCut_n$. Then $G^{\delta(T)}$ is a facet of $OCut_n$ if and only if $T,\overline{T}\in R(G)$, and then $R(G^{\delta(T)})=\{S\Delta T:S\in R(G)\}$.* □

Theorem 6 asserts that the set of facets of the cone $OCut_n$ is partitioned onto equivalence classes by switchings $G\to G^{\delta(T)}$, where $T,\overline{T}\in R(G)$.

The case $T=V$ in Theorem 6 plays a special role. Recall that $V\in R(F)$ if F is a facet of Cut_{n+1} such that $\psi(F)$ is a facet of $OCut_n$. Hence Lemma 1 and Proposition 3 imply the following fact.

Proposition 9. *Let F be a facet of Cut_{n+1} such that $\psi(F)$ is a facet of $OCut_n$. Let $g=g^s+g^a$ be a facet vector of the facet $\psi(F)$. Then the vector $g^*=g^s-g^a$ is a facet vector of the facet $\psi(F^{\delta(V)})=(\psi(F))^*=(\psi(F))^{\delta(V)}$ such that $R((\psi(F))^*)=\{\overline{S}:S\in R(F)\}$.* □

Recall that roughly speaking $OCut_n$ is projection of Cut_{n+1} along the vector $\delta(V)=\delta(\{0\})$.

Let $\sigma\in\Sigma_n$ be a permutation of the set V. For a vector $q\in\mathbb{R}^{E^{\mathcal{O}}}$, we have $\sigma(q)_{ij}=q_{\sigma(i)\sigma(j)}$. Obviously if g is a facet vector of a facet G of $OCut_n$, then $\sigma(g)$ is the facet vector of the facet $\sigma(G)=\{\sigma(q):q\in G\}$.

Note that, by Proposition 9, the switching by V is equivalent to the operation $q\to q^*$. Hence the symmetry group of $OCut_n$ contains the group $\Sigma_n\times\Sigma_2$, where Σ_2 relates to the map $q\to q^*$ for $q\in OCut_n$.

Theorem 7. *The group $\Sigma_n\times\Sigma_2$ is the symmetry group of the cone $OCut_n$.*

Proof. Let γ be a symmetry of $OCut_n$. Then γ is a symmetry of the set $\mathcal{F}(e_0)$ of facets F of the cone Cut_{n+1} containing the vector e_0. The symmetry group $\Gamma(e_0)$ of the set $\mathcal{F}(e_0)$ is a subgroup of the symmetry group of the cut-polytope $Cut^{\square}_{n+1}$. In fact, $\Gamma(e_0)$ is stabilizer of the edge e_0 of the polytope $Cut^{\square}_{n+1}$. But it is well-known that

$\Gamma(e_0)$ consists of the switching by V and permutations $\sigma \in \Sigma_{n+1}$ leaving the edge e_0 non-changed. The map ψ transforms these symmetries of $\mathcal{F}(e_0)$ into symmetries $\sigma \in \Sigma_n$ and $q \to q^*$ of the cone $OCut_n$. □

The set of all facets of $OCut_n$ is partitioned onto orbits of facets that are equivalent by the symmetry group $\Sigma_n \times \Sigma_2$. It turns out that, for some facets G, subsets $S \in R(G)$ and permutations $\sigma \in \Sigma_n$, we have $G^{\delta(S)} = \sigma(G)$.

By Proposition 5, if a facet of Cut_{n+1} is zero-lifting of a facet F^V of Cut_n, then the facet $G = \psi(F)$ of $OCut_n$ is symmetric and $G = G^* = G^{\delta(V)}$ is zero-lifting of F^V.

So, there are two important classes of orbits of facets of $OCut_n$. Namely, the orbits of symmetric facets, that are zero-lifting of facets of Cut_n, and orbits of asymmetric facets that are ψ-images of facets of Cut_{n+1} and are not zero-lifting.

15 Cases $3 \leq n \leq 6$

It is worth to compare results of this Section with Table 2 of [DDV11].

Most of described below facets are hypermetric or negative type. We give here the corresponding vectors b in accordance with Section 9.

n=3. Note that $Cut_4 = Hyp_4 = Met_4$. Hence

$$OCut_3 = WQHyp_3 = WQMet_3.$$

All these cones have two orbits of facets: one orbit of non-negativity facets with $b = (1, 0, -1)$ and another orbit of triangular facets with $b = (1^2, -1)$.

n=4. We have $Cut_5 = Hyp_5 \subset Met_5$. Hence

$$OCut_4 = WQHyp_4 \subset WQMet_4.$$

The cones $Hyp_5 = Cut_5$ have two orbits of facets: triangular and pentagonal facets. Recall that a triangular facet with facet vector τ_{ijk} is zero-lifting if $0 \notin \{ijk\}$. Hence the cones $WQHyp_4 = OCut_4$ have three orbits of facets: of non-negativity with $b = (1, 0^2, -1)$, triangular with $b = (1^2, 0, -1)$ and weighted version of negative type with $b = (1^2, -1^2)$.

n=5. We have again $Cut_6 = Hyp_6 \subset Met_6$. Hence

$$OCut_5 = WQHyp_5 \subset WQMet_5.$$

The cones $Hyp_6 = Cut_6$ have four orbits of facets, all are hypermetric: triangular with $b = (1^2, 0^3, -1)$, pentagonal with $b = (1^3, 0, -1^2)$ and two more types, one with $b = (2, 1^2, -1^3)$ and its switching with $b = (1^4, -1, -2)$. These four types provide 6 orbits of facets of the cones $WQHyp_5 = OCut_5$: non-negativity with $b = (1, 0^3, -1)$, triangular with $b = (1^2, 0^2, -1)$, of negative type with $b = (1^2, 0, -1^2)$, pentagonal with $b = (1^3, -1^2)$, and two of negative type with $b = (2, 1, -1^3)$ and $b = (1^3, -1, -2)$.

The last two types belong to the same orbit of the full symmetry group $\Sigma_5 \times \Sigma_2$. Hence the cone $OCut_5$ has 5 orbits of facets under action of its symmetry group.

n=6. Now, we have $Cut_7 \subset Hyp_7 \subset Met_7$. Hence

$$OCut_6 \subset WQHyp_6 \subset WQMet_6.$$

The cone Cut_7 has 36 orbits of facets under action of the permutation group Σ_7. Switchings contract these orbits into 11 types F_k, $1 \leq k \leq 11$, (see [DL97], Sect. 30.6). J.Vidali compute orbits of facets of $OCut_6$ under action of the group Σ_6. Using these computations, we give in Table below numbers of orbits of facets of cones Cut_7 and $OCut_6$ (cf. Figure 30.6.1 of [DL97]).

The first row of Table gives types of facets of Cut_7. In the second row of Table, for each type F_k, numbers of orbits of facets of Cut_7 of type F_k under action of the group Σ_7. The third row of Table, for each type F_k, gives numbers of orbits of facets of $OCut_6$ that are obtained from facets of type F_k under action of the group Σ_6. The fourth row gives, for each type F_k, numbers of orbits of facets of $OCut_6$ that are obtained from facets of type F_k under action of the group $\Sigma_6 \times \Sigma_2$.

The last column of Table gives total numbers of orbits of facets of the cones Cut_7 and $OCut_6$.

Table.

types	F_1	F_2	F_3	F_4	F_5	F_6	F_7	F_8	F_9	F_{10}	F_{11}	$\|\Omega\|$
Σ_7	1	1	2	1	3	2	4	7	5	3	7	36
Σ_6	2	2	4	1	3	2	7	13	6	6	15	61
$\Sigma_6 \times \Sigma_2$	2	2	3	1	2	1	4	7	3	4	8	37

The first three types F_1, F_2, F_3 relate to 4 orbits of hypermetric facets $F(b)$ of Cut_7 that are zero-lifting, where $b = (1^2, 0^4, -1)$, $b = (1^3, 0^2, -1^2)$ and $b = (2, 1^2, 0, -1^3)$, $b = (1^4, 0, -1, -2)$. Each of these four orbits of facets of Cut_7 under action of Σ_7 gives two orbits of facets of $OCut_6$ under action of the group Σ_6.

The second three types F_4, F_5, F_6 relate to 6 orbits of hypermetric facets $F(b)$ of Cut_7 that are not zero-lifting. Each of these 6 orbits gives one orbit of facets of $OCut_6$ under action of the group Σ_6.

The third three types F_7, F_8, F_9 relate to 16 orbits of facets of clique-web types $CW_1^7(b)$. These 16 orbits give 26 orbits of facets of $OCut_6$ under action of Σ_6.

The last two types $F_{10} = Par_7$ and Gr_7 are special (see [DL97]). They relate to 10 orbits of Cut_7, that give 21 orbits of facets of $OCut_6$ under action of Σ_6.

The subgroup Σ_2 of the full symmetry group $\Sigma_6 \times \Sigma_2$ contracts some pairs of orbits of the group Σ_6 into one orbit of the full group. The result is given in the forth row of Table.

Note that the symmetry groups of Cut_7 and $OCut_6$ have 36 and 37 orbits of facets, respectively.

Bibliography

[AACMP97] O.Aichholzer, F.Auerhammer, D.Z.Chen, D.T.Lee, A.Mukhopadhyay and E.Papadopoulou, *Voronoi diagrams for direction-sensitive distances*, Proceedings of 13^{th} Annual ACM Simposium Computational Geometry, Nice, France (1997), 418–420.

[Aig79] M.Aigner, *Combinatorial Theory*, Springer-Verlag, Berlin 1979, (Chapter VII 3B).

[AM11] D.Avis and C.Meagher, *On the Directed Cut Cone and Polytope*, Manuscript Draft No. MAPR-D-11-00057, 2011.

[Bir67] G.Birkhoff, *Lattice Theory*, AMS, Providence, Rhode Island, 1967.

[CMM06] M.Charikar, K.Makarychev, and Y.Makarychev, *Directed metrics and directed graph partitioning problem* Proc. of 17th ACM-SIAM Symposium on Discrete Algorithms (2006) 51–60.

[DD10] M.Deza and E.Deza, *Cones of Partial Metrics*, Contributions in Discrete Mathematics, **6** (2010), 26–41.

[DDV11] M.Deza, E.Deza and J.Vidali, *Cones of Weighted and Partial Metrics*, arXiv: 1101.o517v2[math.Co]04 Jan 2011.

[DL97] M.Deza and M.Laurent, *Geometry of cuts and metrics*, Springer-Verlag, 1997.

[Ha14] F. Hausdorff, *Grundzüge der Mengenlehre*, Leipzig,Verlag "Veit and Co", 1914.

[Se97] A.K.Seda, *Quasi-metrics and semantic of logic programs*, Fundamenta Informaticae, **29** (1997), 97–117.

Authors' Information

Michel Deza *- Ecole Normale Superieure, Paris.*

Vyacheslav P. Grishukhin *- CEMI, Russian Academy of Sciences, Moscow, the speaker and corresponding author.*

Elena Deza *- Moscow State Pedagogical University, Moscow.*

CUBE-LIKE POLYTOPES AND COMPLEXES

Andrew Duke, Egon Schulte

Abstract: *The main purpose of this paper is to popularize Danzer's power complex construction and establish some new results about covering maps between two power complexes. Power complexes are cube-like combinatorial structures that share many structural properties with higher-dimensional cubes and cubical tessellations on manifolds. Power complexes that are also abstract polytopes have repeatedly appeared somewhat unexpectedly in various contexts, although often under a different name. However, the non-polytope case is largely unexplored.*

Keywords: *cube; cubical tessellation; abstract polytope; incidence complex; covering.*

MSC (2000)*: Primary: 51M20. Secondary: 52B15.*

1 Introduction

Combinatorial structures built from cubes or cube-like elements have attracted a lot of attention in geometry, topology, and combinatorics. In this paper we study a particularly interesting class of cube-like structures known as *power complexes*. These power complexes were first discovered by Danzer in the early 1980's (see [7; 15; 22]). Power complexes that are also abstract polytopes have repeatedly appeared somewhat unexpectedly in various contexts, although often under a different name; for example, see Coxeter [4], Effenberger-Kühnel [9], Kühnel [13], McMullen-Schulte [15, Ch. 8] and Ringel [20]. However, most power complexes are not abstract polytopes, and have not been very well researched.

The main purpose of this paper is to popularize Danzer's power complex construction and establish some new results about covering maps between power complexes. Our discussion is in terms of incidence complexes, a class of ranked incidence structures closely related to polytopes, ranked partially ordered sets, and incidence geometries (Danzer-Schulte [8; 21]). In Section 2 we begin by reviewing key facts about incidence complexes and their automorphism groups. Then in Section 3 we define power complexes and establish some of their basic properties. A number of applications of power complexes are summarized in Section 4. Finally, Section 5 describes fairly general circumstances that guarantee the existence of covering maps between two power complexes.

2 Incidence complexes

An incidence complex has some of the key combinatorial properties of the face lattice of a convex polytope; in general, however, an incidence complex need not be a lattice, need not be finite, need not be an abstract polytope, and need not admit any familiar geometric realization. The notion of an *incidence complex* is originally due to Danzer [7; 8] and was inspired by Grünbaum [11]. Incidence complexes can also be viewed as incidence geometries or diagram geometries with a linear diagram (see Buekenhout-Pasini [3], Leemans [14], Tits [24]), although here we study them from the somewhat different discrete geometric and combinatorial perspective of polytopes and ranked partially ordered sets.

Following Danzer-Schulte [8] (and [21]), an *incidence complex $\mathcal{K}$ of rank k*, or briefly a *k-complex*, is defined by the properties **(I1)**,...,**(I4)** below. The elements of $\mathcal{K}$ are called *faces* of $\mathcal{K}$.

(I1) $\mathcal{K}$ is a partially ordered set with a unique least face and a unique greatest face.

(I2) Every totally ordered subset of $\mathcal{K}$ is contained in a (maximal) totally ordered subset with exactly $k+2$ elements, a *flag*, of $\mathcal{K}$.

These two conditions make $\mathcal{K}$ into a ranked partially ordered set, with a strictly monotone rank function with range $\{-1, 0, \ldots, k\}$. A face of rank i is called an *i-face*; often F_i will indicate an i-face. The least face and greatest face are the *improper faces* of $\mathcal{K}$ and have ranks -1 and k, respectively; all other faces of $\mathcal{K}$ are *proper faces* of $\mathcal{K}$. A face of rank 0, 1 or $n-1$ is also called a *vertex*, an *edge* or a *facet*, respectively. We let $\mathcal{F}(\mathcal{K})$ denote the set of flags of $\mathcal{K}$.

(I3) $\mathcal{K}$ is *strongly flag-connected*, meaning that if Φ and Ψ are two flags of $\mathcal{K}$, then there is a finite sequence of flags $\Phi = \Phi_0, \Phi_1, \ldots, \Phi_{m-1}, \Phi_m = \Psi$, all containing $\Phi \cap \Psi$, such that successive flags are *adjacent* (differ in just one face).

Call two flags *i-adjacent*, for $i = 0, \ldots, k-1$, if they are adjacent and differ exactly in their i-faces. With this notion of adjacency, $\mathcal{F}(\mathcal{K})$ becomes the *flag graph* for $\mathcal{K}$ and acquires a natural edge-labelling where edges labelled i represent pairs of i-adjacent flags.

Our last defining condition is a homogeneity requirement for the numbers of i-adjacent flags for each i.

(I4) There exist cardinal numbers $c_0, \ldots, c_{k-1} \geqslant 2$, for our purposes taken to be finite, such that, whenever F is an $(i-1)$-face and G a $(i+1)$-face with $F < G$, the number of i-faces H with $F < H < G$ equals c_i.

If F is an i-face and G a j-face with $F < G$, we call

$$G/F := \{H \in \mathcal{K} \mid F \leqslant H \leqslant G\}$$

a *section* of $\mathcal{K}$. It follows that G/F is an incidence complex in its own right, of rank $j - i - 1$ and with cardinal numbers $c_{i+1}, \ldots, c_{j-1}$. It is useful to identify a j-face G of $\mathcal{K}$ with the j-complex G/F_{-1}. Likewise, if F is an i-face, the $(k-i-1)$-complex F_k/F is the *co-face* of F in $\mathcal{K}$; if F is a vertex (and $i = 0$), this is also called the *vertex-figure* at F.

An *abstract k-polytope*, or simply *k-polytope*, is an incidence complex of rank k such that $c_i = 2$ for $i = 0, \ldots, k-1$ (see McMullen-Schulte [15]). Thus a polytope is a complex in which every flag has precisely one i-adjacent flag for each i. For polytopes, the last condition (I4) is also known as the *diamond condition*.

The *automorphism group* $\Gamma(\mathcal{K})$ of an incidence complex $\mathcal{K}$ consists of all order-preserving bijections of $\mathcal{K}$. We say that $\mathcal{K}$ is *regular* if $\Gamma(\mathcal{K})$ is transitive on the flags of $\mathcal{K}$. Note that a regular complex need not have a simply flag-transitive automorphism group (in fact, $\Gamma(\mathcal{K})$ may not even have a simply flag-transitive subgroup), so in general $\Gamma(\mathcal{K})$ has nontrivial flag-stabilizer subgroups. However, the group of a regular polytope is always simply flag-transitive.

It was shown in [21] (for a proof for polytopes see also [15, Ch. 2]) that the group $\Gamma := \Gamma(\mathcal{K})$ of a regular k-complex $\mathcal{K}$ has a well-behaved system of generating subgroups. Let $\Phi := \{F_{-1}, F_0, \ldots, F_k\}$ be a fixed, or *base flag*, of $\mathcal{K}$, where F_i designates the i-face in Φ for each i. For each $\Omega \subseteq \Phi$ let Γ_Ω denote the stabilizer of Ω in Γ. Then Γ_Φ is the stabilizer of the base flag Φ, and $\Gamma_\emptyset = \Gamma$. Moreover, for $i = -1, 0, \ldots, k$ set

$$R_i := \Gamma_{\Phi \setminus \{F_i\}} = \langle \varphi \in \Gamma \mid F_j\varphi = F_j \text{ for all } j \neq i \rangle.$$

Then each R_i contains Γ_Φ, and coincides with Γ_Φ when $i = -1$ or k; in particular,

$$c_i := |R_i : \Gamma_\Phi| \quad (i = 0, \ldots, k-1). \tag{1}$$

Moreover, these subgroups have the following commutation property:

$$R_i \cdot R_j = R_j \cdot R_i \qquad (-1 \leqslant i < j - 1 \leqslant k - 1). \tag{2}$$

Note here that R_i and R_j commute as subgroups, not generally at the level of elements.

The groups $R_{-1}, R_0, \ldots, R_k$ form a *distinguished system of generating subgroups* of Γ, that is,

$$\Gamma = \langle R_{-1}, R_0, \ldots, R_k \rangle. \tag{3}$$

Here the subgroups R_{-1} and R_k are redundant when $k > 0$. More generally, if Ω is a proper subset of Φ, then

$$\Gamma_\Omega = \langle R_i \mid -1 \leqslant i \leqslant k,\ F_i \notin \Omega \rangle.$$

For each nonempty subset I of $\{-1, 0, \ldots, k\}$ define $\Gamma_I := \langle R_i \mid i \in I \rangle$; and for $I = \emptyset$ define $\Gamma_I := R_{-1} = \Gamma_\Phi$. (As a warning, the notation $\Gamma_\emptyset$ can have two meanings, either as Γ_Ω with $\Omega = \emptyset$ or Γ_I with $I = \emptyset$; the context should make it clear which of the two is being used.) Thus

$$\Gamma_I = \Gamma_{\{F_j \mid j \notin I\}} \quad (I \subseteq \{-1, 0, \ldots, k\});$$

or equivalently,

$$\Gamma_\Omega = \Gamma_{\{i \mid F_i \notin \Omega\}} \quad (\Omega \subseteq \Phi).$$

The automorphism group Γ of $\mathcal{K}$ and its distinguished generating system satisfy the following important *intersection property*:

$$\Gamma_I \cap \Gamma_J = \Gamma_{I \cap J} \qquad (I, J \subseteq \{-1, 0, \ldots, k\}). \tag{4}$$

The combinatorial structure of $\mathcal{K}$ can be completely described in terms of the distinguished generating system of $\Gamma(\mathcal{K})$. In fact, bearing in mind that Γ acts transitively on the faces of each rank, the partial order is given by

$$F_i\varphi \leqslant F_j\psi \iff \psi^{-1}\varphi \in \Gamma_{\{i+1,\ldots,k\}}\Gamma_{\{-1,0,\ldots,j-1\}} \quad (-1 \leqslant i \leqslant j \leqslant k;\ \varphi, \psi \in \Gamma),$$

or equivalently,

$$F_i\varphi \leqslant F_j\psi \iff \Gamma_{\{-1,0,\ldots,k\}\setminus\{i\}}\varphi \cap \Gamma_{\{-1,0,\ldots,k\}\setminus\{j\}}\psi \neq \emptyset \quad (-1 \leqslant i \leqslant j \leqslant k;\ \varphi, \psi \in \Gamma). \tag{5}$$

Conversely, if Γ is any group with a system of subgroups $R_{-1}, R_0, \ldots, R_k$ such that (2), (3) and (4) hold, and $R_{-1} = R_k$, then Γ is a flag-transitive subgroup of the full automorphism group of a regular incidence complex $\mathcal{K}$ of rank k (see again [21], or [15, Ch. 2] for polytopes). The i-faces of $\mathcal{K}$ are the right cosets of $\Gamma_{\{-1,0,\ldots,k\}\setminus\{i\}}$ for each i, and the partial order is given by (5). The homogeneity parameters $c_0, \ldots, c_{k-1}$ are determined by (1).

For abstract regular polytopes, these structure results lie at the heart of much research activity in this area (see [15]). In this case the flag stabilizer Γ_Φ is the trivial group, and each nontrivial subgroup R_i (with $i \neq -1, k$) has order 2 and is generated by an involutory automorphism ρ_i that maps Φ to its unique i-adjacent flag. The group of an abstract regular polytope is then a *string C-groups*, meaning that the *distinguished involutory generators* $\rho_0, \ldots, \rho_{k-1}$ satisfy both the commutativity relations typical of a Coxeter group with string diagram, and the intersection property (4).

3 Power complexes

In this section we briefly review the construction of the *power complexes* $n^\mathcal{K}$, an interesting family of incidence complexes with n vertices on each edge, and with each vertex-figure isomorphic to $\mathcal{K}$ (see [22], and [15, Section 8D] for $n = 2$). These power complexes were first discovered by Danzer in the early 1980's; however, the construction announced in [7] was never published by Danzer, and first appeared in print in [22]. The power complexes $n^\mathcal{K}$, with $n = 2$ and $\mathcal{K}$ a polytope, are abstract polytopes and have attracted a lot of attention (see [15, Ch. 8]). In a sense, these power complexes are generalized cubes; and in certain cases (when $\mathcal{K}$ has simplex facets) they can also be viewed as cubical complexes (see [2; 18]). We briefly review some applications in Section 4.

To begin with, we say that an (incidence) complex $\mathcal{K}$ is *vertex-describable* if its faces are uniquely determined by their vertex-sets. A complex is vertex-describable if and only if its underlying face poset can be represented by a family of subsets of the vertex-set ordered by inclusion. If a complex $\mathcal{K}$ is a lattice, then $\mathcal{K}$ is vertex-describable. For example, the torus map $\mathcal{K} = \{4, 4\}_{(s,0)}$ is vertex-describable if and only if $s \geqslant 3$. The faces of a vertex-describable complex are again vertex-describable.

Now let $n \geqslant 2$ and define $N := \{1, \ldots, n\}$. Suppose $\mathcal{K}$ is a finite vertex-describable $(k-1)$-complex with v vertices and vertex-set $V := \{1, \ldots, v\}$. Then $\mathcal{P} := n^{\mathcal{K}}$ will be a finite k-complex with vertex-set

$$N^v = \bigotimes_{i=1}^{v} N, \tag{6}$$

the cartesian product of v copies of N; its n^v vertices are written as row vectors $\varepsilon := (\varepsilon_1, \ldots, \varepsilon_v)$. Now recall that, since $\mathcal{K}$ is vertex-describable, we may view the faces of $\mathcal{K}$ as subsets of V. With this in mind we take as j-faces of $\mathcal{P}$, for any $(j-1)$-face F of $\mathcal{K}$ and any vector $\varepsilon = (\varepsilon_1, \ldots, \varepsilon_v)$ in N^v, the subsets $F(\varepsilon)$ of N^v defined by

$$F(\varepsilon) := \{(\eta_1, \ldots, \eta_v) \in N^v \mid \eta_i = \varepsilon_i \text{ if } i \notin F\} \tag{7}$$

or, abusing notation, the cartesian product

$$F(\varepsilon) := (\bigotimes_{i \in F} N) \times (\bigotimes_{i \notin F} \{\varepsilon_i\}).$$

In other words, the j-face $F(\varepsilon)$ of $\mathcal{P}$ consists of the vectors in N^v that coincide with ε precisely in the components determined by the vertices of $\mathcal{K}$ not lying in the $(j-1)$-face F of $\mathcal{K}$. It follows that, if F, F' are faces of $\mathcal{K}$ and $\varepsilon = (\varepsilon_1, \ldots, \varepsilon_v)$, $\varepsilon' = (\varepsilon_1, \ldots, \varepsilon_v)$ are vectors in N^v, then $F(\varepsilon) \subseteq F'(\varepsilon')$ if and only if $F \leqslant F'$ in $\mathcal{K}$ and $\varepsilon_i = \varepsilon'_i$ for each i not contained in F'.

It can be shown that the set of all faces $F(\varepsilon)$, where F is a face of $\mathcal{K}$ and ε a vector in N^v, partially ordered by inclusion (and supplemented by the empty set as least face), is an incidence complex of rank k. This is the desired complex $\mathcal{P} = n^{\mathcal{K}}$.

The following theorem summarizes a number of key properties of power complexes.

Theorem 3.1. *Let $\mathcal{K}$ be a finite incidence complex of rank $k-1$ with v vertices, and let $\mathcal{K}$ be vertex-describable. Then the power complex $\mathcal{P} := n^{\mathcal{K}}$ has the following properties.*

(a) $\mathcal{P}$ is an incidence complex of rank k with vertex-set N^v and each vertex-figure isomorphic to $\mathcal{K}$.

(b) If F is a $(j-1)$-face of $\mathcal{K}$ and $\mathcal{F} := F/F_{-1}$ is the $(j-1)$-complex determined by F, then the j-faces of $\mathcal{P}$ of the form $F(\varepsilon)$ with ε in N^v are isomorphic to the power complex $n^{\mathcal{F}}$ of rank j.

(c) $\Gamma(\mathcal{P})$ contains a subgroup Λ isomorphic to $S_n \wr \Gamma(\mathcal{K}) = S_n^v \rtimes \Gamma(\mathcal{K})$, the wreath product of S_n and $\Gamma(\mathcal{K})$ defined by the natural action of $\Gamma(\mathcal{K})$ on the vertex-set of $\mathcal{K}$. Moreover, Λ acts vertex-transitively on $\mathcal{P}$ and has vertex stabilizers isomorphic to $S_{n-1} \wr \Gamma(\mathcal{K})$.

(d) If $\mathcal{K}$ is regular, then so is $\mathcal{P}$. In this case the subgroup Λ of $\Gamma(\mathcal{P})$ of part (c) acts flag-transitively on $\mathcal{P}$; in particular, if $n = 2$ and $\mathcal{K}$ is polytope, then $\Lambda = \Gamma(\mathcal{P})$.

Proof. For power complexes $2^{\mathcal{K}}$ regular polytopes $\mathcal{K}$ these facts are well-known (see [15, Section 8D] and [19; 22]). Here we briefly outline the proof for general power complexes, as no general proof has been published anywhere. So, as before, let $\mathcal{K}$ be a finite vertex-describable complex of rank $k-1$.

Begin by making the following important observation regarding inclusion of faces in $\mathcal{P}$: if $F(\varepsilon) \subseteq F'(\varepsilon')$, with $F, F', \varepsilon, \varepsilon'$ as above, then $F'(\varepsilon') = F'(\varepsilon)$. Thus, in designating the larger face we may take $\varepsilon' = \varepsilon$. It follows that every face containing a given vertex ε must necessarily be of the form $F(\varepsilon)$ with $F \in \mathcal{K}$, and that any two such faces $F(\varepsilon)$ and $F'(\varepsilon)$ are incident in $\mathcal{P}$ if and only if F and F' are incident in $\mathcal{K}$. As an immediate consequence, $\mathcal{P}$ must have vertex-figures isomorphic to $\mathcal{K}$. It is straightforward to prove that $\mathcal{P}$ actually is an incidence complex of rank k.

For part (b), let F be a $(j-1)$-face of $\mathcal{K}$ with v_F vertices and vertex-set V_F, and let ε be a vector in N^v. Now, if $F'(\varepsilon')$ is any face of $\mathcal{P}$ with $F'(\varepsilon') \subseteq F(\varepsilon)$ in $\mathcal{P}$, then necessarily $F' \leqslant F$ in $\mathcal{K}$ and $\varepsilon'_i = \varepsilon_i$ for each $i \notin F$; in other words, the vectors ε and ε' agree on each component representing a vertex i of $\mathcal{K}$ that lies outside F. It follows that the components of vectors in N^v corresponding to vertices i of $\mathcal{K}$ outside of F do not matter in determining the structure of the j-face $F(\varepsilon)$ of $\mathcal{P}$. Hence, if we omit these components and simply write

$\eta_F := (\eta_i)_{i\in F}$ for the "trace" of a vector η on F, then η_F lies in the cartesian product $N^{v_F} := \bigotimes_{i\in V_F} N$, and the faces $F(\varepsilon)$ and $F'(\varepsilon')$ of $\mathcal{P}$ can safely be designated by $F(\varepsilon_F)$ and $F'(\varepsilon'_F)$, respectively. Then, in particular, $F(\varepsilon_F) = N^{v_F}$ is the unique greatest face of $n^{\mathcal{F}}$, and $F'(\varepsilon'_F)$ becomes a face of $n^{\mathcal{F}}$. Moreover, the partial order on the j-face $F(\varepsilon)$ of $\mathcal{P}$ is just the standard inclusion of faces in $n^{\mathcal{F}}$. Thus, as a complex, $F(\varepsilon)$ is isomorphic to $n^{\mathcal{F}}$. This proves part (b).

The automorphism group $\Gamma(\mathcal{P})$ always contains a subgroup Σ isomorphic to S_n^v, the direct product of v copies of the symmetric group S_n. In fact, for each $i = 1, \ldots, v$, the symmetric group S_n can be viewed as acting on the i^{th} component of the vectors in N^v (while leaving all other components unchanged), and this action on the vertex-set N^v induces an action as a group of automorphisms on $\mathcal{P}$. In particular, Σ acts vertex-transitively on $\mathcal{P}$, so the same holds for $\Gamma(\mathcal{P})$ as well.

Moreover, $\Gamma(\mathcal{K})$ is naturally embedded in $\Gamma(\mathcal{P})$ as a subgroup of the vertex-stabilizer of $\varepsilon = (0, \ldots, 0)$ in $\Gamma(\mathcal{P})$. In fact, each automorphism φ of $\mathcal{K}$ determines an automorphism $\widehat{\varphi}$ of $\mathcal{P}$ as follows. Define $\widehat{\varphi}$ on the set of vertices $\eta = (\eta_1, \ldots, \eta_v)$ by [1]

$$(\eta)\widehat{\varphi} := (\eta_{(1)\varphi}, \ldots, \eta_{(v)\varphi}) =: \eta_\varphi,$$

and more generally on the set of faces $F(\eta)$ of $\mathcal{P}$ by

$$F(\eta)\widehat{\varphi} := (F\varphi)(\eta_\varphi).$$

Then it is straightforward to verify that $\widehat{\varphi}$ is indeed an automorphism of $\mathcal{P}$, and that $\widehat{\varphi}$ fixes $\varepsilon = (0, \ldots, 0)$. It follows that the two subgroups Σ and $\Gamma(\mathcal{K})$ together generate a subgroup Λ of $\Gamma(\mathcal{P})$ isomorphic to $S_n \wr \Gamma(\mathcal{K}) \cong S_n^v \rtimes \Gamma(\mathcal{K})$. Clearly, Λ acts vertex-transitively and has vertex-stabilizers isomorphic to $S_{n-1} \wr \Gamma(\mathcal{K})$. Now part (c) follows.

Finally, suppose $\mathcal{K}$ is regular. Then Λ acts flag-transitively on $\mathcal{P}$, and so does $\Gamma(\mathcal{P})$. Thus $\mathcal{P}$ is regular. If $n = 2$ and $\mathcal{K}$ is a regular polytope, then $\mathcal{P}$ is also a regular polytope and $\Gamma(\mathcal{P}) = \Lambda$. This proves part (d). □

We do not know of an example of a power complex $n^{\mathcal{K}}$, with $\mathcal{K}$ regular, where the full automorphism group of $n^{\mathcal{K}}$ is strictly larger than its subgroup $S_n \wr \Gamma(\mathcal{K})$.

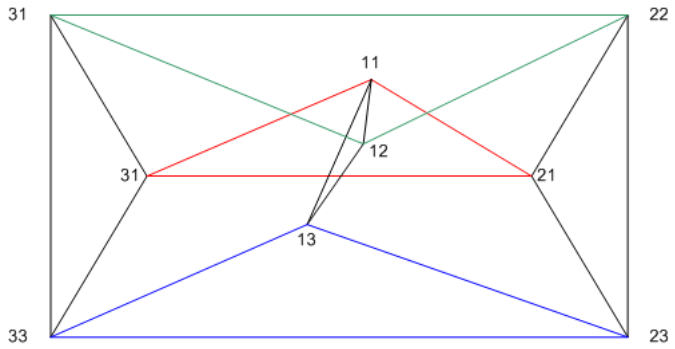

Figure 1: Combinatorics of the complex square γ_2^3

In Section 4, we discuss a number of interesting applications of the $n^{\mathcal{K}}$ construction. Here we just describe the most basic example obtained when $\mathcal{K} = \alpha_{v-1}$ (see [5]), the $(v-1)$-simplex (with v vertices). In this case $n^{\mathcal{K}}$ is combinatorially isomorphic to the *complex v-cube*

$$\gamma_v^n = n\{4\}2\{3\}2\cdots 2\{3\}2$$

in v-dimensional unitary complex v-space $\mathbb{C}^v$, that is, $n^{\alpha_{v-1}} = \gamma_v^n$. The unitary complex symmetry group of γ_v^n is isomorphic to $C_n \wr S_v$ (see Coxeter [6] and Shephard [23]). However, the combinatorial automorphism group of

[1] Throughout we write maps on the right.

γ_v^n is much larger when $n > 2$, and includes a subgroup isomorphic to $S_n \wr S_v$. The case $n = 2$ always gives the ordinary real v-cube $\gamma_v := \gamma_v^2 = \{4, 3^{v-2}\}$ (see [5]).

The combinatorics of the *complex square* $\gamma_2^3 = 3\{4\}2$ in $\mathbb{C}^2$ (obtained when $v = 2$ and $n = 3$) is illustrated in Figure 1; there are 9 vertices (denoted $i\,j$ with $i, j = 1, 2, 3$), each contained in 2 edges (drawn as 3-cycles), as well as 6 edges, each containing 3 vertices.

Now let $\mathcal{K}$ be an arbitrary incidence complex of rank k, and let $0 \leqslant j \leqslant k-1$. The *$j$-skeleton* $skel_j(\mathcal{K})$ of $\mathcal{K}$ is the incidence complex, of rank $j+1$, whose faces of rank less than or equal to j are those of $\mathcal{K}$, with the partial order inherited from $\mathcal{K}$; as greatest face, of rank $j+1$, we may simply take the greatest face of $\mathcal{K}$.

The following lemma says that taking skeletons and taking power complexes are commuting operations.

Lemma 3.2. *Let $\mathcal{K}$ be a finite vertex-describable k-complex, let $0 \leqslant j \leqslant k-1$, and let $n \geqslant 2$. Then*

$$skel_{j+1}(n^{\mathcal{K}}) = n^{skel_j(\mathcal{K})}.$$

Proof. The proof is straightforward. First note that a skeleton of a vertex-describable complex is again vertex-describable, with the same vertex set as the underlying complex. The proper faces of $skel_{j+1}(n^{\mathcal{K}})$ are the faces $F(\varepsilon)$ of $n^{\mathcal{K}}$ where F has rank at most j and ε lies in N^v. On the other hand, the proper faces of $n^{skel_j(\mathcal{K})}$ are of the form $F(\varepsilon)$ where F is a face of $skel_j(\mathcal{K})$ of rank at most j and ε lies in N^v. But the faces of $\mathcal{K}$ of rank at most j are precisely the faces of $skel_j(\mathcal{K})$ of rank at most j. Now the lemma follows. □

We conclude this section with a nice application of the lemma. Suppose $n \geqslant 2$ and $\mathcal{K}$ is the (unique) complex of rank 1 with v vertices. Now identifying $\mathcal{K}$ with $skel_0(\alpha_{v-1})$ we then have

$$n^{\mathcal{K}} = n^{skel_0(\alpha_{v-1})} = skel_1(n^{\alpha_{v-1}}) = skel_1(\gamma_v^n). \tag{8}$$

Thus the 2-complex $n^{\mathcal{K}}$ is isomorphic to the 1-skeleton of the unitary complex v-cube γ_v^n described above.

4 Applications

In this section we briefly review a number of interesting applications of the power complex construction that have appeared in the literature.

First suppose $n = 2$ and $\mathcal{K} = \{q\}$ is a q-gon with $3 \leqslant q < \infty$. It was shown in [15, Ch. 8D] that $2^{\{q\}}$ is isomorphic to Coxeter's regular map $\{4, q \mid 4^{\lfloor q/2 \rfloor - 1}\}$ in the 2-skeleton of the ordinary q-cube $\gamma_q = \{4, 3^{q-2}\}$, whose edge-graph coincides with that of the cube (see [4, p. 57]). In fact, the method of construction directly produces a realization of $2^{\{q\}}$ in the 2-skeleton of γ_q, which is identical with the realization outlined in [4]. This map and its realizations were rediscovered several times in the literature. For example, Ringel [20] and Beineke-Harary [1] established that the genus $2^{q-3}(q-4)+1$ of Coxeter's map is the smallest genus of any orientable surface into which the edge-graph of the q-cube can be embedded without self-intersections. It is rather surprising that each map $\{4, q \mid 4^{\lfloor q/2 \rfloor - 1}\}$, as well as its dual $\{q, 4 \mid 4^{\lfloor q/2 \rfloor - 1}\}$, can also be embedded as a polyhedron without self-intersections in ordinary 3-space (see McMullen-Schulz-Wills [17] and McMullen-Schulte-Wills [16]). When $q \geqslant 12$, the genus of this polyhedron exceeds the number of vertices, 2^q, of $\{4, q \mid 4^{\lfloor q/2 \rfloor - 1}\}$, which is somewhat hard to visualize.

When $n = 2$ and $\mathcal{K}$ is an abstract $2m$-polytope given by a neighborly simplicial $(2m-1)$-sphere, the corresponding power complex $2^{\mathcal{K}}$ gives an *m-Hamiltonian* $2m$-manifold embedded as a subcomplex of a higher-dimensional cube (see Kühnel-Schulz [12], Effenberger-Kühnel [9]). Recall here that a polytope is *neighborly* if any two of its vertices are joined by an edge. The m-Hamiltonicity then refers to the distinguished property that $2^{\mathcal{K}}$ contains the full m-skeleton of the ambient cube. In this sense, Coxeter's map $\{4, q \mid 4^{\lfloor q/2 \rfloor - 1}\}$ gives a 1-Hamiltonian surface.

The case when $n = 2$ and $\mathcal{K}$ is an (abstract) regular polytope has inspired a number of generalizations of the $2^{\mathcal{K}}$ construction that have proved important in the study of universality questions and extensions of regular polytopes (see [15, Ch. 8]). A particularly versatile generalization is to polytopes $2^{\mathcal{K},\mathcal{D}}$, where $\mathcal{K}$ is a vertex-describable

regular k-polytope with v vertices, and $\mathcal{D}$ is a Coxeter diagram on v nodes admitting a suitable action of $\Gamma(\mathcal{K})$ as a group of diagram symmetries. The corresponding Coxeter group $W(\mathcal{D})$ then can be extended by $\Gamma(\mathcal{K})$ to obtain the automorphism group $W(\mathcal{D}) \ltimes \Gamma(\mathcal{K})$ of a regular $(k+1)$-polytope denoted $2^{\mathcal{K},\mathcal{D}}$. This polytope is generally infinite, and its vertex-figures are isomorphic to $\mathcal{K}$. When $\mathcal{D}$ is the *trivial* diagram, without branches, on the vertex set of $\mathcal{K}$, the $(k+1)$-polytope $2^{\mathcal{K},\mathcal{D}}$ is isomorphic to the power complex $2^{\mathcal{K}}$ and the Coxeter group $W(\mathcal{D})$ is just C_2^v. This provides an entirely different construction of power complexes $2^{\mathcal{K}}$ based on regular polytopes $\mathcal{K}$.

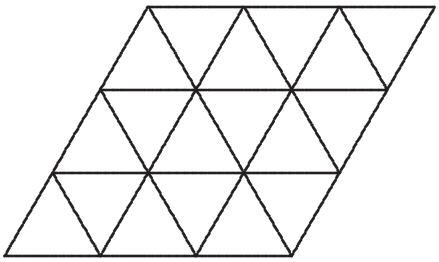

Figure 2: The torus map $\{3,6\}_{(3,0)}$

The polytopes $2^{\mathcal{K},\mathcal{D}}$ are very useful in the study of universal regular polytopes, as the following example illustrates (again, see [15, Ch. 8]). Let $\mathcal{K}$ be a (polytopal) regular map of type $\{3,r\}$ on a surface, for instance, a torus map $\{3,6\}_{(b,0)}$ or $\{3,6\}_{(b,b)}$ (see Figure 2). Suppose we wish to investigate regular 4-polytopes (if they exist) with cubes $\{4,3\}$ as facets and with copies of $\mathcal{K}$ as vertex-figures. In particular this would involve determining when the universal such structure, denoted

$$\mathcal{U} := \{\{4,3\},\mathcal{K}\},$$

is a finite polytope. It turns out that this universal polytope $\mathcal{U}$ always exists (for any $\mathcal{K}$), and that $\mathcal{U} = 2^{\mathcal{K},\mathcal{D}}$ for a certain Coxeter diagram $\mathcal{D}$ depending on $\mathcal{K}$ (see [15, Thm. 8E10]). In particular, $\mathcal{U}$ is finite if and only if $\mathcal{K}$ is neighborly. In this case $\mathcal{U} = 2^{\mathcal{K}}$ and $\Gamma(\mathcal{U}) = C_2^v \ltimes \Gamma(\mathcal{K})$ (and $\mathcal{D}$ is trivial). For example, if $\mathcal{K}$ is the hemi-icosahedron $\{3,5\}_5$ (with group $[3,5]_5$), then

$$\mathcal{U} = \{\{4,3\},\{3,5\}_5\} = 2^{\{3,5\}_5}$$

and

$$\Gamma(\mathcal{U}) = C_2 \wr [3,5]_5 = C_2^6 \ltimes [3,5]_5.$$

5 Coverings

In this section we investigate coverings of power complexes. We begin with some terminology; see [15, Ch. 2D] for similar notions for abstract polytopes.

Let $\mathcal{K}$ and $\mathcal{L}$ be (incidence) complexes of rank k. A map $\gamma : \mathcal{K} \to \mathcal{L}$ is called a *homomorphism* if γ preserves incidence in one direction; that is, $F\gamma \leqslant G\gamma$ in $\mathcal{L}$ whenever $F \leqslant G$ in $\mathcal{K}$. (Automorphisms are bijections that are order preserving in both directions.) A homomorphism γ is a *rap-map* if γ is rank preserving and adjacency preserving; that is, faces of $\mathcal{K}$ are mapped to faces of $\mathcal{L}$ of the same rank, and pairs of adjacent flags of $\mathcal{K}$ are mapped onto pairs of adjacent flags of $\mathcal{L}$. A surjective rap-map γ is called a *covering* (*map*). Similarly we call a homomorphism $\gamma : \mathcal{K} \to \mathcal{L}$ a *weak rap-map* if γ is rank preserving and *weakly adjacency preserving*, meaning that γ maps a pair of adjacent flags of $\mathcal{K}$ onto a pair of flags of $\mathcal{L}$ that are adjacent or identical.

Figure 3 illustrates an example of a covering $\gamma : \mathcal{K} \to \mathcal{L}$ between a hexagon $\mathcal{K}$ with vertices $1,\ldots,6$, and a triangle $\mathcal{L}$ with vertices $1,2,3$, given by $i, i+3 \mapsto i$ for $i = 1,2,3$. The edges are mapped by $\{i,i+1\}$, $\{i+3,i+4\} \mapsto \{i,i+1\}$. Thus γ wraps the hexagon twice around the triangle.

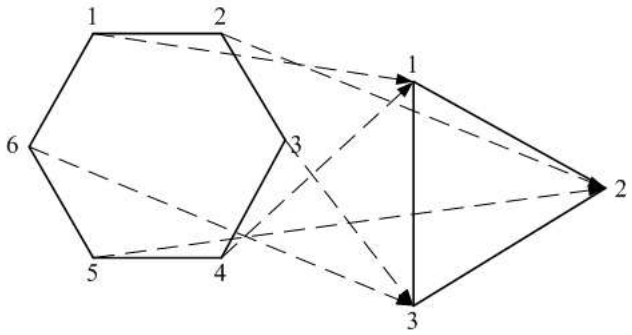

Figure 3: A hexagon wrapped around the triangle

Returning to the general discussion, let $\mathcal{K}$ be a k-complex and Σ be a subgroup of $\Gamma(\mathcal{K})$. Denote the set of orbits of Σ in $\mathcal{K}$ by $\mathcal{K}/\Sigma$, and the orbit of a face F of $\mathcal{K}$ by $F \cdot \Sigma$. Then introduce a partial ordering on $\mathcal{K}/\Sigma$ as follows: if $\widehat{F}, \widehat{G} \in \mathcal{K}/\Sigma$, then $\widehat{F} \leqslant \widehat{G}$ if and only if $\widehat{F} = F \cdot \Sigma$ and $\widehat{G} = G \cdot \Sigma$ for some faces F and G of $\mathcal{K}$ with $F \leqslant G$. The set $\mathcal{K}/\Sigma$ together with this partial order is the *quotient of $\mathcal{K}$ with respect to Σ*. The triangle in Figure 3 is a quotient of the hexagon obtained by identifying opposite vertices; here Σ is generated by the central involution in D_6, the group of the hexagon.

Coverings $n^{\mathcal{K}} \to m^{\mathcal{L}}$ with $n \geqslant m$.

The following theorem says that coverings between (vertex-describable) incidence complexes naturally induce coverings or weak coverings between the corresponding power complexes.

Theorem 5.3. *Let $\mathcal{K}$ and $\mathcal{L}$ be finite vertex-describable incidence complexes of rank k, and let $\gamma : \mathcal{K} \to \mathcal{L}$ be a covering. Moreover, let $n \geqslant m \geqslant 2$ and $f : \{1, \ldots, n\} \to \{1, \ldots, m\}$ be a surjective mapping. Then γ and f induce a weak covering $\pi_{\gamma,f} : n^{\mathcal{K}} \to m^{\mathcal{L}}$ between the power complexes $n^{\mathcal{K}}$ and $m^{\mathcal{L}}$. Moreover, $\pi_{\gamma,f}$ is a covering if and only if f is a bijection (and $n = m$).*

Proof. Suppose $V(\mathcal{K}) := \{1, \ldots, v(\mathcal{K})\}$ and $V(\mathcal{L}) := \{1, \ldots, v(\mathcal{L})\}$ are the vertex sets of $\mathcal{K}$ and $\mathcal{L}$, respectively. (It will be clear from the context if a label j refers to a vertex of $\mathcal{K}$ or a vertex of $\mathcal{L}$.) Then $v(\mathcal{L}) \leqslant v(\mathcal{K})$ since there is a covering map from $\mathcal{K}$ to $\mathcal{L}$. Define $N := \{1, \ldots, n\}$ and $M := \{1, \ldots, m\}$.

First note that a typical flag in $n^{\mathcal{K}}$ has the form

$$\Phi(\varepsilon) := \{\emptyset, \varepsilon, F_0(\varepsilon), \ldots, F_k(\varepsilon)\},$$

where ε is a vector in $N^{v(\mathcal{K})}$ and $\Phi := \{F_{-1}, F_0, \ldots, F_k\}$ is a flag of $\mathcal{K}$. Clearly, if $r \geqslant 1$ and Φ, Φ' are $(r-1)$-adjacent flags of $\mathcal{K}$, then $\Phi(\varepsilon), \Phi'(\varepsilon)$ are r-adjacent flags of $n^{\mathcal{K}}$. Similar statements also hold for $m^{\mathcal{L}}$.

Now consider the given covering map $\gamma : \mathcal{K} \to \mathcal{L}$. For a vertex j of $\mathcal{K}$ write $\overline{j} := j\gamma$, so $\overline{j}$ is a vertex of $\mathcal{L}$. Since γ is surjective, we may assume that the vertex labeling for $\mathcal{K}$ and $\mathcal{L}$ is such that the vertices $\overline{1}, \overline{2}, \ldots, \overline{v(\mathcal{L})}$ comprise all the vertices of $\mathcal{L}$, and in particular that $\overline{j} = j$ for each $j = 1, \ldots, v(\mathcal{L})$. Now define the mapping

$$\begin{array}{rccc} \pi_{\gamma,f}: & n^{\mathcal{K}} & \to & m^{\mathcal{L}} \\ & F(\varepsilon) & \to & (F\gamma)(\varepsilon_f), \end{array} \tag{9}$$

where as usual F denotes a face of $\mathcal{K}$ and ε a vector in $N^{v(\mathcal{K})}$, and

$$\varepsilon_f := (\varepsilon_1 f, \ldots, \varepsilon_{v(\mathcal{L})} f)$$

is the vector in $M^{v(\mathcal{L})}$ given by the images under f of the first $v(\mathcal{L})$ components of ε. We claim that $\pi := \pi_{\gamma,f}$ is a well-defined weak covering.

First we prove that π is well-defined. For a face F of a complex we let $V(F)$ denote its vertex set. Now suppose we have $F(\varepsilon) = F'(\varepsilon')$ in $n^{\mathcal{K}}$, where $\varepsilon = (\varepsilon_1, \ldots, \varepsilon_{v(\mathcal{K})})$ and $\varepsilon' = (\varepsilon'_1, \ldots, \varepsilon'_{v(\mathcal{K})})$ belong to $N^{v(\mathcal{K})}$ and F, F' are faces of $\mathcal{K}$. Then necessarily $F = F'$, since the vertex sets of F and F' must be the same; recall here that $\mathcal{K}$ is vertex-describable. Thus $F\gamma = F'\gamma$. Moreover, $\varepsilon_i = \varepsilon'_i$ for each $i \notin V(F) = V(F')$, so ε_f and ε'_f certainly agree on all components indexed by vertices i with $i \notin V(F)$. All other components of ε_f and ε'_f are indexed by a vertex i of F; but if $i \in V(F)$ then $\overline{i} = (i)\gamma \in V(F\gamma) = V(F'\gamma)$, and hence i indexes a component where entries are allowed to range freely over $M = (N)f$. Therefore, $(F\gamma)(\varepsilon_f) = (F'\gamma)(\varepsilon'_f)$. Thus π is well-defined. Clearly, π is a homomorphism since this is true for γ. For the same reason, π is rank-preserving and surjective.

It remains to show that π is weakly adjacency preserving. To this end, let

$$\Phi(\varepsilon) := \{\emptyset, \varepsilon, F_0(\varepsilon), \ldots, F_k(\varepsilon)\}, \quad \Phi'(\varepsilon') := \{\emptyset, \varepsilon', F'_0(\varepsilon'), \ldots, F'_k(\varepsilon')\}$$

be flags of $n^{\mathcal{K}}$, where

$$\Phi := \{F_{-1}, F_0, \ldots, F_k\}, \quad \Phi' := \{F'_{-1}, F'_0, \ldots, F'_k\}$$

are flags of $\mathcal{K}$ and $\varepsilon, \varepsilon'$ are vectors in $N^{v(\mathcal{K})}$. Suppose $\Phi(\varepsilon)$ and $\Phi'(\varepsilon')$ are r-adjacent for some $r \geqslant 0$. Then two possibilities can arise.

If $r > 0$, then $\varepsilon = \varepsilon'$ and Φ, Φ' must be $(r-1)$-adjacent flags of $\mathcal{K}$. It follows that $\varepsilon_f = \varepsilon'_f$, and that $\Phi\gamma, \Phi'\gamma$ are $(r-1)$-adjacent flags of $\mathcal{L}$ since γ is adjacency preserving. Hence the image flags of $\Phi(\varepsilon)$ and $\Phi'(\varepsilon')$ under π, which are given by

$$(\Phi(\varepsilon))\pi = \{\emptyset, \varepsilon_f, (F_0\gamma)(\varepsilon_f), \ldots, (F_k\gamma)(\varepsilon_f)\}$$

and

$$(\Phi'(\varepsilon'))\pi = \{\emptyset, \varepsilon'_f, (F'_0\gamma)(\varepsilon'_f), \ldots, (F'_k\gamma)(\varepsilon'_f)\}$$

respectively, are also r-adjacent. Thus, when $r > 0$, the map π takes r-adjacent flags of $n^{\mathcal{K}}$ to r-adjacent flags of $m^{\mathcal{L}}$.

Now suppose $r = 0$. Then $\Phi = \Phi'$ (but $\varepsilon \neq \varepsilon'$), since the faces F_s and F'_s of $\mathcal{K}$ must have the same vertex sets for each $s \geqslant 0$; bear in mind that $\mathcal{K}$ is vertex-describable. Moreover, since $F_0 = F'_0$ and $r \neq 1$, we have $F_0(\varepsilon) = F'_0(\varepsilon') = F_0(\varepsilon')$, so $\varepsilon_i = \varepsilon'_i$ for each vertex i of $\mathcal{K}$ distinct from $i_0 := F_0$; hence ε and ε' differ exactly in the position indexed by i_0. Then we certainly have $(F_s\gamma)(\varepsilon_f) = (F'_s\gamma)(\varepsilon'_f)$ for all $s \geqslant 0$. Hence $(\Phi(\varepsilon))\pi$ and $(\Phi'(\varepsilon'))\pi$ are either 0-adjacent or identical.

At this point we know that $\pi\colon n^{\mathcal{K}} \to m^{\mathcal{L}}$ is weakly adjacency preserving, that is, π is a weak covering. This proves the first part of the theorem.

Moreover, since the two vectors ε and ε' differ precisely in the position indexed by i_0, the corresponding shortened vectors $(\varepsilon_1, \ldots, \varepsilon_{v(\mathcal{L})})$ and $(\varepsilon'_1, \ldots, \varepsilon'_{v(\mathcal{L})})$ in $N^{v(\mathcal{L})}$ (underlying the definition of ε_f and ε'_f) also differ only in the position indexed by i_0; note here that $\overline{i_0} = i_0$, by our labeling of the vertices in $\mathcal{K}$ and $\mathcal{L}$. Hence the two vertices $\varepsilon_f = (\varepsilon_1 f, \ldots, \varepsilon_{v(\mathcal{L})} f)$ and $\varepsilon'_f = (\varepsilon'_1 f, \ldots, \varepsilon'_{v(\mathcal{L})} f)$ of $m^{\mathcal{L}}$ in $(\Phi(\varepsilon))\pi$ and $(\Phi'(\varepsilon'))\pi$, respectively, either coincide or differ in a single position, indexed by i_0; the former occurs precisely when $\varepsilon_{i_0} f = \varepsilon'_{i_0} f$. Therefore, since ε_{i_0} and ε'_{i_0} can take any value in N, the mapping π is a covering if and only if f is a bijection. This completes the proof. □

Coverings $n^{\mathcal{K}} \to m^{\mathcal{L}}$ with $n^l \geqslant m$.

The previous Theorem 5.3 describes quite general circumstances under which coverings or weak coverings between power complexes $n^{\mathcal{K}}$ and $m^{\mathcal{L}}$ are guaranteed to exist. Under the basic condition that $n \geqslant m$ this generally leads to a host of possible weak covering maps. Our next theorem deals with coverings or weak coverings between power complexes in situations where certain well-behaved (equifibered) coverings between the original complexes $\mathcal{K}$ and $\mathcal{L}$ exist. This also permits many examples with $n \leqslant m$.

To begin with, let $\mathcal{K}$ and $\mathcal{L}$ be finite vertex-describable complexes of rank k, and let $V(\mathcal{K}) := \{1, \ldots, v(\mathcal{K})\}$ and $V(\mathcal{L}) := \{1, \ldots, v(\mathcal{L})\}$, respectively, denote their vertex sets. Suppose there is a covering $\gamma\colon \mathcal{K} \to \mathcal{L}$ that is

equifibered (with respect to the vertices), meaning that the *fibers* $\gamma^{-1}(j)$ of the vertices j of $\mathcal{L}$ under γ all have the same cardinality, l (say). In other words, the restriction of γ to the vertex sets of $\mathcal{K}$ and $\mathcal{L}$ is $l:1$, so in particular $v(\mathcal{K}) = l \cdot v(\mathcal{L})$.

Important examples of this kind are given by the regular k-polytopes $\mathcal{K}$ that are (*properly*) *centrally symmetric*, in the sense that the group $\Gamma(\mathcal{K})$ contains a central involution that does not fix any of the vertices (see [15, p. 255]); any such central involution α pairs up the vertices of $\mathcal{K}$ and naturally determines an equifibered covering $\mathcal{K} \to \mathcal{K}/\langle\alpha\rangle$, of $\mathcal{K}$ onto its quotient $\mathcal{K}/\langle\alpha\rangle$, satisfying the desired property with $l = 2$.

Now returning to the general discussion, let $m, n \geqslant 2$ and l be as above. Define $N := \{1, \ldots, n\}$, $M := \{1, \ldots, m\}$ and $L := \{1, \ldots, l\}$. We wish to describe coverings $n^{\mathcal{K}} \to m^{\mathcal{L}}$ that can balance the effect of γ as an $l:1$ mapping on the vertex sets, by a controlled change in the base parameters from n to m, provided $m \leqslant n^l$. To this end, we may assume that the vertices of $\mathcal{K}$ and $\mathcal{L}$ are labeled in such a way that

$$\gamma^{-1}(j) = L_j := \{(j-1)l + 1, \ldots, (j-1)l + l\} \qquad (\text{for } j \in V(\mathcal{L})).$$

Thus for each j, the map γ takes the vertices of $\mathcal{K}$ in L_j to the vertex j of $\mathcal{L}$. By a slight abuse of notation, we then can write a vector $\varepsilon = (\varepsilon_1, \ldots, \varepsilon_{v(\mathcal{K})})$ in $N^{v(\mathcal{K})} = (N^l)^{v(\mathcal{L})}$ in the form $\varepsilon = (\widehat{\varepsilon}_1, \ldots, \widehat{\varepsilon}_{v(\mathcal{L})})$, where

$$\widehat{\varepsilon}_j := (\varepsilon_{(j-1)l+1}, \ldots, \varepsilon_{(j-1)l+l})$$

lies in N^l for each $j = 1, \ldots, v(\mathcal{L})$.

Now suppose that, in addition to γ, we also have a surjective mapping $g\colon N^l \to M$ (and hence $m \leqslant n^l$). Then γ and g determine a mapping

$$\begin{array}{rccc} \pi^{\gamma,g}\colon & n^{\mathcal{K}} & \to & m^{\mathcal{L}} \\ & F(\varepsilon) & \to & (F\gamma)(\varepsilon_g), \end{array} \tag{10}$$

where again F denotes a face of $\mathcal{K}$ and ε a vector in $N^{v(\mathcal{K})}$, and

$$\varepsilon_g := (\widehat{\varepsilon}_1 g, \ldots, \widehat{\varepsilon}_{v(\mathcal{L})} g)$$

is the vector in $M^{v(\mathcal{L})}$ given by the images under g of the components of ε in its representation as $(\widehat{\varepsilon}_1, \ldots, \widehat{\varepsilon}_{v(\mathcal{L})})$. We must prove that $\pi := \pi^{\gamma,g}$ is a covering.

First we must show that π is well-defined. Suppose we have $F(\varepsilon) = F'(\varepsilon')$ in $n^{\mathcal{K}}$, where $\varepsilon = (\varepsilon_1, \ldots, \varepsilon_{v(\mathcal{K})})$ and $\varepsilon' = (\varepsilon'_1, \ldots, \varepsilon'_{v(\mathcal{K})})$ belong to $N^{v(\mathcal{K})}$ and F, F' are faces of $\mathcal{K}$. Then, as in the proof of the previous theorem, $F = F'$, $F\gamma = F'\gamma$, and $\varepsilon_i = \varepsilon'_i$ for $i \notin V(F) = V(F')$. Now bear in mind that γ is a covering. Hence, if $i \in V(F)$ then $(i)\gamma \in V(F\gamma)$; or equivalently, if $j \notin V(F\gamma)$ then $V(F) \cap L_j = \emptyset$. It follows that, if $j \notin V(F\gamma)$, then $\varepsilon_i = \varepsilon'_i$ for every i in L_j, and therefore $\widehat{\varepsilon}_j = \widehat{\varepsilon'_j}$ and $\widehat{\varepsilon}_j g = \widehat{\varepsilon'_j} g$. Hence ε_g and ε'_g agree on every component represented by vertices of $\mathcal{L}$ outside of $F\gamma = F'\gamma$. As the remaining components are allowed to take any value in M, we conclude that $(F\gamma)(\varepsilon_g) = (F'\gamma)(\varepsilon'_g)$. Thus π is well-defined.

It is straightforward to verify that π is a rank-preserving surjective homomorphism. To show that π is also weakly adjacency preserving, let

$$\Phi(\varepsilon) := \{\emptyset, \varepsilon, F_0(\varepsilon), \ldots, F_k(\varepsilon)\}, \quad \Phi'(\varepsilon') := \{\emptyset, \varepsilon', F'_0(\varepsilon'), \ldots, F'_k(\varepsilon')\}$$

be r-adjacent flags of $n^{\mathcal{K}}$, where

$$\Phi := \{F_{-1}, F_0, \ldots, F_k\}, \quad \Phi' := \{F'_{-1}, F'_0, \ldots, F'_k\}$$

are flags of $n^{\mathcal{K}}$ and $\varepsilon, \varepsilon'$ lie in $N^{v(\mathcal{K})}$. Again two possibilities arise. First, if $r > 0$ then $\varepsilon = \varepsilon'$ and Φ, Φ' are $(r-1)$-adjacent in $\mathcal{K}$. Hence $\varepsilon_g = \varepsilon'_g$ and $\Phi\gamma, \Phi'\gamma$ are $(r-1)$-adjacent in $\mathcal{L}$. It follows that the two image flags under π,

$$\begin{aligned} (\Phi(\varepsilon))\pi &= \{\emptyset, \varepsilon_g, (F_0\gamma)(\varepsilon_g), \ldots, (F_k\gamma)(\varepsilon_g)\}, \\ (\Phi'(\varepsilon'))\pi &= \{\emptyset, \varepsilon'_g, (F'_0\gamma)(\varepsilon'_g), \ldots, (F'_k\gamma)(\varepsilon'_g)\}, \end{aligned}$$

are also r-adjacent. Now, if $r = 0$ then $\Phi = \Phi'$ (but $\varepsilon \neq \varepsilon'$); in fact, $V(F_s) = V(F'_s)$ and hence $F_s = F'_s$ for each $s \geqslant 0$. When $s = 0$ this gives $F_0(\varepsilon) = F'_0(\varepsilon') = F_0(\varepsilon')$ (since $r \neq 1$), and therefore $\varepsilon_i = \varepsilon'_i$ for each vertex i of $\mathcal{K}$ distinct from $i_0 := F_0$; hence ε and ε' only differ in the position indexed by i_0. This already implies that $(F_s\gamma)(\varepsilon_g) = (F'_s\gamma)(\varepsilon'_g)$ for all $s \geqslant 0$, and hence that $(\Phi(\varepsilon))\pi$ and $(\Phi'(\varepsilon'))\pi$ are weakly 0-adjacent flags of $m^{\mathcal{L}}$. Thus π is a weak covering.

Moreover, since $\varepsilon_i = \varepsilon'_i$ if and only if $i \neq i_0$, we also know that $\widehat{\varepsilon}_j = \widehat{\varepsilon'_j}$ if and only if $j \neq j_0 := (i_0)\gamma$. Hence the two vertices

$$\varepsilon_g := (\widehat{\varepsilon}_1 g, \ldots, \widehat{\varepsilon}_{v(\mathcal{L})} g), \quad \varepsilon'_g := (\widehat{\varepsilon'_1} g, \ldots, \widehat{\varepsilon'_{v(\mathcal{L})}} g)$$

of $m^{\mathcal{L}}$ lying in $(\Phi(\varepsilon))\pi$ and $(\Phi'(\varepsilon'))\pi$, respectively, either coincide or differ in a single position, indexed by j_0; the former occurs precisely when $\widehat{\varepsilon}_{j_0} g = \widehat{\varepsilon'_{j_0}} g$. Since $\widehat{\varepsilon}_{j_0}$ can take any value in N^l, the mapping π is a covering if and only if g is a bijection.

Finally, suppose g is a bijection, so in particular $m = n^l$. Then $n^{\mathcal{K}}$ and $m^{\mathcal{L}}$ must have the same number of vertices,

$$n^{v(\mathcal{K})} = n^{l \cdot v(\mathcal{L})} = m^{v(\mathcal{L})},$$

and hence π must be a covering that is one-to-one on the vertices.

In summary, we have established the following theorem.

Theorem 5.4. *Let $\mathcal{K}$ and $\mathcal{L}$ be finite vertex-describable incidence complexes of rank k, let $\gamma : \mathcal{K} \to \mathcal{L}$ be a covering, and let $m, n \geqslant 2$ and $l \geqslant 1$. Suppose that γ is equifibered with vertex fibers of cardinality l, and that $g : \{1, \ldots, n\}^l \to \{1, \ldots, m\}$ is a surjective mapping (and hence $m \leqslant n^l$). Then γ and g induce a weak covering $\pi^{\gamma,g} : n^{\mathcal{K}} \to m^{\mathcal{L}}$ between the power complexes $n^{\mathcal{K}}$ and $m^{\mathcal{L}}$. Moreover, $\pi^{\gamma,g}$ is a covering if and only if g is a bijection (and $m = n^l$); in this case $\pi^{\gamma,g}$ is one-to-one on the vertices.*

As an example consider finite regular polygons $\mathcal{K} = \{2p\}$ and $\mathcal{L} = \{p\}$, with $2p$ or p vertices, respectively, for some $p \geqslant 2$. The central symmetry of $\mathcal{K}$ gives an obvious equifibered covering $\gamma : \mathcal{K} \to \mathcal{L}$ between $\mathcal{K}$ and $\mathcal{L}$ with fibers of size $l = 2$. Now choose $m = n^2$ and pick any bijection $g : \{1, \ldots, n\}^2 \to \{1, \ldots, n^2\}$. Then

$$\pi^{\gamma,g} : n^{\{2p\}} \to (n^2)^{\{p\}}$$

is a covering. Either complex has n^{2p} vertices, and $\pi^{\gamma,g}$ is one-to-one on the vertices. For example, when $n = 2$ we obtain a covering

$$\pi^{\gamma,g} : 2^{\{2p\}} \to 4^{\{p\}}.$$

Here $2^{\{2p\}}$ is Coxeter's regular map $\{4, 2p \,|\, 4^{\lfloor p \rfloor - 1}\}$ described in Section 4.

Acknowledgements

Egon Schulte's work was supported by NSF-grant DMS–0856675.

Bibliography

[1] L.W. Beineke and F. Harary, The genus of the n-cube, *Canad. J. Math.* **17** (1965), 494–496.

[2] V.M. Buchstaber and T.E. Panov, *Torus actions and their applications in topology and combinatorics*, American Mathematical Society (Providence, RI, 2002).

[3] F. Buekenhout and A. Pasini, Finite diagram geometries extending buildings, In *Handbook of Incidence Geometry* (ed. F. Buekenhout), Elsevier Publishers (Amsterdam, 1995), 1143–1254.

[4] H.S.M. Coxeter, Regular skew polyhedra in 3 and 4 dimensions and their topological analogues, *Proc. London Math. Soc.* (2) **43** (1937), 33–62. (Reprinted with amendments in *Twelve Geometric Essays*, Southern Illinois University Press (Carbondale, 1968), 76–105.)

[5] H.S.M. Coxeter, *Regular Polytopes* (3rd edition), Dover (New York, 1973).

[6] H.S.M. Coxeter, *Regular Complex Polytopes* (2nd edition), Cambridge University Press (Cambridge, 1991).
[7] L. Danzer, Regular incidence-complexes and dimensionally unbounded sequences of such, I, In *Convexity and Graph Theory (Jerusalem 1981)*, North-Holland Math. Stud. 87, North-Holland (Amsterdam, 1984), 115–127.
[8] L.Danzer and E.Schulte, Reguläre Inzidenzkomplexe, I, *Geom. Dedicata* **13** (1982), 295–308.
[9] F. Effenberger and W. Kühnel, Hamiltonian Submanifolds of Regular Polytopes, *Discrete Comput. Geometry* **43** (2010), 242–262.
[10] B. Grünbaum, *Convex Polytopes*, Graduate Texts in Mathematics, Springer, 2003.
[11] B. Grünbaum, Regularity of graphs, complexes and designs, In *Problèmes combinatoires et théorie des graphes*, Coll. Int. C.N.R.S. 260, Orsey (1977), 191–197.
[12] W. Kühnel and C. Schulz, Submanifolds of the cube, In *Applied Geometry and Discrete Mathematics, The Victor Klee Festschrift* (P. Gritzmann, B. Sturmfels, eds.), DIMACS Series in Discrete Math. and Theor. Comp. Sci., vol. 4, pp. 423Ð432. Am. Math. Soc. (Providence, 1991).
[13] W. Kühnel, *Tight Polyhedral Submanifolds and Tight Triangulations*, Lecture Notes in Mathematics Vol. 1612, Springer-Verlag (Berlin-Heidelberg-New York, 1995).
[14] D. Leemans, *Residually weakly primitive and locally two-transitive geometries for sporadic groups*, Acad. Roy. Belgique, Mem. Cl. Sci., Coll. 4, Ser. 3, Tome XI(2008).
[15] P. McMullen and E. Schulte, *Abstract regular polytopes*, Encyclopedia of Mathematics and its Applications, Vol. 92, Cambridge University Press, Cambridge, UK, 2002.
[16] P. McMullen, E. Schulte and J.M. Wills, Infinite series of combinatorially regular maps in three-space, *Geom. Dedicata* **26** (1988), 299–307.
[17] P. McMullen, Ch. Schulz and J.M. Wills, Polyhedral manifolds in E^3 with unexpectedly large genus, *Israel J. Math.* **46** (1983), 127–144.
[18] S.P. Novikov, *Topology 1, Contemporary Problems of Mathematics, Fundamental Directions*, Vol. 12, VINITI, Moscow, 1986; English transl., Encyclopedia Math. Sci., Vol. 12, Springer-Verlag, BerlinÐNew York, 1988.
[19] T. Pisanski, E. Schulte and A. Ivić Weiss, On the size of equifacetted semi-regular polytopes, *Glasnik Matematički* (10 pp, to appear).
[20] G. Ringel, Über drei kombinatorische Probleme am n-dimensionalen Würfel und Würfelgitter, *Abh. Math. Sem. Univ. Hamburg* **20** (1956), 10–19.
[21] E. Schulte, Reguläre Inzidenzkomplexe, II, *Geom. Dedicata* **14** (1983), 33–56.
[22] E. Schulte, Extensions of regular complexes, In *Finite Geometries* (eds. C.A. Baker and L.M. Batten), Lecture Notes Pure Applied Mathematics **103**, Marcel Dekker (New York, 1985), 289–305.
[23] G.C. Shephard, Regular complex polytopes, *Proc. London Math. Soc.* (3) **2** (1952), 82–97.
[24] J. Tits, *Buildings of Spherical type and finite BN-Pairs*, Lecture Notes in Mathematics Vol. 386, Springer-Verlag (New York-Heidelberg-Berlin, 1974).

Authors' Information

Andrew Duke *- Northeastern University, Boston, Massachussetts, USA, 02115*

Egon Schulte *- Northeastern University, Boston, Massachussetts, USA, 02115*

A BRIEF SURVEY OF METRICS IN CODING THEORY

Ernst Gabidulin

Abstract: *The main objects of Coding theory are metric vector or matrix spaces. Subsets of spaces are known as codes. The main problem is constructing codes of given pairwise distance and having maximal cardinality. Most known and most investigated spaces are Hamming spaces. Thousands papers and books are devoted to codes in the Hamming metric. We mention here only two books [1; 2] and will not consider this metric in details. Other metrics are investigated much less. In this paper, we give many examples of useful metrics. It is still non exhaustive review.*

Keywords: *metrics and norms, the uniform and non-uniform Hamming metrics, the Lee and Sharma-Kaushik metrics, the city block (Manhattan) metric, the Varshamov metric, the burst metric, the 2-dimensional burst metric, the term rank metric, the rank metric, combinatorial metrics, projective metrics, graph metrics, the subspace metric.*

ACM Classification Keywords: A.0 General Literature - Conference proceedings

MSC*: 94B05, 94B20, 94B25*

Introduction

Coding theory studies techniques to correct errors arising during communications through noisy channels. Its distinguishing features are using discrete signals and introducing the artificial redundancy. Discrecity allows to describe signals in terms of abstract symbols not connected with any physical realization. The artificial redundancy gives possibilities to correct errors using hard enough combinatorial constructions of signals. One can say that coding theory uses a wide spectrum of mathematical tools from simple binary arithmetic to modern algebraic geometry. The main objects of Coding theory are metric vector spaces. Subsets of spaces are known as codes. Main problem is constructing codes of given cardinality and having maximal pairwise distance as large as possible. Most known and most investigated spaces are Hamming spaces. The distance function between two vectors is defined as the number of non identical their coordinates. Thousands papers and books are devoted to the Hamming metrics. We mention here only two books [1; 2]. Other metrics are investigated much less.

In this paper, we describe connections between channels and metrics and give many examples of useful metrics. It is still non exhaustive review. Also it is important to mention that not all metrics allow the good mathematic theory.

General properties of codes

Let $\mathcal{X}$ be an alphabet of q elements. Let $\mathcal{X}^n$ be the space of all vectors over $\mathcal{X}$ of dimension n.

A code $\mathcal{C} \subseteq \mathcal{X}^n$ of size $|\mathcal{C}| = M$ and length n is defined as any set of n-vectors over $\mathcal{X}^n$:

$$\mathcal{C} = \{\underline{\mathbf{x}}_1, \underline{\mathbf{x}}_2, \ \ldots, \underline{\mathbf{x}}_M\}.$$

We assume also that the space of vectors $\mathcal{X}^n$ is considered as a *metric* space. A metric can be defined either by a *distance function*, or by a *norm function*.

We shall consider only integer-valued distance functions and norms.

A distance $d(\underline{\mathbf{x}}, \underline{\mathbf{y}})$ between a n-vectors $\underline{\mathbf{x}}, \underline{\mathbf{y}}$ is a function satisfying conditions

$$\begin{array}{rcll} d(\underline{\mathbf{x}}, \underline{\mathbf{y}}) & \geq & 0, \ \forall \ \underline{\mathbf{x}}, \underline{\mathbf{y}}; & \text{(Non-negative).} \\ d(\underline{\mathbf{x}}, \underline{\mathbf{y}}) & = & 0 \iff \underline{\mathbf{x}} = \underline{\mathbf{y}}; & \text{(Zero value).} \\ d(\underline{\mathbf{x}}, \underline{\mathbf{y}}) & = & d(\underline{\mathbf{y}}, \underline{\mathbf{x}}); & \text{(Symmetry).} \\ d(\underline{\mathbf{x}}, \underline{\mathbf{y}}) & \leq & d(\underline{\mathbf{x}}, \underline{\mathbf{z}}) + d(\underline{\mathbf{z}}, \underline{\mathbf{y}}), \ \forall \ \underline{\mathbf{x}}, \underline{\mathbf{y}}, \underline{\mathbf{z}} & \text{(Triangle inequality).} \end{array}$$

A norm function $\mathcal{N}(\underline{\mathbf{x}})$ should satisfy next axioms:

$$\begin{array}{rcll} \mathcal{N}(\underline{\mathbf{x}}) & \geq & 0, \ \forall \ \underline{\mathbf{x}}; & \text{(Non-negative).} \\ \mathcal{N}(\underline{\mathbf{x}}) & = & 0 \iff \underline{\mathbf{x}} = 0; & \text{(Zero value).} \\ \mathcal{N}(\underline{\mathbf{x}} + \underline{\mathbf{y}}) & \leq & \mathcal{N}(\underline{\mathbf{x}}) + \mathcal{N}(\underline{\mathbf{y}}), \ \forall \ \underline{\mathbf{x}}, \underline{\mathbf{y}} & \text{(Triangle inequality).} \end{array}$$

The norm function allows to construct the distance function as follows:

$$d(\underline{\mathbf{x}}, \underline{\mathbf{y}}) := \mathcal{N}(\underline{\mathbf{x}} - \underline{\mathbf{y}}).$$

Often distance and norm functions are defined coordinate-wise. A distance $d(x, y)$ between letters of the alphabet $\mathcal{X}$ (respectively, $\mathcal{N}(x), \ x \in \mathcal{X}$) is defined first. Assume that the distance takes all values $0, 1, \ldots, D$, where D is the maximal possible value. Then the distance between n-vectors $\underline{\mathbf{x}}, \underline{\mathbf{y}} \in \mathcal{X}^n$ is defined as follows:

$$d(\underline{\mathbf{x}}, \underline{\mathbf{y}}) = \sum_{i=1}^{n} d(x_i, y_i).$$

This distance takes values $0, 1, \ldots, nD$.

There exist still distance functions which are not coordinate-wise. For instance, the Varshamov distance and the rank distance (see, below) can not be represented in such a manner.

Similarly, for the coordinate-wise norm, we have

$$\mathcal{N}_n(\underline{\mathbf{x}}) = \sum_{i=1}^{n} \mathcal{N}(x_i).$$

It is useful for applications to introduce the generator norm function

$$W(z) = \sum_{i=0}^{D} N(i) z^i,$$

where $N(i) = |x \in \mathcal{X} : \mathcal{N}(x) = i| \ , \ i = 0, 1, \ldots, D$, is the number of elements $\mathcal{X}$ with norm i. D means the maximal norm.

The generator norm function of the extended norm $\mathcal{N}_n(\cdot)$ is clearly

$$W_n(z) = \sum_{i=0}^{nD} N_n(i) z^i = W(z)^n = \left(\sum_{i=0}^{D} N(i) z^i \right)^n .$$

We shall consider metrics defined by a coordinate-wise norm $\mathcal{N}_n(\cdot)$. The main problem of coding theory is constructing codes $\mathcal{C}_n \subseteq \mathcal{X}^n$ of maximal cardinality M if minimal distance d is given. For a metric on $\mathcal{X}$ we define the *average norm* $\overline{N}$ and the *average* pair-wise *distance* $\overline{D}$ by

$$\begin{array}{rcccl} \overline{N} & = & \frac{\sum\limits_{x \in \mathcal{X}} \mathcal{N}(x)}{q} & = & \frac{\sum\limits_{i=0}^{D} i N(i)}{q}; \\ \overline{D} & = & \frac{\sum\limits_{x \in \mathcal{X}} \sum\limits_{y \in \mathcal{X}} \mathcal{N}(x-y)}{q(q-1)} & = & \frac{\sum\limits_{x \in \mathcal{X}} \overline{N}(x)}{q}, \end{array}$$

where $\overline{N}(x)$ denotes the average distance from $\mathcal{X}\backslash x$ to x.

If $\mathcal{X}$ is an additive group, then $\overline{N}(x)$ does not depend on x. Moreover $\overline{N}(x) = \frac{q}{q-1}\overline{N}$. Hence in this case $\overline{D} = \frac{q}{q-1}\overline{N}$.

For the extended metric $\mathcal{N}_n(\underline{\mathbf{x}})$ we have $\overline{N}_n = \overline{N}n,\ \overline{D}_n = \frac{q^n}{q^n-1}\overline{N}_n$.

If $\mathcal{C}_n$ is a code of cardinality M and of distance $d > \overline{N}_n$, then the Plotkin-style bound is valid:

$$M \leq \frac{d}{d - \overline{N}_n}.$$

Let

$$S_{d-1}(\underline{\mathbf{0}}) = \left\{\underline{\mathbf{y}} :\ \mathcal{N}_N(\underline{\mathbf{y}}) \leq d-1\right\}$$

be the ball of radius $d-1$ with the center at the all zero vector $\underline{\mathbf{0}}$. Then asymptotically, when $n \to \infty$ and $x = \frac{d-1}{Dn} < \overline{N}$, the volume of the ball is equal to

$$V_{d-1} = |S_{d-1}(\underline{\mathbf{0}})| \asymp cq^{n(1-R)},$$

where

$$\begin{aligned} 1 - R &= H(\alpha_0, \alpha_1, \ldots, \alpha_D) + \sum_{i=1}^{D} \alpha_i \log_q N_i; \\ \alpha_i &= \tfrac{N_i \gamma^i}{W(\gamma)}, \quad i = 0, 1, \ldots, D; \\ \gamma &\quad \text{is the positive root of} \quad \tfrac{\gamma W'(\gamma)}{W(\gamma)} = xD, \\ H(\alpha_0, \alpha_1, \ldots, \alpha_D) &= -\sum_{i=0}^{D} \alpha_i \log_q \alpha_i. \end{aligned}$$

It follows the upper Gilbert-style bound for a code with rate $R = \frac{\log_q M}{n}$ and distance $d - 1 = xDn$:

$$R = 1 - H(\alpha_0, \alpha_1, \ldots, \alpha_D) - \sum_{i=1}^{D} \alpha_i \log_q N_i.$$

One can show that this equation can be reduced to the next simple form:

$$\begin{aligned} R &= 1 - \log_q W(\gamma) + xD \log \gamma; \\ xD &= \tfrac{\gamma W'(\gamma)}{W(\gamma)}. \end{aligned}$$

Examples of metrics

Hamming metric

The most known is the Hamming metric.

The Hamming norm $w_H(\underline{\mathbf{x}})$ of a vector $\underline{\mathbf{x}}$ is defined as the number of its non zero coordinates.

The Hamming distance between $\underline{\mathbf{x}}$ and $\underline{\mathbf{y}}$ is the norm of its difference: $d(\underline{\mathbf{x}}, \underline{\mathbf{y}}) = w_H(\underline{\mathbf{x}} - \underline{\mathbf{y}})$.

The Hamming metric is matched strongly with all full symmetrical memoryless channels.
Full symmetrical channels are channels such that all non diagonal elements of the transfer probability matrix are identical.

Huge amount of papers are devoted to this metric.

Norms and metrics for $\mathbb{Z}_q$

Let the alphabets $\mathcal{X}$ be the integer ring $\mathbb{Z}_q = \{0, 1, \ldots, q-1\}$. Integer-valued norms and metrics can be defined in many ways.

It is clear that for any norm $\mathcal{N}(i) = \mathcal{N}(q-i),\ i \in \mathbb{Z}_q$.

All elements of $\mathbb{Z}_q$ can be divided into subsets of equal weight elements $B_j = \{a : a \in \mathbb{Z}_q,\ \mathcal{N}(a) = j\}\,,\ j = 0, 1, \ldots, D$, where $D \leq \left\lfloor \frac{q}{2} \right\rfloor$ is the maximal norm. If $a \in B_j$, then also $q - a \in B_j$.
The maximal norm D can take values between 1 and $\left\lfloor \frac{q}{2} \right\rfloor$.

Open problem: find all possible values of D for $\mathbb{Z}_q$.

Open problem: describe all non-equivalent norms for $\mathbb{Z}_q$.

Two extreme cases are the **Hamming** metric ($D = 1$) and the **Lee** metric ($D = \left\lfloor \frac{q}{2} \right\rfloor$).

The Hamming metric is defined by

$$\mathcal{N}(i) = \begin{cases} 0, & \text{if } i = 0; \\ 1, & \text{if } i = 1, \ldots, q-1; \end{cases} \quad ,$$

so $D = 1$. The subsets of equal weight elements are

$$B_0 = \{0\}\,,\ B_1 = \{1, 2, \ldots, q-1\}\,.$$

The Lee metric is defined by

$$\mathcal{N}(i) = \begin{cases} 0, & \text{if } i = 0; \\ i, & \text{if } 1 \leq i \leq \left\lfloor \frac{q}{2} \right\rfloor; \\ \mathcal{N}(q-i), & \text{if } \left\lfloor \frac{q}{2} \right\rfloor < i \leq q-1; \end{cases} \quad ,$$

so $D = \left\lfloor \frac{q}{2} \right\rfloor$. The subsets of equal weight elements are

$$B_0 = \{0\}\,,\ B_1 = \{1, q-1\}\,, B_2 = \{2, q-2\}\,, \ldots, B_{\left\lfloor \frac{q}{2} \right\rfloor} = \left\{ \left\lfloor \frac{q}{2} \right\rfloor, q - \left\lfloor \frac{q}{2} \right\rfloor \right\}.$$

Main results for codes with the Lee metric were obtained by Berlekamp [7]:

- The weight generator function

$$W(z) = \begin{cases} 1 + 2z + 2z^2 + \cdots + 2z^{\frac{q-1}{2}}, & \text{if } q \text{ odd}; \\ 1 + 2z + 2z^2 + \cdots + 2z^{\frac{q-2}{2}} + z^{\frac{q}{2}}, & \text{if } q \text{ even}. \end{cases}$$

- The average vector weight

$$\overline{N}_n = \begin{cases} n\frac{q^2-1}{4q}, & \text{if } q \text{ odd}; \\ n\frac{q}{4}, & \text{if } q \text{ even}. \end{cases}$$

- The Plotkin-style bound for cardinality M of a code with Lee distance d:

$$M \leq \frac{d}{d - \overline{N}_n},\ \text{if } d > \overline{N}_n.$$

- The asymptotic Gilbert-style bound: a code with cardinality M and Lee distance d exists, if

$$\begin{aligned} R = \frac{\log_q M}{n} &= 1 - \log_q W(\gamma) + xD \log \gamma; \\ xD &= \frac{\gamma W'(\gamma)}{W(\gamma)}, \end{aligned}$$

where $D = \left\lfloor \frac{q}{2} \right\rfloor$ and $xD = \frac{d-1}{n}$.

All non-equivalent norms for $\mathbb{Z}_4$

1. The Hamming metrics with the subsets of equal weight elements $B_0 = \{0\},\ B_1 = \{1,2,3\}$, and with the distance matrix

$$\mathbf{D} = \left[\begin{array}{c|cccc} x\backslash y & 0 & 1 & 2 & 3 \\ \hline 0 & 0 & 1 & 1 & 1 \\ 1 & 1 & 0 & 1 & 1 \\ 2 & 1 & 1 & 0 & 1 \\ 3 & 1 & 1 & 1 & 0 \end{array}\right].$$

2. The Lee metrics with the subsets of equal weight elements $B_0 = \{0\},\ B_1 = \{1,3\}, B_2 = \{2\}$, and with the distance matrix

$$\mathbf{D} = \left[\begin{array}{c|cccc} x\backslash y & 0 & 1 & 2 & 3 \\ \hline 0 & 0 & 1 & 2 & 1 \\ 1 & 1 & 0 & 1 & 2 \\ 2 & 2 & 1 & 0 & 1 \\ 3 & 1 & 2 & 1 & 0 \end{array}\right].$$

3. A new non-Lee metrics (never investigated) with the subsets of equal weight elements $B_0 = \{0\},\ B_1 = \{2\}, B_2 = \{1,3\}$, and with the distance matrix

$$\mathbf{D} = \left[\begin{array}{c|cccc} x\backslash y & 0 & 1 & 2 & 3 \\ \hline 0 & 0 & 2 & 1 & 2 \\ 1 & 2 & 0 & 2 & 1 \\ 2 & 1 & 2 & 0 & 2 \\ 3 & 2 & 1 & 2 & 0 \end{array}\right].$$

Sharma-Kaushik metrics for $\mathbb{Z}_q$

Many norms for $\mathbb{Z}_q$ were proposed by Sharma and Kaushik [3; 4; 5; 6].

The Sharma-Kaushik norm $\mathcal{N}_{SK}$ is defined in terms of disjoint sets $B_0 \bigcup B_1 \bigcup \cdots \bigcup B_{m-1}$ with conditions:

1. $B_0 = \{0\}$.

2. If $x \in B_i$, then $q - x \in B_i$.

3. If $x \in B_i, y \in B_j$ and $i < j$, then the **Lee** norm $\mathcal{N}_{Lee}(x) < \mathcal{N}_{Lee}(y)$.

4. $|B_0| \leq |B_1| \leq \cdots \leq |B_{m-2}|$, but $|B_{m-1}| \geq |B_{m-2}|/2$.

5. $\mathcal{N}_{SK}(x) = s \Longleftrightarrow x \in B_s$.

6. $d_{SK}(\underline{\mathbf{x}}, \underline{\mathbf{y}}) = \sum_{i=1}^{n} \mathcal{N}_{SK}(x_i - y_i)$

Example: Sharma-Kaushik metrics for $\mathbb{Z}_9$.

Let

$$1.\ B_0 = \{0\}, B_1 = \{1,8\}, B_2 = \{2,3,6,7\}, B_3 = \{4,5\}.$$

This is a Sharma-Kaushik metric.

Let

$$2.\ B_0 = \{0\}, B_1 = \{4,5\}, B_2 = \{2,3,6,7\}, B_3 = \{1,8\}.$$

This is not a metric because Triangle inequality axiom is not satisfied: $\mathcal{N}(4+4) = \mathcal{N}(8) = 3 > \mathcal{N}(4)+\mathcal{N}(4) = 2$.

City block metric

The city block metric is known also as the Manhattan metric, or, the modular metric.

Let $\underline{\mathbf{x}} = (x_1, x_2, \ldots, x_n)$ and $\underline{\mathbf{y}} = (y_1, y_2, \ldots, y_n)$ be integer-valued vectors, $x_i,\ y_i \in \{0, 1, \ldots, q-1\}, i = 1, 2, \ldots, n$. Then the distance function is defined by

$$d_M(\underline{\mathbf{x}}, \underline{\mathbf{y}}) = \sum_{i=1}^{n} |x_i - y_i|.$$

This metrics is popular in psychology and related areas but not well known in communications. The possible reason is that *there exist no channels* matched MLD with city block metrics, *there exist no channels* matched MDD with city block metrics. Still channels exist matched ECD with city block metrics. Such channels appear when a signal limiter is used at the receiver. Error correcting was investigated first by [8] (without any metrics). Few results and code constructions are known. We present several new results.

- The weight generator function

$$W(z) = 1 + z + z^2 + \cdots + z^{q-1}.$$

- The average vector weight

$$\overline{N} = \frac{q-1}{2}; \quad \overline{N}_n = n\frac{q-1}{2}.$$

- The average pair-wise distance

$$\overline{D} = \frac{q+1}{3}; \quad \overline{D}_n = n\frac{q+1}{3}\frac{q^n - q^{n-1}}{q^n - 1}.$$

- The Plotkin-style bound for cardinality M of a code with city block distance d:

$$M \leq \frac{d}{d - \overline{N}_n}, \text{ if } d > \overline{N}_n.$$

- The asymptotic Gilbert-style bound is unknown for city block metrics because balls of radius t have different cardinalities for different centers. For example, if $q = 3, n = 3, t = 3$, then the ball with the center $(0, 0, 0)$ has cardinality 17, while the ball with the center $(1, 1, 1)$ has cardinality 27, i.e., contains all elements!
  For integer s, define the s-ary entropy by

$$H_s(x) = x\log_s(s-1) - x\log_s x - (1-x)\log_s(1-x).$$

  We explain by examples how to derive the alternative bound. Let $q = 3$. We want to get the rate as a function of the normalized minimal city distance $x = \frac{d}{n(q-1)} = \frac{d}{2n}$. Note that any ternary code in the Hamming metric with minimal distance d_H is a code with the same distance in city block metric. We have the Gilbert bound for these codes in the form

$$R_1 = 1 - H_3\left(\frac{d_H}{n}\right),$$

  or, in terms of city block distance

$$R_{1CB} = 1 - H_3(2x),$$

  Hence we have the non-zero rate for small distances $2x \leq 2/3$. It goes to the 1, when x runs to 0. Consider now *binary* codes in the Hamming metrics with distance d_H. If we replace each "1" in code words

by $q-1=2$, we obtain a code in city block metrics with minimal distance $d=(q-1)d_H=2d_H$. We have the Gilbert bound for these codes in the form

$$R_2=1-H_2\left(\frac{d_H}{n}\right),$$

or, in terms of city block distance

$$R_{2CB}=(1-H_2(x))\log_3 2.$$

It gives the non-zero exponent for all allowable distances but for small distances the rate is less than 1. We get, combine both bounds, that a code with cardinality $M=q^{nR_{CB}}$ and with city block distance $d=x(q-1)n$ exists, if

$$R^{(3)}_{CB}=\max\left\{R_{1CB},R_{2CB}\right\}=\max\left\{1-H_3(2x),(1-H_2(x))\log_3 2\right\},$$

for $0\le x\le\frac{1}{2}$. We can obtain in a similar manner for $q=5$ that

$$R^{(5)}_{CB}=\max\left\{R^{(5)}_{1CB},R^{(5)}_{2CB},R^{(5)}_{3CB}\right\},$$

where

$$\begin{aligned}R^{(5)}_{1CB}&=1-H_5(5x);\\ R^{(5)}_{2CB}&=(1-H_3(2x))\log_5 3;\\ R^{(5)}_{3CB}&=(1-H_2(x))\log_5 2.\end{aligned}$$

Rates as functions of the normalized city block distance are shown on Fig.1.

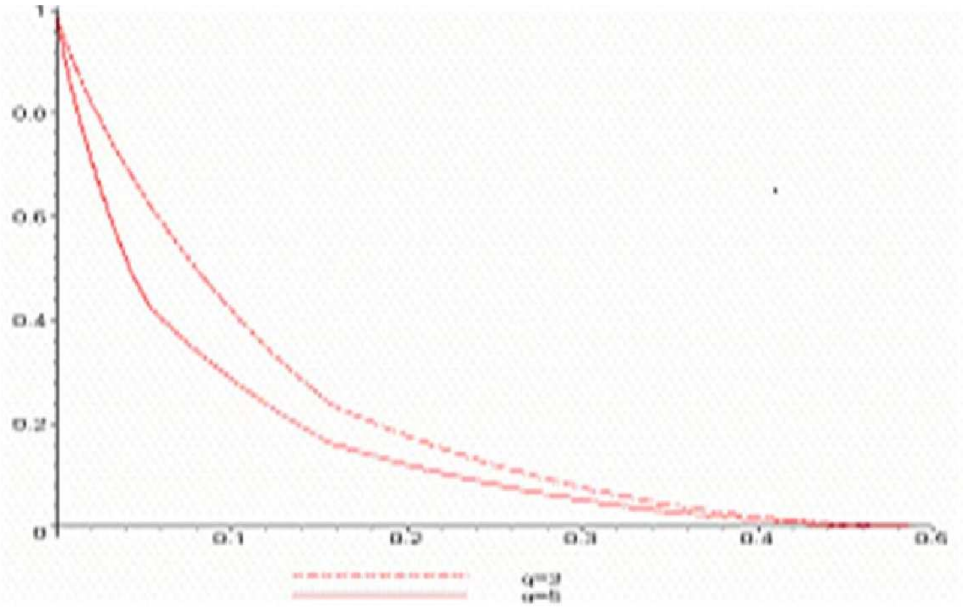

Figure 1: Bounds for City block metrics, q=3 (dash), q=5 (solid)

The Varshamov metric was introduced to describe asymmetric errors in the paper [9]. Let $\underline{\mathbf{x}} = (x_1, x_2, \ldots, x_n)$ and $\underline{\mathbf{y}} = (y_1, y_2, \ldots, y_n)$ be binary n-vectors. The distance-function is defined as

$$d_V(\underline{\mathbf{x}}, \underline{\mathbf{y}}) = \frac{1}{2}\left[w_H(\underline{\mathbf{x}} - \underline{\mathbf{y}}) + |w_H(\underline{\mathbf{x}}) - w_H(\underline{\mathbf{y}})|\right],$$

where $w_H(\underline{\mathbf{x}})$ denotes the Hamming weight of $\underline{\mathbf{x}}$.

The equivalent definition was introduced in [10]:

$$d_V(\underline{\mathbf{x}}, \underline{\mathbf{y}}) = \max\left\{N_{01}(\underline{\mathbf{x}}, \underline{\mathbf{y}}), N_{10}(\underline{\mathbf{x}}, \underline{\mathbf{y}})\right\},$$

where

$$N_{01}(\underline{\mathbf{x}}, \underline{\mathbf{y}}) = \#\left\{(x_i, y_i) : x_i = 0, y_i = 1\right\}, N_{10}(\underline{\mathbf{x}}, \underline{\mathbf{y}}) = \#\left\{(x_i, y_i) : x_i = 1, y_i = 0\right\}$$

Many results and code constructions are known.

Main theoretical result sounds that

$$M_H(n, 2d-1) \le M_V(n, d) \le dM_H(n, 2d-1),$$

where $M_H(n, d)$ and $M_V(n, d)$ denote maximal cardinalities of codes with minimal distance d in the Hamming metric and in the Varshamov metric, respectively.

The burst metric for dependent errors

The b-burst metric was introduced first in the paper [11], though codes correcting burst were invented much earlier. The burst norm $\mathcal{N}_b(\underline{\mathbf{x}})$ of a vector $\underline{\mathbf{x}}$ is defined as follows. Represent this vector as

$$\underline{\mathbf{x}} = (x_1, x_2, \ldots, x_n) = (0^{m_1}u_1v_1^{b-1}0^{m_2}u_2v_2^{b-1}\ldots),$$

where $u_j \neq 0$, 0^m means the all zero string of length $m \ge 0$, v^{b-1} means any string of length $b-1$. Such representation is unique. Then the b-burst norm of $\underline{\mathbf{x}}$ is equal to the number of b-tuples:

$$\mathcal{N}_b(\underline{\mathbf{x}}) = \#\left(b\text{-tuples of type } (uv^{b-1})\right).$$

For example, if $b = 4$ and the ternary vector is $\underline{\mathbf{x}} = (0,0,2,2,1,1,1,1,0,0,2,0,0,0,0,1,2,1)$, then the representation as a sequence of b-tuples is $\underline{\mathbf{x}} = (0,0,\ \vdots\mathbf{2},\mathbf{2},\mathbf{1},\mathbf{1},\vdots\ \vdots\mathbf{1},\mathbf{1},\mathbf{0},\mathbf{0},\vdots\ \vdots\mathbf{2},\mathbf{0},\mathbf{0},\mathbf{0},\vdots,\ 0,\ \vdots\mathbf{1},\mathbf{2},\mathbf{1}\vdots)$, so $\mathcal{N}_4(\underline{\mathbf{x}}) = 4$.

The b-burst distance is defined as

$$d_b(\underline{\mathbf{x}}, \underline{\mathbf{y}}) = \mathcal{N}_b(\underline{\mathbf{x}} - \underline{\mathbf{y}}).$$

Many constructions and decoding algorithms are published devoted to correcting burst errors. Still the notion "metric" is used not very often.

Several general facts about b-burst correcting codes are listed below.

1. The generator weight function of n-dimensional vectors:

$$W_n(z) = \sum_{i=1}^{D_n} A_i(n) z^i,$$

where $A_i(n)$ denotes the number of vectors with the b-burst i and $D_n = \left\lceil \frac{n}{b} \right\rceil$ is the maximal possible b-norm of $\underline{\mathbf{x}}$. Here

$$\begin{aligned} A_1(n) &= \begin{cases} q^n - 1, & 1 \le n \le b; \\ (q-1)q^{b-1}(n-b+1) + q^{b-1} - 1, & n > b; \end{cases} \\ A_i(n) &= \left[(q-1)q^{b-1}\right]^{i-1} \sum_{j=0}^{n-b(i-1)} \binom{j+i-2}{i-2} A_1\left(n - b(i-1) - j\right); \quad i > 1. \end{aligned}$$

For large n, the average norm $W_n = \frac{\sum_{i=0}^{D_n} N_i}{q^n} \approx \frac{q-1}{1+b(q-1)}$. The normalized average norm $\delta = \frac{N_n}{D_n} \approx \frac{b(q-1)}{1+b(q-1)}$.

2. The upper bound (can be improved) [12].
For any q-ary code with minimal b-distance d and cardinality M we have

$$R = \frac{\log_q M}{n} \leq b\left[1 - H_{q^b}\left(\frac{q_b-1}{q_b} - \frac{q_b-1}{q_b}\sqrt{1-\frac{q_b}{q_b-1}x}\right)\right],$$

where $x = \frac{d}{D_n}$ is the normalized minimal distance.

3. The lower bound (can be improved) [12].
There exists a q-ary code with minimal b-distance d and cardinality M such that

$$\begin{aligned} R &= \tfrac{\log_q M}{n} = \max\{R_1, R_2\}, \\ R_1 &= (1-\tfrac{b-1}{b}x)\left[1 - H_2\left(\tfrac{x}{b-(b-1)x}\right)\log_2 q\right] - \tfrac{x}{b}\log_q(q-1), \\ R_2 &= \max_{s\geq 2}\tfrac{1}{s}\left[1 - H_{q^b}\left(\tfrac{xs}{s-1}\right)\right]. \end{aligned}$$

Combinatorial Metrics

Combinatorial metrics were introduced in [13]. Sometimes specific spots of errors are most probable in channels. Then often we can define a matched metric.

We shall consider both vector signals ($\underline{\mathbf{x}} \in \mathcal{X}^n$) and matrix signals ($\mathbf{X} \in \mathcal{X}^{m\times n}$). To describe coordinates of signals, we consider two types of index sets:
the Line index set

$$\mathbf{I} = \{i \mid 0 \leq i \leq n-1\},$$

and the Array index set

$$\mathbf{I} = \{\{i,j\} \mid 0 \leq i \leq m-1,\ 0 \leq j \leq n-1\}.$$

Hence the set of all signals can be denote equally

$$\mathcal{X}^{\mathbf{I}} = \{\mathbf{x} \mid \mathbf{x} = (x(u),\ u \in \mathbf{I})\}.$$

For a signal $\mathbf{x} \in \mathcal{X}^{\mathbf{I}}$, the **support** is defined by

$$Q(\mathbf{x}) = \{i \mid x_i \neq 0,\ i \in \mathbf{I}\}.$$

Choose a subset $T \in \mathbf{I}$.
A word $\mathbf{x} \in \mathcal{X}^{\mathbf{I}}$ is said to be a T-spot, or T-burst, if

$$Q(\mathbf{x}) \subseteq T.$$

General Definition.
Consider a set of **Basic subsets**

$$\mathbf{T} = \{T_0 = \emptyset, T_1, T_2, \ldots, T_s\},\ T_j \subseteq \mathbf{I}$$

with the only restriction

$$\bigcup_{i=0}^{s} = \mathbf{I}.$$

The $\mathbf{T}$-norm is defined by

1. $\mathcal{N}_{\mathbf{T}}(\mathbf{x}) = 0 \Longleftrightarrow Q(\mathbf{x}) = \emptyset$.

2. $\mathcal{N}_{\mathbf{T}}(\mathbf{x}) = 1 \Longleftrightarrow Q(\mathbf{x}) \subseteq T_i$ for some i.

3. $\mathcal{N}_{\mathbf{T}}(\mathbf{x}) = k \Longleftrightarrow$
$Q(\mathbf{x}) \subseteq \{$ a junction of exactly k subsets from $\mathbf{T}\}$,
but
$Q(\mathbf{x}) \not\subseteq \{$ a junction of $k-1$ or less subsets from $\mathbf{T}\}$

A combinatorial metric for the Line index set is said to be Translation invariant if and only if

$$T_i = T_1 + (i-1) \pmod{n},\ i = 1, \ldots, n.$$

A combinatorial metric for the Array index set is said to be Translation invariant if and only if

$$T_{ij} = T_{11} + \{(i-1),(j-1)\}\,(\pmod{n_1}, \pmod{n_2})$$
$$i = 1, \ldots, n_1,\ j = 1, \ldots, n_2.$$

Let $\mathcal{N}_{\mathbf{T}_1}(\mathbf{x})$ and $\mathcal{N}_{\mathbf{T}_2}(\mathbf{x})$ be two metrics defined on $\mathcal{X}^{\mathbf{I}}$, such that $\mathcal{N}_{\mathbf{T}_1}(\mathbf{x}) \leq \mathcal{N}_{\mathbf{T}_2}(\mathbf{x}),\ \forall \mathbf{x} \in \mathcal{X}^{\mathbf{I}}$. Then $M_1(n,d) \leq M_2(n,d)$, where $M_i(n,d), i = 1,2$, are maximal cardinalities of codes.

Examples of combinatorial metrics

Previous metrics

The ***Hamming metric*** can be considered as a combinatorial metric defined by Basic subsets

$$T_1 = \{0\}, T_2 = \{1\}, \ldots, T_n = \{n-1\}.$$

Its generalization is ***the non-uniform Hamming Metric*** defined by the following Basic subsets:

$$\begin{array}{rcl} T_1 & = & \{0,1,\ldots,n_1-1\}, \\ T_2 & = & \{n_1, n_1+1, \ldots, n_1+n_2-1\}, \\ \cdots & \cdots & \cdots \\ T_s & = & \left\{\sum_{k=1}^{s-1} n_k, \sum_{k=1}^{s-1} n_k + 1, \ldots, \sum_{k=1}^{s-1} n_k + n_s - 1\right\}; \\ \sum_{k=1}^{s} n_k & = & n \end{array}$$

The metric is useful to construct codes when the different coordinates belong to different alphabets. Main results about codes in this metric can be found in [14].

The b-burst metric can be considered as a combinatorial metric defined by Basic subsets

$$\begin{array}{rcl} T_1 & = & \{0,1,\ldots,b-1\}, \\ T_2 & = & \{1,2,\ldots,b\}, \\ \cdots & \cdots & \cdots \\ T_{n-b+1} & = & \{n-b, n-b+1, \ldots, n\}. \end{array}$$

Vectors of weight 1 in this metric are vectors such that all the non zero coordinates can be covered by the only string of length b.

Its generalization is the 1-dimensional ***cyclic*** b*-burst metric* defined by Basic subsets

$$\begin{array}{lcl} T_1 & = & \{0,1,\ldots,b-1\}, \\ T_2 & = & \{1,2,\ldots,b\}, \\ \cdots & \cdots & \cdots \\ T_{n-b+1} & = & \{n-b,n-b+1,\ldots,n\}, \\ T_{n-b+2} & = & \{n-b+1,n-b+2,\ldots,0\}, \\ \cdots & \cdots & \cdots \\ T_n & = & \{n,0,\ldots,b-2\}, \end{array}$$

Vectors of weight 1 are vectors such that all the non zero coordinates can be covered by the only *cyclic* string of length b.

The 1-dimensional Hamming-burst (t,b) metric

This metric is defined by Basic subsets

$$\begin{array}{lcl} T_\alpha & = & \{\alpha=\{i_1,i_2,\ldots,i_t\} \mid 0 \le i_1 < i_2 < \cdots < i_t \le n-1\} \\ T_1 & = & \{0,1,\ldots,b-1\}, \\ T_2 & = & \{1,2,\ldots,b\}, \\ \cdots & \cdots & \cdots \\ T_{n-b+1} & = & \{n-b,n-b+1,\ldots,n\}, \\ T_{n-b+2} & = & \{n-b+1,n-b+2,\ldots,0\}, \\ \cdots & \cdots & \cdots \\ T_n & = & \{n,0,\ldots,b-2\}, \end{array}$$

Vectors of weight 1 are: all the vectors of the Hamming weight t and all vectors such that all the non zero coordinates can be covered by the only cyclic string of length b.
Codes of T-distance 3 correct all single errors in this metric, i. e., t-fold random errors, or all single b-burst errors. Such linear (n,k) codes exist, if

$$\begin{array}{lcl} \sum\limits_{i=0}^{2t-1}\binom{n-1}{i}(q-1)^i & + & \left[\sum\limits_{i=t+1}^{b-1}\binom{b-1}{i}(q-1)^i\right]\left[\sum\limits_{i=0}^{t-1}\binom{n-b-1}{i}(q-1)^i\right] \; + \\ \left[\sum\limits_{i=t}^{b-1}\binom{b-1}{i}(q-1)^i\right]\left[\sum\limits_{i=0}^{t}(i+1)\binom{n-b}{i}(q-1)^i\right] & + & \left[\sum\limits_{i=t+1}^{b-1}\binom{b-1}{i}(q-1)^i\right]\left[\sum\limits_{i=t}^{b-1}\binom{b-1}{i}(q-1)^i\right] \; + \\ \left[\sum\limits_{i=t}^{b-1}\binom{b-1}{i}(q-1)^i\right]^2(n-2b+1)(q-1) & < & q^{n-k}. \end{array}$$

Let $\delta = 2t/n,\ \gamma = b/n$. Then we have asymptotically that there exist linear codes with rate

$$R = \begin{cases} 1-2\gamma, & 0 \le \delta \le \delta_1()\gamma; \\ (1-\gamma)H_2\left(\frac{\delta}{2(1-\gamma)}\right)\log_2 q + \frac{\delta}{2}\log_q(q-1), & \delta_1(\gamma) \le \delta \le \delta_2(\gamma); \\ 1-H_q(\delta), & \delta_2(\gamma) \le \delta \le \frac{q-1}{q} \end{cases},$$

where $\delta_1(\gamma),\ \delta_2(\gamma)$ are roots of equations

$$\begin{array}{lcl} (1-\gamma)H_2\left(\frac{\delta_1}{2(1-\gamma)}\right)\log_2 q + \frac{\delta_1}{2}\log_q(q-1) & = & \gamma; \\ (1-\gamma)H_2\left(\frac{\delta_2}{2(1-\gamma)}\right)\log_2 q + \frac{\delta_2}{2}\log_q(q-1)+\gamma & = & H_q(\delta_2). \end{array}$$

In particular, this means that ordinary linear codes correcting up to t random errors can also correct single b- bursts, if $\delta \ge \delta_2(\gamma)$.

The 2-dimensional $(b_1 \times b_2)$-burst metric

The Basic subsets for this metrics are all the 2-dimensional cyclic shifts $(\mod n_1, \mod n_2)$ of the subset T_{11}, where T_{11} is a rectangle of size $b_1 \times b_2$ in the upper left hand corner of the Array index set:

$$T_{11} = \begin{bmatrix} (0,0) & (0,1) & \cdots & (0,b_2-1) \\ \cdots & \cdots & \cdots & \cdots \\ (b_1-1,0) & (b_1-1,1) & \cdots & (b_1-1,b_2-1) \end{bmatrix}$$

Matrices of weight 1 are matrices such that all the non zero coordinates can be covered by the only *cyclic* $b_1 \times b_2$ rectangle.
The Weight Enumerator is known for special cases only.
Several results can be found in [15].

The Term Rank Metric

The metric was proposed in [16; 18]. The Array index set is used. The Basic subsets are as follows:

$$\{\text{All rows of the Array Index Set }\} \bigcup \{\text{All columns of the Array Index Set }\}$$

This metric is not translation invariant. Matrices of weight 1 are all matrices such that all the non zero coordinates can be covered by the only row or by the only column.
The Weight Enumerator is unknown for this metric.

Another definition can be given in combinatorial terms. If

$$\mathbf{X} = \begin{bmatrix} x_{0,0} & x_{0,1} & \cdots & x_{0,n-1} \\ x_{1,0} & x_{1,1} & \cdots & x_{1,n-1} \\ \cdots & \cdots & \cdots & \cdots \\ x_{m-1,0} & x_{m-1,1} & \cdots & x_{m-1,n-1} \end{bmatrix}$$

is a $m \times n$ matrix over the field $GF(q)$, then the $Term\,Rank\,Norm$ of a matrix $\mathbf{X}$, $\mathcal{N}_{TR}(\mathbf{X})$, is defined as the $minimal$ number of lines (rows or columns) containing all $nonzero$ elements of a matrix.

Easy decodable optimal codes for this metric are described in [19; 20].

Projective metrics

Projective metrics were proposed in [21; 22].

Let F_q^n be a vector space of dimension n over a finite field F_q.
Let

$$\mathcal{F} = \{\mathbf{f}_1, \mathbf{f}_2, \cdots, \mathbf{f}_N\}$$

be a set of non-zero distinct column vectors from F_q^n containing a basis. This means that $N \geq n$ and there exist n linearly independent vectors in $\mathcal{F}$.

It is convenient to treat $\mathcal{F}$ as a $n \times N$ matrix.

Each vector $\mathbf{f} \in F_q^n$ can be represented (not uniquely) as a linear combination of columns from $\mathcal{F}$:

$$\mathbf{f} = a_1\mathbf{f}_1 + a_2\mathbf{f}_2 + \cdots a_N\mathbf{f}_N.$$

The projective $\mathcal{F}$-norm $\mathcal{N}_{\mathcal{F}}(\mathbf{f})$ of a vector $\mathbf{f}$ is defined as a minimal possible number of non-zero coefficients among all representations of $\mathbf{f}$:

$$N_{\mathcal{F}}(\mathbf{f}) = \min \#(a_i \neq 0 : \quad \mathbf{f} = a_1\mathbf{f}_1 + a_2\mathbf{f}_2 + \cdots a_N\mathbf{f}_N).$$

This definition defines very rich family of metrics which can be useful to describe errors in channels with an additive noise.

All the vectors $\mathbf{f}_i \in \mathcal{F}$ and its multiples (and only these vectors) are of norm 1 and are considered as 1-fold errors.

Examples of projective metrics

The Hamming metric. Let $N = n$ and let

$$\mathcal{F} = \left\{ \begin{array}{cccc} 1 & 0 & \cdots & 0 \\ 0 & 1 & \cdots & 0 \\ \vdots & \vdots & \cdots & \vdots \\ 0 & 0 & \cdots & 1 \end{array} \right\}$$

Then this set defines the Hamming norm and the Hamming distance.

If $\mathcal{F}$ is a non singular matrix, then it defines formally the new metric but *equivalent* to the Hamming metric.

The metric for a channel with phase rotation. If a receiver should recover synchronization, then sometimes data are received as negative:

$$\text{Input data } \ldots 0011101 \ldots \implies \ldots 1100010 \ldots \text{ Output data}$$

Extra redundancy is needed to discover and to remove the phase rotation. An alternative is use of a special metric.

Let $N = n + 1$ and let

$$\mathcal{F} = \left\{ \begin{array}{ccccc} 1 & 0 & \cdots & 0 & 1 \\ 0 & 1 & \cdots & 0 & 1 \\ \vdots & \vdots & \cdots & \vdots & \\ 0 & 0 & \cdots & 1 & 1 \end{array} \right\}$$

The phase rotation is treated as adding to transmitted blocks the all 1's block. Declare this block as a 1-fold error. Use codes correcting 1-folds errors. Such codes are constructed in [23; 24].

The Rank metric

This metric was introduced in [17; 18; 25].

Let $q = p^m$, let F_p be a base field and let $\mathrm{rank}(\mathbf{f};F_p)$ be the rank of a vector $\mathbf{f} \in F_q^n$ over the base field F_p. Let $\mathcal{F}$ be the set of all the vectors of rank 1:

$$\mathcal{F} = \left\{\mathbf{f} : \ \mathbf{f} \in F_q^n, \ \mathrm{rank}(\mathbf{f};F_p) = 1.\right\}$$

This set defines the Rank metric.

The theory of codes in the rank metric is presented in [25].

Linear optimal (n, k, d) codes are called Maximal Rank Distance codes, or, MRD codes. They can be defined in terms of *generator* matrices of the form

$$\mathbf{G} = \begin{bmatrix} g_1 & g_2 & \cdots & g_n \\ g_1^q & g_2^q & \cdots & g_n^q \\ g_1^{q^2} & g_2^{q^2} & \cdots & g_n^{q^2} \\ \cdots & \cdots & \cdots & \cdots \\ g_1^{q^{k-1}} & g_2^{q^{k-1}} & \cdots & g_n^{q^{k-1}} \end{bmatrix},$$

where $g_1, g_2, \ldots, g_n$ is a set of elements of $\mathbf{F}_{q^N}$ which are linearly independent over $\mathbf{F}_q$. MRD codes have the following parameters:
Code length $n \leq N$; Dimension k; Rank and Hamming code distance $d = r + 1 = n - k + 1$.
Let $A_i(n, d)$ be the number of vectors of a MRD code of rank weight i. Spectra of (n, k, d) MRD codes are given by the next equations:

$$\begin{aligned} A_0(n,d) &= 1; \\ A_i(n,d) &= \begin{bmatrix} n \\ i \end{bmatrix} \sum_{j=0}^{i-d} (-1)^{j+i-d} \begin{bmatrix} i \\ d+j \end{bmatrix} q^{(m-j)(m-j-1)/2} \left(q^{N(j+1)} - 1\right), \quad i \geq d. \end{aligned}$$

Here $\begin{bmatrix} n \\ i \end{bmatrix}$ is the notation for Gaussian numbers:

$$\begin{bmatrix} n \\ i \end{bmatrix} = \frac{(q^n - 1)(q^n - q) \ldots (q^n - q^{i-1})}{(q^i - 1)(q^i - q) \ldots (q^i - q^{i-1})}.$$

There exist fast decoding algorithms for MRD codes [25].

The Vandermonde metric

The Vandermonde $\mathcal{F}$-metric is defined as follows.
Vectors $\mathbf{f}_1, \mathbf{f}_2, \ldots, \mathbf{f}_N$ that specify the $\mathcal{F}$-metrics are chosen as columns of the Vandermonde matrix:

$$\mathbf{F} = \begin{pmatrix} u_1 & u_2 & \ldots & u_N \\ u_1 x_1 & u_2 x_2 & \ldots & u_N x_N \\ u_1 x_1^2 & u_2 x_2^2 & \ldots & u_N x_N^2 \\ \ldots & \ldots & \ldots & \ldots \\ u_1 x_1^{n-1} & u_1 x_2^{n-1} & \ldots & u_N x_N^{n-1} \end{pmatrix}.$$

Here $n \leq N$, $x_i \in \mathbb{F}_q$ should be different, $u_i \in \mathbb{F}_q$ should be non-zero, $i = 1, \ldots, N$.
Optimal linear (n, k, d) codes in this metric can be defined in terms of generator matrices of the form:

$$\mathbf{G} = \begin{pmatrix} v_1 & v_1 y_1 & \ldots & v_1 y_1^{n-1} \\ v_2 & v_2 y_2 & \ldots & v_2 y_2^{n-1} \\ v_3 & v_3 y_3 & \ldots & v_3 y_3^{n-1} \\ \ldots & \ldots & \ldots & \ldots \\ v_k & v_k y_k & \ldots & v_k y_k^{n-1} \end{pmatrix}.$$

Here $v_i \in \mathbb{F}_q$ are non-zero, and $y_i \in \mathbb{F}_q$ are different. Moreover, we must choose y_j that differs from each x_i.
A dimension k of the code C must satisfy $k + N \leq q + 1$ (it is a necessary condition for the fast decoding algorithm).
There exist a fast decoding algorithm for these codes.

Codes are used in the modified Niederreiter public key cryptosystem [26].

Some graph metrics

It is clear that distance among nodes in a connected graph constitutes a metric. The distance, $d(n_1, n_2)$, between two nodes n_1 and n_2 in a connected graph is the length of the shortest path joining them and the diameter is the maximum of all the distances between any pair of nodes. It is known that Hamming distance among codewords can be seen as the graph distance among vertices in a Hypercube graph. In the same way, the Lee metric in two-dimensional signal sets can be associated to minimal routing in a Torus graph.

Examples of graph metrics

Circulant Graph Distances over Gaussian Integer Constellations. The *Gaussian integers* $\mathbb{Z}[i]$ is the subset of the complex numbers with integer real and imaginary parts, that is:

$$\mathbb{Z}[i] := \{x + yi |\, x, y \in \mathbb{Z}\}.$$

$\mathbb{Z}[i]$ is an Euclidean domain and the norm is defined as:

$$\begin{array}{rccc} \mathcal{N}: & \mathbb{Z}[i] & \longrightarrow & \mathbb{Z}^+ \\ & x + yi & \longmapsto & x^2 + y^2 \end{array}$$

If $0 \neq \alpha \in \mathbb{Z}[i]$, we consider $\mathbb{Z}[i]_\alpha$ the ring of the classes of $\mathbb{Z}[i]$ modulo the ideal (α) generated by α.

A new metric over these subsets of the Gaussian integers is defined in a very natural way. This metric is applicable when using any value of α (not necessarily with prime norm) and it corresponds to the distance among nodes in its associated circulant graph.

For $\beta, \gamma \in \mathbb{Z}[i]_\alpha$, consider $x + yi$ in the class of $\beta - \gamma$ with $|x| + |y|$ minimum. The distance D_α between β and γ is

$$D_\alpha(\beta, \gamma) = |x| + |y|.$$

D_α defines a distance over the quotient ring $\mathbb{Z}[i]_\alpha$.

A new family of circulant graphs of degree four whose nodes are labeled by Gaussian integers and their adjacency is determined by the distance D_α was introduced in [27].

Given $\alpha = a + bi \in \mathbb{Z}[i]$ with $\gcd(a, b) = 1$ we define the graph $G_\alpha = (V, E)$ where:

1. $V = \mathbb{Z}[i]_\alpha$ is the node set, and
2. $E = \{(\beta, \gamma) \in V \times V \mid D_\alpha(\beta, \gamma) = 1\}$ is the edge set.

Perfect codes over quotient rings of Gaussian integers were constructed correcting 1-fold errors.

Eisenstein-Jacobi integers and circulant graphs of degree six. The ring of the *Eisenstein-Jacobi integers* is defined as:

$$\mathbb{Z}[\rho] = \{x + y\rho \mid x, y \in \mathbb{Z}\},$$

where $\rho = (-1 + \sqrt{-3})/2$. The ring $\mathbb{Z}[\rho]$ is an Euclidean domain with norm

$$\begin{array}{rccc} \mathcal{N}: & \mathbb{Z}[\rho] & \longrightarrow & \mathbb{N} \\ & x+y\rho & \longmapsto & x^2+y^2-xy \end{array}$$

The units of $\mathbb{Z}[\rho]$ are the elements with unitary norm, that is $\{\pm 1, \pm\rho, \pm\rho^2\}$.

For every $0 \neq \alpha \in \mathbb{Z}[\rho]$ we can consider $\mathbb{Z}[\rho]_\alpha = \{\beta \pmod{\alpha} \mid \beta \in \mathbb{Z}[\rho]\}$.

Let $0 \neq \alpha = a + b\rho \in \mathbb{Z}[\rho]$ with $\gcd(a, b) = 1$ and consider $\mathbb{Z}[\rho]_\alpha$. Denote the *Eisenstein-Jacobi graph* generated by α as $EJ_\alpha = (V, E)$ and it is defined as follows:

- $V = \mathbb{Z}[\rho]_\alpha$ is the set of nodes and
- $E = \{(\beta, \gamma) \in V \times V \mid (\gamma - \beta) \equiv \pm 1, \pm\rho, \pm\rho^2 \pmod{\alpha}\}$ is the set of edges.

Let $\alpha = a + b\rho \in \mathbb{Z}[\rho]$ be such that $\gcd(a, b) = 1$. Denote the distance between nodes β and γ in EJ_α as $D_\alpha(\beta, \gamma)$. This distance can be expressed as:

$$D_\alpha(\beta, \gamma) = \min\{|x| + |y| + |z| \mid x + y\rho + z\rho^2 \equiv (\gamma - \beta) \pmod{\alpha}\}.$$

Perfect codes over quotient rings of Eisenstein–Jacobi integers were constructed correcting 1-fold errors.

The subspace metric

A subspace approach for network coding has been proposed in [28]. It allows to overcome many previous restrictions on network configurations. Coding schemes using this approach are developed in [29]. The subspace approach is based on the subspace metric.

Let $\mathbb{F}_q$ be a finite field of q elements. Denote by $W_{N,q}$ a fixed N-dimensional vector space over the field $\mathbb{F}_q$. Let $\mathcal{P}(W_{N,q})$ be the set of all subspaces of $W_{N,q}$.

The ***subspace distance*** between two subspaces U and V is defined as follows:

$$d(U, V) = \dim(U \uplus V) - \dim(U \cap V). \tag{1}$$

Codes for network coding are proposed in several papers (see, [28] - [34]).

Conclusion

Metrics are used in many practical applications. The brief survey of such metrics is given.

General properties of codes are considered including simple bounds.

Many examples of metrics are described. In particular, the uniform and non-uniform Hamming metrics, the Lee and Sharma-Kaushik metrics, the city block (Manhattan) metric, the Varshamov metric, the burst metric, the 2-dimensional burst metric, the term rank metric, the rank metric, combinatorial metrics, projective metrics, graph metrics, the subspace metric.

Open problems are pointed.

Acknowledgements

This work is supported in part by Grant of Ministry of Education 8.4414.2011(0704 T 019).

Bibliography

[1] F. J. MacWilliams and N.J.A. Sloane, *The theory of error-correcting codes. I, II.* North-Holland Mathematical Library, Vol. 16, Amsterdam: North-Holland Publishing Co., 1977.

[2] S. G. Vlăduţ, D. J. Nogin, M. A. Tsfasman, *Algebraic-geometric codes. Fundamentals.* (in Russian) — M.:MCCME, 2003.—P. 504.
{See also, M. A. Tsfasman and S. G. Vlăduţ, *Algebraic-geometric codes,* vol. 58 of *Mathematics and Its Applications (Soviet Series)*. Dordrecht: Kluver Academic Publishers Group, 1991.}

[3] Sharma B. D. and Kaushik M. L., Limites intensity random and burst error codes with class-weight considerations, *Elektron. Inform.-verarb. Kybernetik* 15 (1979), 315-321.

[4] Sharma B. D. and Kaushik M. L., Algebra of Sharma and Kaushik's metric inducing partitions of Z_q, *J. Combin. Inform. System Sci.* 11 (1986), 19 - 32.

[5] Sharma, B. D. and Sookoo, N., Association and other schemes related to Sharma-Kaushik class of distances over finite rings, *Le Matematiche*, Vol. XLV, Fasc. I (1990), 163-185.

[6] Sharma B. D. and Sookoo N., The difference matrices of the classes of a Sharma-Kaushik partition, *ARCHIVUM MATHEMATICUM (BRNO)*. Tomus 40 (2004), 23 - 31.

[7] Berlekamp E. R., *Algebraic coding theory*. McGraw-Hill, New York, 1968.

[8] Ulrich, BSTJ, 1957, No. 6

[9] Varshamov R. R., On theory of asymmetric codes.– *Doclady of AS USSR*, 1965, vol. 164, No. 4, P. 757-760.

[10] Rao T. R. N., Chawla A. S., Asymmetric error codes for some LSI semiconductor memories. – Proc. 7-th Ann. Southeast Symp. Syst. Theory, Auburn-Tuskegee, 1975, New York, N. J., 170-171.

[11] Bridewell J. D., Wolf J. K., Burst distance and multiple burst correction.– Bell. Syst. Tech. J., 1979, 49, 889-909.

[12] Gabidulin E. M., Bassalygo L. A., Sidorenko V.R., Varshamov-Gilbert Bound is improvable for Codes Correcting Multiple Burst Errors .–In: Proc. of the 6-th International Symposium on Information Theory, Part II, pp. 78-80, 1984, Moscow-Tashkent.

[13] Gabidulin E. M., Combinatorial metrics in coding theory.– In: *Proc. of the 2-nd International Symposium on Information Theory*, Budapest, 1971, 169-176.

[14] Vladimir Sidorenko, Georg Schmidt, Ernst Gabidulin, Martin Bossert, Valentin Afanassiev, "On polyalphabetic block codes, " Proc. of the ITW2005 - IEEE ITSOC Information Theory Workshop 2005 on Coding and Complexity, 28th/29th Aug. - 1st Sept. 2005 - Rotorua, New Zealand.

[15] Gabidulin E. M., Zanin V. V., Codes Correcting Array Errors.– In: B. Honary, M. Darnell, P. Farrell (Eds), COOMUNICATION THEORY AND APPLICATIONS II, HW Communications Ltd. 1994.

[16] Gabidulin E. M., A Class of Two-Dimensional Codes Correcting Lattice-Pattern Errors.– In: Proc. of the 2-nd International Symposium on Information Theory, pp. 44-47, 1971, Moscow-Yerevan.

[17] P. Delsarte, "Bilinear forms over a finite field, with applications to coding theory," Journal of Combinatorial Theory A, vol. 25, pp. 226-241, 1978.

[18] Gabidulin E. M., Optimal Codes Correcting Array Errors.– In: Proc. of the 6-th International Symposium on Information Theory, Part II, pp. 75-77, 1984, Moscow-Tashkent.

[19] Gabidulin E. M., Optimal Codes Correcting Array Errors.– *Problems of Information Transmission*, v. 21, No. 2, pp. 3-11, 1985.

[20] Gabidulin E. M., Lund D., Honary B., A New Family of Optimal Codes Correcting Term Rank Errors.– In: Proc. of the 2000 IEEE International Symposium on Information Theory, 25 - 30 June, 2000, p. 115, Sorrento, Italy.

[21] Gabidulin E. M., Simonis J., Metrics Generated by a Projective Point Set.– In: Proc. of the 1997 IEEE International Symposium on Information Theory, June 29 - July 4, 1997, p. 248, Ulm, Germany.

[22] Gabidulin E. M., Simonis J., Metrics Generated by Families of Subspaces.– *IEEE Trans. Inform. Theory*, vol. 44, pp. 1336-1341, May 1998.

[23] Gabidulin E. M., Bossert M., Codes Resistant to the Phase Rotation.– In: Proc. of the 4-th Simposium on Communication and Applications, pp. 253-257, July 1997, pp. 65-84, Charlotte Mason College, Lake District, UK.

[24] Gabidulin E. M., Bossert M., Hard and Soft Decision Decoding of Phase Rotation Invariant Block Codes.– In: Proceedings of the 1998 International Zurich Seminar on Broadband Communications - Accessing, Transmission, Networking - 17-19 February, 1998, ETH Zurich, Switzerland.

[25] Gabidulin E. M., Theory of Codes with Maximum Rank Distance.– *Problems of Information Transmission*, v. 21, No. 1, pp. 3-14, 1985.

[26] Gabidulin E. M., Obernikhin V. A., Codes in the Vandermonde $\mathcal{F}$-metric and applications.– *Problems of Information Transmission*, v. 39, No. 2, pp. 3-14, 2003.

[27] C. Martínez, R. Beivide, J. Gutierrez and E. Gabidulin. "On the Perfect t-Dominating Set Problem in Circulant Graphs and Codes over Gaussian Integers". Proceedings of the 2005 IEEE International Symposium on Information Theory (ISIT'05). Adelaide, Australia. September, 2005.

[28] Koetter R., Kschischang F. R.: Coding for errors and erasures in random network coding. In: Proc. of the 2007 IEEE International Symposium on Information Theory (ISIT 2007), pp. 791-795. Nice, France, 24-29 June (2007)

[29] Silva D., Kschischang F. R.: Using rank-metric codes for error correction in random network coding. In: Proc. of the 2007 IEEE International Symposium on Information Theory (ISIT 2007), pp. 796-800. Nice, France, 24-29 June (2007)

[30] Gabidulin E., Bossert M.: Codes for Network Coding. In: Proc. of the 2008 IEEE International Symposium on Information Theory (ISIT 2008), pp. 867-870. Toronto, ON, Canada, 6-11 July (2008)

[31] Gabidulin E.M., Bossert M.: A Family of Algebraic Codes for Network Coding. Probl. Inform. Transm. Vol. 45. No. 4, pp. 54–68 (2009)

[32] Skachek V.: Recursive Code Construction for Random Networks. IEEE Trans. On Inform. Theory. V. 56. No. 3, pp. 1378-1382 (2010)

[33] Etzion T., Silberstein N.: Error-Correcting Codes in Projective Spaces Via Rank-Metric Codes and Ferrers Diagrams. IEEE Trans. On Inform. Theory. V. 55. No. 7, pp. 2909Ű2919 (2009).

[34] Gadouleau M., Yan Z.: Construction and Covering Properties of Constant-Dimension Codes. In: Proc. of the 2009 IEEE International Symposium on Information Theory (ISIT 2009), pp. 2221-2225. Nice, France, 24-29 June (2007)

Authors' Information

Ernst Gabidulin *- Professor, Moscow Institute of Physics and Technology (State University), Dept. of Radio Engineering and Telecommunications,*
P.O. Box: 141700, Dolgoprudny Moscow region, Russia; e-mail: ernst_gabidulin@yahoo.com
Major Fields of Scientific Research: Algebraic coding, Cryptography, Sequences

REGULAR INVERSIVE POLYTOPES

Norman W. Johnson

Abstract: *Corresponding to each regular asymptotic polytope* P *in hyperbolic* ***n****-space* H^n *is an isomorphic figure* °P *in inversive* ($n-1$)*-space* I^{n-1} *having many related metric properties. A regular inversive polytope* °P *has a* midangle ω *and a* radius ρ*, with* 2ω *being its* dihedral angle *and* 2ρ *its* antihedral distance*. The values of* ω *and* ρ *are determined for each regular inversive* ***n****-polytope.*

Keywords: *regular polytopes, inversive geometry, non-Euclidean geometry*

ACM Classification Keywords: *G.2.1 Discrete mathematics — combinatorics*

Introduction

The classical real metric spaces (or "spaces of constant curvature") are the *spherical*, *Euclidean*, and *hyperbolic* ***n***-spaces S^n, E^n, and H^n ($n \geq 1$); *elliptic* ***n****-space* eP^n results from identifying antipodal points of S^n and has many of the same metric properties. The points at infinity of hyperbolic ***n***-space H^n lie on the *absolute hypersphere*, which has the geometry of a Möbius ($n-1$)-sphere or *inversive* ($n-1$)-space I^{n-1}. Each ***k***-plane of H^n meets the absolute hypersphere in a real inversive ($k-1$)-sphere I^{k-1}, with I^1 being an inversive circle and I^0 a pair of points. Two hyperplanes of H^n may be *intersecting*, meeting in an ($n-2$)-plane; *parallel*, having a single absolute point in common; or *diverging*, with a common perpendicular. The corresponding inversive ($n-2$)-spheres are respectively *separating*, *tangent*, or *separated*.

An ***n****-polytope* $\mathcal{P}$ is a partially ordered set of ***j***-dimensional "entities" ($-1 \leq j \leq n$), its ***j****-faces*, satisfying certain incidence conditions, such as those given by McMullen & Schulte (2002, pp. 22–25). A totally ordered subset of ***j***-faces, one of each rank from -1 to ***n***, is a *flag*. When $\mathcal{P}$ is realized as a geometric figure P in some ***n***-dimensional real space, the unique (-1)-face, or *nullity*, can be taken to be the empty set $\varnothing$. The 0-faces are points, the *vertices* of P, and the 1-faces joining adjacent vertices are *edges*. The unique ***n***-face is the *body* of P, essentially its "interior." The ($n-1$)-faces are called *facets*, and the ($n-2$)-faces in which adjacent facets meet are *ridges*. A 2-polytope is a *polygon*, and a 3-polytope is a *polyhedron*. An ***n***-polytope P is *regular* if its symmetry group is transitive on the flags.

Dihedral Angles

It is convenient to denote a regular ***p***-gon of (interior) angle $2\pi/q$ by the extended Schläfli symbol $\{p\}:q$. Then the polygon is spherical, Euclidean, or hyperbolic according as ***q*** is less than, equal to, or greater than $2p/(p-2)$. A regular hyperbolic polygon can be *ordinary*, with all its vertices lying on an ordinary circle, or *asymptotic*, with adjacent sides parallel, so that the vertices all lie on the absolute circle of H^2 and the angles are all zero; a regular asymptotic ***p***-gon thus has the symbol $\{p\}:\infty$. The center of an ordinary or asymptotic ***p***-gon is an ordinary point. An infinite-sided *apeirogon* $\{\infty\}:q$ of angle $2\pi/q$ ($q>2$), whose center is an absolute point, can be inscribed in a horocycle, and an *asymptotic apeirogon* $\{\infty\}:\infty$ in the absolute circle.

A regular polyhedron whose faces are p-gons, arranged q at a vertex, having dihedral angle $2\pi/r$, is denoted by $\{p, q\}:r$. The polyhedron is spherical, Euclidean, or hyperbolic according as $\sin \pi/p \sin \pi/r$ is greater than, equal to, or less than $\cos \pi/q$, and it is asymptotic when the vertex section $\{q\}:r$ is Euclidean, i.e., when $r = 2q/(q-2)$. The regular asymptotic polyhedra of H^3 consist of the five convex polyhedra

$$\{3, 3\}:6, \quad \{3, 4\}:4, \quad \{4, 3\}:6, \quad \{3, 5\}:10/3, \quad \{5, 3\}:6,$$

the four star polyhedra

$$\{5/2, 5\}:10/3, \quad \{5, 5/2\}:10, \quad \{5/2, 3\}:6, \quad \{3, 5/2\}:10,$$

and the three apeirohedra

$$\{4, 4\}:4, \quad \{3, 6\}:3, \quad \{6, 3\}:6.$$

In similar fashion, a regular 4-polytope with facets $\{p, q\}$, r surrounding each edge, and dihedral angle $2\pi/s$ is denoted by $\{p, q, r\}:s$, the polytope being spherical, Euclidean, or hyperbolic depending on the value of s. It is asymptotic when the vertex section $\{q, r\}:s$ is Euclidean, i.e., when $\sin \pi/q \sin \pi/s = \cos \pi/r$. Analogous criteria can be developed for higher-dimensional regular polytopes

$$\{p, q, \ldots, u, v\}:w.$$

Going in the other direction, a one-dimensional polytope comprises a line segment (or a circular arc) and its two endpoints; the whole figure may be called a *ditel*. This can be a circular ditel $\{\}:a$ ($a > 2$) in S^1, a straight ditel $\{\}:\infty$ in E^1, an ordinary hyperbolic ditel $\{\}:b\,\mathrm{i}$ ($b > 0$) in H^1, or an asymptotic ditel $\{\}:0$ (an entire hyperbolic line with its two absolute points). Each finite ditel $\{\}:a$, $\{\}:\infty$, or $\{\}:b\,\mathrm{i}$ has a unique midpoint, halfway between the endpoints. An asymptotic ditel, however, does not have a well-defined midpoint.

Each vertex of a regular asymptotic n-polytope P in hyperbolic n-space H^n lies on the absolute hypersphere, and each j-face ($1 \le j \le n-1$) lies in a unique j-plane. The j-plane of a j-face meets the absolute hypersphere in an inversive $(j-1)$-sphere. The vertices of P and these $(j-1)$-spheres can be taken as the j-faces ($0 \le j \le n-1$) of an isomorphic *regular inversive n-polytope* °P. The (-1)-face of °P is (as usual) the empty set, and the n-face of °P is the whole absolute hypersphere, regarded as an inversive $(n-1)$-sphere I^{n-1}.

The *dihedral angle* between two adjacent facets of the inversive n-polytope °P is, in general, the angle between two $(n-2)$-spheres on I^{n-1}, which is the same as the dihedral angle between the corresponding facets of the asymptotic n-polytope P. For $n = 1$, P is an asymptotic ditel $\{\}:0$, and °P is an inversive *dyad* $°\{\}:0$, whose two facets are points, the "angle" between which is infinite. For $n = 2$, P is a regular asymptotic p-gon $\{p\}:\infty$, and °P is a *regular inversive p-gon* $°\{p\}:\infty$, adjacent facets of which are tangent point-pairs (i.e., they have one point in common) on an inversive circle, the angle between which is zero. For $n \ge 3$, the dihedral angle between adjacent facets of a regular inversive n-polytope °P is the positive angle between two separating $(n-2)$-spheres on an inversive $(n-1)$-sphere.

For $n \ge 2$, joining the center of a regular asymptotic n-polytope P to any ridge, or $(n-2)$-face, determines a *median hyperplane* of P. The angle between the median hyperplane and either of the facets that meet at the ridge is the *midangle*, half the dihedral angle. For both P and the corresponding regular inversive polytope °P, it often turns out to be simpler to work with the midangle ω rather than the dihedral angle 2ω.

Metric Formulas

In the Beltrami–Klein model for hyperbolic n-space H^n, the ordinary points of H^n are represented by the interior of an oval $(n-1)$-quadric Φ in projective n-space P^n, with the points of Φ itself representing the absolute hypersphere. Let the points X and hyperplanes $\check{U}$ of P^n have homogeneous coordinates

$$(\!(x)\!) = (x_0,\ x_1, \ldots,\ x_n) \quad \text{and} \quad [\![u]\!] = [u_0,\ u_1, \ldots,\ u_n]$$

with $(\!(x)\!)$ treated as a row and $[\![u]\!]$ as a column. Point X lies on hyperplane $\check{U}$, written $X \diamondsuit \check{U}$, whenever $(\!(x)\!)[\![u]\!] = 0$. Then the $(n-1)$-quadric Φ can be taken to be the locus of self-conjugate points, or the envelope of self-conjugate hyperplanes, in an absolute *hyperbolic polarity* defined by dual bilinear forms

$$(\!(x\ \ y)\!) = (\!(x)\!)H(\!(y)\!)^{\mathrm{v}} \quad \text{and} \quad [\![u\ \ v]\!] = [\![u]\!]^{\mathrm{v}}H^{-1}[\![v]\!].$$

Here H is a symmetric $(n+1) \times (n+1)$ matrix congruent to the pseudo-identity matrix $I_{n,1} = \backslash 1, \ldots,\ 1, -1 \backslash$, and the caron denotes the transpose, making $(\!(y)\!)^{\mathrm{v}}$ a column and $[\![u]\!]^{\mathrm{v}}$ a row. We may, for instance, take H to be the diagonal matrix $\backslash -1,\ 1, \ldots,\ 1 \backslash$, so that the absolute hypersphere $(\!(x\ \ x)\!) = 0$ has the equation

$$x_1^{\,2} + \cdots + x_n^{\,2} = x_0^{\,2}.$$

Every ordinary point X with coordinates $(\!(x)\!)$ has $(\!(x\ \ x)\!) < 0$, and every ordinary hyperplane $\check{U}$ with coordinates $[\![u]\!]$ has $[\![u\ \ u]\!] > 0$. The *discriminant* of two ordinary hyperplanes $\check{U}$ and $\check{V}$ may be defined by

$$\|u\ \ v\| = [\![u\ \ u]\!][\![v\ \ v]\!] - [\![u\ \ v]\!]^2,$$

and the hyperplanes are then

intersecting if $\|u\ \ v\| > 0$,
parallel if $\|u\ \ v\| = 0$,
diverging if $\|u\ \ v\| < 0$.

When H^n is taken to have constant curvature -1, we have simple expressions for distances and angles (cf. Coxeter 1998, pp. 209–210). In place of the Euclidean distance $|XY|$, the hyperbolic distance between two ordinary points X and Y is given by

$$]XY[\ = \ \cosh^{-1} \ \frac{|(\!(x\ \ y)\!)|}{\sqrt{-(\!(x\ \ x)\!)}\sqrt{-(\!(y\ \ y)\!)}}. \tag{1}$$

The angle between two intersecting or parallel hyperplanes $\check{U}$ and $\check{V}$ is given by

$$(\check{U}\check{V}) \ = \ \cos^{-1} \ \frac{|[\![u\ \ v]\!]|}{\sqrt{[\![u\ \ u]\!]}\sqrt{[\![v\ \ v]\!]}}, \tag{2}$$

and the minimum distance between two diverging hyperplanes $\check{U}$ and $\check{V}$ by

$$)\check{U}\check{V}(\ = \ \cosh^{-1} \ \frac{|[\![u\ \ v]\!]|}{\sqrt{[\![u\ \ u]\!]}\sqrt{[\![v\ \ v]\!]}}. \tag{3}$$

The distance between a point X and a hyperplane $\check{U}$ is given by

$$]X\check{U}(\;=\; \sinh^{-1} \;\frac{|(\!(x)\!)[\![u]\!]|}{\sqrt{-(\!(x\;\;x)\!)}\sqrt{[\![u\;\;u]\!]}}. \tag{4}$$

Given any hyperplane $\check{U}$ and a point X not on $\check{U}$, a line through X and one of the absolute points of $\check{U}$ is parallel to $\check{U}$ in that direction. Following Lobachevsky, the angle between the perpendicular from X to $\check{U}$ and the parallel is called the *angle of parallelism* for the distance $x =]X\check{U}($ and is given by

$$\Pi(x) \;=\; \cos^{-1} \tanh x \;=\; 2 \tan^{-1} e^{-x}. \tag{5}$$

As x increases from zero to infinity, $\Pi(x)$ decreases from $\pi/2$ to 0.

A projective hyperplane $\check{U}$, with coordinates $[\![u]\!]$, meets the $(n-1)$-quadric Φ, i.e., the absolute hypersphere of H^n regarded as the inversive $(n-1)$-sphere I^{n-1}, in an inversive $(n-2)$-sphere $\mathring{u}$, a *hypersphere* of I^{n-1}, which is

$$\begin{aligned} &\textit{real} && \text{if } [\![u\;\;u]\!] > 0, \\ &\textit{degenerate} && \text{if } [\![u\;\;u]\!] = 0, \\ &\textit{imaginary} && \text{if } [\![u\;\;u]\!] < 0. \end{aligned}$$

Taking the discriminant of two real or degenerate hyperspheres $\mathring{u}$ and $\mathring{v}$ to be the discriminant $\|u\;\;v\|$ of the corresponding hyperplanes $\check{U}$ and $\check{V}$, we find that the hyperspheres are

$$\begin{aligned} &\text{separating} && \text{if } \|u\;\;v\| > 0, \\ &\text{tangent} && \text{if } \|u\;\;v\| = 0, \\ &\text{separated} && \text{if } \|u\;\;v\| < 0. \end{aligned}$$

Applied to point-pairs $\ddot{u} = \{U_1, U_2\}$ and $\ddot{v} = \{V_1, V_2\}$ on an inversive circle, separation has the usual meaning associated with cyclic order (Coxeter 1966a, p. 218; 1998, pp. 22–23). That is, $\ddot{u}$ and $\ddot{v}$ are separating if $U_1U_2 \,//\, V_1V_2$, tangent if they have a point in common, and separated otherwise. For $n \geq 3$, two hyperspheres of I^{n-1} are separating, tangent, or separated according as they intersect in a real, degenerate, or imaginary $(n-3)$-sphere.

The angle between two separating hyperspheres $\mathring{u}$ and $\mathring{v}$ of I^{n-1}, which is the same as the angle between the corresponding intersecting hyperplanes of H^n, is given by

$$(\mathring{u}\mathring{v}) \;=\; \cos^{-1} \;\frac{|[\![u\;\;v]\!]|}{\sqrt{[\![u\;\;u]\!]}\sqrt{[\![v\;\;v]\!]}}. \tag{6}$$

Two separated hyperspheres $\mathring{u}$ and $\mathring{v}$ of I^{n-1} have an analogous *inversive distance* (Coxeter 1966b; 1998, pp. 292–298); this is the same as the minimum distance between the corresponding diverging hyperplanes of H^n and is given by

$$)\mathring{u}\mathring{v}(= \cosh^{-1} \frac{|[\![u\ v]\!]|}{\sqrt{[\![u\ u]\!]}\sqrt{[\![v\ v]\!]}}. \quad (7)$$

The last two formulas are especially relevant to the properties of regular inversive polytopes.

Antihedral Distances

If P is a regular *n*-polytope in a real metric space, the distance from the center *O* of the body of P to one of its vertices is the *circumradius* ${}_0R$, and the perpendicular distance from *O* to (the center of) a facet is the *inradius* ${}_{n-1}R$. When P is centrally symmetric, the *antihedral distance* between a pair of opposite facets is twice the inradius of P. Although an odd polygon $\{p\}:q$ or a regular simplex $\{3^{n-1}\}:w$ is not centrally symmetric, the regular compound $\{\{p\}\}:q$ or $\{\{3^{n-1}\}\}:w$ of two such polygons or simplexes in dual positions is. The distance between two opposite facets of the compound, one belonging to each component, can be taken as the antihedral distance of the polytope. The inradius of a regular asymptotic apeirotope is infinite, but there is no antihedral distance, since there are no opposite facets.

The *radius* ρ of a regular inversive polytope °P and its *antihedral distance* 2ρ are respectively the inradius and the antihedral distance of the corresponding regular asymptotic polytope P. When ρ is finite, the antihedral distance of °P is the inversive distance between two separated hyperspheres of I^{n-1}, opposite facets either of °P or of a regular compound of two °P's. For an inversive apeirotope, ρ is infinite. The *subradius* σ of °P is the radius of a facet of °P.

The inradius ${}_0R$ of an asymptotic ditel $\{\}:0$ or the radius ρ of an inversive dyad $°\{\}:0$ is infinite. For a regular inversive *p*-gon $°\{p\}:\infty$, ρ is the distance for which the angle of parallelism is π/p, and it follows from (5) that $\tanh\rho = \cos\pi/p$. Values for particular polygons are given in the table below, where we write τ and $\bar{\tau}$ for the golden-section number $\frac{1}{2}(\sqrt{5}+1)$ and its inverse $\frac{1}{2}(\sqrt{5}-1)$.

Table 1. *Regular Inversive Polygons*

Polygon	ω	$2\tanh\rho$
$°\{3\}:\infty$	0	1
$°\{4\}:\infty$	0	$\sqrt{2}$
$°\{5\}:\infty$	0	τ
$°\{\frac{5}{2}\}:\infty$	0	$\bar{\tau}$
$°\{6\}:\infty$	0	$\sqrt{3}$
$°\{p\}:\infty$	0	$2\cos\pi/p$
$°\{\infty\}:\infty$	0	2

With the help of some hyperbolic trigonometry, we obtain a simple formula for the radius ρ of a regular inversive polyhedron $°\{p, q\}:r$ in terms of its subradius σ and midangle ω:

$$\tanh \rho = \sinh \sigma \tan \omega = \frac{\tan \pi/r}{\tan \pi/p}. \tag{8}$$

The particular cases are listed in the following table.

Table 2. *Regular Inversive Polyhedra*

Polyhedron	$\tan \omega$	$\tanh \rho$
$°\{3, 3\}:6$	$\frac{1}{3}\sqrt{3}$	$\frac{1}{3}$
$°\{3, 4\}:4$	1	$\frac{1}{3}\sqrt{3}$
$°\{4, 3\}:6$	$\frac{1}{3}\sqrt{3}$	$\frac{1}{3}\sqrt{3}$
$°\{3, 5\}:\frac{10}{3}$	$\sqrt{(3+4\tau)/5}$	$\sqrt{(3+4\tau)/15}$
$°\{5, 3\}:6$	$\frac{1}{3}\sqrt{3}$	$\sqrt{(3+4\tau)/15}$
$°\{\frac{5}{2}, 5\}:\frac{10}{3}$	$\sqrt{(3+4\tau)/5}$	$\frac{1}{5}\sqrt{5}$
$°\{5, \frac{5}{2}\}:10$	$\sqrt{(3-4\bar{\tau})/5}$	$\frac{1}{5}\sqrt{5}$
$°\{\frac{5}{2}, 3\}:6$	$\frac{1}{3}\sqrt{3}$	$\sqrt{(3-4\bar{\tau})/15}$
$°\{3, \frac{5}{2}\}:10$	$\sqrt{(3-4\bar{\tau})/5}$	$\sqrt{(3-4\bar{\tau})/15}$
$°\{4, 4\}:4$	1	1
$°\{3, 6\}:3$	$\sqrt{3}$	1
$°\{6, 3\}:6$	$\frac{1}{3}\sqrt{3}$	1

From the relationship $\tanh \rho = \sinh \sigma \tan \omega$, which holds for all regular inversive n-polytopes with $n \geq 3$, we obtain the parameters for the seventeen regular inversive 4-polytopes $°\{p, q, r\}:s$, as given in the following table. The last figure is an apeirotope. Irrational values of s are rounded to four decimal places.

Table 3. *Regular Inversive 4-Polytopes*

4-Polytope	tan ω	tanh ρ
°{ 3, 3, 3 } : 5.1043	$\frac{1}{2}\sqrt{2}$	$\frac{1}{4}$
°{ 3, 3, 4 } : 3.2885	$\sqrt{2}$	$\frac{1}{2}$
°{ 4, 3, 3 } : 5.1043	$\frac{1}{2}\sqrt{2}$	$\frac{1}{2}$
°{ 3, 4, 3 } : 4	1	$\frac{1}{2}\sqrt{2}$
°{ 3, 3, 5 } : 2.6051	τ^2	$\frac{1}{4}\sqrt{2}\,\tau^2$
°{ 5, 3, 3 } : 5.1043	$\frac{1}{2}\sqrt{2}$	$\frac{1}{4}\sqrt{2}\,\tau^2$
°{ $\frac{5}{2}$, 5, 3 } : 3.0884	τ	$\frac{1}{2}\tau$
°{ 3, 5, $\frac{5}{2}$ } : 5.6751	$\bar{\tau}$	$\frac{1}{2}\tau$
°{ 5, $\frac{5}{2}$, 5 } : 3.0884	τ	$\frac{1}{2}\tau$
°{ $\frac{5}{2}$, 3, 5 } : 2.6051	τ^2	$\frac{1}{2}$
°{ 5, 3, $\frac{5}{2}$ } : 8.6103	$\bar{\tau}^2$	$\frac{1}{2}$
°{ $\frac{5}{2}$, 5, $\frac{5}{2}$ } : 5.6751	$\bar{\tau}$	$\frac{1}{2}\bar{\tau}$
°{ 3, $\frac{5}{2}$, 5 } : 3.0884	τ	$\frac{1}{2}\bar{\tau}$
°{ 5, $\frac{5}{2}$, 3 } : 5.6751	$\bar{\tau}$	$\frac{1}{2}\bar{\tau}$
°{ $\frac{5}{2}$, 3, 3 } : 5.1043	$\frac{1}{2}\sqrt{2}$	$\frac{1}{4}\sqrt{2}\,\bar{\tau}^2$
°{ 3, 3, $\frac{5}{2}$ } : 8.6103	$\bar{\tau}^2$	$\frac{1}{4}\sqrt{2}\,\bar{\tau}^2$
°{ 4, 3, 4 } : 3.2885	$\sqrt{2}$	1

There are six regular inversive 5-polytopes °{ p, q, r, s } : t, whose midangles ω and radii ρ can be determined from the following table. The last three are apeirotopes.

Table 4. *Regular Inversive 5-Polytopes*

5-Polytope	tan ω	tanh ρ
°{ 3, 3, 3, 3 } : 4.7668	$\frac{1}{5}\sqrt{15}$	$\frac{1}{5}$
°{ 3, 3, 3, 4 } : 3	$\sqrt{3}$	$\frac{1}{5}\sqrt{5}$
°{ 4, 3, 3, 3 } : 4.7668	$\frac{1}{5}\sqrt{15}$	$\frac{1}{5}\sqrt{5}$
°{ 4, 3, 3, 4 } : 3	$\sqrt{3}$	1
°{ 3, 3, 4, 3 } : 3	$\sqrt{3}$	1
°{ 3, 4, 3, 3 } : 4	1	1

For $n \geq 6$, there are just four regular asymptotic polytopes in hyperbolic n-space H^n: the asymptotic versions of the regular *n-simplex* and the dual *n-orthoplex* (cross polytope) and *n-orthotope* (block polytope)

$$\{ 3^{n-1} \} : a_n, \quad \{ 3^{n-2}, 4 \} : b_n, \quad \{ 4, 3^{n-2} \} : a_n,$$

and the asymptotic *orthic n-apeirotope* (grid apeirotope)

$$\{ 4, 3^{n-3}, 4 \} : b_n.$$

Each of these figures has a corresponding regular inversive polytope in I^{n-1}. The parameters a_n and b_n are defined by

$$\tan \frac{\pi}{a_n} = \sqrt{\frac{n-2}{n}} \quad \text{and} \quad \tan \frac{\pi}{b_n} = \sqrt{n-2}. \tag{9}$$

Note that $\lim_{n\to\infty} a_n = 4$ and $\lim_{n\to\infty} b_n = 2$. The following table gives the midangle ω and radius ρ of each regular inversive n-polytope ($n \geq 6$).

Table 5. *Regular Inversive n-Polytopes*

n-Polytope	$\tan \omega$	$\tanh \rho$
$^\circ\{ 3, 3, \ldots, 3, 3 \} : a_n$	$\sqrt{\frac{n-2}{n}}$	$\frac{1}{n}$
$^\circ\{ 3, 3, \ldots, 3, 4 \} : b_n$	$\sqrt{n-2}$	$\frac{1}{\sqrt{n}}$
$^\circ\{ 4, 3, \ldots, 3, 3 \} : a_n$	$\sqrt{\frac{n-2}{n}}$	$\frac{1}{\sqrt{n}}$
$^\circ\{ 4, 3, \ldots, 3, 4 \} : b_n$	$\sqrt{n-2}$	1

Regular inversive polytopes with identical vertex sections have the same midangle ω, and dual polytopes

$$^\circ\{ p, q, \ldots, u, v \} : w \quad \text{and} \quad ^\circ\{ v, u, \ldots, q, p \} : o$$

have the same radius ρ. Also, except for polygons $^\circ\{ p \} : \infty$ with more than six sides, $\tan \omega$ and $\tanh \rho$ either are rational numbers or have expressions involving nothing worse than nested square roots.

Conformal Models

The Euclidean plane can be given the topology of a sphere by means of a "one-point compactification," i.e., by adjoining a single point at infinity $\dot{O}$ that lies on every line. If such extended lines are treated as infinite (or "great") circles on the same footing as ordinary (or "small") circles, and if we allow a circle-preserving transformation, or *circularity*, to move the point $\dot{O}$, the resulting "inversive plane" or *parabolic sphere* $\dot{\mathrm{S}}^2$ provides a conformal model for the inversive sphere I^2. A circularity is called a *homography* or an *antihomography* according as it preserves or reverses orientation; homographies are also known as Möbius transformations.

An ordinary point with Cartesian coordinates (x, y) has *parabolic coordinates*

$$(\tfrac{1}{2}(x^2 + y^2 + 1),\ x,\ y,\ \tfrac{1}{2}(x^2 + y^2 - 1)),$$

while the exceptional point $\dot{O}$ is

$$(1,\ 0,\ 0,\ 1).$$

A small circle with center (h, k) and radius r has parabolic coordinates

$$[\tfrac{1}{2}(r^2 - h^2 - k^2 - 1),\ h,\ k,\ \tfrac{1}{2}(r^2 - h^2 - k^2 + 1)],$$

The equation of a small circle is $(x - h)^2 + (y - k)^2 = r^2$. A great circle, i.e., a line, with inclination θ and displacement c has coordinates

$$[c,\ \sin\theta,\ -\cos\theta,\ -c],$$

with $0 \le \theta < \pi$. The equation of a line is $y \cos\theta = x \sin\theta + c$; if $\theta \ne \pi/2$, the line has slope $m = \tan\theta$ and y-intercept $b = c \sec\theta$. Parabolic coordinates for points and circles of $\dot{\mathrm{S}}^2$ (and nonzero scalar multiples thereof) can be taken as homogeneous coordinates for points and circles of I^2.

An inversive circle $\mathring{c}$, with coordinates $[\![c]\!] = [c_0,\ c_1,\ c_2,\ c_3]$, is real, degenerate, or imaginary according as the quadratic form

$$[\![c\ \ c]\!] = c_1^{\,2} + c_2^{\,2} + c_3^{\,2} - c_0^{\,2}$$

Is positive, zero, or negative. In the nondegenerate cases an *inversion* in $\mathring{c}$ is the involutory circularity $\mathrm{I}^2 \to \mathrm{I}^2$ induced by the pseudo-orthogonal *inversion matrix*

$$C = \frac{1}{[\![c\ \ c]\!]} \begin{pmatrix} c_0^{\,2} + c_1^{\,2} + c_2^{\,2} + c_3^{\,2} & -2c_0c_1 & -2c_0c_2 & -2c_0c_3 \\ 2c_1c_0 & -c_0^{\,2} - c_1^{\,2} + c_2^{\,2} + c_3^{\,2} & -2c_1c_2 & -2c_1c_3 \\ 2c_2c_0 & -2c_2c_1 & -c_0^{\,2} + c_1^{\,2} - c_2^{\,2} + c_3^{\,2} & -2c_2c_3 \\ 2c_3c_0 & -2c_3c_1 & -2c_3c_2 & -c_0^{\,2} + c_1^{\,2} + c_2^{\,2} - c_3^{\,2} \end{pmatrix} \tag{10}$$

(cf. Schwerdtfeger 1962, pp. 117–118). Each point $(\!|p|\!) = (p_0,\ p_1,\ p_2,\ p_3)$ is interchanged with the point $(\!|p|\!)C$. If $[\![c\ \ c]\!] > 0$, this is a *hyperbolic inversion*, leaving all points on the real circle $\mathring{c}$ invariant and taking each circle orthogonal to $\mathring{c}$ into itself. If $[\![c\ \ c]\!] < 0$, the circularity is an *elliptic inversion* in the imaginary circle $\mathring{c}$, leaving no real points invariant. Every circularity of I^2 is the product of (at most four) hyperbolic inversions.

If we now fix a *central* inversion in a particular real inversive circle Ω, say the unit circle or the x-axis, we obtain a conformal model for the metric *hyperbolic sphere* $\ddot{\mathrm{S}}^2$ (cf. Johnson 1981, pp. 452–454). A point on one side

of Ω inverts into a point on the other side, and such *antipodal* point-pairs represent the ordinary points of the *hyperbolic plane* H^2. The self-antipodal points on the "equator" Ω are the absolute points of H^2. Inversive circles orthogonal to Ω ("great" circles of $\ddot{\mathrm{S}}^2$) represent ordinary lines of H^2. A circularity of I^2 that takes Ω into itself is an isometry of H^2. The mapping $\mathrm{I}^2 \to \mathrm{H}^2$ preserves angular measure, and the minimum distance between two diverging lines in H^2 is the same as the inversive distance between the representative separated circles in I^2 (cf. Coxeter 1998, pp. 308–311). Note that a regular inversive polygon $^\circ\{p\}:\infty$ whose vertices all lie on Ω is the trace on Ω of a regular asymptotic polygon $\{p\}:\infty$.

The mapping just described can be made one-to-one by identifying antipodal points of $\ddot{\mathrm{S}}^2$ or, equivalently, by restricting the domain to points on one side of Ω, e.g., the interior of the unit circle or points with positive y-coordinates, with hyperbolic lines represented by inversive circular arcs instead of whole circles. In this manner we obtain Poincaré's "conformal disk" and "upper half-plane" models for the hyperbolic plane.

As a model for the inversive sphere I^2, the completed Euclidean plane can be replaced by the *elliptic sphere* S^2, taken as the unit sphere in Euclidean 3-space. A conformal mapping from the "equatorial plane" $z = 0$ to S^2 can be achieved by stereographic projection, in which a line through an arbitrary point $(x, y, 0)$ and the "north pole" $(0, 0, 1)$ meets the sphere again in the point (ξ, η, ζ), with $(0, 0, 1)$ itself corresponding to the exceptional point $\dot{O}$ (cf. Schwerdtfeger 1962, pp. 22–29). The relationship between two-dimensional Cartesian coordinates (x, y) and spherical coordinates (ξ, η, ζ) is given by

$$\xi = \frac{2x}{x^2 + y^2 + 1}, \qquad \eta = \frac{2y}{x^2 + y^2 + 1}, \qquad \zeta = \frac{x^2 + y^2 - 1}{x^2 + y^2 + 1}. \tag{11}$$

The parabolic coordinates $(\tfrac{1}{2}(x^2 + y^2 + 1), x, y, \tfrac{1}{2}(x^2 + y^2 - 1))$ of a point can be replaced by *normalized coordinates* $(1, \xi, \eta, \zeta)$, with $\xi^2 + \eta^2 + \zeta^2 = 1$.

A regular asymptotic polyhedron $\{p, q\}:r$ of finite inradius can be represented in the Beltrami–Klein model for H^3 by a regular Euclidean polyhedron $\{p, q\}:r'$ inscribed in the unit sphere. Although it does not preserve angles between ordinary planes, so that $r' \neq r$, the Beltrami–Klein model is conformal on the absolute sphere. Thus the inversive circles in which adjacent face-planes of $\{p, q\}:r'$ meet the sphere intersect in an angle of $2\pi/r$, producing a regular inversive polyhedron $^\circ\{p, q\}:r$.

The above procedures can be extended to construct conformal Euclidean and spherical models for hyperbolic n-space and inversive $(n-1)$-space and for regular inversive n-polytopes $^\circ\{p, q, \ldots, u, v\}:w$.

Bibliography

H. S. M. Coxeter 1966a. "The inversive plane and hyperbolic space," *Abh. Math. Sem. Univ. Hamburg* **29**, 217–242.

———— 1966b. "Inversive distance," *Ann. Mat. Pura Appl.* (4) **71**, 73–83.

———— 1998. *Non-Euclidean Geometry*, 6th ed. Math. Assoc. of America, Washington, 1998.

N. W. Johnson 1981. "Absolute polarities and central inversions," in *The Geometric Vein: The Coxeter Festschrift*, C. Davis, B. Grünbaum, and F. A. Sherk, eds. (Springer-Verlag, New York–Heidelberg–Berlin, 1981), 443–464.

P. McMullen and E. Schulte 2002. *Abstract Regular Polytopes*, Encyclopedia of Mathematics and Its Applications, Vol. 92. Cambridge Univ. Press, Cambridge–New York, 2002.

H. Schwerdtfeger 1962. *Geometry of Complex Numbers: Circle Geometry, Moebius Transformation, Non-Euclidean Geometry*, Mathematical Expositions, No. 13, Univ. of Toronto Press, Toronto, 1962; Dover, New York, 1979.

Author's Information

Norman W. Johnson *– Professor of Mathematics Emeritus, Wheaton College, Norton, Mass. 02766, U.S.A.; e-mail: njohnson@wheatonma.edu*

Major Fields of Scientific Research: Non-Euclidean geometry, discrete geometry, regular polytopes, Coxeter groups

CONSTRUCTION OF GEOMETRIC DIVERGENCE ON q-EXPONENTIAL FAMILY

Hiroshi Matsuzoe

Abstract: *A divergence function is a skew-symmetric distance like function on a manifold. In the geometric theory of statistical inference, such a divergence function is useful. In complex systems, Tsallis anomalous statistics is developing rapidly. A q-exponential family is an important statistical model in Tsallis statistics. For this q-exponential family, a divergence function is constructed from the viewpoint of affine differential geometry.*

Keywords: *information geometry, affine differential geometry, Tsallis statistics, divergence, q-exponential family*

ACM Classification Keywords*: G.0 General*

MSC*: 53A15, 62B10, 53A30*

Introduction

A divergence function is a skew-symmetric squared distance like function on a manifold. In information geometry, which is a geometric theory of statistical inference, divergence functions play important roles. The Kullback-Leibler divergence is a typical example of such divergence functions [Amari and Nagaoka, 2000].

Recently, theory of complex systems has been developing rapidly. In complex systems, Tsallis statistics is one of anomalous statistics based on generalized entropies [Tsallis, 2009]. A q-exponential family is an important statistical model in Tsallis statistics, which includes various long tail probability distributions.

In this paper, we construct a divergence function on a q-exponential family from the viewpoint of affine differential geometry. For this purpose, we study generalized conformal geometry and affine hypersurface theory.

In information geometry, affine differential geometry is more useful than Riemannian geometry, and it is known that affine differential geometry generalizes geometry of distance. See [Matsuzoe, 2009], for example.

Statistical manifolds and generalized conformal geometry

First, let us recall geometry of statistical manifolds. Further details about statistical manifolds and generalized conformal equivalence relations, see [Matsuzoe, 2009; Matsuzoe, 2010], for example.

Definition 1 ([Kurose, 1994]). Let (M, h) be a semi-Riemannian manifold and let ∇ be a torsion-free affine connection on M. We say that the triplet (M, ∇, h) is a *statistical manifold* if the covariant derivative ∇h is a totally symmetric, that is, the following equation folds:

$$(\nabla_X h)(Y, Z) = (\nabla_Y h)(X, Z),$$

where X, Y and Z are arbitrary vector fields on M. The symmetric $(0, 3)$-tensor field $C := \nabla h$ is called the *cubic form* of (M, ∇, h). (In information geometry, the triplet (M, h, C) is also called a statistical manifold.)

For a statistical manifold (M, ∇, h), we can define another torsion-free affine connection by

$$Xh(Y, Z) = h(\nabla_X Y, Z) + h(Y, \nabla^*_X Z).$$

We call ∇^* the *dual connection* of ∇ with respect to h. In this case, the triplet (M, ∇^*, h) is a statistical manifold, which is called the *dual statistical manifold* of (M, ∇, h).

Here let us recall that a statistical model is a statistical manifold [Amari and Nagaoka, 2000]. Let $(\Omega, \mathcal{F})$ be a measurable space, and let S be a parametric statistical model on Ω. That is, S is a set of all probability densities on Ω parametrized by $\theta = (\theta^1, \dots, \theta^n) \in \Theta \subset \mathbf{R}$ such that

$$S = \left\{ p(x;\theta) \,\middle|\, p(x;\theta) > 0,\ \int_\Omega p(x;\theta)dx = 1 \right\},$$

where x is a random variable on Ω. We assume that S is a manifold with a local coordinate system $(\theta^1, \dots, \theta^n)$. For simplicity, set $\partial_i := \partial/\partial\theta^i$. We define a symmetric matrix (g^F_{ij}) $(i, j = 1, 2, \dots, n)$ by

$$g^F_{ij}(\theta) := \int_\Omega (\partial_i \log p(x;\theta))\,(\partial_j \log p(x;\theta))\, p(x;\theta)dx.$$

If $(g^F_{ij}(\theta))$ is positive definite, it determines a Riemannian metric on M. We call g^F the *Fisher metric* on M.

For an arbitrary constant $\alpha \in \mathbf{R}$, we can define a torsion-free affine connection $\nabla^{(\alpha)}$ on S by

$$\Gamma^{(\alpha)}_{ij,k}(\theta) := \int_\Omega \left\{ \partial_i\partial_j \log p(x;\theta) + \frac{1-\alpha}{2} (\partial_i \log p(x;\theta))\,(\partial_j \log p(x;\theta)) \right\} (\partial_k \log p(x;\theta))\, p(x;\theta)dx,$$

where $\Gamma^{(\alpha)}_{ij,k}(\theta)$ is the Christoffel symbol of the first kind, i.e., $g^F(\nabla^{(\alpha)}_{\partial_i}\partial_j, \partial_k) = \Gamma^{(\alpha)}_{ij,k}(\theta)$. The affine connection $\nabla^{(\alpha)}$ is called the *α-connection* on M. For an arbitrary constant $\alpha \in \mathbf{R}$, $\nabla^{(\alpha)}$ and $\nabla^{(-\alpha)}$ are mutually dual with respect to g^F, and the triplets $(M, \nabla^{(\alpha)}, g^F)$ and $(M, \nabla^{(-\alpha)}, g^F)$ are dual statistical manifolds. We remark that $(M, \nabla^{(\alpha)}, g^F)$ is invariant under the choice of the reference measure on Ω. Hence we call $(M, \nabla^{(\alpha)}, g^F)$ an *invariant statistical manifold*.

A statistical model S_e is an *exponential family* if $S_e = \left\{ p(x;\theta) \,\middle|\, p(x;\theta) = \exp\left[\sum_{i=1}^n F_i(x)\theta^i - \psi(\theta)\right] \right\}$, where $F_1(x), \dots, F_n(x)$ are random variables on Ω, and ψ is a convex function on Θ. For an exponential family, the Fisher metric g^F and the α-connection $\nabla^{(\alpha)}$ are given by

$$g^F_{ij}(\theta) = \partial_i\partial_j\psi(\theta), \quad \Gamma^{(\alpha)}_{ij,k} = \frac{1-\alpha}{2} C^F_{ijk}(\theta) = \frac{1-\alpha}{2}\partial_i\partial_j\partial_k\psi(\theta).$$

Since $\Gamma^{(1)}_{ij,k} \equiv 0$, the 1-connection $\nabla^{(1)}$ is flat and $\{\theta^1, \dots, \theta^n\}$ is an affine coordinate system on S_e. For this reason, the 1-connection $\nabla^{(1)}$ on an exponential family S_e is called an *exponential connection*.

Next, we consider the 1-conformal equivalence relation on statistical manifolds.

Definition 2 ([Kurose, 1994]). We say that statistical manifolds (M, ∇, h) and $(M, \bar\nabla, \bar h)$ are *1-conformally equivalent* if there exists a function λ such that

$$\begin{aligned} \bar h(X,Y) &= e^\lambda h(X,Y), \\ \bar\nabla_X Y &= \nabla_X Y - h(X,Y)\mathrm{grad}_h\lambda, \end{aligned}$$

where $\mathrm{grad}_h\lambda$ is the gradient vector field of λ with respect to h. A statistical manifold (M, ∇, h) is said to be *1-conformally flat* if (M, ∇, h) is locally 1-conformally equivalent to some flat statistical manifold.

Geometry of q-exponential family

In this section, we consider geometry of q-exponential families. First, let us recall the definitions of q-exponential functions and q-exponential families

For a fixed positive number q, the *q-exponential function* and the *q-logarithm function* are defined by

$$\exp_q x := \begin{cases} (1+(1-q)x)^{\frac{1}{1-q}}, & q \neq 1, \quad (1+(1-q)x > 0), \\ \exp x, & q = 1, \end{cases}$$

$$\log_q x := \begin{cases} \dfrac{x^{1-q}-1}{1-q}, & q \neq 1,\ (x > 0), \\ \log x, & q = 1,\ (x > 0), \end{cases}$$

respectively. When $q \to 1$, the q-exponential function recovers the standard exponential, and the q-logarithm function recovers the standard logarithm. A statistical model S_q is said to be a *q-exponential family* if $S_q = \left\{p(x,\theta)\,\middle|\, p(x;\theta) = \exp_q\left[\sum_{i=1}^n \theta^i F_i(x) - \psi(\theta)\right], \theta \in \Theta \subset \mathbf{R}^n\right\}$. We remark that a q-exponential family is obtained from the maximization principle of the generalized entropy in Tsallis statistics [Tsallis, 2009].

In the same manner as an exponential family, we can define geometric objects on S_q. We define the *q-Fisher metric* g^q, the *q-cubic form* C^q, and the *q-exponential connection* $\nabla^{q(e)}$ by

$$g^q_{ij} := \frac{\partial^2 \psi}{\partial\theta^i \partial\theta^j}, \quad C^q_{ijk} := \frac{\partial^3 \psi}{\partial\theta^i \partial\theta^j \partial\theta^k}, \quad g^q(\nabla^{q(e)}_X Y, Z) := g^q(\nabla^{q(LC)}_X Y, Z) - \frac{1}{2} C^q(X,Y,Z),$$

respectively, where $\nabla^{q(LC)}$ is the Levi-Civita connection with respect to g^q. In this case, $(S_q, \nabla^{q(e)}, g^q)$ is a flat statistical manifold. Denote by $\nabla^{(2q-1)}$ the $(2q-1)$-connection on S_q, i.e., $\alpha = 2q-1$. The triplet $(S_q, \nabla^{(2q-1)}, g^F)$ is an invariant statistical manifold. The following lemma is given in [Matsuzoe and Ohara, 2011].

Lemma 1. *For a q-exponential family S_q, consider a flat statistical manifold $(S_q, \nabla^{q(e)}, g^q)$, and an invariant statistical manifold $(S_q, \nabla^{(2q-1)}, g^F)$. Then these two statistical manifolds are 1-conformally equivalent, that is,*

$$\begin{aligned} g^q(X,Y) &= \frac{q}{Z_q} g^F(X,Y), \\ \nabla^{q(e)}_X Y &= \nabla^{(2q-1)}_X Y - g^F(X,Y)\mathrm{grad}_h\left(\log\frac{q}{Z_q}\right), \end{aligned}$$

where $Z_q(\theta) = \int_\Omega p(x;\theta)^q dx$. In particular, $(S_q, \nabla^{(2q-1)}, g^F)$ is 1-conformally flat.

The geometric divergence on q-exponential family

In this section, we consider realizations of q-exponential families into affine space, and constructions of geometric divergences. For more details about affine differential geometry, see [Nomizu and Sasaki, 1994].

Let M be an n-dimensional manifold, and let f be an immersion from M to $\mathbf{R}^{n+1}$. Denote by ξ a *transversal vector field*, that is, the tangent space is decomposed as $T_{f(p)}\mathbf{R}^{n+1} = f_*(T_pM) \oplus \mathrm{Span}\{\xi_p\}, (^\forall p \in M)$. We call the pair $\{f, \xi\}$ an *affine immersion* from M to $\mathbf{R}^{n+1}$.

Denote by D the standard flat affine connection. Then we have the following decompositions:

$$D_X f_* Y = f_*(\nabla_X Y) + h(X,Y)\xi, \tag{1}$$
$$D_X \xi = -f_*(SX) + \tau(X). \tag{2}$$

We call ∇ a *induced connection*, h an *affine fundamental form*, S an *affine shape operator*, and τ a *transversal connection form*. If the affine fundamental form h is nondegenerate, the immersion f is said *nondegenerate*. If $\tau = 0$, the affine immersion $\{f, \xi\}$ is said *equiaffine*. It is known that the induced objects (M, ∇, h) becomes a 1-conformally flat statistical manifold if the affine immersion is nondegenerate and equiaffine [Kurose, 1994].

The induced objects depend on the choice of transversal vector field. For a function ϕ on M, and a vector field Z on M, if we change a transversal vector field ξ to $\bar{\xi} = e^\phi \xi + f_*(Z)$,Then the induced objects change as follows (See Chapter 2 in [Nomizu and Sasaki, 1994]):

$$\bar{h}(X,Y) = e^{-\phi} h(X,Y), \tag{3}$$
$$\overline{\nabla}_X Y = \nabla_X Y - e^{-\phi} h(X,Y) Z, \tag{4}$$
$$\bar{\tau}(X) = \tau(X) + e^{-\phi} h(X,Z) - d\phi(X). \tag{5}$$

Theorem 1. *For a q-exponential family $S_q = \left\{p(x,\theta)\,\middle|\, p(x;\theta) = \exp_q\left[\sum_{i=1}^n \theta^i F_i(x) - \psi(\theta)\right]\right\}$, set*

$$\begin{aligned} f_q(p(\theta)) &= \{\theta^1, \ldots, \theta^n, \psi(\theta)\}^T, \\ \xi_q &= \{0, \ldots, 0, 1\}^T, \\ \xi^F_q &= \{e^{-\phi}\xi_q + f_* \mathrm{grad}_h \phi\}, \end{aligned}$$

where $\phi = \log(Z_q/q)$ *and* $Z_q(\theta) = \int_\Omega p(x;\theta)^q dx$. *Then the pair* $\{f_q, \xi_q\}$ *is an affine immersion which realizes the flat statistical manifold* $(S_q, \nabla^{q(e)}, g^q)$. *The pair* $\{f_q, \xi_q^F\}$ *is an affine immersion which realizes the invariant statistical manifold* $(S_q, \nabla^{2q-1)}, g^F)$.

Proof. From the definitions of q-Fisher metric, q-exponential connection and Equations (1)-(2), the affine immersion $\{f_q, \xi_q\}$ realizes $(S_q, \nabla^{q(e)}, g^q)$ in $\mathbf{R}^{n+1}$. From Lemma 1 and Equations (3)-(5), the affine immersion $\{f_q, \xi_q^F\}$ realizes $(S_q, \nabla^{2q-1)}, g^F)$ in $\mathbf{R}^{n+1}$. □

Finally, we define the geometric divergence on q-exponential family. For a nondegenerate equiaffine immersion $\{f, \xi\}$, the *conormal map* $\nu : M \to \mathbf{R}_{n+1}$ of $\{f, \xi\}$ by $\nu_p(f_* X) = 0$ and $\nu_p(\xi(p)) = 1$. Then we define a skew-symmetric function ρ on $M \times M$ by

$$\rho(p, q) = \nu_p(f(q) - f(p)).$$

The function ρ is called the *geometric divergence* [Kurose, 1994; Matsuzoe, 2010]. In fact, ρ induces the given statistical manifold structure, that is, the geometric divergence ρ_q for $\{f_q, \xi_q\}$ induces $(S_q, \nabla^{q(e)}, g^q)$, and ρ_F for $\{f_q, \xi_q^F\}$ induces $(S_q, \nabla^{2q-1)}, g^F)$.

Conclusion

A q-exponential family is an important statistical model in Tsallis statistics. In this paper, we give a hypersurface affine immersion of q-exponential family. As a consequence, we obtain a divergence function on a q-exponential family, which is an important distance like function in information geometry.

Acknowledgments

This research was partially supported by JSPS, Grant-in-Aid for Young Scientists (B), No. 23740047.

Bibliography

[Amari and Nagaoka, 2000] S. Amari and H. Nagaoka, Methods of information geometry, Amer. Math. Soc., Providence, Oxford University Press, Oxford, 2000.

[Kurose, 1994] T. Kurose, On the divergences of 1-conformally flat statistical manifolds, Tôhoku Math. J., 46, 427-433, 1996.

[Matsuzoe, 2009] H. Matsuzoe, Computational Geometry from the Viewpoint of Affine Differential Geometry, Lecture Notes in Computer Science, 5416, 103-123, 2009.

[Matsuzoe, 2010] H. Matsuzoe, Statistical manifolds and affine differential geometry, Adv. Stud. Pure Math., 57, 303-321, 2010.

[Matsuzoe and Ohara, 2011] H. Matsuzoe and A. Ohara, Geometry for q-exponential families, Recent Progress in Differential Geometry and Its Related Fields: Proceedings of the 2nd International Colloquium on Differential Geometry and its Related Fields, World Sci. Publ., 55-71, 2011.

[Nomizu and Sasaki, 1994] K. Nomizu and T. Sasaki, Affine differential geometry – Geometry of Affine Immersions –, Cambridge University Press, 1994.

[Tsallis, 2009] C. Tsallis, Introduction to Nonextensive Statistical Mechanics: Approaching a Complex World, Springer, 2009.

Authors' Information

Hiroshi Matsuzoe *- Associate Professor, Ph.D., Department of Computer Science and Engineering, Graduate School of Engineering, Nagoya Institute of Technology, Nagoya 466-8555, Japan; e-mail: matsuzoe@nitech.ac.jp*

PART 2

Applications of Mathematics of Distances

METRIC BASED RECOMMENDER SYSTEMS

Ali Akhtarzada, Cristian S. Calude, John Hosking

Abstract: *Information overload and an abundance of choices create situations where selecting one option becomes extremely difficult or even worse, a guessing game. Collaborative ranking systems address this problem by creating intelligent rankings of items based on user opinions aggregation. This paper presents a metric-based multi-criteria recommender system that can be used on non-rigid sets of criteria. These systems fare well with respect to accuracy, transparency and flexibility.*

Keywords: *Multi-dimensional recommender system, metric method.*

ACM Classification Keywords*: H.4: Information systems applications*

MSC*: 68N30: Mathematical aspects of software engineering*

Introduction

This paper presents metric-based multi-criteria recommender systems that can be used on non-rigid sets of criteria (that may be defined by the users of a system). The approach uses a novel concept of an ideal candidate, which is an aggregation of users' digital belief systems: the algorithm first calculates a hypothetical ideal candidate, which is then used as the pivot point.

The paper is structured as follows. First, we briefly present the motivation and related results. Then, an overview of the algorithm is informally described, an example scenario in which the algorithm is applied is discussed, and a detailed description of the algorithm itself is given. We then describe a proof of concept implementation of the algorithm and a user study evaluating the perceived accuracy of the algorithm and usability of the system. We finish with conclusions and a brief discussion of future work.

Motivation and related facts

The biggest motivating factor for recommendation systems in general is that of information overload. Our society produces more information than it produces anything else [13; 27; 28][1]. Information overload leads to situations where the inputs to one's decision making process exceed the "capacity to assimilate and act on the information as well as the ability to evaluate every alternative" [25]. Information overload has also been linked with negative psychological impacts created by the illusion that more choices lead to better results [19]. Recommendation systems generally use single criteria ratings that define how good an entity is. For example [15] uses a single 10 star rating for each movie for their recommendations. More recently, multi-criteria recommendation systems have become popular, as evidenced by Yahoo! Movies' recent movie recommender system. Various surveys and papers [1; 2] have shown the increase in accuracy multi-criteria rating systems can achieve and have indicted the need for research activity in this area. Because of the amount of research out there, other papers [31] present methods on how to efficiently evaluate a recommender system. Transparency, "the opposite of secrecy" [17], is important because it goes hand-in-hand with trust and accountability. Transparency increases trust, hence the acceptance of a recommendation [11]. Transparency increases accountability too, as seen in numerous situations presented in Wikileaks (`http://www.wikileaks.org`). Fundamentally, a multi-criteria system allows for more transparency because one sees how each rating is broken down to create the overall rating. Flexibility is also paramount: it allows users to participate with their own preferences and knowledge. There has also been extensive work done

[1] The amount of digitally stored information in 2009 was estimated to be 500 exabytes [29].

on content, collaborative and hybrid based recommender systems and social information filtering, see for example [5; 22; 7; 2; 24]. Demographic, utility and knowledge based systems have been proposed by [7]. Recently, matrix factorisation methods have been used in [16].

Multi-criteria approaches to recommendation and ranking systems have been considered in [1; 12]. The authors crawled Yahoo! Movies and extracted a number of movie ratings decomposed into 4 criteria; they found that using multi-criteria ratings allows for more accurate ratings than single ratings. One approach they used was to simply divide the multi-criteria problem into M single criteria recommendation problems, thus treating each criteria as a single rating. Another approach taken by [21] treats tags as multiple dimensions and first infers users' preferences for tags and then resultantly for items (movies).

Multi-criteria approaches to recommendation and ranking systems are subject to limitations which were first proved for voting systems. The most famous result, Arrow's Impossibility Theorem [4] (also known as Arrow's Paradox), states that no voting system can turn individual preferences into a global (community) ranking if there are three or more options to choose from and a few "innocent-looking" conditions (such as, non-dictatorship, Pareto efficiency, and independence of irrelevant alternatives) are satisfied. Another limitation may appear because of the lack of independence of preferences.

Metric-Based Algorithms

Overview

Our main algorithm applies on a system composed of 5 parts: the users, the entities, the value dimensions, the belief system and the ideal candidate. *Entities* are anything that the system is recommending or ranking. For example in a movie recommender system, the movies would be the entities. *Value dimensions* are a set of factors that influence the ratings of an entity. For example, taste and price are value dimensions that influence the ratings of menu items in a restaurant. All entities are defined over a set of value dimensions. *Users* collaborate within the system by rating an entity over the set of value dimensions. For example a user may rate price high and taste poor, or price low and taste excellent.

The *belief system* is personal to each user. Each user is allowed to tell the system what ideal value they want a value dimension to have, and how important that value dimension is to them. For example, most people's belief system would have a value of 'low' for the dimension 'price' but depending on your level of income, the importance of price may vary. Finally, the *ideal candidate* is the set of ideal value dimensions. The system determines the ideal value dimensions by aggregating all users' belief systems into an average. That is, if there were 2 people in the system, and user one's belief system had the ideal value for price set to high, and user two's belief system had the ideal value for price set to low, then the ideal candidate will have it's ideal value for price set to 'in between low and high'. The ideal candidate can be thought of as the belief system of a hypothetical user that takes everyone's opinions into account.

Value dimensions can be either hard or soft. Hard value dimensions are factual, such as the price of an item, or the location of a building. Soft value dimensions are subjective, i.e. an opinion. The major difference between a soft and hard value dimension is that a hard dimension cannot be rated, while a soft one can. While a hard value dimension cannot be rated, it's belief weight can still be set. The price of an entity is a factual piece of information (bar bargaining practices), so it is an example of a hard value dimension. On the other hand, quality is a subjective (hence soft) value dimension as there are no standard measurements to quality which is subject to individual perspectives.

The ideal candidate discussed above is the global ideal candidate (i.e. all users' belief systems are aggregated into one). The system also uses a local ideal candidate, which is simply equivalent to a single user's belief system. The distinction between a local and global ideal candidate results in two different types of rankings and two different types of recommendations—a global and local ranking and a global and local recommendation. A global ranking

Dimension	Low value	High value
Humour (d_1)	not funny	hilarious
Complexity (d_2)	no brainer	very complex
Action (d_3)	no action	action packed
Acting (d_4)	bad	excellent

Table 1: Ranges for each dimension.

	Inception				Rush Hour				Dumb and Dumber			
	d_1	d_2	d_3	d_4	d_1	d_2	d_3	d_4	d_1	d_2	d_3	d_4
Frodo	2	5	4	5	4	1	4	4	3	1	1	4
Gimly	2	4	4	5	5	1	3	4	4	1	1	5
Bilbo	1	5	5	4	4	2	4	4	5	2	2	5
Sam	2	5	5	4	5	3	5	5	5	1	2	4
Pippin	2	5	4	4	3	2	5	4	4	1	1	5
Average	1.8	4.8	4.4	4.4	4.2	1.8	4.2	3.2	4.2	1.2	1.4	4.6

Table 2: Ratings given to each dimension per user and an average of all the ratings per entity.

of entities is one which calculates distances between an entity and the global ideal candidate, and a local ranking calculates distances between an entity and a local ideal candidate. Likewise, a global recommendation uses the global ideal candidate, which represents a community at large, and a local recommendation uses the local ideal candidate (personal to each individual). The ideal candidate refers to the global ideal candidate unless explicitly stated otherwise.

The algorithm that has been developed for the multi-criteria recommendation process is based on a distance metric that calculates the distance between an entity and the ideal candidate. The distances are then weighted to take into account importance levels. Two types of recommendations can be performed. One recommends similar items by finding similar entities to a pivot entity. The second recommends any items that match each user's belief system. That is, the second method is the same as the ranking algorithm, except instead of using the ideal candidate, it uses the specific user's belief system.

An example

We present an example to illustrate the developed algorithms, formally defined in the next section. In the scenario we have defined 5 users, 3 entities and 4 criteria. The entities we are rating are movies and the value dimensions that they are rated over are d_1 = humour, d_2 = complexity, d_3 = action and d_4 = acting. The five different users have all rated each movie along a set of 4 value dimensions.

The data we use is shown in Table 1, Table 2 and Table 3. All the data is presented as ratings between 1 and 5. This means that dimensions are rated on a 5-point scale, as are all the weights. What the scales represent per dimension is described in Table 1.

From Table 3 we can loosely categorize each user as follows: Frodo likes a well balanced movie and the quality of acting is very important. Gimly likes complicated, preferably action movies with some comedy, where complexity and acting matters most to him. Bilbo likes simple funny movies but no one particular dimension is overly important to him. Sam likes funny and dumb movies, and would prefer no action, but is not that fussed about action movies; the dumb part is important to him. Pippin likes action movies with no complexity (important). In short: Frodo is well balanced, Gimly likes complicated action with comic relief, Bilbo likes simple action comedies, Sam likes comedy sans action and Pippin likes action sans comedy.

	Value dimensions				Weights			
	d_1	d_2	d_3	d_4	w_1	w_2	w_3	w_4
Frodo	3	3	3	5	2	2	2	5
Gimly	3	4	5	5	2	4	3	4
Bilbo	5	2	3	5	3	3	3	3
Sam	5	1	1	5	4	5	3	1
Pippin	1	1	5	5	5	5	5	1

Table 3: Users' belief system.

Dimension	Ideal value	Ideal weight
d_1	3.4	3.2
d_2	2.2	3.8
d_3	3.4	3.2
d_4	5.0	2.8

Table 4: The ideal candidate calculated from all the user belief systems.

The three entities the algorithms will be applied to are the movies 'Inception', 'Rush Hour' and 'Dumb and Dumber', the ratings of which can be seen in Table 2.

The first step is to calculate the ideal candidate, which is an average of all the belief systems. The ideal candidate can be seen in Table 4. From this table we can see that the most important dimension is d_2 with a height of 3.8. The dimension that matters least in the system is d_4. Next we can determine the rankings of the entities by calculating the additive distance between each entity's average dimensional ratings, and the ideal candidate. We also apply the ideal weights to the calculations. Table 5 shows the global rankings of the system because the distances are calculated from the *global ideal candidate*. There is also the concept of the *local ideal candidate* which calculates the distance between an entity and a belief system which is local to the user in question. So we may also have a local ranking for each user, which is shown in Table 6. The local rank list is also the recommendation list.

From Table 5 and Table 6 we see that, according to the data provided, the rankings make sense. In Table 6, the person who likes complicated movies gets Inception ranked highest, the person who likes fun and dumb movies gets Dumb and Dumber. Table 7 shows the rankings for Sam, after we take out all of his rating data. So the system now has no information on Sam's ratings, but retains his belief system. We can see that, while the distances have changed, the order of recommended movies is perfect for him.

In Table 8 we see the second recommendation method, which finds the similarity between entities. In that table Inception is more similar to Dumb and Dumber than it is to the Rush Hour. This is a result of using the global ideal candidate as the pivot point. Alternatively, we can use specific belief systems as the pivot point for computing similarities. This is shows in Table 9, which is specific to the user Gimly, who likes complicated action movies. In that table, it shows that Inception is more similar to Rush Hour than to Dumb and Dumber (which would hold true for a recommendation personal to Gimly). A system using this recommendation process would recommend Rush Hour to Gimly if he was looking at the Inception page.

Entity	Rank	Distance
Rush Hour	1	0.1506
Dumb and Dumber	2	0.1857
Inception	3	0.1983

Table 5: Rankings of each entity.

	Rank	Entity	Distance		Rank	Entity	Distance
Frodo	1^{st}	Inception	0.2402	Gimly	1^{st}	Inception	0.1541
	2^{nd}	Rush Hour	0.242		2^{nd}	Rush Hour	0.173
	3^{rd}	Dumb and Dumber	0.272		3^{rd}	Dumb and Dumber	0.2545
Bilbo	1^{st}	Rush Hour	0.14	Sam	1^{st}	Dumb and Dumber	0.0934
	2^{nd}	Dumb and Dumber	0.155		2^{nd}	Rush Hour	0.195
	3^{rd}	Inception	0.22		3^{rd}	Inception	0.2721
Pippin	1^{st}	Inception	0.163				
	2^{nd}	Rush Hour	0.1761				
	3^{rd}	Dumb and Dumber	0.2053				

Table 6: Local rankings of each entity for each user.

Sam		
Rank	Entity	Distance
1^{st}	Dumb and Dumber	0.2882
2^{nd}	Rush Hour	0.3647
3^{rd}	Inception	0.4514

Table 7: Recommended movies for Sam created from Sam's belief system and ignoring all his ratings in Table 2.

	Inception	Rush Hour	Dumb and Dumber
Inception	1.0	0.9523	0.9868
Rush Hour	0.9523	1.0	0.9655
Dumb and Dumber	0.9868	0.9655	1.0

Table 8: Similarities between each movie, with 1 representing full similarity.

Gimly			
	Inception	Rush Hour	Dumb and Dumber
Inception	1.0	0.9811	0.8997
Rush Hour	0.9811	1.0	0.9186
Dumb and Dumber	0.8997	0.9186	1.0

Table 9: Similarities between each movie, personalized to Gimly's belief system.

Main Algorithm

The algorithm developed for the multi-criteria recommender system in [3] uses a weighted sum approach which is defined in multi-objective optimization literature [14]. The goal of a recommendation system is to construct the $Users \times Items$ 2-dimensional matrix by predicting the missing values in the matrix. The approach we take involves the reconstruction of a 3-dimensional matrix, with the third dimension being the set of criteria defined over the items, i.e. the value dimensions. Additionally, we use a weighted approach so that more important value dimensions make more of a difference to the final calculations.

For the rest of this section we use the following notation. The set of users U has $n = |U|$ elements. The set of entities denoted by E has $m = |E|$ elements. The set of value dimensions is denoted by V; let $l = |V|$ be the number of dimensions for each entity. Finally, let W be the set of weights such that $|W| = |V|$.

Our goal is to predict values in the $n \times m \times l$ matrix. There are three concepts used by the proposed algorithm: 1) value dimensions (i.e. criteria), 2) the belief system, and 3) the ideal candidate. *Value dimensions* determine the ratings of each entity in E. Each entity is defined by l value dimensions, which are collaboratively rated and then normalized to the range $[0, 1]$ before being used as the input to the algorithm. Therefore, each entity is a vector $e = (v_1, v_2, \cdots, v_l)$ for all $v \in V$.

A *belief system* (see Table 3) allows each user to define their beliefs using two components: 1) the values for each criteria and 2) the weights attached to each criteria. The weights are normalized to the range $[0, 1]$ with 0 representing no importance and 1 indicating utmost importance. Formally, each user u has a belief system B, which is the ordered pair $B_u = (v_u, w_u)$ where $v_u = (v_1, v_2, \cdots, v_l), w_u = (w_1, w_2, \cdots, w_l)$ are vectors and v_i, w_i represent the user's preferred value for value dimension i and weight i, respectively.

The *ideal candidate* is used as the pivot point for all distance calculations. Instead of calculating the distance of entities from the origin or from other entities, the algorithm makes use of a hypothetical ideal entity that is an aggregation of each users' belief system (see Table 4). Formally, the ideal candidate is an ordered pair $I = (v_I, w_I)$, where $v_I = (v_1, v_2, \cdots, v_l), w_I = (w_1, w_2, \cdots, w_l)$ and are calculated as follows:

$$I = \frac{1}{N}\sum_{i=1}^{N} B_i = \left(\frac{1}{N}\sum_{i=1}^{N} v_i, \frac{1}{N}\sum_{i=1}^{N} w_i\right). \tag{1}$$

Equation (1) is referred to as the global ideal candidate I_G, which takes into account every user's belief system. The local ideal candidate I_L is specific to each user and is simply equal to B_u. The ideal candidate is an entity as well, hence any algorithm that can calculate the distance or similarity between two entities can operate similarly with the ideal candidate.

Discrete Metrics and Similarities

Let $\mathbb{M}$ be a nonempty set of nonnegative real numbers with the greatest element $a = 1$. Then $d : \mathbb{M} \times \mathbb{M} \to \mathbb{R}$ is a metric on M and the ordered pair $(\mathbb{M}, d)$ is a metric space [9]:

$$d(x, y) = \begin{cases} \frac{1}{2}(1 + |x - y| - |1 - x - y|), \text{if } x \neq y, \\ 0, \text{if } x = y, \end{cases} \tag{2}$$

For our multi-criteria problem we can naturally extend the metric to $\mathbb{M}^l$

$$d_l(x, y) = \frac{1}{l}\sum_{i=1}^{l} d(x_i, y_i), x, y \in \mathbb{M}^l, \tag{3}$$

and to a weighted metric $d_w : \mathbb{M}^l \times \mathbb{M}^l \times \mathbb{M}^l \to \mathbb{R}$:

$$d_l(x, y, w) = \frac{1}{l} \sum_{i=1}^{l} (1 - w_i) d(x_i, y_i), x, y, w \in \mathbb{M}^l \tag{4}$$

The weights have to be normalized in the range $0 \leq w \leq 1$. From Table 3 we can see that the higher the weight w_i is, the more important it is. The more important a weight is the less it increases the distance results. Therefore, as a weight approaches 0, it's importance is reduced and the distance is increased. See more details in [3].

From equation (4) we can define a multi-criteria rating function in terms of $e \in E$, $u \in U$ and I. We define two rating functions, the global rating function $r_G : E \times I \rightarrow \mathbb{R}$:

$$r_G(e, I_G) = d_w(e, v_I, w_I), \tag{5}$$

and the local rating function $r_L : E \times I \rightarrow \mathbb{R}$:

$$r_L(e, I_L) = d_w(e, v_u, w_u). \tag{6}$$

The difference between r_G and r_L is that the global rating function calculates the distance between an entity and the global ideal candidate I_G while the local one calculates the distance between the local ideal candidate I_L.

There are two ways in which recommendations can be made using the algorithms. The first is a ranking of items obtained by using function (6). The results of this can be seen in Table 7. The second method uses a similarity metric to recommend entities that are similar to other entities. The similarity method can also be divided into two functions, one which uses the global ideal candidate I_G to obtain global recommendations, and one which uses a local ideal candidate I_L to obtain personalized recommendations.

From [10], any normalized distance metric d can be converted into a similarity metric s defined as follows: $s = 1 - d : 0 \leq d \leq 1$. Equations (2), (3) and (4) are normalized distance metrics that return a value in the range $[0, 1]$. If d is a normalized distance between two entities e_1 and e_2, then we can define a global similarity metric s_G as:

$$s_G(e_1, e_2, I_G) = 1 - |d_w(e_1, v_I, w_I) - d_w(e_2, v_I, w_I)|, \tag{7}$$

and the local similarity metric as:

$$s_L(e_1, e_2, I_L) = 1 - |d_w(e_1, v_u, w_u) - d_w(e_2, v_u, w_u)|. \tag{8}$$

Since s_G and s_L are both normalized similarity metrics, because d is normalized, they both satisfy the following "coherence" properties [10] for all x, y, z, I: $s_{G|L}(x, x, I) \geq 0$, $s_{G|L}(x, x, I) \geq s_{G|L}(x, y, I)$, $s_{G|L}(x, y, I) = s_{G|L}(y, x, I)$, $s_{G|L}(x, y, I) + s_{G|L}(x, z, I) \leq s_{G|L}(x, z, I) + s_{G|L}(y, y, I)$, $s_{G|L}(x, x, I) = s_{G|L}(y, y, I) = s_{G|L}(x, y, I) \iff x = y$.

The following functions showcase part of the pseudo code used for the developed prototype system. The function *distance* represents equation (4), the function *rating* represents equations (6), (5), and the function *similarity* represents equations (7,) (8).

```
Function distance( rating, ideal, weight )
  min = 1
  max = 5
  x = (min - rating) / (min - max)
  y = (min - ideal) / (min - max)
  if x == y, return 0
  return (1 - weight) * (0.5 * (1 + |x - y| - |1 - x - y|))
End

Function rating( entity )
```

```
  num_dims_used = 0
  total_distance = 0
  For each dimension dim in entity.category
    rating = average_rating(dim)
    total_distance += distance(rating, dim.ideal, dim.weight)
    num_dims_used += 1
  End For
  // Return a rating in between 0 and 1 (1 means perfect)
  return 1 - (num_dims_used / total_distance)
End

Function similarity( entity1, entity2 )
  return 1 - |rating(entity1) - rating(entity2)|
End
```

Implementation

A proof of concept system was developed for a local restaurant in Auckland, New Zealand. Users are required to sign up to obtain personalized recommendations. Signing up also requests demographic information so it can be used for extracting intelligence from the data (segmenting user preferences in to region, for example). Signed in users can add or edit a value dimension, set their beliefs, rate a menu item or view details about a menu item.

Adding a value dimension and editing a value dimension use the same input screen. End users can only add soft value dimensions. Only administrators can add hard value dimensions, such as Price, via a different input screen. Once a hard value dimension is added it becomes part of an entity's profile. For example, having added Price, each priced entity has attached to it a new property, called price, the value of which can be changed on the entity's edit page. Furthermore, the type of scale that is used can be chosen by the user as well. The prototype implementation supports the addition of ordinal and nominal scales. The user must also specify which category the value dimension applies over.

Once value dimensions are provided, users can set their beliefs. Figure 1 shows the belief entry screen. Two columns are shown, one for the ideal value for a belief and the other for the weight of the value dimension. There are two scale types: one is an ordinal scale with a low and high range and the other a nominal scale. These ideal values are used to calculate the global ideal value and importance of a dimension.

Users can also obtain valuable statistics at this point. For example clicking on the value dimension 'healthiness', you will be informed that 44 people in the system care about this dimension and that most people think that the healthiness of mains, desserts and starters should be, ideally, almost as healthy as you can get and that while healthiness matters, it is not vital nor is it very important in determining the rating of food. You will also be told that while healthiness matters somewhat in the United States, it's more important in Germany, and less important in Canada. This is of course reflective of the beliefs of the system's users.

The prototype allows users to rate menu items over all soft value dimensions entered into the system; hard value dimensions are facts and can only be changed by the administrators of the system. The rating screen can be seen in Figure 2. Users are free to ignore certain value dimensions. The more a value dimension is ignored, the more obvious it becomes that this value dimension is not worth having in the system. A straightforward extension would be for the system to provide a confidence level to each value dimension's importance level.

The system can perform two types of recommendations, one based on entity-to-entity similarity and one showing users predicted ratings of all the entities in the system (that have been rated by anyone). The second type of recommendation does not depend on entity-to-entity similarity, nor on user similarity, only on the similarity between a user's belief system and the entity's profile (which is composed of value dimensions and their aggregated values). The first type of recommendation (entity-to-entity) is shown in Figure 3. It uses the user's belief system as the pivot point if the user is logged in.

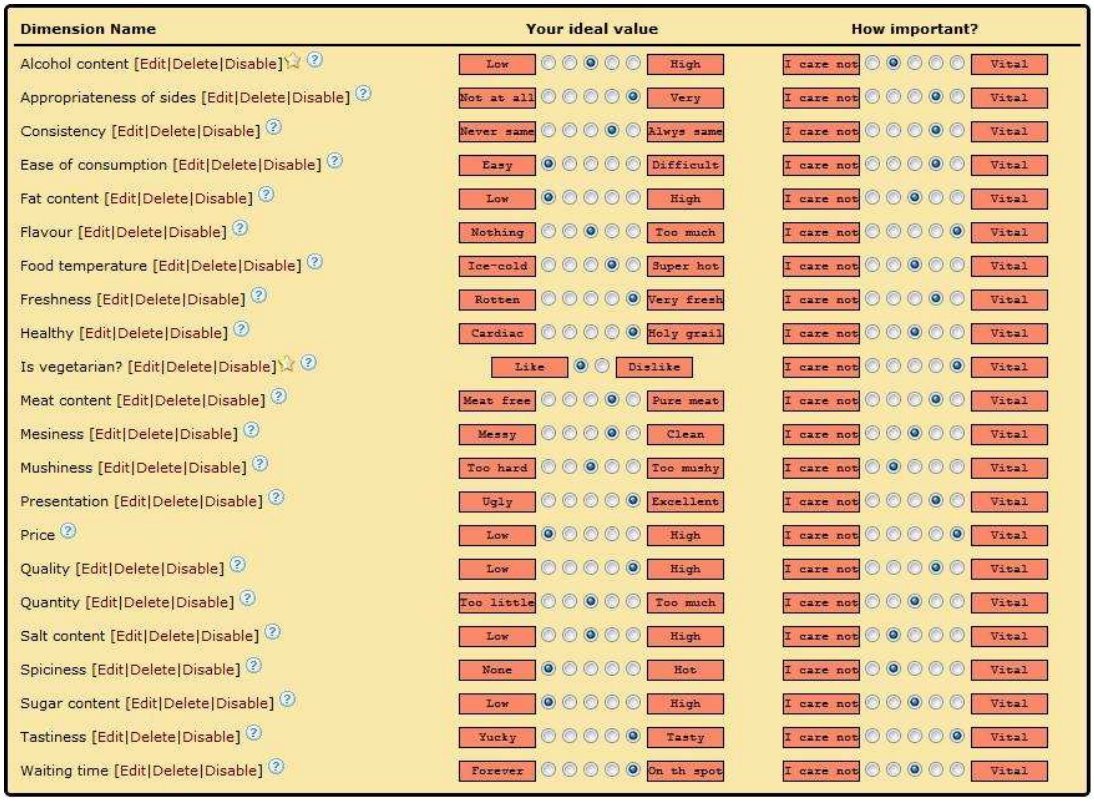

Figure 1: Setting your beliefs involves setting an ideal value and a weight.

The system will list all the details about the entity in question. This includes how many users have rated it, what the global rating is, what the predicted rating for the user is and any hard values. It will then show the user the rating screen in the case that a user wants to rate it, and this will be followed by a number of item-to-item recommendations based on the similarity calculations between this entity and every other entity, with the user's belief system used as the pivot point.

Evaluation

A user survey was carried out on a random sample of 20 patrons of the restaurant that the prototype was developed for. Each user was asked to use the system and rate items that they had tried. They were then given a list of 5 recommendations and asked to rank the algorithms in order from most to least accurate. We obtained 85 unfiltered orderings of the algorithms. After filtering them out for incomplete orderings we had 78 orderings. In addition to ranking the algorithms that were employed, the participants of the survey were also asked a number of questions regarding the usability of the system. The following five algorithms were rated:

1. Algorithm A: Rating based on global ideal candidate and average ratings–equation 5.
2. Algorithm B: The predicted rating based on user's belief system and average ratings–equation 6.
3. Algorithm C: Weighted sum [2].
4. Algorithm D: Adjusted weighted sum [2].
5. Algorithm E: Rating based on global ideal candidate and user's personal ratings.

The results of the algorithm rankings are presented in Table 10. The first 5 columns of the table represent how many times the algorithm was ranked at that position. So, the Algorithm B was ranked first 29 times, second 14 times, etc.

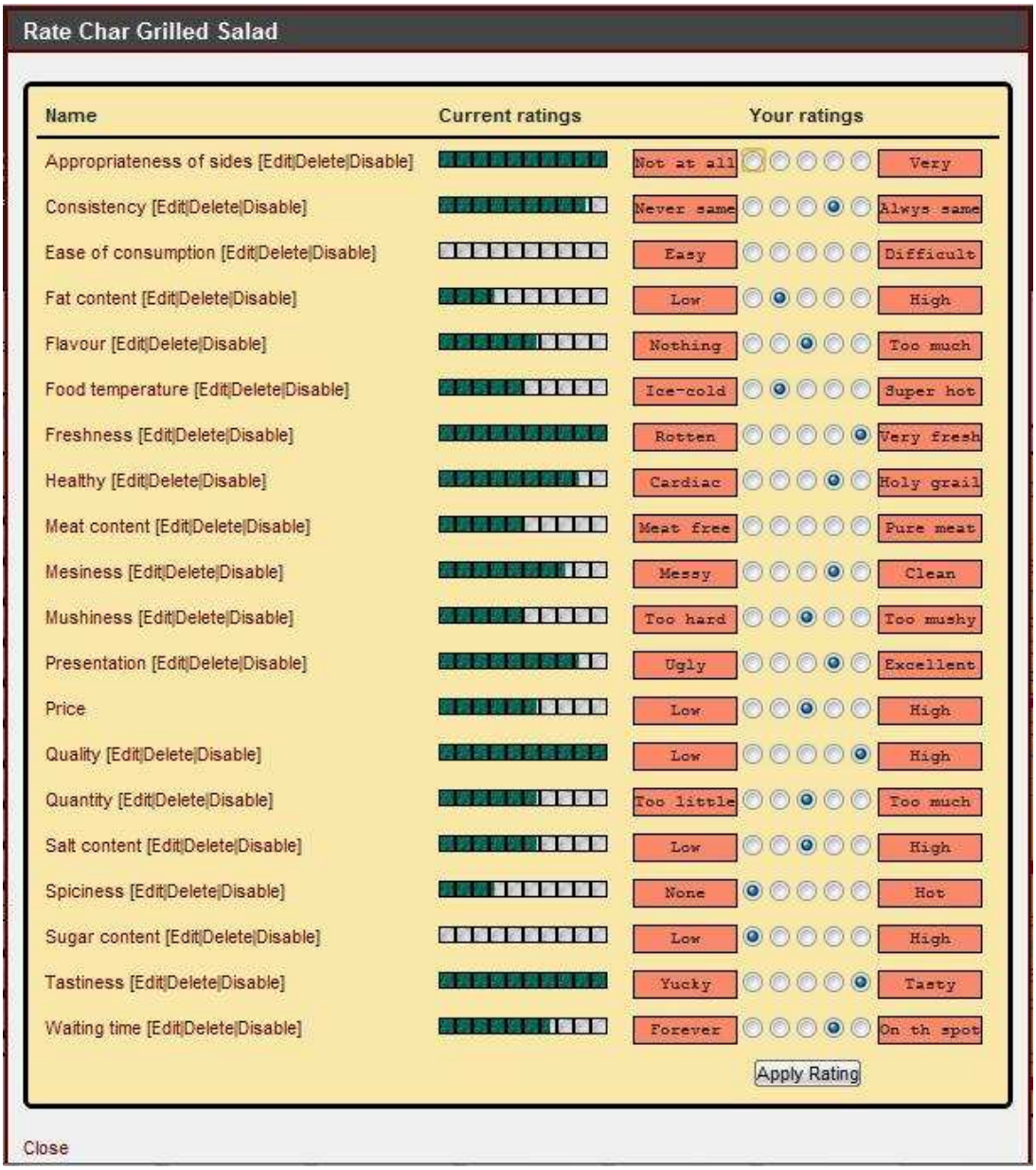

Figure 2: Rating a menu item.

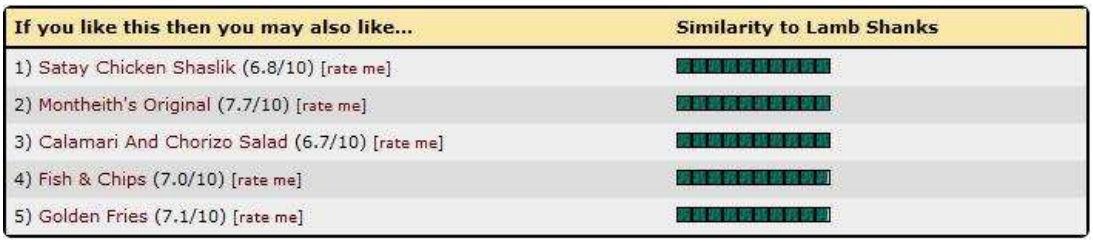

Figure 3: Recommended items when viewing the Lamb Shank page.

	1^{st}	2^{nd}	3^{rd}	4^{th}	5^{th}	$\%1^{st}$	Linear rating	Exp rating	% exp	% lin
Algorithm A	13	21	32	8	4	16.7	265	1048	21.4	22.4
Algorithm B	26	14	12	24	3	33.3	273	1250	25.6	23.1
Algorithm C	12	21	18	21	7	15.4	247	962	19.7	20.9
Algorithm D	7	4	4	6	58	9	133	460	9.4	11.2
Algorithm E	21	19	13	19	7	27	265	1170	24	22.4

Table 10: The rankings of each of the algorithms and their additive scores.

The algorithm that has been proposed in this paper is Algorithm B. It can be seen from the results that it does better than all the others. Algorithm A is also used by the system, not for personal results, but for global rankings of items. The only difference between A and B is that B uses the user's personal belief system to calculate the ratings and A uses the global ideal candidate. As it turns out, the personalized algorithm, based on a digitized belief system, is the most accurate of them all.

A number of other statistics were also calculated. The $\%1^{st}$ column represents the percentage that the algorithm came first. Algorithm B dominates this by being the most accurate 33 percent of the time out of all 5 algorithms and algorithm E comes in second with 27 percent. The 2 algorithms together, both of which add in a personal aspect to the rating process, are the most accurate 60 percent of the time.

The next 4 columns are an additive ranking that was calculated for each algorithm by taking into account the number of times the algorithms came in each position rather than in just first spot. Each position was given a weighting and then a total rating was calculated. The algorithm with the highest rating wins, and again it shows that B came in on top with A and E a close second. One may note here that even though algorithm E came in first place almost 2 times more frequently than algorithm A, their linear rating is exactly the same. This happens because algorithm A came in third place almost 3 times more frequently than algorithm E, which linearly made a significant difference.

The linear rating for algorithm L was calculated using the formula $rating_L = \sum_{i=1}^{M} (M-i) * L_i$ and the exponential rating was calculated with $rating_L = \sum_{i=1}^{M} 2^{M-i} * L_i$, where L_i represents the number of times algorithm L came on the i^{th} place. The linear rating gives a consistent weight to each of the positions, which assumes that the most accurate algorithm is worth as much more than the second most accurate algorithm is worth over the third most. The exponential model seems to be more accurate; it gives more value to the difference in weight between the first and second place than the difference in weight between the second and third place.

Methods on evaluating recommender systems are presented in [31]. The evaluation method we used was a mix of a user study and online study. While the users were given specific tasks to do, those tasks were prerequisites for allowing/encouraging them to roam free within the system. This allowed us to also collect data that was not relevant to the algorithm presented in this paper, but on the dynamics of the user interface, the experienced speed of the calculations and the perceived accuracy of the results (described above).

A number of properties are considered desirable in a recommender system [31]. *Prediction accuracy* was shown to be better than for some of the other algorithms. *Ranking measures* was explicit in the system because the recommendations use the user's own belief system (i.e. ideal candidate) as the pivot point to determine the similarity between items. Measuring the accuracy of this ranking would require the user to have tried all the dishes in the list (given the nature of the prototype) and so was unfeasible to perform.

Item coverage is an important property for a recommendation system. While some algorithms may be limited to recommending only items that have a lot of associated data, our algorithm has 100 percent coverage. The accuracy of cases where one item has a large number of ratings and another item has only one was not tested, but adding a confidence level to ratings is a technique that may be used to alleviate that situation. A similar property is user coverage (i.e. providing recommendations based on a given number of users within the system). The prototype we developed provides full coverage, and may also be enhanced with the addition of a confidence level.

One flaw of this algorithm is that it is extremely susceptible to the cold start problem, in which items that have not been given data would be quite useless. If value dimensions have not been given importance levels, or belief systems have not been defined, then the system would be unusable.

Conclusion

The system that has been implemented is a proof of concept for the envisioned final system. The current implementation provides a ranking based on any number of value dimensions, with weights and ideal values definable by the users. There are many directions the work on this framework can take.

First, the ontology system, which provides the ability for users to arrange the entities under categories and link categories if need be, can be made much more robust with the addition of the ability to categorize. It is still not clear if a universal ontology would be best for the framework, or if other methods should be used to categorize entities into classes of value dimensions. One such method would be collaborative tagging as described in [26]. That is, instead of arranging the structure in a directory-like manner, the users can tag a category instead, and the entities within that group will implicitly have the same tags, creating a folksonomy. The value dimensions could be attached to tags instead of the category as well. This may work better to enable the ability to share value dimensions across categories as well as impressive recommendations.

Secondly, the governance mechanisms have not been implemented in a way that is scalable. The governance mechanisms determine how the system governs itself at the micro and macro levels. Concepts such as policy citations on 'talk-pages' enhance governance at the micro-level on website such as Wikipedia [6]. The macro-level governance mechanisms (namely the aggregation of the belief systems and rankings) are in place, but there is a lot of work that needs to be done at the micro-level.

Thirdly, work is needed on trust and reputation support. Incorporating trust into users' profiles would be one direction. Perhaps the framework should take a user's reputation into account when applying the value dimension weightings in the algorithms, maybe just for the global rankings. These extra calculations could, however, give rise to performance. The current system implementation can be slow at times because it is running five different algorithms at the same time for the purpose of allowing users to rank various algorithms (as discussed in Section **Evaluation**).

And finally, the system does not take temporal dynamics in to account. As time goes by, items become less valuable and no longer appealing in the same way. One approach that tackles this problem keeps degradation information along with the rating data and creates a temporal model out of the rating patterns [33].

Giving users less work to do in the system, i.e. by automating certain processes, is also desirable. One example may be the weighting system for value dimensions. The trust system [30] developed for Wikipedia could be used to create implicit weightings over the value dimensions by determining collaborative importance through analyzing a value dimension's revision history.

Knowledge extraction mechanisms are needed for the framework to be useful. This is the component that will provide the most value to users in the long run. The ranking algorithm is a central part of the entire knowledge extraction system. This part can answer questions such as: What is a positive contribution to the world? What is a negative contribution to this world, and why? What is the most important value-dimension for universities, for countries, or for various businesses?

A problem faced by this recommendation system and many others is the cold-start problem. How do we get initial input form users so that the system gets in to a usable state. Wikipedia addressed this by appealing to the expert community [6]. Other systems, which are not that appealing to "experts" have adopted a hybrid approach [32] that assigns ratings to items based on their similarity to other items that have already been rated, e.g. in a trial run of the system.

Another area of future work is method to enable iterative aggregation, that is, how to enable the inclusion of nominal value dimensions.

The evaluation section showed that user's ranked the proposed algorithm at a higher *subjective* accuracy than the other algorithms that were implemented. Another area of research in this regard would be to implement various

other algorithms and carry out another evaluation study against the proposed system. Furthermore, [31] pointed out a number of evaluation criteria for recommendation systems that were not included in this evaluation, such as the user's intent (which in our case was to test the system since they were hand picked—but this is not the intent of a real user of a recommendation system), how much they trust the recommendations, the novelty of a recommendation (i.e. whether the user knew about the recommended item or not), serendipity, diversity, utility, adaptability and scalability.

Acknowledgements

We thank M. Stay (Google, Mountainview) and the anonymous referee for comments which improved the paper and Professor Michel Petitjean for generous support. The paper is published with financial support by the project ITHEA XXI of the Institute of Information Theories and Applications FOI ITHEA (www.ithea.org) and the Association of Developers and Users of Intelligent Systems ADUIS Ukraine (www.aduis.com.ua).

Bibliography

[1] Adomavicius, G. and Kwon, Y. (2007). New recommendation techniques for multi-criteria rating systems. *Intelligent Systems*, 22(3), pp.48-55.

[2] Adomavicius, G. and Tuzhilin, A. (2005). Toward the next generation of recommender systems: a survey of the state-of-the-art and possible extensions. *IEEE Transactions on Knowledge and Data Engineering*, 17(6), pp.734–749.

[3] Akhtarzada, A., Calude, C. S., Hosking, J. (2011). A multi-criteria metric algorithm for recommender systems, *Fundamenta Informaticae* 110, 1–11.

[4] Arrow, K. J. (1950). A difficulty in the concept of Social Welfare. *Journal of Political Economy*, 58(4), pp.328–346.

[5] Belkin, N. J. and Croft, W. B. (1992) Information filtering and information retrieval: two sides of the same coin? *Communications of the ACM*, 35(12), pp.29–38.

[6] Beschastnikh, I., Kriplean, T. and W. McDonald, D. (2008). Wikipedian Self-Governance in Action: Motivating the Policy Lens. *International AAAI Conference on Weblogs and Social Media*, Menlo Park, CA, AAAI Press.

[7] Burke, R. (2002). Hybrid recommender systems: survey and experiments. *User Modeling and User-Adapted Interaction*, 12(4), pp.331–370.

[8] Calude, C. and Calude, E. (1982). A metrical method for multicriteria decision making. *St. Cerc. Mat.* 34, pp.223–234. (in Romanian)

[9] Calude, C. and Calude, E. (1983). On some discrete metrics. *Bull. Math. Soc. Sci. Math. R. S. Roumanie (N. S.)* 27(75), pp.213–216.

[10] Chen, S., Ma, B. and Zhang, K. (2009). On the similarity metric and the distance metric. *Theoretical Computer Science*, 410(24-25), pp.2365–2376.

[11] Cramer, H., Evers, V., Ramlal, S., Someren, M. v., Rutledge, L., Stash, N., Aroyo, L. and Wielinga, B. (2008). The effects of transparency on trust in and acceptance of a content-based art recommender. *User Modeling and User Adapted Interaction*, 18(5), pp.455–496.

[12] Dinu, L. P., Popescu, M. (2008). Multi-criteria decision method based on rank distance, *Fundamenta Informaticae* 86(1-2), pp. 79–91.

[13] Edmunds, A. and Morris, A. (2000). The problem of information overload in business organizations: a review of the literature. *International Journal of Information Management*, 20(1), pp.17–28.

[14] Fishburn, P. C. (1967). Additive utilities with incomplete product sets: application to priorities and assignments. *Operations Research*, 15(3), (May - Jun., 1967), pp. 537–542.

[15] IMdB ([Online]) http://www.imdb.com. Visited at 10, May, 2009.

[16] Koren, Y., Bell, R. and Volinsky, C. (2009). Matrix factorization techniques for recommender systems. *Computer*, 42(8), pp.30–7.

[17] Meyer, P. D. (2003). The truth about transparency. *ASAE and The Center for Association Leadership*, http://www.asaecenter.org/PublicationsResources/EUArticle.cfm?ItemNumber=11786. Visited at Sept 30, 2010.

[18] Schafer, J. B. , Konstan, J. and Riedl, J. (2002). Meta-recommendation systems: User-controlled integration of diverse recommendations. *Proceedings of the 2002 International ACM CIKM Conference on Information and Knowledge Management*, pp.43–51. McLean, VA, USA.

[19] Schwartz, B. (2003). *The Paradox of Choice. Why More Is Less*. Ecco Publishing, New York.

[20] Sen, A. (1979). Personal utilities and public judgements: or what's wrong with welfare economics. *The Economic Journal*, 89(355), pp. 537–55.

[21] Sen, S., Vig, J. and Riedl, J. (2009). Tagommenders: connecting users to items through tags. *Proceedings of the 18th international conference on World wide web*, pp.671–680, ACM, New York, NY, USA.

[22] Shardanand, U., Maes, P. (1995) Social information filtering: algorithms for automating "word of mouth". *Proceedings of the SIGCHI Conference on Human Factors in Computing Systems*. ACM/Addison-Wesley, Denver, Colorado, USA, pp.210–217.

[23] Stuer, R. E. (1986). *Multiple Criteria Optimization: Theory, Computation and Application*. Wiley and Sons, Inc.

[24] Su, X. and Khoshgoftaar, T. M. (2009). A survey of collaborative filtering techniques. *Advances in Artificial Intelligence*, 2009 (Jan. 2009), 2-2. Hindawi Publishing Corporation.

[25] Walker, J. P. (1971). Decision-making under conditions of information overload: alternative response modes and their consequences. *American Educational Research Association Annual Meeting*, New York, USA.

[26] Xu, Z., Fu, Y., Mao, J. and Su, D. (2006). Towards the semantic web: collaborative tag suggestions. *Workshop on Collaborative Web Tagging*, Edinburgh, Scotland.

[27] Kelly, K. (2006). The speed of information. *The Technicum*, http://www.kk.org/thetechnium/archives/2006/02/the_speed_of_in.php. Visited Oct 30, 2010.

[28] Lyman, P and Varian, H. R. (2003). How much information? *School of Information Management and Systems, University of California, Berkley*, http://www2.sims.berkeley.edu/research/projects/how-much-info-2003. Visited Oct 30, 2010.

[29] Wray, R. (2009). Internet data heads for 500bn gigabytes. *The Guardian*, http://www.guardian.co.uk/business/2009/may/18/digital-content-expansion. Visited May 14, 2010.

[30] Adler, B., T., Chatterjee, K., de Alfaro, L., Faella, M., Pye, I. Raman, V. (2008). Assigning trust to Wikipedia content. *WikiSym 2008: International Symposium on Wikis*, Porto, Portugal.

[31] Shani, G., Gunawardana, A. (2011). Evaluating recommendation systems. *Recommender Systems Handbook*, pp.257–297. Springer US, 2011.

[32] Schein, A. I., Popescu, A. Ungar, L. H., Pennock, A. M. (2002). Methods and metrics for cold-start recommendation systems. *Proceedings of the 25th Annual International ACM SIGIR Conference on Research and Development in Information Retrieval (SIGIR 2002)*, pp.253–260. ACM 2002.

[33] Koren, Y. (2009). Collaborative filtering with temporal dynamics. *Proceedings of the 15th ACM SIGKDD international conference on Knowledge Discovery and Data Mining*, pp.447–456. ACM 2009.

Authors' Information

Ali Akhtarzada *- Department of Computer Science, University of Auckland, Auckland, New Zealand; e-mail: ali.akhtarzada@gmail.com*
Major Fields of Scientific Research: Software engineering, multi-dimensional information systems

Cristian S. Calude *- Department of Computer Science, University of Auckland, Auckland, New Zealand; e-mail: cristian@@cs.auckland.ac.nz*
Major Fields of Scientific Research: Algorithmic information theory and quantum theory

John Hosking *- ANU College of Engineering and Computer Science Australian National University, Canberra, Australia; e-mail: john.hosking@anu.edu.au*
Major Fields of Scientific Research: Software engineering, software tools and meta-tools, visual languages

RANK CODES OVER GAUSSIAN INTEGERS AND SPACE TIME BLOCK CODES

Hafiz M.Asif, Ernst Gabidulin, Bahram Honary

Abstract: *Maximum rank distance (MRD) codes have been used for the construction of space time block code (STBC) using a matrix method. Like orthogonal STBC's in most popular cases, MRD-STBC's can also achieve full diversity. Though an OSTBC is known to yield the best BER performance, a unique case is described where MRD-STBC performs better than Alamouti code (OSTBC). Moreover, the viability of Gabidulin's decoding algorithm has been established by decoding complex symbols generated from MRD-STBC's. Under this decoding scheme, MRD-STBC's have been shown to be preferred candidate for higher antenna configuration as the decoding complexity of Gabidulin's algorithm is far less than that of maximum likelihood (ML) decoding algorithm.*

Keywords: *Rank codes, Gaussian integers, space time block codes, orthogonal space time block codes.*

MSC*: 12E20*

Introduction

The design of error-correcting codes for two dimensional signal spaces has been widely considered. Different authors have constructed new error-correcting codes over quotient rings of Gaussian integers by using the Mannheim measure as it was introduced in [Huber, 1994]. Complex constellations based on graphs allow to construct rank codes over Gaussian integers. In turn, such codes can be used as space time block codes.

The idea of exploiting transmit diversity was introduced by Vahid Tarokh et al. [Tarokh et al., 1998] and it was later on adopted for much simpler structure by Alamouti [Alamouti, 1998]. His work was later on extended and formally developed to originate space time block codes (STBC) [Tarokh et al., 1999]. In addition, for 2×1 scenario, Alamouti code achieves full diversity gain. In [Lusina et al., 2003], the application of rank codes for forming STBC was introduced. Rank codes [Gabidulin, 1985], due to rank distance property, make themselves useful candidate for STBC's. The construction of rank codes is presented based on direct matrix method as MRD-STBC's. MRD-STBC codes performs better than orthogonal STBC (OSTBC) under certain criteria. Moreover, little work was found on decoding MRD-STBC except ML scheme which is extremely complex for higher antenna configuration. Therefore, first, the idea of using interleaved MRD codes ($\mathcal{I}$) is introduced to construct MRD-STBC's for $N_{tx} > 4$. Second, a decoding algorithm has been described that can effectively decode MRD-STBC.

The Gaussian integers

The set $\mathbb{Z}[i]$ of *Gaussian integers* is the subset of the complex numbers $\mathbb{C}$ with integer real and imaginary parts, i.e.,

$$\mathbb{Z}[i] := \{a + bi \mid a, b \in \mathbb{Z}\}.$$

If $0 \neq \pi = u + vi \in \mathbb{Z}[i]$, then we denote, $\mathbb{Z}[i]_\pi$, the ring of the classes of $\mathbb{Z}[i]$ modulo the ideal (π) generated by π. Therefore, we write $\beta \equiv \beta' \pmod{\pi}$ if β and β' belong to the same class modulo (π). It is well known that the cardinality $\mathcal{N}$ of $\mathbb{Z}[i]_\pi$ equals $\mathcal{N} = u^2 + v^2$. From now on, we consider the case when $0 < u < v$ and $u^2 + v^2 = p \equiv 1 \pmod{4}$, p is a prime. $\mathcal{Z}_\pi$ is a set of representatives of the residue classes $\mathbb{Z}[i]_\pi$. These constellations have been previously modeled by quotient rings of Gaussian integers, [Huber, 1994], [Costa et al., 2004], [Nóbrega et al., 2001]. Constellations and the metric based on associated graphs were introduced in [Martínez et al., 2005]. We denote by $\mathcal{MZ}_\pi$ the constellation defined by K.Huber [Huber, 1994] and by $\mathcal{GZ}_\pi$ the constellation based on graphs. In general, for a given π they are different as well as associated metrics.

The Mannheim constellation $\mathcal{MZ}_\pi$

For a given π and any Gauss integer $\alpha = a + bi$, define the projection α on $\mathcal{MZ}_\pi$ as $\rho_\alpha := \alpha - q_\alpha \pi$ where,

$$q_\alpha := \left[\frac{\alpha\overline{\pi}}{p}\right].$$

The operation $[c + di]$ denotes rounding in Gaussian integers and is defined by $[c + di] = [c] + [d]i$ with $[c]$ denoting rounding to the closest integer.
Next statements are evident.

1. $\rho_\alpha(\rho_\alpha) = \rho_\alpha$.

2. The Mannheim set $\mathcal{MZ}_\pi$ is the image of the set $\{0, 1, \ldots, p-1\}$ under the projection ρ_*.

3. For any $\alpha \in \mathcal{MZ}_\pi$, $\rho_\alpha = \alpha$.

For $\alpha = a + bi \in \mathcal{MZ}_\pi$, the Mannheim weight is defined by $w_M(\alpha) = |a| + |b|$. For any $\alpha = a + bi$, the Mannheim weight is defined by $w_M(\alpha) = w_M(\rho_\alpha)$. The Mannheim distance between two elements α and β in $\mathbb{Z}[i]_\pi$ is defined as $d_M(\alpha, \beta) = w_M(\alpha - \beta)$. In fact, the Mannheim distance is not true distance as it was shown first by example in [Martínez et al., 2005]. We give more general explanations.
Let $\pi = u + vi,\ 0 < u < v,\ u^2 + v^2 = p$. Introduce

$$r = \frac{v + u - 1}{2},\ \ m = v - r = \frac{v - u + 1}{2},\ \ \&\ \ s = \left\lfloor \frac{v(u-1) - u^2}{2v} \right\rfloor.$$

Lemma 1. *Let p be a prime such that $u = 1$, or, $u = v - 1$. Then the Mannheim distance is a true distance.*

Proof. In this case the sets $\mathcal{MZ}_\pi$ and $\mathcal{GZ}_\pi$ associated metrics coincide. The proof for the graph based metric can be used (see, [Martínez et al., 2005]). □

Theorem 1. *Let p be a prime such that $u \neq 1$ and $u \neq v - 1$. Then the Mannheim distance is **not** a true distance. More precisely, it does not fulfil the triangular inequality.*

Proof. First show that $v(u-1) > u^2$. Since $u \neq v - 1$, it follows that $u \leq v - 2$. It is impossible that $u = v - 2$ since the left and the right parts must have the different parity. Hence $u \leq v - 3,\ v \geq u + 3$. If we assume that $v(u-1) < u^2$, we obtain $v < u + 1 + 1/(u-1)$, or, $v \leq u + 1$ with contradiction to $v \geq u + 3$. Therefore the integer s introduced above is non negative.
For a true distance function and any three elements x, y, z must be $d(x, z) \leq d(x, y) + d(y, z)$ (the triangular inequality). We present three elements $x, y, z \in \mathcal{MZ}_\pi$ such that $d_M(x, z) > d_M(x, y) + d_M(y, z)$. Namely, let $x = u + (m+s)i,\ y = -i,\ z = 0$. By direct calculation, one can show that $\rho_x = x$. Hence all three x, y, z are in $\mathcal{MZ}_\pi$. We have $d_M(x, z) = w_M(x - z) = w_M(x) = u + m + s$ and $d_M(y, z) = w_M(y - z) = w_M(-i) = 1$. Also we have $x - y = u + (m + s + 1)i$ and by direct calculation $\rho_{x-y} = x - y - \pi = -(v - m - s - 1)i$. Thus $d_M(x, y) = w_M(x - y) = w_M(\rho_{x-y}) = w_M(-(v - m - s - 1)i) = v - m - s - 1$. Finally, $d_M(x, z) - d_M(x, y) - d_M(y, z) = u + m + s - v + m + s = 1 + 2s > 0$. The triangular inequality fails. □

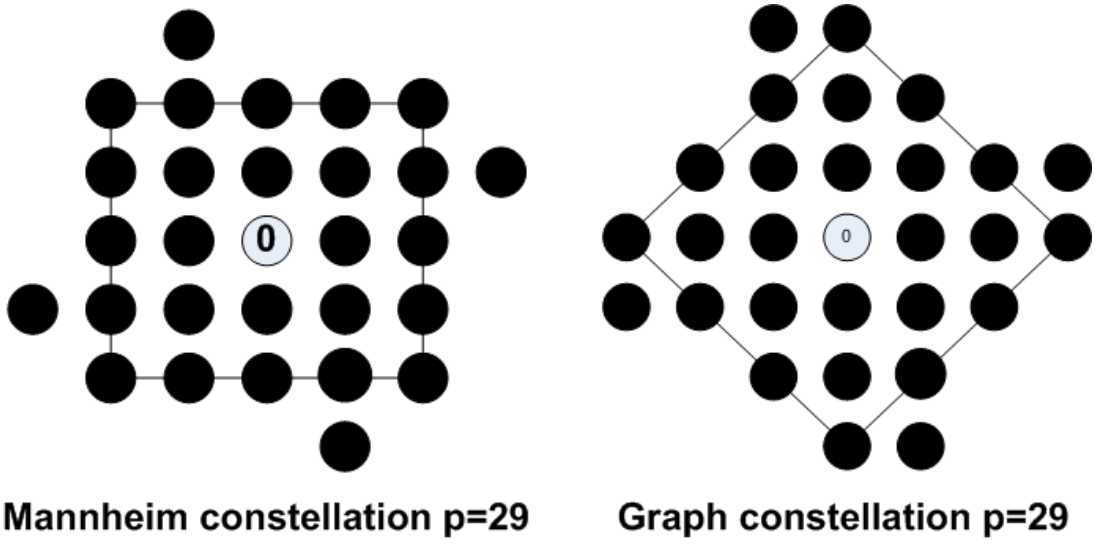

Figure 1: Constellations $\mathcal{Z}_{2+5i}, p = 29$.

The graph constellation $\mathcal{GZ}_\pi$

For $\beta, \gamma \in \mathbb{Z}[i]_\pi$, consider $x + yi$ in the class of $\beta - \gamma$ with $|x| + |y|$ minimum. The distance D_π between β and γ is $D_\pi(\beta, \gamma) = |x| + |y|$. This distance function is called the graph distance since it coincides with the distance function of the following graph.

Given $\pi = u + vi \in \mathbb{Z}[i]$ we define the graph $G_\pi = (V, E)$ where:

1. $V = \mathbb{Z}[i]_\pi$ is the node set, and
2. $E = \{(\beta, \gamma) \in V \times V \mid D_\pi(\beta, \gamma) = 1\}$ is the edge set.

We call G_π the Gaussian Graph generated by π.

The constellation $\mathcal{GZ}_\pi$ consists of Gaussian integers in the square with vertices $(ri, r, -ri, -r)$ and in four triangles with vertices $(r+i, r+(m-1)i, r-m+2+(m-1)i)$, $(-r-i, -r-(m-1)i, -(r-m+2)-(m-1)i)$, $(ri-1, ri-m+1, (r-m+2)i-m+1)$, $(-ri+1, -ri+m-1, -(r-m+2)i+m-1)$. Constellations $\mathcal{MZ}_\pi$ and $\mathcal{GZ}_\pi$ are presented below for $\pi = 2 + 5i, p = 2^2 + 5^2 = 29$.

Rank codes over Gaussian integers

The constellation $\mathcal{GZ}_\pi$ can be considered as a representation of the finite field $GF(p)$. Extension fields of degree n over Gaussian integers can be represented as n-tuples of $\mathcal{GZ}_\pi^n$. Also they can be defined in the matrix representation. Let $f(x) = x^n + f_{n-1}x^{n-1} + \cdots + f_1 x + f_0$ be a primitive polynomial over $GF(p)$. Then the companion matrix

$$M_n = \begin{bmatrix} 0 & 1 & 0 & \dots & 0 & 0 \\ 0 & 0 & 1 & \dots & 0 & 0 \\ 0 & 0 & 0 & \ddots & 0 & 0 \\ \vdots & \vdots & \vdots & \vdots & \ddots & \vdots \\ 0 & 0 & 0 & \ddots & 0 & 1 \\ -f_0 & -f_1 & -f_2 & \dots & -f_{n-2} & -f_{n-1} \end{bmatrix} \tag{1}$$

represents a primitive element of the extension field $GF(p^n)$. Matrices $M_n^i,\ i = 1, \dots, p^n - 1$, represent all non zero elements of the extension field. To obtain an extension field over $\mathcal{GZ}_\pi$, one can replace each entry by

corresponding value of $\mathcal{GZ}_\pi$. Afterwards all matrix operations should be fulfilled modulo π.

Example. Let $\pi = 1 + 2i,\ p = 5$. Then $\mathcal{GZ}_\pi$ consists of $\{0, \pm 1, \pm i\}$. Let $f(x) = x^2 + x + 2$ be the primitive polynomial over $GF(5)$. We have,

$$M_2 = \begin{bmatrix} 0 & 1 \\ -2 & -1 \end{bmatrix},\ M_2^2 = \begin{bmatrix} -2 & -1 \\ 2 & -1 \end{bmatrix}, \ldots, M_2^{23} = \begin{bmatrix} 2 & 2 \\ 1 & 0 \end{bmatrix},\ M_2^{24} = \begin{bmatrix} 1 & 0 \\ 0 & 1 \end{bmatrix}.$$

The corresponding matrices over $\mathcal{GZ}_\pi$ are as follows:

$$\widetilde{M_2} = \begin{bmatrix} 0 & 1 \\ -i & -1 \end{bmatrix},\ \widetilde{M_2^2} = \begin{bmatrix} -i & -1 \\ i & -1 \end{bmatrix}, \ldots, \widetilde{M_2^{23}} = \begin{bmatrix} i & i \\ 1 & 0 \end{bmatrix},\ \widetilde{M_2^{24}} = \begin{bmatrix} 1 & 0 \\ 0 & 1 \end{bmatrix}.$$

A rank code with rank distance d is a set of $n \times n$ matrices over $GF(p)$ such that the difference of two code matrices has rank not less than d. This property holds true, if elements of $GF(p)$ are replaced by elements of $\mathcal{GZ}_\pi$.

Rank codes as space time codes

Code construction

It was investigated that if a linear code of block size 4 is formed in such a way that the absolute value of the determinant of each pairwise difference is equal to 4 then rank code (and all its coset codes) performs better than Alamouti code. The construction of such is described as follows.

Let $x^2 + x + 1$ be a primitive irreducible polynomial over GF(2), then the elements of $GF(2^2)$ form an MRD code of block size 4. The direct matrix construction (using Eq.(1)) is obtained as follows: $\begin{bmatrix} 0 & 0 \\ 0 & 0 \end{bmatrix}, \begin{bmatrix} 0 & 1 \\ 1 & 1 \end{bmatrix}, \begin{bmatrix} 1 & 1 \\ 1 & 0 \end{bmatrix}, \begin{bmatrix} 1 & 0 \\ 0 & 1 \end{bmatrix}$.

Having mapped 0 to 1 and 1 to -1 (BPSK), the code becomes $\begin{bmatrix} 1 & 1 \\ 1 & 1 \end{bmatrix}, \begin{bmatrix} 1 & -1 \\ -1 & -1 \end{bmatrix}, \begin{bmatrix} -1 & -1 \\ -1 & 1 \end{bmatrix}, \begin{bmatrix} -1 & 1 \\ 1 & -1 \end{bmatrix}$.

Two important observations can be made on the above MRD; (1) The sum of square modules in each is equal to 4 and (2) The absolute value of the determinant of each pairwise difference is equal to 4. From physical point of view, the first condition is a transmitting power for a matrix while the second condition is a measure of difference between code matrices.

Next we consider orthogonal STBC (OSTBC) construction and select four such codes which fulfil the above mentioned two properties.

Let $G = \{0, 1, \alpha, \alpha^2, \alpha^3, ..., \alpha^{14}\}$ be an additive group of 16 elements. Let $G_S = \{0, 1, \alpha, \alpha^2\}$ be a subgroup of G comprising 4 elements. The first coset of G_S is equal to G_S, i.e., addition of 0 to G_S which in turn yields G_S. Now, 16 different Alamouti codes (16 blocks) can be constructed out of which the following four are selected: $\begin{bmatrix} 0 & -0^* \\ 0 & 0^* \end{bmatrix}, \begin{bmatrix} 0 & -\alpha^* \\ \alpha & 0^* \end{bmatrix}, \begin{bmatrix} \alpha^2 & -1^* \\ 1 & \alpha^{2^*} \end{bmatrix}, \begin{bmatrix} 1 & -1^* \\ 1 & 1^* \end{bmatrix}$.

The symbol $\{.\}^*$ indicates conjugate of the element. It can easily be verified that the blocks are orthogonal blocks (i.e., the determinant is identity matrix). After modulation or the mapping $(0, 1, \alpha, \alpha^2)$ to $(1, j, -1, -j)$, which has been selected by exhaustive search approach, we obtain: $\begin{bmatrix} 1 & -1 \\ 1 & 1 \end{bmatrix}, \begin{bmatrix} 1 & 1 \\ -1 & 1 \end{bmatrix}, \begin{bmatrix} -j & j \\ j & j \end{bmatrix}, \begin{bmatrix} j & j \\ j & -j \end{bmatrix}$.

It can be checked the above four OSTBC blocks satisfy the above mentioned two conditions. Hence, the two sets, each of 4 different 2×2 block, can be compared.

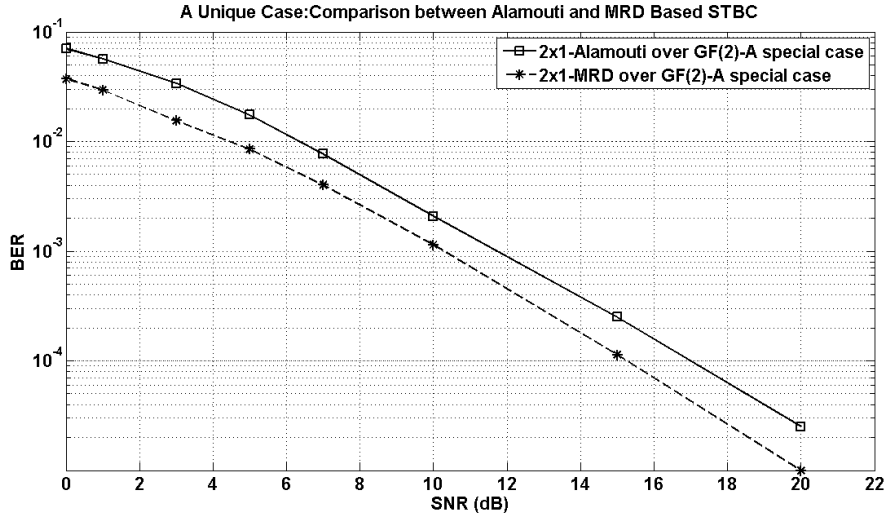

Figure 2: Orthogonal codes vs. MRD over GF(2^2) for 2×1 scenario

Simulation analysis

Simulation was carried out for comparing all described configurations of MRD with the corresponding OSTBC's described in the previous section. 2×10^5 symbols per SNR value were transmitted in each case.

The channel matrix H_C was calculated based on Rayleigh fading. The received signal y is calculated as $y = H_C c + n$, where c is the transmitted block code (2×2) and n is $AWGN$. Maximum likelihood decoding was used to decode the transmitted symbols in both cases (MRD and orthogonal). Each received signal is compared against all possible blocks ($q^{N_{tx}}$) to select the block with minimum error, i.e., with minimum Euclidean distance.

Fig.2 shows BER performance comparison of 2×1 OSTBC and 2×1 MRD-STBC which were designed based on the construction given in Section . First, it is important to note that MRD-STBC achieves full rate diversity because its slope is parallel to that of OSTBC. Second, there is a coding gain of about 1.8 dB over OSTBC which can further be multiplied by using different primitive polynomial or so. It is to be noted that OSTBC performs better than MRD-STBC for general case, i.e., if the above two conditions are not fulfilled.

Rank codes, when used as complex symbols, may lose the rank of the code block if traditional modulation schemes, such as $n - PSK$, are applied. As mentioned earlier, Gaussian integers can be used to map rank codes to corresponding complex constellations. In what next follows we describe how Gaussian integers can improve MRD-STBC's performance to some extent, especially in low SNR region, in two systems, i.e., 3×3 and 5×5 systems over GF(5^3) and GF(5^5) respectively.

3 MRD-STBC over GF(5^3)

Let $x^3 + 3x + 2$ be the primitive polynomial of degree 3, where the coefficients of the polynomial are from GF(5). Then the first non-zero companion matrix, with extension degree 3, can be written as follows (i.e., the elements of GF(5^3):

$$C = \begin{bmatrix} 0 & 0 & 3 \\ 1 & 0 & 2 \\ 0 & 1 & 0 \end{bmatrix}$$

Let β be a root of the above polynomial then the above companion matrix, in vector form, is as follows:

$$C_{vec} = G = \begin{bmatrix} \beta & \beta^2 & \beta^3 \end{bmatrix} \tag{2}$$

where,

$\beta^3 = 2x + 3$ and note that it is our generator matrix, G, as well. We can calculate the corresponding parity check matrix, H, by using the relationship $GH^T = 0$. The corresponding calculated H is as follows:

$$H = \begin{bmatrix} h_1 & h_2 & h_3 \\ h_1^5 & h_2^5 & h_3^5 \end{bmatrix} = \begin{bmatrix} 1 & \beta^{103} & \beta^{98} \\ 1 & \beta^{19} & \beta^{118} \end{bmatrix} \tag{3}$$

Afterwards, MRD-STBC symbols are mapped to complex domain using Gaussian integers, and finally Gabidulin's decoding was applied on the received signal which will be discussed shortly.

5 MRD-STBC over GF(5^5)

Let $x^5 + 2x^4 + 2x^2 + x + 2$ be the primitive polynomial of degree 5, where the coefficients of the polynomial are from GF(5). Then the first non-zero companion matrix, with extension degree 5, can be written as follows (i.e., the elements of GF(5^5):

$$C = \begin{bmatrix} 0 & 0 & 0 & 0 & 3 \\ 1 & 0 & 0 & 0 & 4 \\ 0 & 1 & 0 & 0 & 3 \\ 0 & 0 & 1 & 0 & 0 \\ 0 & 0 & 0 & 1 & 3 \end{bmatrix}$$

Let β be a root of the above polynomial then the above companion matrix, in vector form, is as follows:

$$C_{vec} = G = \begin{bmatrix} \beta & \beta^2 & \beta^3 & \beta^4 & \beta^5 \end{bmatrix} \tag{4}$$

where,

$\beta^5 = 3x^4 + 3x^2 + 4x + 3$ and note that it is our generator matrix, G, as well. The corresponding parity check matrix (H) is as follows:

$$H = \begin{bmatrix} h_1 & h_2 & h_3 & h_4 & h_5 \\ h_1^5 & h_2^5 & h_3^5 & h_4^5 & h_5^5 \\ h_1^{25} & h_2^{25} & h_3^{25} & h_4^{25} & h_5^{25} \\ h_1^{125} & h_2^{125} & h_3^{125} & h_4^{125} & h_5^{125} \end{bmatrix} = \begin{bmatrix} 1 & \beta^{3011} & \beta^{1464} & \beta^{1459} & \beta^{2348} \\ 1 & \beta^{2559} & \beta^{1072} & \beta^{1047} & \beta^{2368} \\ 1 & \beta^{299} & \beta^{2236} & \beta^{2111} & \beta^{2468} \\ 1 & \beta^{1495} & \beta^{1808} & \beta^{1183} & \beta^{2968} \end{bmatrix} \tag{5}$$

Interleaved MRD

A 4×1 MRD-STBC code can easily be constructed for 4 transmit antennas, i.e., $N_{tx} = 4$. In order to increase the code length N_{tx} to certain extent, we can use a direct concatenation of consecutive M matrices such that the concatenated code is also a unique MRD [Sidorenko and Bossert, 2010], i.e.,

$$\mathcal{I} = \begin{bmatrix} M^{(1)} & M^{(2)} & M^{(3)} \dots M^{(i)} \end{bmatrix}, \ M^i \in \mathcal{M}, \tag{6}$$

Algorithm 1 Decoding MRD-STBC $(q^m; n, k, d)$

1: **Input**: Received y $\in$ GF$(q^m)^{N_{tx}}$
2: Demodulate received signal, y, use Eq.(7) to nullify channel effect and then write the result in vector form.
3: Compute syndrome $s = yH^T$ where H is parity check matrix.
4: Compute matrix M_i using Eq.(8) such that $M_i \neq 0$ starting with $i = t, t-1, ...$ The value of i determines rank of the error vector, m.
5: Solve Eq.(9) to find $\sigma_i \; \forall \; i = 0, 1, \ldots, m-1$, where m =rank of the error vector. Also, write $\sigma(x)$ as shown by Eq.(10).
6: Solve Eq.(10) using Berlekamp-Massey type algorithm [Berlekamp, 1968] in order to find m number of roots of this equation. Represent these roots as $z_1, z_2, \ldots, z_m$.
7: Solve Eq.(11) for any value of i to find E_i, where $i = 1, 2, \ldots, m$.
8: Solve Eq.(12) using again Berlekamp-Massey algorithm to find Y.
9: Calculate error vector, e, using Eq.(13).
10: Codeword $c = y - e$ or decoding failure
11: If success, write c again in matrix form to find BER etc.

where M is defined by Eq.(1) and $i = 1, 2, 3 \ldots, i$ is the *interleaving order*. The matrix $\mathcal{I}$ is known as interleaved MRD code [Sidorenko and Bossert, 2010]. Based on this definition, three MRD-STBC's were constructed for $N_{tx} = 4, 8,$ and 12 respectively. Finally, the advantage of using $\mathcal{I}$ codes is to increase the error-correction ability of the algorithm while the time complexity of the algorithm becomes $\mathcal{O}(id_r^2)$ (i is the interleaving order) which is still better than ML decoding. If d_r be the rank distance, then number of errors that can be corrected (t) in $\mathcal{I}$ code, for i interleaving order, is $i(i+1)/(d_r - 1)$ [Sidorenko and Bossert, 2010]:

Decoding 4×1 MRD-STBC using Gabidulin's algorithm

In this section, it is presented how Gabidulin's algorithm [Gabidulin, 1995] can be used to decode MRD-STBC which is symbolically written as MRD$(q^m; n, k, d)$. The complete steps of the algorithm to decode STBC blocks have been shown in Algorithm I.

Followings are the equations which have been referred to in Algorithm 1:

$$y_{rec} = H^\top (c + n) = c + H^\top n \quad H \; is \; parity \; check \; matrix. \tag{7}$$

$$M_i = \begin{bmatrix} s_0 & s_1^{2^{-1}} & \ldots & s_{i-1}^{2^{-i+1}} \\ s_1 & s_2^{2^{-1}} & \ldots & s_i^{2^{-i+1}} \\ \vdots & \vdots & \vdots & \vdots \\ s_{i-1} & s_i^{2^{-1}} & \ldots & s_{2i-2}^{2^{-i+1}} \end{bmatrix}. \tag{8}$$

$$(\sigma_0, \sigma_1, ..., \sigma_{m-1}) M_m = -\left[s_m, s_{m+1}^{2^{-1}}, ... s_{2m-1}^{2^{-m+1}} \right]. \tag{9}$$

$$\sigma(x) = \sum_{i=0}^{m} \sigma_i x^{2^i}, \; \sigma_m = 1. \tag{10}$$

$$\sum_{j=1}^{m} E_j z_j^{2^i} = s_i, \quad i = 0, 1, ..., d-2. \tag{11}$$

$$Z^t = Y H^t. \tag{12}$$

$$e = EY. \tag{13}$$

The complexity of this decoding algorithm is $\mathcal{O}(d_r^2)$ where $d_r = n - k + 1 = 4$ is the rank distance of the code. It guarantees to correct all errors with rank $\leq \lfloor \frac{d_r - 1}{2} \rfloor$ [Sidorenko and Bossert, 2010]. It can easily be seen that the decoding complexity is far less than that of ML decoding which runs full search and compares all possible

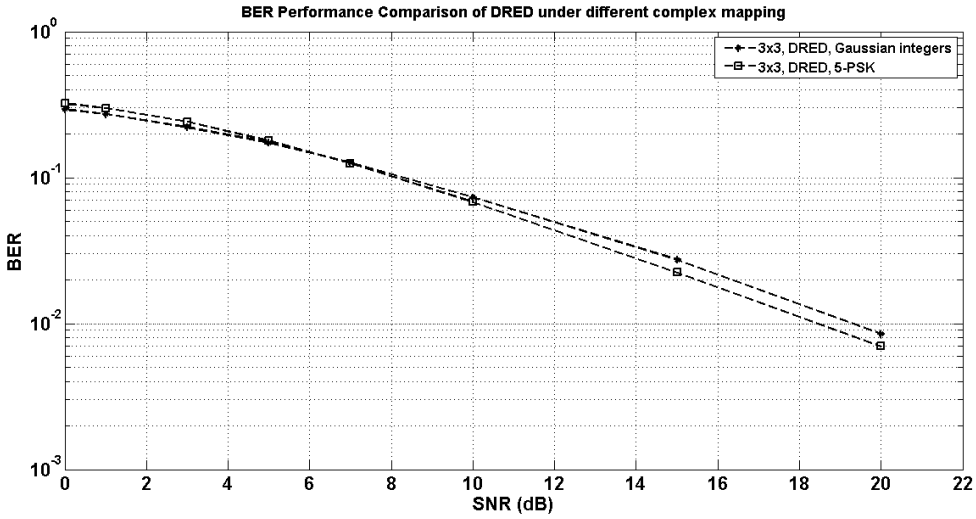

Figure 3: Gaussian integers vs 5-PSK for mapping 3×3 MRD-STBC.

combinations, i.e., $\mathcal{O}(q^{N_{tx}})$ where N_{tx} is the number of transmitting antennas. Furthermore, Interleaved MRD codes ($\mathcal{I}$) that have been used to construct $N_{tx} > 4$ STBC's are based on MRD-STBC for $N_{tx} = 4$, i.e., for $N_{tx} = 8$, and $N_{tx} = 12$.

First, simulation was run to analyze the performance of 3×3 and 5×5 mentioned above. Gaussian integers were used to map the blocks to complex symbols. At the receiver, Gabidulin's decoding algorithm was used to decode the symbols. 2×10^5 symbols per SNR value were transmitted in each case. The noise was AWGN and Rayleigh fading was used to model channel response of the system. Fig.3 shows performance curves for 3×3 MRD-STBCs that were constructed according to the above described procedure. The system was first modulated by $5 - PSK$ followed by Gaussian integers mapping. The figure shows the comparison of MRD-STBCs under two complex mapping schemes. It is evident from the figure that slight performance gain can be obtained in low SNR region by the use of Gaussian integers. The rank conservation property is better maintained by these integers in low SNR region. Furthermore, it is also clear from the graph that the gain reduces with the increase in SNR and Gaussian integers do not perform well for high SNR values. More or less, the same can be said for 5×5 system as depicted in Fig.4. Further experiments are required to investigate these integers for modulation. For instance, Gaussian integers over different fields (GF(7), GF(11) etc.) may produce better results. These investigations are left for future work.

Second, simulation was carried out to assess the viability of Gabidulin's decoding scheme for MRD-STBC especially under higher antenna configuration due to its low complexity. Because Gabidulin's decoding scheme requires vector form to function, 4×4 MRD-STBC has been constructed to exhibit 4-transmit antenna configuration. The 4-receiving antennas increase the rank of the channel matrix and thus help to nullify channel effect and convert received symbols in a vector for the decoding scheme. In a similar fashion, 8×4, and 12×4 MRD-STBC's were constructed using interleaved MRD codes represented by Eq.6.

Fig.5 shows BER comparison of 4×4, 8×4, and 12×4 MIMO systems. In each case, Gabidulin's algorithm was used to decode recovered received symbols. We can see a gradual performance improvement due to $\mathcal{I}$ codes with incremental increase in interleaving order. From the curves in Fig.5, we can see that almost over 1.5dB gain of 12×4 system is observed over 8×4 system. Similarly, there is a gain of 4dB of 12×4 over 4×4 system. The performance will be much better if the same system is decoded using ML scheme but decoding complexity increases significantly. Asymptotically, Gabidulin's algorithm is far better than ML decoder because its complexity is $\mathcal{O}\left(d_r^2\right)$ whereas that of ML is $\mathcal{O}\left(q^{N_{tx}}\right)\big)$. This implies that (1) ML is not suitable to delay sensitive applications or the applications which cannot afford high computational complexity and (2) ML-decoder is almost impractical for higher antenna configuration ($N_{tx} \geq 4$) as its complexity grows exponentially with increase in N_{tx}. Hence, it

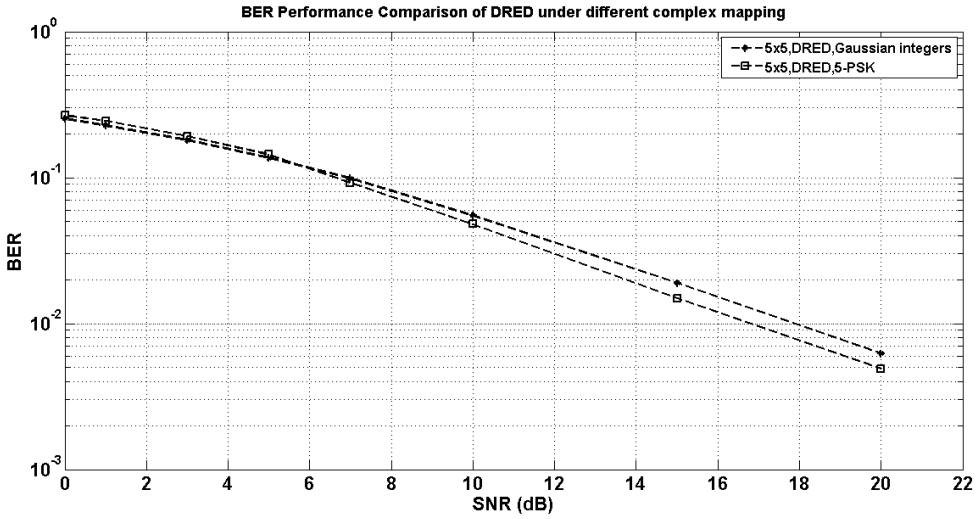

Figure 4: Gaussian integers vs 5-PSK for mapping 5×5 MRD-STBC.

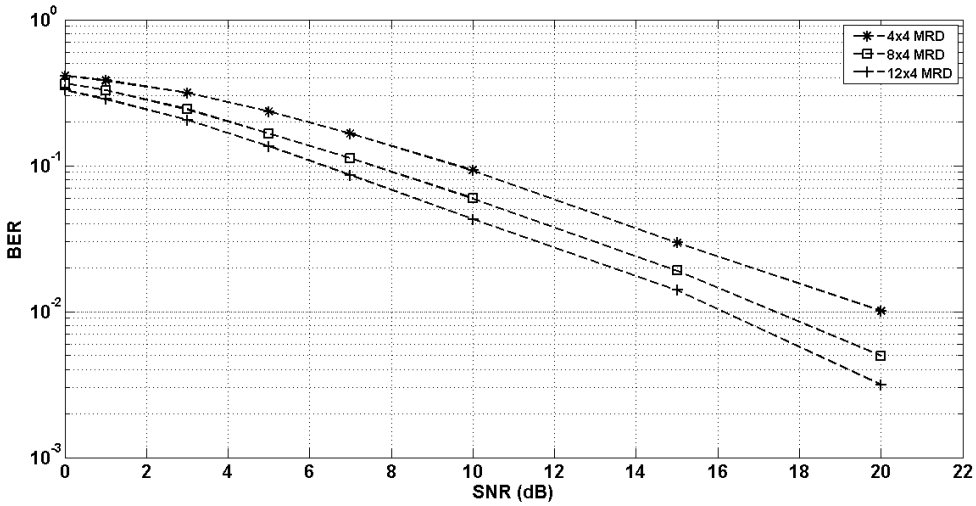

Figure 5: BER Performance Comparison of Gabidulin's Decoding Scheme for $N_{tx} = 4$, $N_{tx} = 8$, and $N_{tx} = 12$.

is reasonable to say that depending upon the trade-off between computational complexity and antennas number (N_{tx}), $\mathcal{I}$ with Gabidulin's decoding may be an elegant replacement to traditional ML-decoder for STBC's. We observe that Gabidulin's algorithm is approximately 5 times faster than ML-decoder.

Concluding Remarks

In this paper, the direct matrix construction of MRD-STBC has been presented and it was shown that the rank codes can achieve full diversity gain much like OSTBC's. Though, the performance of OSTBC is generally better than MRD-STBC yet it does outperform OSTBC provided the absolute value of the determinant of each pairwise difference is equal to 4 for both types of block code. The role of Gaussian integers has been highlighted especially low SNR region by exhibiting two STBC cases. Furthermore, we have also evaluated the viability of Gabidulin's decoding algorithm to decode MRD-STBC. The algorithm is well-suited to higher transmit antenna codes which have been constructed using interleaved MRD-STBC's and which output reasonable BER performance at the cost of low complexity.

Acknowledgements

The first and third authors would like to thank HW Communications Ltd. and COMSATS Institute of Information Technology for their support.
The paper is published with financial support by the project ITHEA XXI of the Institute of Information Theories and Applications FOI ITHEA (www.ithea.org) and the Association of Developers and Users of Intelligent Systems ADUIS Ukraine (www.aduis.com.ua).

Bibliography

[Huber, 1994] K. Huber. “Codes Over Gaussian Integers". *IEEE Transactions on Information Theory*, Vol. 40, No. 1, pp. 207-216, 1994.

[Costa et al., 2004] S.I.R. Costa, M. Muniz, E. Agustini and R. Palazzo. "Graphs, Tessellations, and Perfect Codes on Flat Tori". IEEE Transactions on Information Theory, Vol. 50, No. 10, pp. 2363-2377, October 2004.

[Nóbrega et al., 2001] T. P. da Nóbrega, J. C. Interlando, O. Milaré, M. Eliaand R. Palazzo. "Lattice Constellations and Codes from Quadratic Number Fields". IEEE Transactions on Information Theory, Vol 47, No 4, May 2001, pp. 1514-1527.

[Martínez et al., 2005] C. Martínez, R. Beivide, J. Gutierrez and E. Gabidulin. "On the Perfect t-Dominating Set Problem in Circulant Graphs and Codes over Gaussian Integers". Proceedings of the 2005 IEEE International Symposium on Information Theory (ISIT'05). Adelaide, Australia. September, 2005.

[Tarokh et al., 1998] V. Tarokh, N. Seshadri, and A. R. Calderbank, ŞSpace-time codes for high data rate wireless communication: Performance criteria and code construction,Ť IEEE Transactions on Information Theory, March 1998.

[Alamouti, 1998] S. M. Alamouti, ŞA simple transmit diversity technique for wireless communications,Ť IEEE JOURNAL ON SELECT AREAS IN COMMUNICATIONS, vol. 16, no. 8, pp. 1451Ű1458, October 1998.

[Tarokh et al., 1999] V. Tarokh, H. Jafarkhani, and A. Calderbank, ŞSpace-time block codes from orthogonal designs,Ť IEEE Transactions on Information Theory, vol. 45, no. 5, pp. 1456Ű1467, July 1999.

[Lusina et al., 2003] P. Lusina, E. Gabidulin, and M. Bossert, ŞMaximum rank distance codes as space-time codes,Ť IEEE Transactions on Information Theory, vol. 49, no. 10, pp. 2757Ű 2760, October 2003.

[Gabidulin, 1985] E. Gabidulin, ŞTheory of codes with maximum rank distance,ŤProblemy Peredachi Informatsii, vol. 21, no. 1, pp. 1Ű12, 1985.

[Gabidulin, 1995] E. Gabidulin, ŞPublic-key cryptosystems based on linear codes,Ť Technische Universiteit Delft Delft University of Technology, Tech. Rep., 1995.

[Berlekamp, 1968] E. Berlekamp, Algebraic coding theory. New York: McGraw-Hill, 1968.

[Sidorenko and Bossert, 2010] V. Sidorenko and M. Bossert, ŞDecoding interleaved gabidulin codes and multisequence linearized shift-register synthesis,Ť in IEEE International Symposium on Information Theory Proceedings (ISIT), 2010, pp. 1148Ű1152.

Authors' Information

Hafiz M.Asif *- PhD student, School of Computing & Communication Systems, Lancaster University, UK; e-mail: h.asif1@lancaster.ac.uk*
Major Fields of Scientific Research: Space time block coding, Rank codes, Wireless communication systems

Ernst Gabidulin *- Professor, Department of Radio Engineering and Telecommunications, Moscow Institute of Physics and Technology, Russia; email: ernst_gabidulin@yahoo.com*
Major Fields of Scientific Research: Information theory, rank codes, cryptography, network coding

Bahram Honary *- Professor, School of Computing & Communication Systems, Lancaster University, UK; e-mail: b.honary@lancaster.ac.uk*
Major Fields of Scientific Research: Channel coding/decoding, Low-density parity-check codes, Ultra wide band technology

ULTRAMETRIC FECHNERIAN SCALING OF DISCRETE OBJECT SETS

Hans Colonius, Ehtibar N. Dzhafarov

Abstract: *Universal Fechnerian Scaling (UFS) is a principled approach to computing "subjective" distances among objects (stimuli) from their pairwise discrimination probabilities. It is based on the concept of 'dissimilarity function' leading to a locally symmetrical quasimetric in the context of Dissimilarity Cumulation (DC) theory developed by Dzhafarov and Colonius. Here we show that, for finite sets of objects, the replacement of dissimilarity cumulation with a dissimilarity maximization procedure results in "subjective" distances satisfying the ultrametric inequality.*

Keywords: *Fechnerian scaling; dissimilarity function; quasimetric; ultrametric.*

ACM Classification Keywords*: G.2.3 Discrete Mathematics – Applications;*

MSC*: 54E05, 54E15, 54E35, 05C12*

Introduction

In experimental psychology, there are many different procedures for gaining insight into a person's subjective representation of a given set of objects, like colors or tones, pictures of faces, semantic terms, etc. Eliciting numerical judgments about the perceived similarity of a pair of stimuli (objects), or estimating the probability with which a stimulus $\mathbf{x}$ is recognized as stimulus $\mathbf{y}$ (confusion probabilities), are among the most common methods with a long tradition in this field [Shepard, 1957]. A discrimination paradigm focal for this paper involves a set of stimuli $\mathfrak{S} = \{\mathbf{s_1}, \mathbf{s_2}, \ldots, \mathbf{s_N}\}$, $N > 1$, presented two at a time to a perceiver whose task is to respond to each ordered pair $(\mathbf{x}, \mathbf{y})$ by "$\mathbf{x}$ and $\mathbf{y}$ are the same" or by "$\mathbf{x}$ and $\mathbf{y}$ are different". Each ordered pair $(\mathbf{x}, \mathbf{y})$ is then assigned (an estimate of) the discrimination probability function[1]

$$\psi\mathbf{xy} = \text{Pr}\,[\mathbf{x} \text{ and } \mathbf{y} \text{ are judged to be different}] \tag{1}$$

Often the investigator seeks an embedding of subjects' judgments in a Euclidian (or, Minkowskian) space via multidimensional scaling (MDS), or in an ultrametric space (rooted tree structure) via cluster analysis (CA), such that distances among the points representing the stimuli correspond as closely as possible to the observed discrimination probabilities. Both procedures are based on the *probability-distance hypothesis* [Dzhafarov, 2002], that is, the assumption that for some distance function $H\mathbf{xy}$ and some increasing transformation f

$$\psi\mathbf{xy} = f(H\mathbf{xy}). \tag{2}$$

The problem for MDS and CA is that experimental data show systematic violations of *symmetry* and *constant self-dissimilarity* (i.e., generally, $\psi\mathbf{xy} = \psi\mathbf{yx}$ and $\psi\mathbf{xx} = \psi\mathbf{yy}$, respectively, for distinct $\mathbf{x}$ and $\mathbf{y}$).

Dzhafarov and Colonius [Dzhafarov, Colonius, 2007] developed a principled approach to solve this problem, *Universal Fechnerian Scaling* (UFS), which is applicable to all possible (finite or infinite) stimulus spaces endowed with "same-different" discrimination probabilities. UFS is based on the theory of *Dissimilarity Cumulation* (DC) [Dzhafarov, Colonius, 2007; Dzhafarov, 2008a; Dzhafarov, 2008b], which provides a general definition of a *dissimilarity function* and shows how to impose topological and metric properties on stimulus sets.

[1] Notation convention: real-valued functions of one or more arguments that are elements of a stimulus set are indicated by strings without parentheses, e.g., $\psi\mathbf{xy}$ instead of $\psi(\mathbf{x}, \mathbf{y})$

The next section gives an outline of only those aspects of UFS and DC theory that are relevant for finite object sets. For the general case, we refer to the papers above and [Dzhafarov, 2010a]. Subsequently, a new (finite) variant based on the ultrametric property will be introduced.

Concepts and Results from DC Theory and UFS for Finite Spaces

Notation conventions. Let $\mathfrak{S}$ be a finite set of objects (stimuli). A *chain*, denoted by boldface capitals, $\mathbf{X}, \mathbf{Y}, \ldots$, is a finite sequence of objects. The set $\bigcup_{k=0}^{\infty} \mathfrak{S}^k$ of all chains with elements in $\mathfrak{S}$ is denoted by $\mathcal{S}$. It contains the empty chain and one-element chains (conveniently identified with their elements, so that $\mathbf{x} \in \mathfrak{S}$ is also the chain consisting of $\mathbf{x}$). Concatenations of two or more chains are presented by concatenations of their symbols, $\mathbf{XY}$, $\mathbf{xYz}$, etc. Given a chain $\mathbf{X} = \mathbf{x}_1, \ldots \mathbf{x}_n$ and a binary (real-valued) function F, the notation $F\mathbf{X}$ stands for

$$\sum_{i=1}^{n-1} F\mathbf{x}_i\mathbf{x}_{i+1},$$

with the obvious convention that the quantity is zero if n is 1 (one-element chain) or 0 (empty chain).

Dissimilarity function and quasimetric. For a finite set $\mathfrak{S}$, a real-valued function $D : \mathfrak{S} \times \mathfrak{S} \to \Re$ is a *dissimilarity function* if it has the following properties:

$\mathcal{D}1$ (positivity) $D\mathbf{ab} > 0$ for any distinct $\mathbf{a}, \mathbf{b} \in \mathfrak{S}$;

$\mathcal{D}2$ (zero property) $D\mathbf{aa} = 0$ for any $\mathbf{a} \in \mathfrak{S}$.

Note that a dissimilarity function need not be symmetric and need not satisfy the triangle inequality. A dissimilarity function M that does satisfy the triangle inequality is called a *quasimetric*:

$$M\mathbf{ab} + M\mathbf{bc} \geq M\mathbf{ac} \tag{3}$$

for all $\mathbf{a}, \mathbf{b}, \mathbf{c} \in \mathfrak{S}$.

Definition 1. Given a dissimilarity D on a finite set $\mathfrak{S}$, the **quasimetric G induced by D** is defined as

$$G\mathbf{ab} = \min_{\mathbf{X} \in \mathcal{S}} D\mathbf{aXb}, \tag{4}$$

for all $\mathbf{a}, \mathbf{b} \in \mathfrak{S}$.

That G is a quasimetric is easy to prove (see, e.g., [Dzhafarov, Colonius, 2006; Dzhafarov, Colonius, 2007]).

Psychometric increments and Fechnerian distance. If $\mathfrak{S}$ is endowed with ψ, as defined in (1), then (following a certain "canonical" transformation of the stimuli)[2], the dissimilarity function can be defined as either of the two kinds of *psychometric increments*

$$\Psi^{(1)}\mathbf{ab} = \psi\mathbf{ab} - \psi\mathbf{aa} \quad \text{and} \quad \Psi^{(2)}\mathbf{ab} = \psi\mathbf{ba} - \psi\mathbf{aa}. \tag{5}$$

Due to the canonical form of ψ, these quantities are always positive for $\mathbf{b} \neq \mathbf{a}$. Denoting by D either $\Psi^{(1)}$ or $\Psi^{(2)}$, one uses (4) to compute, respectively, the quasimetrics $G_1\mathbf{ab}$ or $G_2\mathbf{ab}$ (called *Fechnerian distances*).

The quantity

$$G^*\mathbf{ab} = G_1\mathbf{ab} + G_1\mathbf{ba} = G_2\mathbf{ab} + G_2\mathbf{ba} \tag{6}$$

then is a metric on $\mathfrak{S}$, called the *overall Fechnerian distance*. The equality of the two computations is easy to establish [Dzhafarov, Colonius, 2006].

[2] For details, including the concept of *regular minimality* see [Dzhafarov, Colonius, 2006]

Ultrametric Fechnerian Scaling of Discrete Object Sets

Any empirical data set being finite, DC theory for finite sets can be viewed as an alternative data-analytic tool to nonmetric (MDS): rather than seeking a nonlinear transformation of a given set of dissimilarities into a (usually Euclidean) metric, DC replaces the dissimilarity value for each ordered pair of points with the shortest length ("cumulated dissimilarity") of a finite chain of points connecting the first element of the pair with the second one resulting in a quasimetric induced by the dissimilarity function.

However, for many empirical dissimilarities on sets of high-dimensional stimuli, or with an underlying collection of hierarchical features, a representation by a rooted tree structure may sometimes be more appropriate. Thus, it seems reasonable to look for a data-analytic alternative to CA based on the principles of Fechnerian Scaling. The basic idea consists in replacing the "dissimilarity cumulation" procedure by "dissimilarity maximization". Given a chain $\mathbf{X} = \mathbf{x}_1, \ldots \mathbf{x}_n$ and a binary (real-valued) function F, the notation $\Delta_F \mathbf{X}$ stands for

$$\max_{i=1,\ldots,n-1} F\mathbf{x_i x_{i+1}},$$

again with the obvious convention that the quantity is zero if n is 1 or 0. A dissimilarity function M on a finite set $\mathfrak{S}$ is called a *quasi-ultrametric* if it satisfies the ultrametric inequality,

$$\max\{M\mathbf{ab}, M\mathbf{bc}\} \geq M\mathbf{ac} \tag{7}$$

for all $\mathbf{a}, \mathbf{b}, \mathbf{c} \in \mathfrak{S}$.

Definition 2. Given a dissimilarity D on a finite set $\mathfrak{S}$, the *quasi-ultrametric G^∞ induced by D* is defined as

$$G^\infty\mathbf{ab} = \min_{\mathbf{X}\in\mathcal{S}} \Delta_D \mathbf{aXb}, \tag{8}$$

for all $\mathbf{a}, \mathbf{b} \in \mathfrak{S}$.

That G^∞ is a quasi-ultrametric is easy to prove. A reasonable symmetrization procedure, yielding a metric that can be called the *overall Fechnerian ultrametric*, is

$$G^{\infty^*}\mathbf{ab} = \max\{G^\infty\mathbf{ab}, G^\infty\mathbf{ba}\} \tag{9}$$

then yields a (symmetric) ultrametric on $\mathfrak{S}$, called the *overall Fechnerian ultrametric*.

Conclusion and Further Developments

On a finite set, any dissimilarity function induces a quasimetric by the "dissimilarity cumulation" procedure of DC theory [Dzhafarov, Colonius, 2006; Dzhafarov, Colonius, 2007]. Here we have suggested a complementary approach inducing a quasi-ultrametric by a "dissimilarity maximization" procedure. A systematic comparison between the two procedures for different types of dissimilarity data sets is left for future investigation, but the following can be noted right away.

First, unlike the DC theory, its ultrametric counterparts does not generalize to arbitrary stimulus sets. Thus, for arc-connected spaces the Fechnerian ultrametric is identically equal to zero.

Second, unlike in the UFS, the overall Fechnerian ultrametric is not the same for the two kinds of psychometric increments, as defined in (5): the equality of the two sums in (6) does not have an analog with (9) in which G^∞ is computed from $\Psi^{(1)}$ and from $\Psi^{(2)}$.

There is, however, one important similarity. [Dzhafarov, 2010b] has shown that the procedure of computing quasimetric distances from dissimilarities can also be described in terms of a series of recursive corrections of the dissimilarity

values for violations of the triangle inequality. It can be shown that a corresponding series of recursive corrections on the dissimilarity values for violations of the ultrametric inequality would yield the induced quasi-ultrametric distances.

One can consider procedures intermediate between cumulation and maximization of dissimilarities by defining, for any dissimilarity function D, the length of a chain $\mathbf{X} = \mathbf{x}_1, \ldots \mathbf{x}_n$ by

$$D\mathbf{X} = ((D\mathbf{x_1x_2})^k + \ldots + (D\mathbf{x}_{n-1}\mathbf{x}_n)^k)^{1/k}. \tag{10}$$

For $k \to \infty$ this would result in the ultrametric approach outlined above. For finite k, the procedure is generalizable to arbitrary dissimilarity spaces. This follows from the fact the use of (10) is equivalent to the use of the original DC in which one, first, redefines D into D^k (which yields another dissimilarity function), and then redefines the locally symmetrical quasimetric G induced by D^k into $G^{1/k}$ (which yields another locally symmetrical quasimetric).

Acknowledgements

H.C. acknowledges support by DFG (Grant SFB-TRR31 Active Listening). E.D. acknowledges support by AFOSR grant FA9550-09-1-0252.

Bibliography

[Dzhafarov, 2002] E.N.Dzhafarov. Multidimensional Fechnerian scaling: Probability-distance hypothesis. J Math Psychol, vol. 46, 352-374

[Dzhafarov, 2008a] E.N.Dzhafarov. Dissimilarity cumulation theory in arc-connected spaces. J Math Psychology, vol. 52, 73-92.

[Dzhafarov, 2008b] E.N.Dzhafarov. Dissimilarity cumulation theory in smoothly-connected spaces. J Math Psychology, vol. 52, 93-115.

[Dzhafarov, 2010a] E.N.Dzhafarov. Dissimilarity, quasidistance, distance. J Math Psychology, vol 54, 334-337.

[Dzhafarov, 2010b] E.N.Dzhafarov. Dissimilarity Cumulation as a procedure correcting for violations of triangle inequality. J Math Psychology, vol. 54, 284-287.

[Dzhafarov, Colonius, 2006] E.N.Dzhafarov and H.Colonius. Reconstructing distances among objects from their discriminability. Psychometrika, vol. 71, 365-386.

[Dzhafarov, Colonius, 2007] E.N.Dzhafarov and H.Colonius. Dissimilarity cumulation theory and subjective metrics, J of Math Psychology, vol. 51(5), 290-304.

[Shepard, 1957] R.N.Shepard. Stimulus and response generalization: A stochastic model relating generalization to distance in psychological space, Psychometrika, vol. 22, 325-345, 1957.

Authors' Information

Hans Colonius *- Carl von Ossietzky Universitaet Oldenburg, 26111 Oldenburg, Germany; e-mail: hans.colonius@uni-oldenburg.de*
Major Fields of Scientific Research: Mathematical modeling of elementary cognitive processes, Psychophysics

Ehtibar N. Dzhafarov *- Purdue University, Department of Psychological Sciences, 703 Third Street, West Lafayette, IN 47907-2081, USA; e-mail: ehtibar@purdue.edu*
Major Fields of Scientific Research: Mathematical psychology, Psychophysics

SYMMETRIZATION: RANKING AND CLUSTERING IN PROTEIN INTERFACES

Giovanni Feverati, Claire Lesieur, Laurent Vuillon

Abstract: *Purely geometric arguments are used to extract information from three-dimensional structures of oligomeric proteins, that are very common biological entities stably made of several polypeptidic chains. They are characterized by the presence of an interface between adjacent amino acid chains and can be investigated with the approach proposed here. We introduce a method, called symmetrization, that allows one to rank interface interactions on the basis of inter-atomic distances and of the local geometry. The lowest level of the ranking has been used previously with interesting results. Now, we need to complete this picture with a careful analysis of the higher ranks, that are for the first time introduced here, in a proper mathematical set up. The interface finds a very nice mathematical abstraction by the notion of weighted bipartite graph, where the inter-atomic distance provides the weight. Thus, our approach is partially inspired to graph theory decomposition methods but with an emphasis to "locality", namely the idea that structures constructed by the symmetrization adapt to the local scales of the problem. This is an important issue as the known interfaces may present major differences in relation to their size, their composition and the local geometry. Thus, we looked for a local method, that can autonomously detect the local structure. The physical neighborhood is introduced by the concept of cluster of interactions. We discuss the biological applications of this ranking and our previous fruitful experience with the lowest symmetrized level. An example is given, using the prototypical cholera toxin.*

Keywords: *symmetrization, protein interfaces, oligomeric proteins, graphs, bonds ranking, interaction clusters.*

ACM Classification Keywords*:*
J.2 Physical sciences - Mathematics and statistics
J.3 Life and medical sciences - Biology and genetics

Conference topic*: MDA 2012 - "Mathematics of Distances and Applications" : Distances in Natural Sciences*

PACS*: 87.15.bk Structure of aggregates, 87.15.km Protein-protein interactions, 87.15.hg Dynamics of intermolecular interactions*

MSC*: 52-XX Convex and discrete geometry, 52C99 None of the above, but in this section, 92-XX Biology and other natural sciences, 92B99 None of the above, but in this section*

Introduction

The present work is motivated by the biological problem of understanding and possibly predicting the assembly of biological molecules. This is one of the most common processes in living cells: proteins and, more generally, biological molecules, interact with each other by temporary or permanently associating into a unit that realises some biological function. Actually, the majority of proteins are permanently formed of several subunits organized into small polymers known as oligomeric proteins [Goodsell, 2000]. Understanding the mechanisms of their formation is particularly important due to their implication in several pathologies, from bacterial infections to protein misfolding diseases (Alzheimer, Parkinson, ...) [Iacovache, 2008; Lesieur, 1997; Kirkitadze, 2002; Harrison, 2007]. The association of different subunits requires the formation of specific intermolecular bonds, thus constituting what is called an interface. Unfortunately, in spite of extensive analyses, the identification of the patterns, in the polypeptidic chain, responsible for the establishment of an interface remains difficult.

The long term perspective of our work is to rationalize the interface, namely to establish a clear understanding of its sequence-structure relationship, in order to perform interface prediction as well as interface design. The shape

and the function of proteins are encoded within their sequence, i.e. in their amino acid composition. But it is not yet possible, by simply reading the primary sequence of a protein, to know its three-dimensional structure or the quaternary organization, in the case of a protein oligomer. One of the difficulties is the non linear encoding of the information in the sequence, that requires three-dimensional analysis. Another difficulty is due to the degeneracy between sequences and structures, consisting in the observation that several sequences can code for the same shape, that indicates a versatile role of the amino acids. The secondary structures of proteins which are mainly composed of α helices, β structures and loops are partially understood, and several prediction programs are now available.

One possible strategy to decipher the sequence-structure relationship of protein interfaces is through the analysis of the interface geometry. This is motivated by the observation, made in the early 50's by F. Crick [Crick, 1953], that the formation of the coiled-coil interface is due to the appropriate geometrical and chemical complementarity of the two interacting domains, as in a lock and key mechanism. The key has a particular geometry combined to some contact points which together provide it the capacity to associate to one lock. Moreover, he also observed that protein interfaces of similar geometry have similar chemistry, namely similar contact points.

Here we follow the same line of thinking, moving from the geometry toward the chemistry. We develop the "symmetrization", a method to decipher interface properties through the analysis of its geometry and interactions. Their strength is measured by some "distance". Indeed, we rely on the notion that physical interactions decrease with increasing distance. With this, the symmetrization produces a hierarchical ranking of the interactions. The notion of physical neighborhood appears by a concept of "clusters of interactions" (see later).

In [Feverati, 2010] we succeeded in showing that it is possible to encode some information of the interface in a graph (interaction network). Comparative statistics on many protein graphs has been a fruitful method to extract useful features for the intermolecular beta sheet interface geometry [Feverati, 2012]. These results were based on the lowest level of ranking, called S_0. All the higher levels were neglected: possibly a 90% of the actual interactions was ignored, focusing on the strongest only. It is important now to explore the structure of the neglected interactions and estimate the information they may contain. To assess this, we need a careful mathematical understanding of the symmetrization, that will be revisited from a more mathematical point of view, in order to develop its full potential.

Methods and results

The symmetrization, first introduced in [Feverati, 2010] and fully developed here for the first time, extract information on the interfaces from the three-dimensional PDB protein structures. The term information is understood in a very wide sense: which atoms form intermolecular bonds, which is the role of the different amino acids in the interface, how the charge or the hydrophobic character of some atomic groups in the amino acids matters in forming or stabilizing the interface, and so on.

In an interface, the typical distances between atoms of two adjacent chains are of the order of 2-5 Angström. Thus it is important to work at the atomic scale, even if the ultimate information must be expressed at the amino acid scale because the formation of proteins always passes through one or few amino acid sequences.

Let A, B the set of atoms of the first, second subunit, respectively. We indicate with $d(a,b)$ a distance between an atom $a \in A$ and an atom $b \in B$. Notice that the notation itself indicates the set to which the atoms belong, namely the first parameter of $d(\ ,\ )$ must be in A, the second in B.

The mathematical development that will be presented in this section is actually independent of the explicit distance function adopted and of the space dimension. Thus, the presentation holds in a generic metric space (or even less than it because we don't actually need the triangular inequality, for the derivation. We need it for the interpretation, in the Discussion section). In the Discussion section, we will present an example based on the Euclidean distance in $\mathbb{R}^3$.

We call raw interface the following set of ordered pairs

$$R_0 = \{(a,b) \in A \times B, \text{ such that } d(a,b) \leq d_0\}, \quad d_0 \geq 0 \quad \text{some cut-off} \tag{1}$$

namely pairs of atoms at distance lower than the cut-off are in the interface. In the present Methods section, the actual cut-off value is immaterial, namely the construction holds whatever its value is. For the purposes of discussing intermolecular interactions, it is often fixed to

$$d_0 = 5 \text{ Angström} \tag{2}$$

This definition of the interface does not provide any measure to distinguish pairs whose atoms are at different distances or in different locations. On the contrary, firstly physical interactions decrease when distance grows, secondly two interactions of equal strength may not play the same role if they are in different parts of the molecules, inserted in different atomic environments.

This means that besides the distances, we need to rank the interactions within an interface, with a ranking sensitive to the local conditions.

The lowest level

We will make large use of the minimum function

$$\min \mathcal{S}\,, \quad \text{where} \quad \mathcal{S} = \text{ some set of reals} \tag{3}$$

to extract the minimum distance in the set. As we have in mind applications, we will use finite sets. Thus, the minimum will always be realized. Let define a first subset of the raw interface by

$$L_A = \Big\{(a,b) \in R_0 \ : \ d(a,b) = \min\big\{d(a,c) : c \in B \text{ and } (a,c) \in R_0\big\}\Big\} \tag{4}$$

This set associates to every atom $a \in A$ its closest neighbour on B (or neighbours, if equidistant), namely it minimizes the distances by respect to the atoms of the first subunit. Similarly, we consider the set of pairs that minimises distances by respect to the atoms of the second subunit

$$L_B = \Big\{(a,b) \in R_0 \ : \ d(a,b) = \min\big\{d(c,b) : c \in A \text{ and } (c,b) \in R_0\big\}\Big\} \tag{5}$$

The symmetrized interface is the subset of the raw interface defined as the intersection of these two sets

$$S_0 = L_A \cap L_B\,, \quad S_0 \subseteq R_0 \tag{6}$$

A restatement of the definition is that a necessary and sufficient condition for a pair $(a,b) \in R_0$ to be in S_0 is to satisfy the system of equations

$$\begin{cases} d(a,b) = \min\Big\{d(a,c) \ : \ c \in B \text{ and } (a,c) \in R_0\Big\} \\ d(a,b) = \min\Big\{d(c,b) \ : \ c \in A \text{ and } (c,b) \in R_0\Big\} \end{cases} \tag{7}$$

Notice that the unknowns are not numbers but pairs of R_0. In practice the logic is the following. Let fix an arbitrary pair (a,b). Is that pair the shortest (or one of the shortest if several have equal length) of all the bonds coming out of a (like rays of a star)? If not, then (a,b) cannot solve the system. If yes, then is (a,b) the shortest (or one of the shortest if several have equal length) of all the bonds coming out of b? If yes, then (a,b) solves the system and belongs to S_0. In other words, when both equations are satisfied, the bond under examination minimizes two distinct sets of bonds, one at each of its extremes: it is a local minimum. This is our notion of symmetrization of a set of bonds.

Theorem 1. *If $R_0 \neq \{\}$, then S_0 cannot be empty.*

Proof. Let consider the pair $(\bar{a}, \bar{b})$ that minimizes the whole set of distances of R_0 (there must be at least one such pair)

$$d(\bar{a}, \bar{b}) = \min\{d(c_1, c_2) \ : \ c_1 \in A \, , \ c_2 \in B \, , \ (c_1, c_2) \in R_0\} \tag{8}$$

It is a global minimum. This implies that the set appearing on the right hand side of the following equation is also minimized

$$d(\bar{a}, \bar{b}) = \min\{d(c_1, \bar{b}) \ : \ c_1 \in A \, , \ (c_1, b) \in R_0\} \tag{9}$$

Similarly, (8) implies also that the following expression is verified

$$d(\bar{a}, \bar{b}) = \min\{d(\bar{a}, c_2) \ : \ c_2 \in B \, , \ (a, c_2) \in R_0\} \tag{10}$$

These last two equations actually constitute the system in (7), thus the pair $(\bar{a}, \bar{b})$ belongs to S_0 which, in that way, cannot be empty. From now on, we will always assume that R_0 is not empty. ■

Corollary 1. *If an atom a appears more than once in S_0, then it appears with equidistant pairs*

$$d(a, b_1) = d(a, b_2) \quad \textit{where} \quad (a, b_1), (a, b_2) \in S_0 \tag{11}$$

Proof. Indeed, multiple minima are allowed. ■

The higher levels

In this subsection we will prove that the procedure of symmetrization can be iterated. We start by defining a new set of bonds

$$R_i = R_{i-1} - S_{i-1} \, , \qquad i = 1, 2, \ldots \tag{12}$$

As in (7), we look for pairs $(a, b) \in R_i$ that solve the following system

$$\begin{cases} d(a, b) = \min\left\{d(a, c) \ : \ c \in B \text{ and } (a, c) \in R_i\right\} \\ d(a, b) = \min\left\{d(c, b) \ : \ c \in A \text{ and } (c, b) \in R_i\right\} \end{cases} \tag{13}$$

The subset that solves this system of equations defines the symmetrized set at level i

$$S_i = \{(a, b) \in R_i \ : \ \text{it solves (13)}\} \, , \qquad S_i \subseteq R_i \tag{14}$$

The proof of theorem 1 can now be repeated here, after replacing R_0 with R_i. This shows that, as long as $R_i \neq \{\}$, its subset S_i cannot be empty as it must contain at least the global minimum, namely a pair $(\bar{a}, \bar{b})$ that minimizes all distances of R_i

$$d(\bar{a}, \bar{b}) = \min\{d(c_1, c_2) \ : \ (c_1, c_2) \in R_i\} \tag{15}$$

All what is stated from (12) to here can be repeated at all orders. Considering that we have a finite number of atoms and that the symmetrized sets are not empty, at some point the recursion (12) will stop with an empty set

$$R_M = \{\} \quad \text{with} \quad R_{M-1} \neq \{\} \, , \quad M = \text{number of levels} \tag{16}$$

By the definition of the recursion (12), it is obvious that a level cannot intersect the previous ones thus we state the following theorem.

Theorem 2. *Different levels are separated:* $S_i \cap S_{i-1} = \{\}$

The initial set of bonds R_0 is now the union of disjoint sets

$$R_0 = \bigcup_{0 \le i < M} S_i \tag{17}$$

Thus the initial set of bonds has been sliced in levels, with each bond uniquely classified into a level. An important theorem that we will use later is now stated.

Theorem 3. *At least one atom in a pair must appear in one pair of the previous symmetrized set, namely*

$$(a_1, b_1) \in S_i \Longrightarrow (a_1, c) \in S_{i-1} \text{ or } (c', b_1) \in S_{i-1} \text{ for some } c, c' \tag{18}$$

(both are possible). Equivalently, one can say that each bond of S_i contains at least one atom of S_{i-1}.

Proof. To show this, let suppose by absurd that they both do not appear. In that case, for the pair (a_1, b_1) it would be equivalent to replace R_i by R_{i-1} in (13), because no record of this pair is present in S_{i-1}. But then, the system of equations that defines the level i (13) would look as the definition of the previous level $i-1$, indicating that the pair belongs to S_{i-1}, that is absurd because of (12). The second formulation re-writes the first one. The following corollary is obvious. ■

Corollary 2. *With respect to S_i, a new pair (a, b), namely one with both new atoms, cannot be found before the level $i+2$, namely in S_{i+2}.*

The flow chart of the whole symmetrization procedure is represented in Figure 1.

Towers and clusters

The pairs at level zero of the symmetrization can be used as the starting point of towers of bonds. The lowest parts of the towers define non intersecting clusters of bonds. Each pair at level zero defines the level zero (ground) of each tower by

$$T_0(a, b) = \{(a, b)\} \quad \forall \quad (a, b) \in S_0 \tag{19}$$

Each tower level higher that the ground is recursively defined by choosing all bonds of S_i that have one atom in common with the lower tower level

$$T_i(a, b) = \{(a', b') \in S_i \ : \ \text{either } (a', c) \in T_{i-1}(a, b) \text{ or } (c, b') \in T_{i-1}(a, b) \text{ for some } c\} \tag{20}$$

The full tower will be the union of all levels

$$T(a, b) = \bigcup_{i \ge 0} T_i(a, b) \tag{21}$$

Notice that the tower and its levels are always labelled by the initial ground pair, namely $(a, b) \in S_0$.

Theorem 4. *At each level, the union of all towers exhausts the corresponding symmetrized set:*

$$\bigcup_{(a,b) \in S_0} T_i(a, b) = S_i \tag{22}$$

Proof. First, this property holds at level 0 (19). For higher i, we prove it by induction, supposing that it holds at $i-1$ and showing that this implies its validity at i. So, at this level we have

$$T = \bigcup_{(a,b) \in S_0} T_i(a, b) =$$

$$\bigcup_{(a,b) \in S_0} \{(a', b') \in S_i \ : \ \text{either } (a', c) \in T_{i-1}(a, b) \text{ or } (c, b') \in T_{i-1}(a, b) \text{ for some } c\}$$

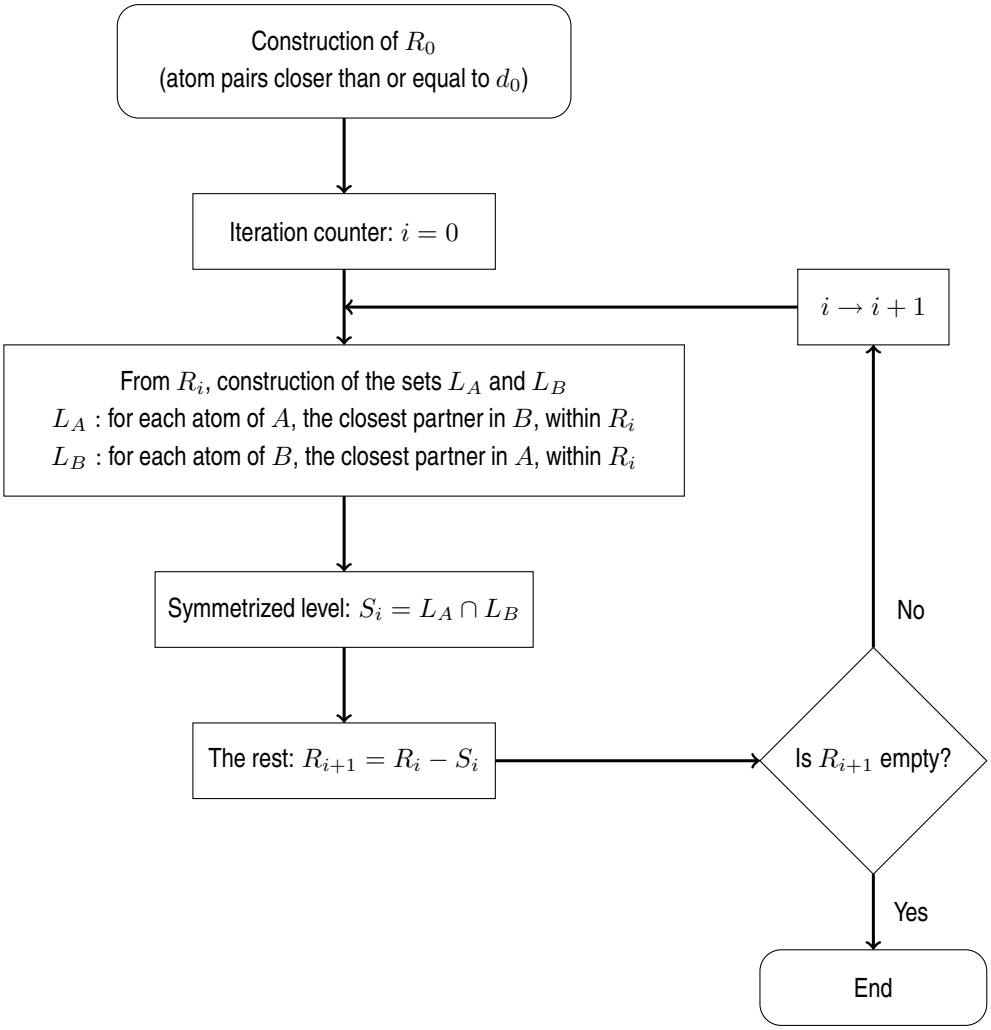

Figure 1. Flow chart of the symmetrization algorithm.

The symmetrized set S_i does not depend on which ground pair (a, b) is considered so the union operation goes inside the braces producing (in two positions) the term

$$\bigcup_{(a,b)\in S_0} T_{i-1}(a, b) = S_{i-1} \tag{23}$$

We have supposed that this holds true so we can write

$$T = \big\{(a', b') \in S_i \ : \ \text{either } (a', c) \in S_{i-1} \text{ or } (c, b') \in S_{i-1} \text{ for some } c\big\} \tag{24}$$

The condition inside the braces is actually the statement of theorem 3 so it is satisfied by all the pairs of S_i, that is precisely the thesis. ■

Corollary 3. *The union of all towers covers R_0:*

$$\bigcup_{(a,b)\in S_0} T(a, b) = R_0 \tag{25}$$

Proof. It is a direct consequence of (22) and (17). ■

Notice that the definition of tower (20) allows the case of bonds belonging to a symmetrized set higher than the ground to be in more than one tower. Thus, two towers can have nonvanishing intersection and the union in (25) redundantly covers the initial set of bonds. On the other hand, it is very easy to provide examples of non intersecting towers: just consider two groups of atoms whose inter-group distances are all larger than the cut-off. The meeting level of two towers is the lowest integer at which they share one or more bonds:

$$T_\ell(a,b) \cap T_\ell(c,d) \neq \{\}\,, \qquad 0 \leq \ell < M\,, \qquad (a,b),\ (c,d) \in S_0 \tag{26}$$

The towers will provide useful information to interpret the bonds organisation of the interface. We define the following relation $\mathcal{R}$ between members of R_0 by saying that two bonds are in relation if one can walk from the first to the last by always traversing intersecting towers:

$$\begin{aligned}(a,b)\mathcal{R}(c,d) \quad \Leftrightarrow \quad & \exists \quad \big\{(e_i,f_i) \in R_0\,, \quad i=1,\ldots,N\big\} \quad \text{for some } N \text{ such that} \\ & \hat{T} \cap T(e_1,f_1) \neq \{\}\,, \quad T(e_1,f_1) \cap T(e_2,f_2) \neq \{\}\,, \quad T(e_2,f_2) \cap \ldots \neq \{\}\,, \\ & \ldots \cap T(e_N,f_N) \neq \{\}\,, \quad T(e_N,f_N) \cap \tilde{T} \neq \{\}\end{aligned} \tag{27}$$

where $\hat{T}$ is a tower that contains (a,b) and $\tilde{T}$ is one that contains (c,d).

Theorem 5. *The binary relation $\mathcal{R}$ is an equivalence relation.*

Proof. First, the relation is reflexive $(a,b)\mathcal{R}(a,b)$, as a tower intersects itself. Second, it is symmetric

$$(a,b)\mathcal{R}(c,d) = (c,d)\mathcal{R}(a,b) \tag{28}$$

because the set intersection is commutative. Third, it is transitive

$$(a,b)\mathcal{R}(c,d) \text{ and } (c,d)\mathcal{R}(e,f) \Rightarrow (a,b)\mathcal{R}(e,f) \tag{29}$$

To see this, one can simply walk back one of the paths of the left hand side, join it with the other and use the joined path to connect the two bonds on the right hand side. ■

This equivalence relation partitions the set R_0 into equivalence classes, members of the quotient set

$$Q = R_0/\mathcal{R} = \{[(a,b)] : (a,b) \in R_0\} \tag{30}$$

Two different equivalent classes represent two groups of bonds that cannot be connected by a bond in R_0. By (1), this means that the respective atoms are separated from each other of more than the cut-off distance (1), thus forming two separated domains of points. They are also called patches, or regions of the interface. By the definition itself, it is obvious that a tower belongs to a single patch. Vice versa, a patch in general contains several towers; actually it contains all the towers that have a (pairwise) nonvanishing intersection.

Two towers at a level lower than the meeting one (26) do not intersect. Thus the bonds belonging to levels lower than the intersection one are well separated and form clusters around the two level 0 bonds that generate the towers. Let ℓ the lowest meeting level for a given tower, namely the lowest integer that satisfies (26) for the tower $T(a,b)$. Then, all its bonds that are ranked at a level lower than ℓ belong to the cluster $\mathcal{C}(a,b)$ that emanates from (a,b)

$$\mathcal{C}(a,b) = \{(e,f) \in T(a,b) : (e,f) \in S_i\,,\ 0 \leq i < \ell\} \tag{31}$$

The bonds at the meeting level or higher are not attributed to this cluster, because they are equally well described as members of the nearby cluster $\mathcal{C}(c,d)$. One can go further. Following (26), one can look for the level ℓ_1 at which a third tower is met, thus form a larger cluster. The construction can go on and will stop when the full patch will be included in the cluster. This hierarchical division into clusters is important because it provides a notion of vicinity between bonds, and thus between atoms, based on the ranks and on the meeting levels.

Complexity of the symmetrization algorithm

For simplicity, we suppose that the two subunits A and B have the same number of atoms n. We compute the complexity of the algorithm by counting the operations needed for the construction of the sets R_i and S_i with $i = 0, 1, \cdots, M-1$.

For the set R_0, the expression (1) considers the pairs of atoms at a distance lower than a given cut-off. Thus, for each atom $a \in A$ we must evaluate the distance to each atom $b \in B$ and make the choice to include or not the pair (a, b) in R_0 by comparing with the cut-off. This construction of R_0 requires n^2 operations. Particularly, in the worst case the cardinality of R_0 is quadratic and of the order of n^2, $O(n^2)$.

The worst case arises when the two subunits are strongly connected; in graph theory such event is called a complete bipartite graph, that occurs when each atom of A is connected to each atom of B, as in the following example

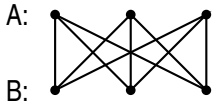

When all the distances between pairs of atoms are less than the cut-off, R_0 turns out to be a complete bipartite graph with exactly n^2 pairs of atoms.

Now, the symmetrization uses the sets defined in (4) and (5). In order to construct L_A, for each atom a we consider all the atoms b such that the pair (a, b) is in R_0. In the worst case we need to consider all the pairs between atoms of A and atoms of B. Thus the construction of L_A uses n^2 operations. The same argument holds for the construction of L_B. The intersection of L_A and L_B requires once more n^2 operations, in the worst case. Thus, at worst, the symmetrization at level 0 needs $3n^2$ operations, that is $O(n^2)$ operations. Notice that the cardinality of L_A and L_B can be estimated to be of order n. Actually, it is precisely n if the distances are all different. The size of S_0 cannot be greater that the one of L_A, L_B; it is expected to be of order n or lower.

A new level is built with the subtraction indicated in (12). This operation is estimated to remove a linear number of pairs of atoms (that is $O(n)$ pairs of atoms). As the removal of a linear set from a quadratic set doesn't affect the order, the cardinality of R_1 turns out to be quadratic. We will use this counting at all levels, claiming that the size of all the R_i is quadratic in n and their symmetrization needs $O(n^2)$ operations. Clearly, this is an overestimation, because we know that the cardinality of R_i decreases, with i, down to zero (16) thus the number of operations needed by its symmetrization decreases accordingly. A more careful counting is possible but has no effect on the final order.

The maximum value of the number of levels in (16) is $M = n^2$, corresponding to a case where at each level we remove only one pair of atoms from R_0, precisely the one that attains the global minimum (15). In practice, the actual number of levels is often less than n (see the example given later).

The total number of operations is evaluated to $n^2 + Mn^2$, that amounts to $n^2 + n^2 n^2$, given the maximum value of M. This means $O(n^4)$ operations for the whole construction.

Comparison with connected components decomposition

It is very natural to express the notion of interface by the form of a graph. Its set of vertices is

$$V = A \cup B \tag{32}$$

The set of edges (bonds) is R_0 itself. As we only consider bonds between A and B, the graph is automatically bipartite. We do not need to consider loops (bonds joining a vertex with itself). Also, the graphs are simple, as we do not attach any meaning to parallel edges.

In [Feverati, 2010] and in later publications, we have systematically represented the level S_0 of interface proteins by undirected bipartite graphs (Gemini graphs) and carefully investigated their properties.

The connected components are a global decomposition of a graph into subgraphs, where the reference length used to separate the different components is the same everywhere. The symmetrization, instead, is a local decomposition of the graph into subgraphs because the ranking is decided by the local features of the graph.

In connected component analysis, a "running" cut-off is used in order to evaluate how far two (or more) parts of the interface are. In the case of an interface, we could introduce a cut-off f with $0 < f < d_0$ in order to consider only pairs of atoms with distance less than f. This construction helps to investigate the structure of the interface and can be used to propose pairs of atoms considered crucial to maintain the interface. On the other hand, it is somehow artificial because the cut-off is not aware of the local "geometry". For example, a very densely populated region and a sparse one are treated on an equal ground by a global cut-off while they are ranked differently by the symmetrization.

Thus, the stratification of R_0 into levels, produced by the symmetrization, is another way to investigate the pertinence of the interface. In particular, there are atoms which are involved at many levels in the towers; these atoms could be important in the construction of the interface itself. We will use all this information in future publications to investigate a new measure of the stability of the interface and to focus on pairs of amino acids with atoms appearing at many different levels of the towers.

Discussion

Example

The subunit B of the cholera toxin protein (CtxB) is a pentamer made of identical chains of 103 amino acids, showing the cyclic group C_5 symmetry. We use the Protein Data Bank structure 1EEI, where the chains are enumerated from D to H. From now on, unless explicitly specified, all the results and the discussion are based on the Euclidean distance in $\mathbb{R}^3$. The raw interface R_0 (1) contains 740 bonds of length smaller that 5 Angström. This interface decomposes in 30 levels S_i, $i = 0, 1, \ldots, 29$ (17), as shown in table 1.

The lowest levels of the towers are indicated in Figure 2 and 3.

At the level 0, one recognizes 10 black straight line segments, namely 10 clusters. Six of them join at level 2, by a purple. Two join at level 3, by a red segment. Two clusters are still disjoint and will join at some higher level.

Table 1. Decomposition of the interface in levels, for the CtxB protein (1EEI). In average, each symmetrized level has 24.7 bonds. The total interface R_0 has 740 members.

level	0	1	2	3	4	5	6	7	8	9	10	11	12	13	14
bonds in the level	33	39	34	32	33	37	32	29	30	32	34	38	38	35	25
level	15	16	17	18	19	20	21	22	23	24	25	26	27	28	29
bonds in the level	29	33	36	25	27	24	17	13	8	7	6	4	4	4	2

Table 2. Effect of the variation of the cut-off in the range [5,25] Angström. The table indicates the number of pairs in S_0, at three different values of the cut-off d_0. The test has been performed on 40 proteins of stoichiometries from 3 to 8. We show one example per stoichiometry.

$d_0 \downarrow$ name $\rightarrow$	1PM4	1J8D	1EEI	1U1S	1HX5	1Q3S
5 Angström	15	36	33	22	18	72
6.5 Angström	16	36	33	23	19	75
25 Angström	18	36	33	23	19	79

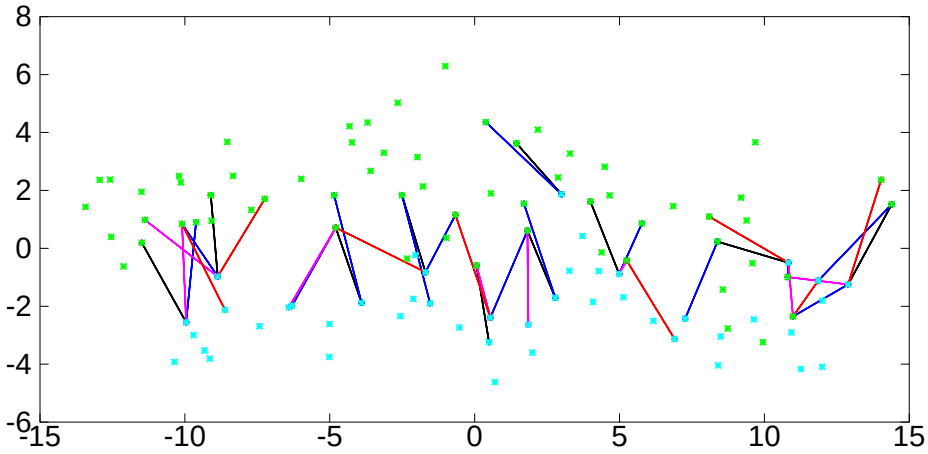

Figure 2. A planar projection of the interface of the CtxB protein is shown; axis coordinates are indicated in Angström. The projection has been chosen to maximise the visibility of the interface. Only atoms belonging to the amino acids in the range $[96, 103]$ in chain D and $[23, 31]$ in chain E are shown. We restrict to it in order to have an image of reasonable size. The four lower levels are shown in colors: S_0 black, S_1 blue, S_2 purple, S_3 red. The stars represent atoms: cyan for the subunit D, green for the subunit E. The unconnected atoms will all join at some level higher than level 3. Here and in the next figure, please notice that the apparent crossing of the straight line segments is an artifact of the projection; in the three dimensional space they actually avoid each other (in general).

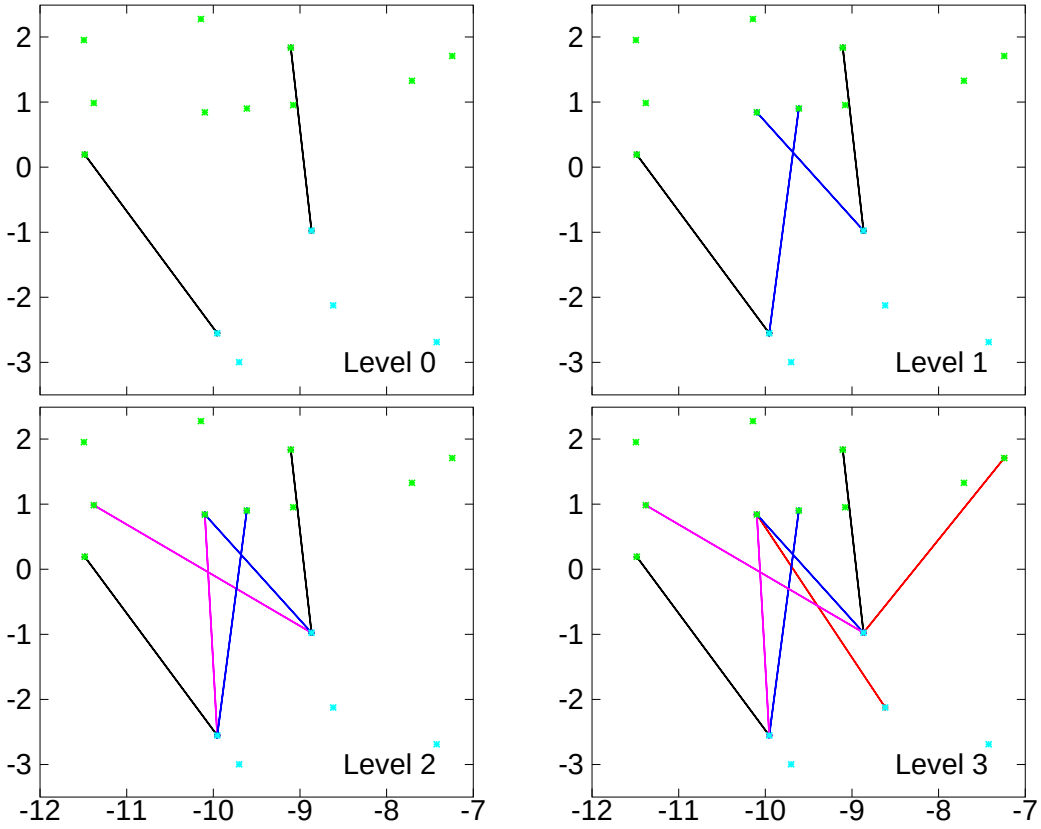

Figure 3. Zoom on the left part of Figure 2. Each image adds one level on top of the previous ones. Two bonds appear at level zero and form the basis of two towers. They meet at level 2, thanks to the purple segment closest to “vertical”, that joins one atom of each tower.

Features of the symmetrization

We present now the features of the symmetrization that we find important in studying the protein interfaces. We also suggest that the symmetrization could help to treat problems issued of different domains, like other biological interfaces.

1. The whole construction is independent on the explicit distance function. In relation to protein interfaces, this means that one could replace the three-dimensional Euclidean distance by some other distance that knows about the actual interaction energy of the pair. This would allow to interpret the ranking in a strict sense: the higher the rank the weaker the strength[1]. Unfortunately, this goal is not easily realized, the major problem being that part of the interaction energy between subunits is accumulated as torsion or bending of covalent bonds. This requires a description based on three or four atoms while the distance is a function of two atoms. Said otherwise, the correct interaction energy is not just the sum of pairwise interactions but also contains three and four atom terms. While here we remain with the Euclidean distance, we plan to perform, in a future publication, several tests in order to appreciate the relative importance of two, three and four atom interaction terms and present a distance expression that (somehow) simulates their effects.

2. The symmetrization self-adapts to the size and packing of the interface. To clarify this point, imagine we define an interface by taking (a) its ten shortest distances, or (b) the three shortest distances for each atom. In (a), the number of representatives would be totally uncorrelated to the actual interface size, while in (b) the local arrangement of points and the interaction strengths would play no role. In particular, an atom connected with three others or a second atom connected with ten others would be treated in the same way. We have observed an enormous variability in the type, number and local organization of atoms or amino acids present in an interface so we mandatorily need to avoid situations as those described in (a) or (b).

3. The symmetrization makes the set S_0, the lower levels content and the clusters (31) weakly dependent upon the cut-off value. Indeed, if $d_0 \to \infty$ (or simply higher that the largest distance in the data set), the full construction becomes cut-off and scale independent. Decreasing it down to a finite value, still sufficiently large by respect to the pairs in S_0, is expected to have a limited influence on the lowest levels, because the whole procedure is based on minimizations while, if we decrease the cut-off, we just slice out widely separated pairs. The validity of this argument strongly depends on the actual data set. In the domain of protein interfaces, it is strongly supported by the data in table 2.

   This indicates that a good strategy to choose the cut-off consists in fixing it to a value such that the effect of a variation on the lowest levels (before meeting) is negligible. Physically, this represents the very common situation where the interaction of sufficiently far apart objects is screened by the interposed ones and the contribution to the bond energy becomes negligible. This is why we choose $d_0 = 5$ Angström in order to capture intermolecular interactions at the interfaces.

4. The symmetrization applies to all scales, namely one could replace the atoms by some interacting entity at some distance scale. Indeed, the only scale length in the problem is the cut-off, that can be removed by simply sending it to infinity. This can be particularly interesting in analysing problems where two or more different scale lengths appear.

5. As the levels are obtained by minimization, they are "fragile" to perturbations or experimental errors, if these are sufficiently large to swap the relative distances of two atoms. Most probably this is not a serious issue if clusters are considered. A more complete analysis will be performed in later publications.

[1] Notice that the triangular inequality is needed to supports this interpretation.

Connection with biology

Having adopted the Euclidean distance, the symmetrization produces a ranking that is purely geometric, because atomic positions only matter while the atom and interaction types do not play any role. The F. Crick approach cited in the Introduction was also purely geometric. If some "improved" distance based on the actual chemical interactions was implemented, as suggested at point 1 in paragraph Features of the symmetrization, the ranking would become geometrical and chemical. With our purely geometric criterion, in previous papers we have show that the lowest symmetrized level S_0 contains useful information on the interfaces. Its use has been validated in [Feverati, 2010]. It has been employed in [Zrimi, 2010] to help investigating the role of histidines in the protein assembly.

More recently, in [Feverati, 2012] it has been shown that the intermolecular β-sheet interfaces are made of two interdigitated interaction networks, one involving backbone (BB) atoms only, the other involving at least one side-chain (SC) atom. The two networks have slightly different amino acids and bond compositions and some specific pattern of charged and hydrophobic amino acids. The hydrophobic amino acids observed in the BB network are similar to those observed in intramolecular β-sheets. The SC network is slightly enriched in charged amino acids and the spatial distribution of the charged amino acids in the interface has some peculiar pattern specific to the intermolecular case.

The work of J. Janin and collaborators [Janin, 2008] indicates that an interface is composed of two parts, the core and the rim. The core is completely inaccessible to the solvent molecules, typically water, while the rim is exposed to them. The distinction is geometrical, based on the position and on steric hindrance of atoms. The core is more conserved during evolution. The complementarity of the two subunits is more pronounced in the core than in the rim.

On the opposite, the symmetrization, albeit geometrical, does classify according to the strength of the interactions. The two classifications (core/rim versus symmetrization) are "dual", in the sense that they complement each other by giving different information on the same entity. For example, atoms of the core can appear at many different levels thus, in general, it would not be appropriate to claim that some levels describe the core, some others the rim.

A consequence of our choice of using the notion of the interaction strength is that we have instruments to characterize the physical neighborhood: the patches, the clusters and the meeting levels.

If the cut-off is well chosen, patches represent different regions of the interface, namely groups of atoms sufficiently far apart to be considered independent. This phenomenon is common, as quite often an interface is made of several patches. Different patches in the same interface can play different roles during assembly and possibly they have different evolutive histories. The notion of independent region or patch is somehow hard to define thus it is very important to have a procedure to construct it. The present definition is based on atomic interactions while the one we used in [Feverati, 2010] was based on the proximity along the amino acid sequence.

The clusters (31) may help to characterize fundamental blocks of an interface, at least for those clusters whose meeting level is very high. A block can mean some group of atoms that is recurrent, in interfaces of similar geometry, or that is conserved during evolution, or that has some special role in the recognition of the two subunits during the assembly.

The assembly is a complex phenomenon where the two partners, namely the subunits, need to recognize each other, then stabilize the interface. In most cases it is not known how these steps develops. Thus, the levels seem to suggest the sequence of events occurring during the assembly, the lower levels accommodating first, the higher levels later.

Conclusion

The whole analysis presented so far has been triggered by the problem of investigating biological interfaces, namely interfaces that form during the biochemical activity in a cell, between or inside proteins, protein-DNA or protein-RNA complexes and so on.

We have proposed a new approach to the treatment of protein interfaces, based on the idea that the ranking of interactions helps clarifying their role. Our previous experience with the lowest level S_0 has been so fruitful that we believe the full set-up constructed here will allow to improve the description of interfaces.

The main tool, in our view, is the cluster. Indeed, it identifies the locally strongest bonds and the meeting level indicates how rich are the interconnections within each cluster.

Higher levels, clusters, towers and patches are presented here for the first time, in a proper mathematical development. The hope is that their full biological relevance will appear after a comparative analysis of many interfaces of similar geometry, as it has been the case with the level 0. Also, with the use of S_0 alone, as we did in our previous papers, it was not possible to evaluate the role of the interactions that were neglected. The need to address this issue has strongly motivated the present work.

Acknowledgements

It's a pleasure to thanks Alexander Grossmann for his most welcome comments.

Bibliography

[Goodsell, 2000] D.S. Goodsell, A.J. Olson. Structural symmetry and protein function. Annu Rev Biophys Biomol Struct 29: 105-153, 2000.

[Iacovache, 2008] I. Iacovache, F.G. van der Goot, L. Pernot. Pore formation: An ancient yet complex form of attack. Biochim Biophys Acta, vol. 1778, num. 7-8, p. 1611-23, 2008.

[Lesieur, 1997] C. Lesieur, B. Vecsey-Semjen, L. Abrami, M. Fivaz, G. F. van der Goot. Membrane insertion: The strategies of toxins (review). Mol Membr Biol 14: 45-64, 1997.

[Kirkitadze, 2002] M.D. Kirkitadze, G. Bitan, D.B. Teplow. Paradigm shifts in Alzheimer's disease and other neurodegenerative disorders: the emerging role of oligomeric assemblies. J Neurosci Res 69: 567-577, (2002).

[Harrison, 2007] R.S. Harrison, P.C. Sharpe, Y. Singh, D.P. Fairlie. Amyloid peptides and proteins in review. Rev Physiol Biochem Pharmacol 159: 1-77, 2007.

[Crick, 1953] F.H.C. Crick. The packing of alpha-helices: simple coiled-coils. Acta Crystallogr 6: 689-697, 1953.

[Feverati, 2010] G. Feverati, C. Lesieur. Oligomeric interfaces under the lens: Gemini. PLoS ONE 5(3): e9897, 2010.

[Zrimi, 2010] J. Zrimi, A. Ng Ling, E. Giri-Rachman Arifint, G. Feverati, C. Lesieur. Cholera toxin B subunits assemble into pentamers: proposition of a fly-casting mechanism. Plos One 5(12) e15347, 2010.

[Feverati, 2012] G. Feverati, M. Achoch, J. Zrimi, L. Vuillon, C. Lesieur. β-strand interfaces of non-dimeric protein oligomers are characterized by scattered charge residues pattern. PLoS ONE 7(4): e32558, 2012.

[Janin, 2008] J. Janin, R.P. Bahadur, P. Chakrabarti. Protein-protein interaction and quaternary structure. Q Rev Biophys 41: 133-180, 2008.

Authors' Information

Giovanni Feverati *- LAPTH, University of Savoie, CNRS, BP: 110, Annecy-le-Vieux 74941, France; e-mail: feverati@lapp.in2p3.fr*
Major Fields of Scientific Research: Mathematical physics, theoretical biophysics, models of Darwinian evolution, models of protein assembly.

Claire Lesieur *- AGIM, University of Grenoble, CNRS, Archamps, France;*
e-mail: claire.lesieur@agim.eu
Major Fields of Scientific Research: Biophysics, protein assembly, kinetics, dynamics, interfaces.

Laurent Vuillon *- LAMA, University of Savoie, CNRS, Le Bourget du lac, France;*
e-mail: Laurent.Vuillon@univ-savoie.fr
Major Fields of Scientific Research: discrete mathematics, combinatorics, discrete dynamical systems.

INTERVALS AS ULTRAMETRIC APPROXIMATIONS ACCORDING TO THE SUPREMUM NORM

Bernard Fichet

Abstract: *Given two distances d and d' defined on a finite set I, with $d \leq d'$, we characterise the set of all ultrametrics lying between d and d' (if any), showing they are the union of finitely many intervals with a common top endpoint, the subdominant ultrametric of d'. We also provide an algorithm to compute the bottom of any interval, given by any upperminimal ultrametric of d less than d'. A series of approximations according to the supremum norm derive from this.*

Keywords: *ultrametric, subdominant ultrametric, upperminimal ultrametrics, approximation, supremum norm*

MSC*: G3: Statistics*

Given a dissimilarity (or a distance) d defined on a finite set I, we here propose an algorithm for computing an upperminimal ultrametric d^* of d bounded by a fixed dissimilarity d' (if any), so yielding a solution of the sandwich problem : find an ultrametric lying between d and d' (we recall that an ultrametric u on I obeys the ultrametric inequality: $u(i,j) \leq max[u(i,k), u(j,k)]$ for all i, j, k in I).

As observed by Chepoi and Fichet (2000), the latter problem admits a very simple characterisation via a subdominant approximation. Namely, the subdominant ultrametric d'_* of d' is (the greatest) solution, provided that it is greater than d (a contrario, there is no solution). Moreover, it is well known that there are efficient algorithms for computing a subdominant, such as the one defined by the single linkage procedure.

Similar results hold with upperminimal ultrametric approximations of d: the sandwich problem has a solution if and only if there is an upperminimal ultrametric of d which is less than d'. We recall that, as opposed to the subdominant which is the best lower approximation, there are finitely many best upper approximations, the upperminimal ultrametrics of d. The complete linkage algorithm builds a particular approximation (several in case of ties), but it was not before the eighties that some dividing procedures compute any of them (Van Cutsem (1984), Leclerc (1986)).

Our algorithm extends the latter ones, in order to satisfy the boundary constraint. It is recursive and (formally) depicts all the solutions (if any). It involves a so-called d-admissibility condition of a given partition of I, and a threshold graph G associated with d'. At a given step, we know whether there is no solution, or there is a possible one related to a new minimal partition less than the one given by the connected components of G.

Thus, the set of solutions of the sandwich problem appears as the finite union of intervals of the type $[d^*, d'_*]$, with common top endpoint d'_*. A series of derivative problems may be solved by this way, such as :

· Characterising all ultrametrics at a least supremum norm of d and d', $d \leq d'$, so recovering the results of (Chepoi-Fichet, 2000), and (Farach et al., 1995).

· Given d, find the minimum $\lambda \geq 1$, such that there is an ultrametric lying between $(1/\lambda)\, d$ and λd.

· Given a partial dissimilarity d, characterising all ultrametric extensions of d.

Authors' Information

Bernard Fichet *- Aix-Marseille University. Laboratoire d'Informatique Fondamentale. bernard.fichet@lif.univ-mrs.fr*

DISTANCES ON ANTIMATROIDS

Yulia Kempner, Vadim E. Levit

Abstract: *An antimatroid is an accessible set system $(U, \mathcal{F})$ closed under union. Every antimatroid may be represented as a graph whose vertices are sets of $\mathcal{F}$, where two vertices are adjacent if the corresponding sets are differ by one element. This graph is a partial cube. Hence an antimatroid with the ground set U of size n may be isometrically embedded into the hypercube $\{0,1\}^n$. Thus the distance on an antimatroid considered as a graph coincides with the Hamming distance. A poset antimatroid is an antimatroid, which is formed by the lower sets of a poset. We consider different definitions of the distance between elements of an antimatroid, and give a new characterization of poset antimatroids.*

Keywords: *antimatroid, partial cube, zigzag distance, Hamming distance.*

ACM Classification Keywords*: G.2*

MSC*: 05C12; 52B40*

Introduction

An antimatroid is an accessible set system closed under union. There are two equivalent definitions of antimatroids, one as set systems and the other as languages [Korte et al., 1991]. An algorithmic characterization of antimatroids based on the language definition was introduced in [Boyd & Faigle, 1990]. Later, another algorithmic characterization of antimatroids which depicted them as set systems was developed in [Kempner & Levit, 2003]. Antimatroids can be viewed as a special case of either greedoids or semimodular lattices, and as a generalization of partial orders and distributive lattices. While classical examples of antimatroids connect them with posets, chordal graphs, convex geometries etc., [Glasserman & Yao, 1994] used antimatroids to model the ordering of events in discrete event simulation systems. In mathematical psychology, antimatroids are used to describe feasible states of knowledge of a human learner [Eppstein et al., 2008]. There are also rich connections between antimatroids and cluster analysis [Kempner & Muchnik, 2003].

Let U be a finite set. A *set system* over U is a pair $(U, \mathcal{F})$, where $\mathcal{F}$ is a family of sets over U, called *feasible* sets.

Definition 1. *[Korte et al., 1991] A finite non-empty set system $(U, \mathcal{F})$ is an antimatroid if $(A1)$ for each non-empty $X \in \mathcal{F}$, there exists $x \in X$ such that $X - x \in \mathcal{F}$*

$(A2)$ for all $X, Y \in \mathcal{F}$, and $X \not\subseteq Y$, there exists $x \in X - Y$ such that $Y \cup x \in \mathcal{F}$.

Any set system satisfying $(A1)$ is called *accessible.*

Proposition 2. *[Korte et al., 1991] For an accessible set system $(U, \mathcal{F})$ the following statements are equivalent:*

(i) $(U, \mathcal{F})$ is an antimatroid

(ii) $\mathcal{F}$ is closed under union ($X, Y \in \mathcal{F} \Rightarrow X \cup Y \in \mathcal{F}$)

A set system $(U, \mathcal{F})$ satisfies the *chain property* [Kempner & Levit, 2010] if for all $X, Y \in \mathcal{F}$, and $X \subset Y$, there exists a chain $X = X_0 \subset X_1 \subset ... \subset X_k = Y$ such that $X_i = X_{i-1} \cup x_i$ and $X_i \in \mathcal{F}$ for $0 \leq i \leq k$.

It is easy to see that this chain property follows from $(A2)$, but these properties are not equivalent. Examples of chain systems include antimatroids, convex geometries, matroids and other hereditary systems (matchings, cliques, independent sets, etc.).

Definition 3. *[Korte et al., 1991] The set system $(U, \mathcal{F})$ is a poset antimatroid if U is the set of elements of a finite partially ordered set (poset) P and $\mathcal{F}$ is a family of lower sets of P. The maximal chains in the corresponding poset antimatroid are the linear extension of P.*

A game theory gives a framework, in which poset antimatroids are considered as permission structures for coalitions [Algaba et al., 2004]. The poset antimatroids can be characterized as the unique antimatroids which are closed under intersection [Korte et al., 1991]. The feasible sets in a poset antimatroid ordered by inclusion form a distributive lattice, and any distributive lattice can be built in this way. Thus, antimatroids can be seen as generalizations of distributive lattices.

Distance on graphs and antimatroids

Definition 4. *For each graph $G = (V, E)$ the distance $d_G(u, v)$ between two vertices $u, v \in V$ is defined as the length of a shortest path joining them.*

Definition 5. *If G and H are arbitrary graphs, then a mapping $f : V(G) \to V(H)$ is an isometric embedding if $d_H(f(u), f(v)) = d_G(u, v)$ for any $u, v \in V(G)$.*

Let $U = \{x_1, x_2, ...x_n\}$. Define a graph $H(U)$ as follows: the vertices are the finite subsets of U, two vertices A and B are adjacent if and only if the symmetric difference $A \triangle B$ is a singleton set. Then $H(U)$ is the *hypercube Q_n on U* [Djokovic,1973]. The hypercube can be equivalently defined as the graph on $\{0, 1\}^n$ in which two vertices form an edge if and only if they differ in exactly one position. The shortest path distance $d_H(A, B)$ on the hypercube $H(U)$ is the Hamming distance between A and B that coincides with the symmetric difference distance: $d_H(A, B) = |A \triangle B|$. A graph G is called a *partial cube* if it can be isometrically embedded into a hypercube $H(U)$ for some set U.

Definition 6. *[Doignon & Falmagne, 1997] A family of sets $\mathcal{F}$ is well-graded if any two sets $P, Q \in \mathcal{F}$ can be connected by a sequence of sets $P = R_0, R_1, ..., R_n = Q$ formed by single-element insertions and deletions ($|R_i \triangle R_{i+1}| = 1$), such that all intermediate sets in the sequence belong to $\mathcal{F}$ and $|P \triangle Q| = n$.*

Any set system $(U, \mathcal{F})$ defines a graph $G_{\mathcal{F}} = (\mathcal{F}, E_{\mathcal{F}})$, where $E_{\mathcal{F}} = \{\{P, Q\} \in \mathcal{F} : |P \triangle Q| = 1\}$.

Since a family $\mathcal{F}$ of every antimatroid $(U, \mathcal{F})$ is well-graded, each antimatroid is a partial cube ([Ovchinnikov, 2008]) and may be represented as a graph $G_{\mathcal{F}}$ that is a subgraph of the hypercube $H(U)$. Thus the distance on an antimatroid $(U, \mathcal{F})$ considered as a graph coincides with the Hamming distance between sets, i.e. $d_{\mathcal{F}}(A, B) = |A \triangle B|$ for any $A, B \in \mathcal{F}$.

Poset antimatroids and zigzag distance

For an antimatroid $(U, \mathcal{F})$ denote $C_k = \{X \in \mathcal{F} : |X| = k\}$ a family of feasible sets of cardinality k. A *lower zigzag* is a sequence of feasible sets $P_0, P_1, ..., P_{2m}$ such that any two consecutive sets in the sequence differ by a single element and $P_{2i} \in C_k$, and $P_{2i-1} \in C_{k-1}$ for all $0 \leq i \leq m$. In the same way we define an *upper zigzag* in which $P_{2i-1} \in C_{k+1}$. Each zigzag $P_0, P_1, ..., P_{2m}$ is a path connecting P_0 and P_{2m}, and so the distance on the zigzag $d(P_0, P_{2m}) = 2m$ is always no less than the distance $d_{\mathcal{F}}(P_0, P_{2m})$ on an antimatroid $(U, \mathcal{F})$.

Figure 1(a) shows two sets ($A = \{1, 2, 3, 5\}$ and $B = \{1, 3, 4, 5\}$) that are connected by a lower zigzag, such that the distance on the zigzag is 4, while $|A \triangle B| = 2$. Note, that the distance on the upper zigzag is indeed 2. For two sets $X = \{1, 2, 5\}$ and $B = \{3, 4, 5\}$ the distance on the lower zigzag and on the upper zigzag is equal to 6, while $|X \triangle Y| = 4$. In order that the distance on zigzags be equal to the distance on an antimatroid, the antimatroid have to be poset antimatroid. This property gives a new characterization of poset antimatroids.

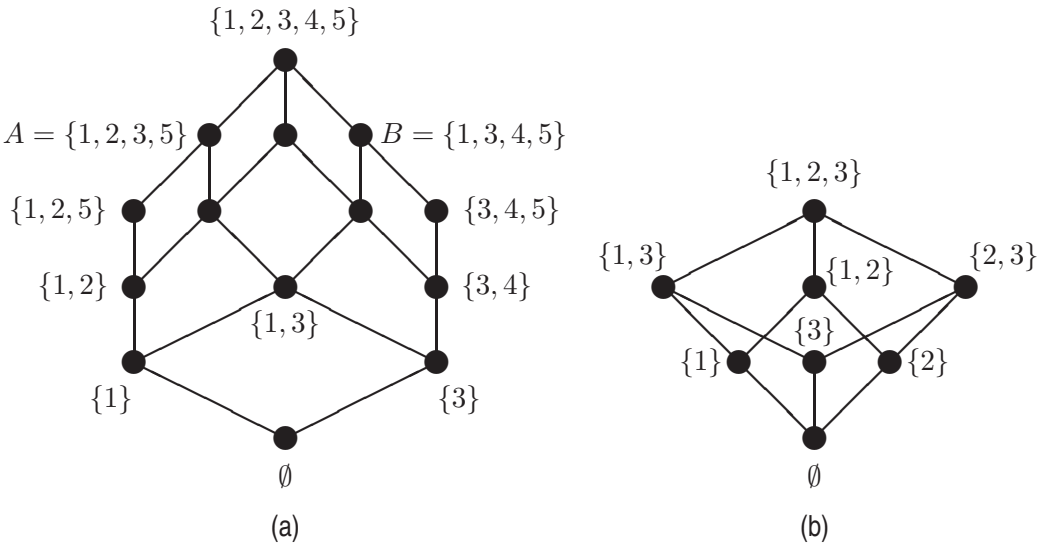

Figure 1: (a) An antimatroid without distance preserving zigzags and (b) a poset antimatroid without total distance preserving zigzags.

Theorem 7. *An antimatroid $(U, \mathcal{F})$ is a poset antimatroid if and only if every two feasible sets A, B of the same cardinality k can be connected by a lower and by an upper zigzags such that the distance between these sets $d_{\mathcal{F}}(A, B)$ coincides with the distance on the zigzags.*

Proof. The proof of the sufficiency may be found in [Kempner & Levit, 2012]. To prove the necessity we show that the antimatroid $(U, \mathcal{F})$ is closed under intersection, i.e., for each $A, B \in \mathcal{F}$ the set $A \cap B \in \mathcal{F}$. If $A \subseteq B$ or $B \subseteq A$ the statement is obvious. So we consider only incomparable sets. We use induction on $d_{\mathcal{F}}(A, B)$.

If $d_{\mathcal{F}}(A, B) = 1$ then the sets are comparable, so we begin from $d_{\mathcal{F}}(A, B) = 2$. Since the sets are incomparable, we have $A = (A \cap B) \cup a$ and $B = (A \cap B) \cup b$. So the lower distance preserving zigzag connecting A and B must go via $A \cap B$, i.e., $A \cap B \in \mathcal{F}$.

Let $d_{\mathcal{F}}(A, B) = m$. If $|A| = |B|$ then there is a distance preserved lower zigzag connecting A with B. Hence there is $a \in A - B$ such that $A - a$ belongs to the zigzag, and $b \in B - A$ with $B - b$ on the zigzag, such that $d_{\mathcal{F}}(A - a, B - b) = |A \triangle B| - 2 = m - 2$. By the induction hypothesis $(A - a) \cap (B - b) = A \cap B \in \mathcal{F}$.

Let $|A| < |B|$. The definition of an antimatroid $(A2)$ implies that there exists $b \in B - A$ such that $A \cup b \in \mathcal{F}$. Since $d_{\mathcal{F}}(A \cup b, B) = d_{\mathcal{F}}(A, B) - 1$, by the induction hypothesis $(A \cup b) \cap B = (A \cap B) \cup b \in \mathcal{F}$. Since $A \nsubseteq B$ and $|A| < |B|$, then $1 \leq |A - B| < |B - A|$. Hence $d_{\mathcal{F}}(A, (A \cap B) \cup b) = |A - (A \cap B)| + 1 = |A - B| + 1 < |A - B| + |B - A| = d_{\mathcal{F}}(A, B)$. By the induction hypothesis $A \cap ((A \cap B) \cup b) = A \cap B \in \mathcal{F}$. □

Note that if for a zigzag $P_0, P_1, ..., P_{2m}$ the distance on the zigzag $d(P_0, P_{2m}) = 2m = d_{\mathcal{F}}(P_0, P_{2m}) = |P_0 \triangle P_{2m}|$ then the zigzag preserves the distance for each pair P_i, P_j, i.e., $d_{\mathcal{F}}(P_i, P_j) = d(P_i, P_j) = |j - i|$.

For poset antimatroids there are distance preserving zigzags connecting two given sets, but these zigzags are not obliged to connect all feasible sets of the same cardinality. In Figure 1(b) we can see that there is a poset antimatroids, for which it is not possible to build a distance preserving zigzag connecting all feasible sets of the same cardinality. To characterize the antimatroids with total distance preserving zigzag we introduce the following definitions.

Each antimatroid $(U, \mathcal{F})$ may be considered as a directed graph $G = (V, E)$ with $V = \mathcal{F}$ and $(A, B) \in E \Leftrightarrow \exists c \in B$ such that $A = B - c$. Denote *in-degree* of the vertex A as $deg_{in}(A) = |\{c : A - c \in \mathcal{F}\}|$, and *out-degree* as $deg_{out}(A) = |\{c : A \cup c \in \mathcal{F}\}|$. Consider antimatroids for which their maximum in-degree and maximum out-degree is at most p, and there is at least one feasible set for which in-degree or out-degree equals p. We will call such antimatroids *p-antimatroids*.

Theorem 8. *In p-antimatroid $(U, \mathcal{F})$ all feasible sets C_k of the same cardinality k can be connected by a lower zigzag and by an upper zigzag such that the distance between any two sets P_i, P_j in each zigzag coincides with distance on the zigzag $d(P_i, P_j) = |j - i|$ if and only if $p < 3$.*

The proof of the sufficiency may be found in [Kempner & Levit, 2012]. To prove the necessity let $(U, \mathcal{F})$ be a p-antimatroid with $p > 2$. Let the out-degree of some A be equal to p. Then there are some $a, b, c \in U$ such that $A \cup a, A \cup b, A \cup c \in \mathcal{F}$. So there is a sub-graph of $G_{\mathcal{F}}$ isomorphic to a cube (see Figure 1(b)), and hence it is not possible to build a distance preserving zigzag connecting all feasible sets of the same cardinality $k = |A| + 1$.

Bibliography

[Algaba et al., 2004] Algaba, E.; Bilbao, J.M.; van den Brink, R. & Jimenez-Losada A. (2004). Cooperative Games on Antimatroids. *Discrete Mathematics*, Vol.282, 1-15.

[Boyd & Faigle, 1990] Boyd, E.A. & Faigle, U. (1990). An Algorithmic Characterization of Antimatroids. *Discrete Applied Mathematics*, Vol.28, 197-205.

[Djokovic,1973] Djokovic, D.Z. (1973). Distance Preserving Subgraphs of Hypercubes. *J. Combin. Theory Ser.B*, Vol.14, 263-267.

[Doignon & Falmagne, 1997] Doignon, J.-P. & Falmagne, J.-Cl. (1997). Well-graded Families of Relations. *Discrete Mathematics*, Vol.173, 35Ű44.

[Eppstein et al., 2008] Eppstein, D.; Falmagne, J.-Cl. & Ovchinnikov, S. (2008). *Media Theory: Interdisciplinary Applied Mathematics*, Springer-Verlag, Berlin.

[Glasserman & Yao, 1994] Glasserman, P. & Yao, D.D. (1994). *Monotone Structure in Discrete Event Systems*, Wiley Inter-Science, Series in Probability and Mathematical Statistics.

[Kempner & Levit, 2003] Kempner, Y. & Levit, V.E. (2003). Correspondence between Two Antimatroid Algorithmic Characterizations. *The Electronic Journal of Combinatorics*, Vol.10.

[Kempner & Levit, 2010] Kempner, Y. & Levit, V.E. (2010). Duality between quasi-concave functions and monotone linkage functions. *Discrete Mathematics*, Vol.310, 3211-3218.

[Kempner & Levit, 2012] Kempner, Y. & Levit, V.E. (2012). Poly-Dimension of Antimatroids. *New Frontiers in Graph Theory*, InTech, Available from: http://www.intechopen.com/books/new-frontiers-in-graph-theory/poly-dimension-of-antimatroids

[Kempner & Muchnik, 2003] Kempner, Y. & Muchnik, I. (2003). Clustering on Antimatroids and Convex Geometries, *WSEAS Transactions on Mathematics*, Vol.2, No.1, 54-59.

[Korte et al., 1991] Korte, B.; Lovász, L. & R. Schrader, R. (1991). *Greedoids*, Springer-Verlag, New York/Berlin.

[Ovchinnikov, 2008] Ovchinnikov, S. (2008). Partial cubes: Structures, Characterizations, and Constructions, *Discrete Mathematics*, Vol.308, 5597Ű5621.

Authors' Information

Yulia Kempner *- Department of Computer Science, Holon Institute of Technology, P.O. Box: 58102, Holon, Israel; e-mail: yuliak@hit.ac.il*
Major Fields of Scientific Research: Combinatorial Optimization

Vadim E. Levit *- Department of Computer Science and Mathematics, Ariel University Center of Samaria, Israel; e-mail: levitv@ariel.ac.il*
Major Fields of Scientific Research: Graph Theory

DISTANCE BETWEEN OBJECTS DESCRIBED BY PREDICATE FORMULAS

Tatiana Kosovskaya

***Abstract**: Functions defining a distance and a distinguish degree between objects described by predicate formulas are introduced. It is proved that the introduced function of distance satisfies all properties of a distance. The function of objects distinguish degree adequately reflects similarity of objects but does not define a distance because the triangle inequality is not fulfilled for it. The calculation of the introduced functions is based on the notion of partial deduction of a predicate formula.*

***Keywords**: artificial intelligence, pattern recognition, distance between objects, predicate calculus.*

***ACM Classification Keywords**: I.2.4 ARTIFICIAL INTELLIGENCE Knowledge Representation Formalisms and Methods – Predicate logic.*

***Conference topic**: Computer-related Distances.*

Introduction

A solution of an Artificial Intelligence (and pattern recognition) problem is often based on the description of an investigated object by means of global features which characterize the whole object but not its parts. In such a case a space of features appears and the distance between objects may be introduced in some natural way, for example, by the formula $\sum_i |x_i - y_i|^k$ for some natural k. In the case $k=1$ we deal with a well-known Hamming metric which is widely used in the information theory for comparison of the same length strings of symbols.

But how we can measure the distance between two objects described by some local features which characterize some parts of an object or relations between such parts? What is the distance between two identical images one of which is situated in the left upper corner of the screen and the second is in the right lower corner? Even if we use a monochrome screen with two degrees of lightness the distance calculated by the formula $\sum_i |x_i - y_i|$ will give the number of pixels in the image itself multiplied by two.

If we analyze a market situation with two participants A and B (the participants of the market are not ordered) with the feature values $(p^1_1, p^1_2,\ldots,p^1_n)$ and $(p^2_1, p^2_2,\ldots,p^2_n)$ then in the dependence of their order $((p^1_1, p^1_2,\ldots,p^1_n), (p^2_1, p^2_2,\ldots,p^2_n))$ or $((p^2_1, p^2_2,\ldots,p^2_n), (p^1_1, p^1_2,\ldots,p^1_n))$ we receive that these two situations are essentially different (the distance between them may be up to $2n$).

To recognize objects from the done set Ω every element of which is a set $\omega = \{\omega_1, \ldots, \omega_t\}$, a logic-objective approach was described in [Kosovskaya, 2007]. Such an approach consists in the following. Let the set of predicates $p_1, \ldots, p_n$ (every of which is defined on the elements of ω) characterizes properties of these elements and relations between them. Let the set Ω is a union of (may be intersected) classes $\Omega = \cup_{k=1}^{K} \Omega_k$.

Logical description $S(\omega)$ of the object ω is a collection of all true formulas of the form $p_i(\tau)$ or $\neg p_i(\tau)$ (where τ is an ordered subset of ω) describing properties of ω elements and relations between them.

Logical description of the class Ω_k is such a formula $A_k(\boldsymbol{x})$ that if the formula $A_k(\boldsymbol{\omega})$ is true then $\omega \in \Omega_k$. The class description always may be represented as a disjunction of elementary conjunctions of atomic formulas.

Here and below the notation $\boldsymbol{x}$ is used for an ordered list of the set x. To denote that all values for variables from the list $\boldsymbol{x}$ are different the notation $\exists \boldsymbol{x}_{\neq} A_k(\boldsymbol{x})$ will be used.

The introduced descriptions allow solving many artificial intelligence problems [Kosovskaya, 2011]. These problems may be formulated as follows. **Identification problem:** to check out such a part of the object ω which belongs to the class Ω_k. **Classification problem:** to find all such class numbers k that $\omega \in \Omega_k$. **Analysis problem:** to find and classify all parts τ of the object ω. The solution of these problems is reduced to the proof of predicate calculus formulas $S(\omega) \Rightarrow \exists \boldsymbol{x}_{\neq} A_k(\boldsymbol{x})$, $S(\omega) \Rightarrow \vee_{k=1}^{K} A_k(\boldsymbol{x})$, $S(\omega) \Rightarrow \vee_{k=1}^{K} \exists \boldsymbol{x}_{\neq} A_k(\boldsymbol{x})$.

The proof of every of these formulas is based on the proof of the sequent

$$S(\omega) \Rightarrow \exists \boldsymbol{x}_{\neq} A(\boldsymbol{x}), \quad (1)$$

where $A(\boldsymbol{x})$ is an elementary conjunction.

The notion of partial deduction was introduced by the author in [Kosovskaya, 2009] to recognize objects with incomplete information. In the process of partial deduction instead of the proof of (1) we search such a maximal sub-formula $A'(\boldsymbol{x}')$ of the formula $A(\boldsymbol{x})$ that $S(\omega) \Rightarrow \exists \boldsymbol{x}'_{\neq} A'(\boldsymbol{x}')$ and there is no information that $A(\boldsymbol{x})$ is not satisfiable on ω.

Let a and a' be the numbers of atomic formulas $A(\boldsymbol{x})$ and $A'(\boldsymbol{x}')$ respectively, m and m' be the numbers of objective variables in $A(\boldsymbol{x})$ and $A'(\boldsymbol{x}')$ respectively. Then partial deduction means that the object ω is an r-th part ($r = m'/m$) of an object satisfying the description $A(\boldsymbol{x})$ with the certainty $q = a'/a$.

More precisely, the formula $S(\omega) \Rightarrow \exists \boldsymbol{x}_{\neq} A(\boldsymbol{x})$ is partially (q,r)-deductive if there exists a maximal sub-formula $A'(\boldsymbol{x}')$ of the formula $A(\boldsymbol{x})$ such that $S(\omega) \Rightarrow \exists \boldsymbol{x}'_{\neq} A'(\boldsymbol{x}')$ is deducible and $\boldsymbol{\tau}$ is the string of values for the list of variables $\boldsymbol{x}'$, but the formula $S(\omega) \Rightarrow \exists \boldsymbol{x}_{\neq} [DA'(\boldsymbol{x})]^{\boldsymbol{x}'}_{\boldsymbol{\tau}}$ is not deducible. Here $[DA'(\boldsymbol{x})]^{\boldsymbol{x}'}_{\boldsymbol{\tau}}$ is obtained from $A(\boldsymbol{x})$ by deleting from it all conjunctive members of $A'(\boldsymbol{x}')$, substituting values of $\boldsymbol{\tau}$ instead of the respective variables of $\boldsymbol{x}'$ and taking the negation of the received formula.

The defined below distance between objects takes into account the non-coincidence of their descriptions as the Hamming metric. It may be calculated not only for descriptions with the same number of atomic formulas which are ordered in some natural way, but for such ones which are sets (not ordered) of an arbitrary finite power.

Distance and Distinguish Degree Between Objects

Let ω_0 and ω_1 be two objects with logical descriptions $S(\omega_0)$ and $S(\omega_1)$ respectively and $A_0(\boldsymbol{x}_0)$ and $A_1(\boldsymbol{x}_1)$ be elementary conjunctions constructed according to these logical descriptions by changing different constants by different variables and putting the sign & between the atomic formulas. It is evident that $S(\omega_i) \Rightarrow \exists \boldsymbol{x}_{\neq} A_i(\boldsymbol{x}_i)$ i.e. ω_i satisfies the formula $A_i(\boldsymbol{x}_i)$ (for $i = 0, 1$). Let $A_i(\boldsymbol{x}_i)$ contains a_i atomic formulas and t_i variables.

Let us construct a partial deduction of a sequent $S(\omega_i) \Rightarrow \exists \boldsymbol{x}_{\neq} A_{1-i}(\boldsymbol{x})$ for every $i = 0,1$.

Let $A'_{i,1\text{-}i}(\mathbf{x}'_{i,1\text{-}i})$ be the maximal (under the number of variables) sub-formula of the formula $A_{1\text{-}i}(\mathbf{x}_{1\text{-}i})$ for which such a partial deduction exists.

Let the formula $A'_{i,1\text{-}i}(\mathbf{x}'_{i,1\text{-}i})$ contains $a'_{i,1\text{-}i}$ atomic formulas and $t'_{i,1\text{-}i}$ variables. Note that $A'_{01}(\mathbf{x}'_{01})$ and $A'_{01}(\mathbf{x}'_{10})$ coincide (up to the names of variables) and hence $a'_{01} = a'_{10}$. Let $\Delta a'_{i,1\text{-}i} = a_i - a'_{i,1\text{-}i}$. $\Delta a'_{01}$ is the number of non-coincidences of atomic formulas (up to the names of constants) in $S(\omega_0)$ with respect to $S(\omega_1)$.

Definition. The distance between objects ω_0 and ω_1 is the sum of the number of non-coincidences of atomic formulas (up to the names of constants)

$$\rho(\omega_0,\omega_1) = \Delta a'_{0,1} + \Delta a'_{1,0}.$$

Remember examples from the introduction. If the image on the display screen is described by a predicate $p(i,j,x)$ "pixel with the number (i,j) has the lightness x" then two identical images one of which is situated in the left upper corner of the screen and the second is in the right lower corner have the same (up to the names of constants) logical descriptions. Therefore the distance between them equals 0.

The logical description of two participants in the example with market participants is a set of atomic formulas $\{p_1(A), p_2(A),\ldots,p_n(A), p_1(B), p_2(B),\ldots,p_n(B)\}$ or $\{p_1(B), p_2(B),\ldots,p_n(B), p_1(A), p_2(A),\ldots,p_n(A)\}$ which are equal and the distance equals 0.

It is natural that in dependence of the chosen initial predicates the distance between objects may differ. Let's give an example of distance calculation between two contour images described by two predicate systems.

Example. Let we have two images A and B represented on the figures 1 and 2.

Consider two systems of initial predicates.

1. $V(x,y,z) \Leftrightarrow \measuredangle yxz < \pi$,

   $I(x,y,z,u,v) \Leftrightarrow$ "the vertex x is a point of intersection of segments $[y,z]$ and $[u,v]$.

In such a case every of the points $a_1, a_2, a_5, a_9, a_{10}$ is represented in $A_a(x_1,\ldots,x_{10})$ by one formula. For example, the point a_1 is represented in $A_a(x_1,\ldots,x_{10})$ by $V(x_1,x_6,x_3)$.

Every of the points $b_1, b_2, b_5, b_9, b_{10}$ is represented in $A_b(x_1,\ldots,x_{10})$ by six formulas. For example, the point b_1 is represented in $A_b(x_1,\ldots,x_{10})$ by $V(x_1,x_2,x_3)$, $V(x_1,x_3,x_4)$, $V(x_1,x_4,x_5)$, $V(x_1,x_2,x_4)$, $V(x_1,x_3,x_5)$, $V(x_1,x_2,x_5)$.

Every of the points a_3, a_4, a_6, a_7, a_8 (as well as b_3, b_4, b_6, b_7, b_8) is represented in $A_a(x_1,\ldots,x_{10})$ (and in $A_b(x_1,\ldots,x_{10})$) by five formulas. For example, the point a_3 is represented in $A_a(x_1,\ldots,x_{10})$ by $V(x_3,x_4,x_1)$, $V(x_3,x_1,x_2)$, $V(x_3,x_2,x_6)$, $V(x_3,x_6,x_4)$, $I(x_3,x_1,x_6,x_2,x_4)$. So, the formula $A_a(x_1,\ldots,x_{10})$ has 30 atomic formulas and the formula $A_b(x_1,\ldots,x_{10})$ has 55 atomic formulas.

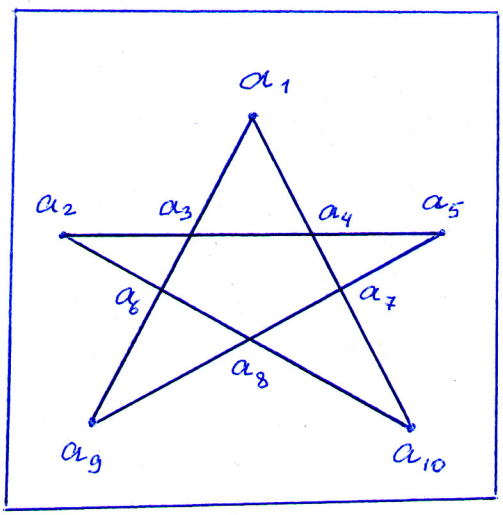

Fig. 1. Image *A*.

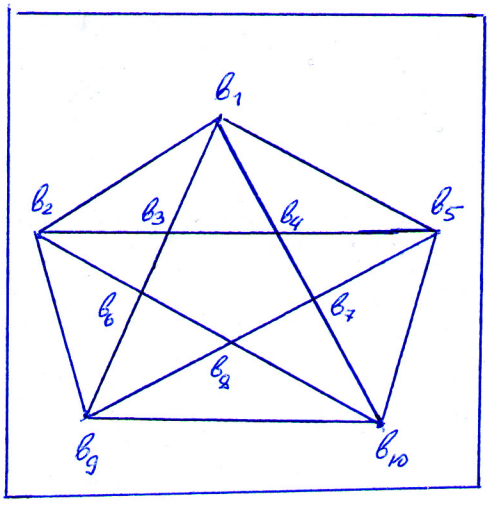

Fig. 2. Image *B*.

While construction partial deduction of $S(A) \Rightarrow \exists \boldsymbol{x}_{\neq}\, A_b(\boldsymbol{x}_b)$ all variables will receive some values but $A'_b(\boldsymbol{x}'_b)$ (coinciding with $A_a(\boldsymbol{x})$) contains only 30 atomic formulas. Hence $\Delta a'_{a,b} = 55 - 30 = 25$.

While construction partial deduction of $S(B) \Rightarrow \square\, \exists \boldsymbol{x}_{\neq}\, A_a(\boldsymbol{x}_a)$ all variables receive some values and all atomic formulas from $A_a(\boldsymbol{x}_a)$ are included into $A'_a(\boldsymbol{x}_a)$. Hence $\Delta a'_{a,b} = 0$.

In such a case $\rho(A,B) = 25 + 0 = 25$.

2. $E(x,y) \Leftrightarrow$ "x and y are adjacent".

This predicate describes not every point individually but a binary relation between them. As a fact we have a set of edges of a planar graph. The formula $A_a(x_1,\ldots,x_{10})$ has 15 atomic formulas and the formula $A_b(x_1,\ldots,x_{10})$ has 20 atomic formulas. While construction partial deductions of $S(A) \Rightarrow \exists \boldsymbol{x}_{\neq}\, A_b(\boldsymbol{x}_b)$ and $S(B) \Rightarrow \square\, \exists \boldsymbol{x}_{\neq}\, A_a(\boldsymbol{x}_a)$ it will be received that $\Delta a'_{a,b} = 20 - 15 = 5$, $\Delta a'_{b,a} = 0$. And $\rho(A,B) = 15$.

These examples demonstrate that besides the fact that different initial predicates provide different distances between objects; the value of the calculated distance does not illustrate the degree of their similarity. To overcome such a lack we may normalize the defined distance in order that it is not greater than 1. It may be done, for example, by dividing the distance by $a_0 + a_1$.

Definition. The degree of distinction between the objects ω_0 and ω_1 is the sum of the number of non-coincidences of atomic formulas (up to the names of constants) divided by the sum of numbers of atomic formulas in elementary conjunctions $A_0(\boldsymbol{x}_0)$ and $A_1(\boldsymbol{x}_1)$

$$d(\omega_0,\omega_1) = (\Delta a'_{0,1} + \Delta a'_{1,0}) / (a_0 + a_1).$$

The distinction degrees between the objects A and B in the previous example are $d(A,B) = 25/55 \approx 0.45$ for the first set of predicates and $d(A,B) = 15/20 = 0.75$ for the second set of predicates.

Properties of the introduced functions

The introduced functions ρ and d have the following properties.

Property 1. For every objects ω_0 and ω_1 $\rho(\omega_0, \omega_1) \geq 0$ and $d(\omega_0, \omega_1) \geq 0$.

This property is an immediate consequence of definitions.

Property 2. If $\omega_0 = \omega_1$ then $\rho(\omega_0, \omega_1) = 0$ and $d(\omega_0, \omega_1) = 0$.

The proof is based on the fact that in such a case the descriptions objects ω_0 and ω_1 contain the same (up to the names of constants) formulas.

Property 3. If ω_0 is a proper subset of ω_1 then $\rho(\omega_0, \omega_1) > 0$ and $0 < d(\omega_0, \omega_1) < 1$.

Proof. As ω_0 is a proper subset of ω_1 so the elementary conjunction $A_0(\boldsymbol{x}_0)$ is a corollary (but not equivalent) of the formula $A_1(\boldsymbol{x}_1)$. Therefore $a_1 > a_0$, $a_1 > \Delta a'_{0,1} > 0$, $\Delta a'_{1,0} = 0$ and $\rho(\omega_0, \omega_1) = \Delta a'_{0,1} + \Delta a'_{1,0} = \Delta a'_{0,1} > 0$, $d(\omega_0, \omega_1) = (\Delta a'_{0,1} + \Delta a'_{1,0}) / (a_0 + a_1) = \Delta a'_{0,1} / a_1 < 1$.

Property 4. If ω_0 and ω_1 have no common (up to the names of constants) formulas in their descriptions then $\rho(\omega_0, \omega_1) = (a_0 + a_1)$ and $d(\omega_0, \omega_1) = 1$.

Proof. As ω_0 and ω_1 have no common (up to the names of constants) formulas in their descriptions so $A_0(\boldsymbol{x}_0)$ and $A_1(\boldsymbol{x}_1)$ also have no common atomic formulas and $a'_{0,1} = a'_{1,0} = 0$. Hence $\rho(\omega_0, \omega_1) = \Delta a'_{0,1} + \Delta a'_{1,0} = (a_0 - a'_{0,1}) + (a_1 - a'_{1,0}) = a_0 + a_1$ and. $\rho_n(\omega_0, \omega_1) = \rho(\omega_0, \omega_1) / (a_0 + a_1) = (a_0 + a_1)/(a_0 + a_1) = 1$.

Property 5. If ω_0 and ω_1 have common (up to the names of constants) formulas in their descriptions but neither of them is a part of the other then $\rho(\omega_0, \omega_1) > 0$, $0 < d(\omega_0, \omega_1) < 1$.

This property is evident.

Theorem 1.

Function ρ defines a distance between objects. I.e. it satisfies the properties of distance:

1. for every objects ω_0 and ω_1 $\rho(\omega_0, \omega_1) \geq 0$;
2. for every objects ω_0 and ω_1 $\rho(\omega_0, \omega_1) = \rho(\omega_1, \omega_0)$;
3. $\omega_0 = \omega_1$ if and only if $\rho(\omega_0, \omega_1) = 0$;
4. triangle inequality is fulfilled for the function ρ, i.e. for every objects ω_1, ω_2 and ω_3 $\rho(\omega_1, \omega_2) + \rho(\omega_2, \omega_3) \geq \rho(\omega_1, \omega_3)$.

Proof. Points 1 and 2 are direct corollaries of the definition of ρ. Point 3 follows from the properties 2 – 5. Let's prove the triangle inequality.

Let $\omega_1, \omega_2, \omega_3$ be objects which descriptions have a_1, a_2, a_3 atomic formulas respectively. $a'_{1,2}$, $a'_{2,3}$, $a'_{3,1}$ are the numbers of atomic formulas contained respectively in maximal sub-formulas $A'_1(\boldsymbol{x}'_1)$, $A'_2(\boldsymbol{x}'_2)$, $A'_3(\boldsymbol{x}'_3)$ obtained while partial deduction of the respective sequents.

Let δ be the number of atomic formulas coinciding (up to the names of variables) simultaneously in $A'_1(x'_1)$, $A'_2(x'_2)$, $A'_3(x'_3)$; a^-_i be the number of atomic formulas which do not take part in partial derivations of $S(\omega_i) \Rightarrow \exists \boldsymbol{x}_{\neq} A_j(\boldsymbol{x}_j)$ $(j = 1, 2, 3, i \neq j)$; $a'_{1,2} = a''_{1,2} + \delta$, $a'_{2,3} = a''_{2,3} + \delta$, $a'_{3,1} = a''_{3,1} + \delta$.

Then

$$a_1 = a^-_1 + a''_{1,2} + a''_{1,3} + \delta,$$

$$a_2 = a^-_2 + a''_{1,2} + a''_{2,3} + \delta,$$

$$a_1 = a^-_1 + a''_{1,2} + a''_{1,3} + \delta,$$

$$a_2 = a^-_2 + a''_{1,2} + a''_{2,3} + \delta,$$

$$a_3 = a^-_3 + a''_{1,3} + a''_{2,3} + \delta.$$

$$\rho(\omega_1, \omega_2) + \rho(\omega_2, \omega_3) = (a_1 - a'_{1,2}) + (a_2 - a'_{1,2}) + (a_2 - a'_{2,3}) + (a_3 - a'_{2,3}) =$$

$$= (a^-_1 + a''_{1,3}) + (a^-_2 + a''_{2,3}) + (a^-_2 + a''_{1,2}) + (a^-_3 + a''_{1,3}).$$

$$\rho(\omega_1, \omega_3) = (a_1 - a'_{1,3}) + (a_3 - a'_{1,3}) = (a^-_1 + a''_{1,2}) + (a^-_3 + a''_{2,3}).$$

The reminder after subtraction of these expressions is $\rho(\omega_1, \omega_2) + \rho(\omega_2, \omega_3) - \rho(\omega_1, \omega_3) = 2a^-_2 + 2a''_{1,3} \geq 0.$

The triangle inequality is proved. The theorem is proved.

Theorem 2.

Function d does not define a distance. It does not satisfy the triangle inequality but satisfies the properties

1. for every objects ω_0 and ω_1 $d(\omega_0, \omega_1) \geq 0$;
2. for every objects ω_0 and ω_1 $d(\omega_0, \omega_1) = d(\omega_1, \omega_0)$;
3. $\omega_0 = \omega_1$ if and only if $d(\omega_0, \omega_1) = 0$.

Proof. Fulfillment of points 1 – 3 is a corollary of such properties for the function ρ.

Let's give an example of such objects ω_1, ω_2 and ω_3 that $d(\omega_1, \omega_2) + d(\omega_2, \omega_3) < d(\omega_1, \omega_3)$.

Let ω_1 be a proper part of ω_2 (hence $a'_{1,2} = a_1$) and $(a_2 - a'_{1,2}) = 0.1\, a_1$ (i.e. $a_2 = 1.1\, a_1$). Then $d(\omega_1, \omega_2) = (a_2 - a'_{1,2})/(a_1 + a_2) = 0.1\, a_1 / 1.1 a_1 = 0.1 / 1.1.$

Let also ω_1 has no common elements with ω_3. Then $d(\omega_1, \omega_3) = 1.$

Let all elements of ω_2 which does not belong ω_1 are elements of ω_3 and $a_3 - a'_{2,3} = a_1$ (i.e. $a_3 = a_1 + a'_{2,3} = 1.1\, a_1$). Then $d(\omega_2, \omega_3) = (a_3 - a'_{2,3})/(a_2 + a_3) = a_1 / 2.1\, a_1 = 1/ 2.1.$

$d(\omega_1, \omega_2) + d(\omega_2, \omega_3) = 0.1/1.1 + 1/ 2.1 \approx 0.09 + 0.043 = 0.133 < 1 = d(\omega_1, \omega_3).$

Conclusion

The presence of a metric between objects involved in an Artificial Intelligence problem allows to state an earlier investigated object which is the mostly similar to the given for investigation one. Algorithms based on the principle “the nearest neighbor” are well-known in pattern recognition, particularly in the training of a neural network.

But usual metrics used in Artificial Intelligence problems are metrics in the fixed-dimensional spaces. This dimension equals to the number of features which describe an object. Usually an object is considered as a single indivisible unit and such a feature is its global characteristic.

If an object is considered as a set of its parts and the features describe properties of its elements and relations between them, then we can't map an object into a fixed-dimensional space. Such descriptions may be simulated by discrete features but the number of such features exponentially depends of the number of elements in the largest object under consideration [Russel, 2003].

Hence, the introduction of a metric for comparison of objects considered as a set of their elements is an important direction in the development of Artificial Intelligence.

Bibliography

[Kosovskaya, 2007] T.M. Kosovskaya. Proofs of the number of steps bounds for solving of some pattern recognition problems with logical description. In: Vestnik of St.Petersburg University. Ser. 1. 2007. No. 4. P. 82 – 90. (In Russian)

[Kosovskaya, 2009] T.M. Kosovskaya. Partial deduction of a predicate formula as an instrument for recognition of an object with incomplete description. In: Vestnik of St.Petersburg University. Ser. 10. 2009. No. 1. P. 77 – 87. (In Russian)

[Kosovskaya, 2011] Kosovskaya T. Discrete Artificial Intelligence Problems and Number of Steps of their Solution // International Journal "Information Theories and Applications", Vol. 18, Number 1, 2011. P. 93 – 99.

[Russel, 2003] S.J.Russel and P.Norvig. Artificial Intelligence. A Modern Approach. Pearson Education, Inc. 2003. ISBN 0-13-790396-2.

Authors' Information

Tatiana Kosovskaya *– Dr., Senior researcher, St. Petersburg Institute of Informatics and Automation of Russian Academy of Science, 14 line, 39, St. Petersburg, 199178, Russia; Professor of St. Petersburg State Marine Technical University, Lotsmanskaya ul., 3, St. Petersburg, 190008, Russia; Professor of St. Petersburg State University, University av., 28, Stary Petergof, St. Petersburg, 198504, Russia, e-mail: kosov@NK1022.spb.edu*

Major Fields of Scientific Research: Logical approach to artificial intelligence problems, theory of complexity of algorithms.

The paper is published with financial support of the project ITHEA XXI of the Institute of Information Theories and Applications FOI ITHEA (www.ithea.org) and the Association of Developers and Users of Intelligent Systems ADUIS Ukraine (www.aduis.com.ua).

ON THE DISCRETIZATION OF DISTANCE GEOMETRY PROBLEMS

Antonio Mucherino, Carlile Lavor, Leo Liberti, Nelson Maculan

Abstract: *Distance geometry consists of finding an embedding of a weighted undirected graph in $\mathbb{R}^n$. Since some years, we are working on suitable discretizations for this problem. Because of the discretization, the search domain is reduced from a continuous to a discrete set which has the structure of a tree. Based on this combinatorial structure, we developed an efficient branch-and-prune (BP) algorithm for the solution of distance geometry problems. In this paper, we focus on two important aspects of the discretization: the identification of suitable vertex discretizing orderings and the analysis of the symmetries that can be found in BP trees.*

Keywords: *distance geometry, discretization, combinatorial optimization, discretizing orderings, symmetries.*

ACM Classification Keywords*: G.2.1 Combinatorics - Combinatorial algorithms; B.5.2 Design Aids - Optimization; J.3 Life and Medical Sciences - Biology and genetics;*

MSC*: 05C85, 90C27, 51K99.*

Introduction

The Distance Geometry Problem (DGP) is the problem of finding an embedding of a weighted undirected graph G in $\mathbb{R}^n$. Let $G = (V, E, d)$ be a weighted undirected graph representing an instance of the DGP, where each vertex $v \in V$ corresponds to a point x_v in $\mathbb{R}^n$, and there is an edge between two vertices if and only if their relative distance is known (the weight associated to the edge). That is, the DGP is the problem of finding a function

$$x : V \longrightarrow \mathbb{R}^n$$

such that

$$\forall (u, v) \in E \qquad || x_u - x_v || = d(u, v), \tag{1}$$

where $x_u = x(u)$ and $x_v = x(v)$. In its basic form, the DGP is a constraint satisfaction problem, because a set of coordinates x_v must be found that satisfies the constraints (1). In the problem definition, the symbol $|| \cdot ||$ represents the computed distance between x_u and x_v, whereas $d(u, v)$ refers to the known distances. The DGP is NP-hard Saxe [1979].

The DGP has various interesting applications. An example is given by the problem of identifying sensors in telecommunication networks Biswas et al. [2006]; Krislock [2010]. The distances between pairs of sensors can be estimated by the time needed for a two-way communication, and such distances can be exploited for identifying the position in space of each sensor. In this application, some sensors are fixed (they are called *anchors* in this domain) and the dimension of the space is usually $n = 2$.

A very interesting application arises in the field of biology. Experiences of Nuclear Magnetic Resonance (NMR) are able to estimate distances between some pairs of atoms of a molecule. Such distances, therefore, can be used for defining a DGP, whose solutions correspond to the set of conformations for the molecules that satisfy all given distances. In this context, the DGP is referred to as Molecular DGP (MDGP) Crippen et al. [1988]; Havel [1995]. This problem is particularly interesting for molecules such as proteins, because the conformation of the protein can provide clues about its function. MDGPs are DGPs in three-dimensional spaces ($n = 3$).

The basic approach to the DGP is to reformulate it as a continuous global optimization problem, where a penalty function is employed in order to measure the satisfaction of the constraints based on the known distances. Many methods and algorithms have been proposed for the solution of this optimization problem, and most of them are

based on a search in a continuous space, and/or on heuristic approaches to optimization. Recent surveys on this topic can be found in Liberti et al. [2010] and Lavor et al. [2012c].

We are working on suitable discretizations of the DGP, which are possible when some assumptions are satisfied. We give in the following the definition of two classes of DGPs that can be discretized.

The Discretizable MDGP (DMDGP) Lavor et al. [2012b]

Supposing there is a *total order relation* on the vertices of V, the DMDGP consists of all the instances of the MDGP satisfying the two assumptions:

A1 E contains all cliques on quadruplets of consecutive vertices;

A2 the triangular inequalities

$$\forall v \in \{1, \ldots, |V| - 2\} \quad d(v, v+2) < d(v, v+1) + d(v+1, v+2)$$

must hold strictly.

The Discretizable DGP (DDGP) Mucherino et al. [2012]

Supposing there is a *partial order relation* on the vertices of V, the DDGP consists of all the instances of the DGP satisfying the two assumptions:

B1 there exists a subset V_0 of V such that

- $|V_0| = 4$;
- the order relation on V_0 is total;
- V_0 is a clique;
- $\forall v_0 \in V_0 \quad \forall v \in V \setminus V_0, \quad v_0 < v$.

B2 $\forall v \in V \setminus V_0, \exists\, u^1, u^2, u^3 \in V$ such that:

- $u^1 < v, u^2 < v, u^3 < v$;
- $\{(u^1, v), (u^2, v), (u^3, v)\} \in E$;
- $d(u^1, u^3) < d(u^1, u^2) + d(u^2, u^3)$.

Note that we removed the word *Molecular* in the definition of the DDGP, because this is a more general problem and not necessarily related to protein molecules. We proved that DMDGP $\subset$ DDGP.

The idea behind the discretization is that the intersection among three spheres in the three-dimensional space can produce, with probability 1, at most two points in the hypothesis in which their centers are not aligned. Consider four vertices u^1, u^2, u^3 and v. If the coordinates for u^1, u^2 and u^3 are known, as well as the distances $d(u^1, v)$, $d(u^2, v)$ and $d(u^3, v)$, then the three spheres can be defined, and their intersection provides the two possible positions in the space for the last vertex v. In the hypothesis of the DMDGP, the four vertices u^1, u^2, u^3 and v are consecutive in the ordering associated to V. In the DDGP, this condition is relaxed, so that the three vertices u^1, u^2, u^3 only have to precede v. In both cases, if the vertices u^1, u^2 and u^3 are already placed somewhere, there are only two possible positions for v.

This suggests a recursive search on a binary tree containing the potential coordinates for the vertices of G. The Branch & Prune (BP) algorithm Liberti et al. [2008] is an exact algorithm which is based on a search on this tree. The binary tree of possible solutions (to which we will also refer as "BP tree") is explored starting from its top, where

the first vertex is positioned, and by placing one vertex per time. At each step, two possible positions for the current vertex v are computed, and two new branches are added to the tree. As a consequence, the size of the binary tree can get very large quite quickly, but the presence of additional distances (not employed in the construction of the tree) can help in verifying the feasibility of the computed positions. To this aim, we consider pruning devices: as soon as a position is found to be infeasible, the corresponding branch can be pruned and the search can be backtracked. We noticed that protein-like instances contain a sufficient number of distances that can be used in the BP pruning phase, so that the complete set of solutions can be found very efficiently Liberti et al. [2011a]. The strong point of the BP algorithm is given by the possibility to enumerate all solutions to a given D(M)DGP.

Solutions to the DMDGP or to the DDGP can be represented as a complete path on the BP tree, from the root (the node associated to the first vertex) to one of the leaf nodes (corresponding to the last vertex). Layer by layer, this path shows all branches associated to the solution: in particular, it shows the selected branches on each layer of the tree. Since only two branches (related to the two positions of the sphere intersection) can be chosen at each layer based on the preceding branches that were already selected, this information can be coded as a binary variable. A solution can therefore be also represented as a binary vector of length $|V|$. If we associate an ordering to the branches having the same root on the previous layer, we can say that each binary variable indicates if the "first" or the "second" branch is selected, or if the "left" or the "right" branch is selected (see Figure 3 for a graphical representation).

In both DMDGP and DDGP, the ordering in which the vertices of G are considered is of fundamental importance. As widely discussed in Mucherino et al. [2012], an instance may or may not satisfy the assumptions for the discretization depending on this ordering. Supposing we have an instance with a predefined ordering for its vertices for which the discretization is not possible, a suitable rearrangement of these vertices may transform the instance in a discretizable instance. Since DMDGP $\subset$ DDGP, this task is, in general, easier for the DDGP.

The problem of sorting the vertices of a graph in order to satisfy certain conditions can be seen as a combinatorial optimization problem. We developed an efficient greedy algorithm for the solution of this problem Lavor et al. [2012a] (for the DDGP), but in the easier case in which all distances are supposed to be exact. Especially in the field of biology, distances are not precisely known, but rather approximations of such distances are available. Since the discretization is still possible if only one of the three reference distances (for both DMDGP and DDGP) is represented by an interval (which gives the uncertainty on the value of the distance), discretization orderings must take this condition into consideration.

Another interesting feature of DMDGPs and DDGPs is given by the definition of BP trees that are symmetric. This implies the possibility to reduce the search on a subset of branches of the tree. If one or more solutions are identified in this subset of branches, other solutions can be reconstructed by applying symmetry rules. As a consequence, the study of the symmetries present in BP trees is essential for improving the algorithm. This is particularly important for instances containing uncertain data, where such an uncertainty makes the computational cost higher.

In this paper, we focus our attention on these two important aspects of the DGP discretization: the identification of suitable vertex discretizing orderings, and the analysis of the symmetries that can be found in BP trees. We will devote the next two session to these two topics. Conclusions will be drawn in the last session.

Discretization orderings

Let $G = (V, E, d)$ be a weighted undirected graph representing an instance of the DGP. As mentioned in the Introduction, the ordering given to the vertices in V plays a very important role in the discretization. There exist indeed orderings for which neither the assumptions for the DMDGP nor the ones for the DDGP can be satisfied. Moreover, there can be orderings for which G represents an instance of the DDGP which is not in the DMDGP class. If the assumptions for the DMDGP are satisfied (**A1** and **A2**), then the assumptions for the DDGP are also satisfied (**B1** and **B2**) Mucherino et al. [2012].

We noticed the importance of the ordering associated to the vertex set V since the beginning of our work. Later, we studied the problem of finding suitable vertex orderings by solving a combinatorial optimization problem and we found an efficient solution for the DDGP Lavor et al. [2012a]. In this work, however, we supposed that all available

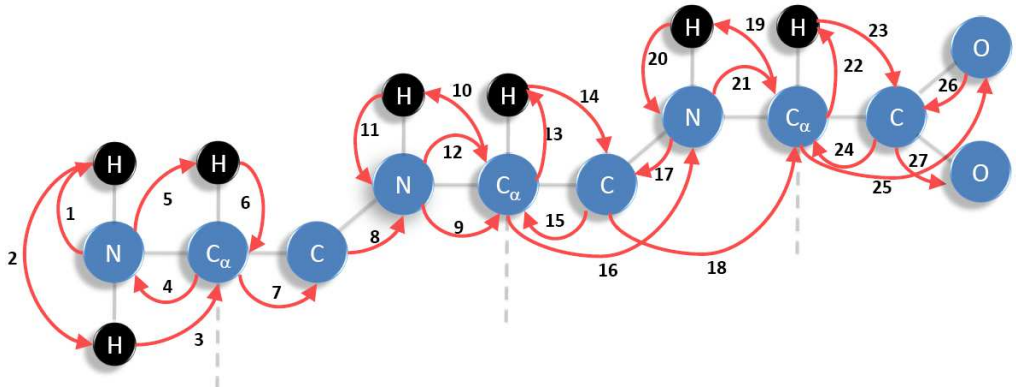

Figure 1: The hand-crafted artificial ordering r_{PB}.

distances were exact, while real-life instances usually contain a percentage of distances whose values are subject to uncertainty. In the field of biology, distances obtained by NMR are commonly represented by a lower bound and an upper bound on the actual value for the distance.

As widely explained in Lavor et al. [2012e], the discretization is still possible in presence of uncertain distances, but, in each sphere intersection, only one reference distance can be imprecise, i.e. at least two of them must be exact. In this case, indeed, the problem of intersecting three spheres (related to 3 exact distances) is transformed in the problem intersecting two spheres with one spherical shell (the uncertainty gives a certain thickness to one of the three spheres). Once two spheres are intersected, the intersection between the obtained circle and the spherical shell produces two disjoint curves in the three-dimensional space. At this point, a predetermined number of sample points can be chosen on the two curves. Notice that, in this case, BP trees are not binary anymore, and that a solution to the problem cannot be represented by a binary vector, but rather by a vector of integer numbers (there are several left branches, and several right branches).

Suitable vertex orderings do not only have to satisfy the assumptions **A1** and **A2** (for the DMDGP) or the assumptions **B1** and **B2** (for the DDGP), but, in addition, for each quadruplet of vertices u^1, u^2, u^3, v, only one of the distances $d(u^1, v)$, $d(u^2, v)$, $d(u^3, v)$ can be represented by an interval. We are currently working for finding a solution to this problem.

Meanwhile, we are also working for identifying suitable orderings for particular classes of molecules. If the chemical composition of a molecule is known, indeed, the distances that are needed for the discretization can be obtained by analyzing its chemical structure. Proteins, for example, are chains of amino acids, and the chemical structure of each amino acid is known. Exact distances can be obtained by observing the atomic bonds, while imprecise distances can be found by analyzing the degrees of freedom of the structure. In this situation, NMR data are not necessary for performing the discretization (they can be rather employed in the pruning phase of BP), and therefore the ordering can be identified independently by the available information.

We carefully hand-crafted a special ordering for the protein backbones Lavor et al. [2012e] (see Figure 1). We found a particular ordering for the generic amino acid which composes a protein, and hence the ordering r_{PB} related to the whole protein backbone as the composition of the several orderings for its amino acids (without side chains):

$$r_{PB} = \{r^1_{PB}, r^2_{PB}, \ldots, r^i_{PB}, \ldots, r^p_{PB}\}.$$

The ordering r^i_{PB} corresponds to the i^{th} amino acid of the protein (superscripts indicate the amino acid to which each atom belongs):

$$r^i_{PB} = \{N^i, C^{i-1}, C^i_\alpha, H^i, N^i, C^i_\alpha, H^i_\alpha, C^i, C^i_\alpha\}.$$

In order to artificially add exact distances, atoms are considered more than once: the distance between two copies of the same atom is 0. It is important to remark that this trick for allowing the discretization does not increase the complexity of the problem, because the second copy of an atom can only be positioned as its first copy. In other

words, there is no branching on the BP tree in correspondence with duplicated atoms. For example, in the ordering for the generic amino acid r^i_{PB}, the nitrogen N^i is considered twice, the carbon C^i_α is considered 3 times, and the carbon C^{i-1} belonging to the previous amino acid is repeated among the atoms of this amino acid. In total, there are four copies of atoms that already appeared earlier in the sequence. Hydrogen atoms are not duplicated.

The first and the last amino acids of the chain have a slightly different structure, and therefore we designed particular orderings for such amino acids. At the beginning of the sequence, we consider the following ordering for the first amino acid:

$$r^1_{PB} = \{N^1, H^1, H^0, C^1_\alpha, N^1, H^1_\alpha, C^1_\alpha, C^1\}.$$

One of the hydrogens bound to N^1 (in general, in r^i_{PB}, there is only one hydrogen) is indicated by the symbol H^0. Between r^1_{PB} and the generic amino acid ordering r^i_{PB}, we consider the following ordering, which makes a sort of *bridge* between the beginning of the sequence and the generic ordering:

$$r^2_{PB} = \{N^2, C^2_\alpha, H^2, N^2, C^2_\alpha, H^2_\alpha, C^2, C^2_\alpha\}.$$

Finally, for the last amino acid of the sequence, we have the following ordering:

$$r^p_{PB} = \{N^p, C^{p-1}, C^p_\alpha, H^p, N^p, C^p_\alpha, H_\alpha, C^p, C^p_\alpha, O^p, C^p, O^{p+1}\}.$$

Note that this is the only case in which oxygen atoms appear. The two oxygens O^p and O^{p+1} which are present in the last amino acid r^p_{PB} correspond to the two oxygens of the C-terminal carboxyl group COO^- of the protein.

The special ordering r_{PB} is constructed in order to satisfy the assumptions for the DMDGP. In particular, for each atom $v \in V$, the three edges $(v-3, v)$, $(v-2, v)$ and $(v-1, v)$ are always contained in E. The corresponding distances are obtained from known bond lengths and bond angles, that only depend on the kind of bonded atoms. The two edges $(v-2, v)$ and $(v-1, v)$ are always associated to exact distances, whereas only the edge $(v-3, v)$ may be associated to an interval distance. In particular, there are three different possibilities. If $d(v-3, v) = 0$, then v represents a duplicated atom, and therefore the only feasible coordinates for v are the same of its previous copy. If $d(v-3, v)$ is an exact distance, the standard discretization process can be applied (intersection among three spheres), and two possible positions for v can be computed. Finally, if $d(v-3, v)$ is represented by an interval, we discretize the interval and take D sample distances from it. For each sample distance, we perform the sphere intersection: $2 \times D$ possible atomic positions can be computed for v.

In order to discretize instances related to entire protein conformations, it is necessary to identify an ordering for all side chains for the 20 amino acids that can be involved in the protein synthesis. This is not trivial, because side chains have more complex structures with respect to the part which is common to each amino acid. Figure 2 shows a discretization ordering for the *glycine*, the smallest amino acid that can be found in proteins, whose side chain is composed by a hydrogen atom only:

$$r_{GLY} = \{C^i_\alpha, N^i, H^i_\alpha, C^i_\alpha, H^i_\beta, C^i, H^i_\alpha, C^i_\alpha, C^i\}.$$

Here, we denote with H^i_β the hydrogen forming the glycine side chain. The ordering r_{GLY} can be plugged in the ordering r_{PB}. If we consider the first amino acid, for example, the last two vertices C^1_α and C^1 need to be replaced by r_{GLY} in order to consider this side chain. In spite of the simplicity of glycine, this ordering is rather complex and it considers various atoms of the protein backbone, which are duplicated in order to satisfy the needed assumptions. Future works will be devoted to the development of suitable hand-crafted orderings for all other 19 amino acids. This will allow us to solve real NMR instances by using our discrete approach to DGPs.

Symmetries

If a D(M)DGP instance admits solutions, then there is an even number of solutions Lavor et al. [2012b]. This is a theoretical result proved for the DMDGP which is immediately extensible to the DDGP. Our computational experiments confirmed this result. However, the sets of solutions found by the BP algorithm always satisfied a stronger property: the cardinality of the set of solutions is always a power of 2.

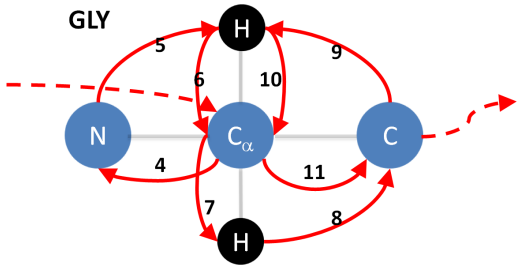

Figure 2: The artificial ordering r_{GLY} for the glycine.

This theoretical result remained unproved for a long time. At a certain point, we found indeed a counterexample, i.e. an instance, artificially generated in a particular way, for which the total number of solutions was not a power of 2. But then we were able to prove that the Lebesgue measure of the subset of instances for which this property is not satisfied is 0 Liberti et al. [2011b]. As a consequence, we can say that, in practice, real-life instances should always have a power of 2 of solutions. This result has been formally proved for the DMDGP; we are currently working for extending this result to the DDGP.

The "power of 2" property is due the presence of various symmetries in BP binary trees Lavor et al. [2012b]. First of all, there is a symmetry at layer 4 of all BP trees, which makes even the total number of solutions. We usually refer to this symmetry as the *first symmetry*. At layer 4, there are no distances for pruning, and the two branches rooted at node 3 are perfectly symmetric. In other words, any solution found on the first branch is related to another solution on the second one, which can be obtained by inverting, at each layer, left with right branches, and vice versa.

In the DMDGP, as for the first symmetry, each partial reflection symmetry appears every time there are no pruning distances concerning some layer v. In such a case, the number of feasible branches on layer v is duplicated with respect to the one of the previous layer $v-1$, and pairs of branches rooted at the same node x_{v-1} are perfectly symmetric. Figure 3 shows a BP tree containing 3 symmetries.

As mentioned in the Introduction, a solution to a DMDGP can be represented in different ways, such as a path on the tree and a list of binary choices 0–1 (we suppose here that all distances are exact). Since solutions sharing symmetric branches of the tree have symmetric local binary representations, we can derive a very easy strategy for generating all solutions to a DMDGP from one found solution and the information on the symmetries in the

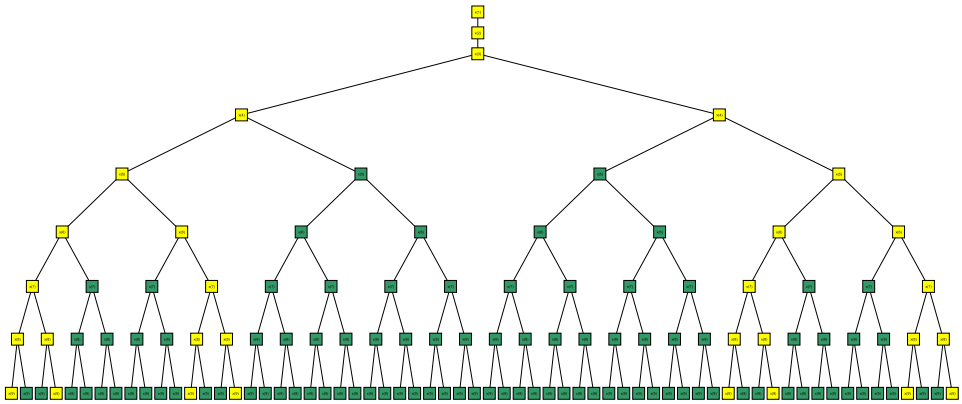

Figure 3: All symmetries of an instance with 9 vertices and $B = \{4, 6, 8\}$. Feasible branches are marked in light yellow.

corresponding tree Mucherino et al. [2011]. Let us consider for example the solution in Fig. 3 corresponding to the second leaf node (from left to right). The binary vector corresponding to this solution is

$$\mathbf{s}_2 = (0, 0, 0, 0, 0, 0, 0, 1, 1),$$

where we suppose that 0 represents the choice *left*, and 1 represents *right* (the first three zeros are associated to the first three fixed vertices of the graph). Since there is a symmetry at layer 6, another solution to the problem can be easily computed by repeating all choices from the root node until the layer 5, and by inverting all other choices. On the binary vector, repeating means *copying*, and inverting means *flipping*. So, another solution to the problem is

$$\mathbf{s}_3 = (0, 0, 0, 0, 0, 1, 1, 0, 0).$$

This solution corresponds to the third feasible leaf node in Fig. 3.

This property can be exploited for speeding up the solution to DMDGPs. The procedure we mentioned above can indeed be used for reconstructing any solution to the problem. Thus, once one solution to the problem is known, all the others can be obtained by exploiting information on the symmetries of BP trees. The set

$$B = \{v \in V : \nexists (u, w) \,\text{s.t.}\, u + 3 < v \leq w\}$$

contains all layers v of the tree where there is a symmetry Mucherino et al. [2011]. As a consequence, $|B|$ is the number of symmetries that are present in the tree. Naturally, since the first symmetry is present in all BP trees, $|B| \geq 1$. The total number of solutions is, with probability 1, equal to $2^{|B|}$.

If the current layer is related to the vertex $v \in B$, for each x_{v-1} on the previous layer, both the newly generated positions for x_v are feasible. If $v \notin B$, instead, only one of the two positions can be part of a branch leading to a solution. The other position is either infeasible or it defines a branch that will be pruned later on at a further layer v, in correspondence with a pruning distance whose graph edge $\{u, w\}$ is such that $u + 3 < v \leq w$. Therefore, we can exploit such information for performing the selection of the branches that actually define a solution to the problem. When $v \notin B$ (only one position is feasible), it is not known a priori which of the two branches (left/right) is the correct one. This is the reason why at least one solution must be computed before having the possibility of exploiting the symmetries for computing all the others.

Computational experiments presented in Mucherino et al. [2011] showed that the BP algorithm can be enhanced by exploiting this a priori knowledge on the symmetries, specially when instances having many solutions are considered. Once one solution is obtained by BP, all the others can be quickly obtained by using this information. Even if protein-like instances usually contain a few symmetries Liberti et al. [2011a], the extension of the BP algorithm to interval data actually needs to be integrated with symmetry-based strategies in order to improve its efficiency. Research in this direction will be performed in the future.

Conclusions

The discretization of DGPs allows us to solve these problems by employing the BP algorithm, which is based on a search on the BP trees. This algorithm is the first exact algorithm which is potentially able to solve DGPs containing interval data. Differently from other proposed algorithms for this problem, BP can enumerate all the solutions for a given instance, allowing to obtain multiple solutions and to leave any other out with certainty.

These works on the DGP also open the doors for suitable discretizations of other important problems, specially in the field of biology. The discretizing ordering for proteins that we detailed in this paper, for example, is completely independent on NMR data, and therefore it could also be applied in the context of *protein folding* and *protein docking*. The exploitation of the symmetries in BP trees can be essential for managing these more complex problems. These are the main directions that we will take for our future research.

Acknowledgements

This work is partially supported by the ANR project "Bip:Bip". The authors would also like to thank the Brazilian research agencies FAPESP and CNPq, and the French research agency CNRS and École Polytechnique, for financial support.

Bibliography

P. Biswas, T.-C. Liang, T.-C. Wang, Y. Ye, *Semidefinite Programming Based Algorithms for Sensor Network Localization*, ACM Transactions on Sensor Networks **2**, 188–220, 2006.

G.M. Crippen and T.F. Havel, *Distance Geometry and Molecular Conformation*, John Wiley & Sons, New York, 1988.

T.F. Havel, *Distance Geometry*, D.M. Grant and R.K. Harris (Eds.), Encyclopedia of Nuclear Magnetic Resonance, Wiley, New York, 1701-1710, 1995.

N. Krislock, *Semidefinite Facial Reduction for Low-Rank Euclidean Distance Matrix Completion*, PhD thesis, University of Waterloo, 2010.

C. Lavor, J. Lee, A. Lee-St.John, L. Liberti, A. Mucherino, M. Sviridenko, *Discretization Orders for Distance Geometry Problems*, Optimization Letters **6**, 783–796, 2012.

C. Lavor, L. Liberti, N. Maculan, A. Mucherino, *The Discretizable Molecular Distance Geometry Problem*, Computational Optimization and Applications, **52**, 115-146, 2012.

C. Lavor, L. Liberti, N. Maculan, A. Mucherino, *Recent Advances on the Discretizable Molecular Distance Geometry Problem*, European Journal of Operational Research **219**, 698–706, 2012.

C. Lavor, L. Liberti, A. Mucherino, *On the Solution of Molecular Distance Geometry Problems with Interval Data*, IEEE Conference Proceedings, International Workshop on Computational Proteomics, International Conference on Bioinformatics & Biomedicine (BIBM10), Hong Kong, 77–82, 2010.

C. Lavor, L. Liberti, A. Mucherino, *The interval Branch-and-Prune Algorithm for the Discretizable Molecular Distance Geometry Problem with Inexact Distances*, to appear in Journal of Global Optimization, 2012.

L. Liberti, C. Lavor, N. Maculan, *A Branch-and-Prune Algorithm for the Molecular Distance Geometry Problem*, International Transactions in Operational Research **15**, 1–17, 2008.

L. Liberti, C. Lavor, A. Mucherino, N. Maculan, *Molecular Distance Geometry Methods: from Continuous to Discrete*, International Transactions in Operational Research **18**, 33–51, 2010.

L. Liberti, B. Masson, C. Lavor, A. Mucherino, *Branch-and-Prune Trees with Bounded Width*, Proceedings of the 10^{th} Cologne-Twente Workshop on Graphs and Combinatorial Optimization (CTW11), Rome, Italy, 189–193, 2011.

L. Liberti, B. Masson, J. Lee, C. Lavor, A. Mucherino, *On the Number of Solutions of the Discretizable Molecular Distance Geometry Problem*, Lecture Notes in Computer Science **6831**, Proceedings of the 5^{th} Annual International Conference on Combinatorial Optimization and Applications (COCOA11), Zhangjiajie, China, 322–342, 2011.

A. Mucherino, C. Lavor, L. Liberti, *A Symmetry-Driven BP Algorithm for the Discretizable Molecular Distance Geometry Problem*, IEEE Conference Proceedings, Computational Structural Bioinformatics Workshop (CSBW11), International Conference on Bioinformatics & Biomedicine (BIBM11), Atlanta, GA, USA, 390–395, 2011.

A. Mucherino, C. Lavor, L. Liberti, *The Discretizable Distance Geometry Problem*, to appear in Optimization Letters, 2012.

J.B. Saxe, *Embeddability of Weighted Graphs in k-space is Strongly NP-hard*, Proceedings of 17^{th} Allerton Conference in Communications, Control, and Computing, Monticello, IL, 480–489, 1979.

Authors' Information

Antonio Mucherino *IRISA, University of Rennes 1, Rennes, France.*
Email: antonio.mucherino@irisa.fr

Carlile Lavor *IMECC-UNICAMP, Campinas-SP, Brazil. Email: clavor@ime.unicamp.br*

Leo Liberti *LIX, École Poleytechnique, Palaiseau, France. Email: liberti@lix.polytechnique.fr*

Nelson Maculan *COPPE, Federal University of Rio de Janeiro, Rio de Janeiro-RJ, Brazil.*
Email: maculan@cos.ufrj.br

GEOMETRICAL TOOLS FOR ALPHA-VORONOI PARTITIONS

Atsumi Ohara and Yuya Nagatani

Abstract: *We consider problems to classify data represented as discrete probability distributions. For the classification we propose the Voronoi partition technique with respect to α-divergence, which is a statistically justified pseudo-distance on the space of probability distributions. In order to improve computational efficiency and performance of the classification, we introduce two nonlinear transformations respectively called the escort and projective transform, and weighted α-centroids. Finally we demonstrate performances of the proposed tools via simple numerical examples.*

Keywords: *α-divergence, α-Voronoi partition, Escort transformation, Projective transformation*

ACM Classification Keywords*: I.3.5 Computational Geometry and Object Modeling*

MSC*: 53A15, 68T10*

Introduction

The Voronoi partitions on the space of probability distributions with the Kullback-Leibler or Bregman divergences have been recognized as significant approaches for various statistical modeling problems involving pattern classification, clustering, likelihood ratio test and so on [1, 2, 3, 4].

Recently we have proposed [7] (See [8] for the proofs and derivations) a computationally efficient method to construct Voronoi diagrams with respect to the α-divergence [5, 6] using conformal flattening technique. One of mathematically natural requirements for divergence functions is an *invariance* property and it is proved that the α-divergence is equipped with the property [5, 6]. Hence the α-divergence is an important candidate to be applied to the above statistical problems.

In this note, we introduce several useful tools when we apply the α-Voronoi partitions on the space of discrete probability distributions for the purpose of pattern classification problems.

Preliminaries

Let $\mathcal{S}^n$ denote the n-dimensional probability simplex, i.e.,

$$\mathcal{S}^n := \left\{ \boldsymbol{p} = (p_i) \,\middle|\, p_i > 0,\ \sum_{i=1}^{n+1} p_i = 1 \right\}, \tag{1}$$

and $p_i, i = 1, \cdots, n+1$ denote probabilities of $n+1$ states.

The α-divergence [5, 6] is a function on $\mathcal{S}^n \times \mathcal{S}^n$ defined for $\alpha \neq \pm 1$ by

$$D^{(\alpha)}(\boldsymbol{p}, \boldsymbol{r}) = \frac{4}{1-\alpha^2} \left\{ 1 - \sum_{i=1}^{n+1} (p_i)^{(1-\alpha)/2} (r_i)^{(1+\alpha)/2} \right\}.$$

Note that it respectively converges to the Kullback-Leibler divergence or its dual when α goes to -1 or 1, and $D^{(0)}$ is called the Hellinger distance.

For $q \in \mathbf{R}$ escort transformation [9] is defined for $\boldsymbol{p} \in \mathcal{S}^n$ by

$$P_i(\boldsymbol{p}) := \frac{(p_i)^q}{\sum_{j=1}^{n+1}(p_j)^q},\ i = 1, \cdots, n+1, \quad Z_q(\boldsymbol{p}) := \sum_{i=1}^{n+1} \frac{(p_i)^q}{q}, \tag{2}$$

and we call $P_i(\boldsymbol{p})$ an escort probability. Note that the escort distribution $\boldsymbol{P}(\boldsymbol{p}) = (P_i(\boldsymbol{p}))$ converges to the uniform distribution independently of $\boldsymbol{p}$, when $q \to 0$. On the other hand, when $q \to \pm\infty$, it converges to a distribution on the boundary of $\mathcal{S}^n$ depending on the maximum or minimum components of $\boldsymbol{p}$. In the sequel we fix the relation between α and q by $q = (1+\alpha)/2$, and assume $q > 0$.

The conformal divergence [7] for $D^{(\alpha)}$ is defined by

$$\begin{aligned} \rho(\boldsymbol{p}, \boldsymbol{r}) &:= \frac{1}{Z_q(\boldsymbol{r})} D^{(\alpha)}(\boldsymbol{p}, \boldsymbol{r}) = -\sum_{i=1}^{n+1} P_i(\boldsymbol{r}) \left(\ln_q(p_i) - \ln_q(r_i)\right) \\ &= \psi(\boldsymbol{\theta}(\boldsymbol{p})) + \psi^*(\boldsymbol{\eta}(\boldsymbol{r})) - \sum_{i=1}^{n} \theta^i(\boldsymbol{p}) \eta_i(\boldsymbol{r}), \end{aligned} \tag{3}$$

where

$$\begin{aligned} \theta^i(\boldsymbol{p}) &:= \ln_q(p_i) - \ln_q(p_{n+1}), \quad \eta_i(\boldsymbol{p}) := P_i(\boldsymbol{p}), \quad i = 1, \cdots, n, \\ \psi(\boldsymbol{\theta}(\boldsymbol{p})) &:= -\ln_q(p_{n+1}), \quad \psi^*(\boldsymbol{\eta}(\boldsymbol{p})) := \frac{1}{\kappa}\left(\frac{1}{Z_q(\boldsymbol{p})} - q\right), \end{aligned}$$

with $\kappa := (1-\alpha^2)/4 = q(1-q)$, $\ln_q(s) := (s^{1-q} - 1)/(1-q)$ for $s \geq 0$ and

$$\eta_i(\boldsymbol{p}) = \frac{\partial \psi}{\partial \theta^i}(\boldsymbol{p}), \quad \theta^i(\boldsymbol{p}) = \frac{\partial \psi^*}{\partial \eta_i}(\boldsymbol{p}), \quad i = 1, \cdots, n. \tag{4}$$

Alpha-Voronoi partitions and pattern classification problems

For given m points $\boldsymbol{p}_1, \cdots, \boldsymbol{p}_m$ on $\mathcal{S}^n$ we define α-*Voronoi regions* on $\mathcal{S}^n$ using the α-divergence as follows:

$$\mathrm{Vor}^{(\alpha)}(\boldsymbol{p}_k) := \bigcap_{l \neq k} \{\boldsymbol{p} \in \mathcal{S}^n | D^{(\alpha)}(\boldsymbol{p}_k, \boldsymbol{p}) < D^{(\alpha)}(\boldsymbol{p}_l, \boldsymbol{p})\}, \quad k = 1, \cdots, m.$$

An α-*Voronoi partition (diagram)* on $\mathcal{S}^n$ is a collection of the α-Voronoi regions and their boundaries.

By the conformal relation between $D^{(\alpha)}$ and ρ in (3) we immediately see that the Voronoi region defined by

$$\mathrm{Vor}^{(\mathrm{conf})}(\boldsymbol{p}_k) := \bigcap_{l \neq k} \{\boldsymbol{p} \in \mathcal{S}^n | \rho(\boldsymbol{p}_k, \boldsymbol{p}) < \rho(\boldsymbol{p}_l, \boldsymbol{p})\}$$

coincides with $\mathrm{Vor}^{(\alpha)}(\boldsymbol{p}_k)$. Furthermore, we have proved [7] that if we regard the escort probabilities $(P_i(\boldsymbol{p}))$ as a new coordinate system for $\boldsymbol{p}$, we can efficiently compute $\mathrm{Vor}^{(\mathrm{conf})}(\boldsymbol{p}_k)$ by the standard algorithm [10] using the polyhedron envelop for the convex potential function ψ. Hence, the boundary for each α-Voronoi region consists of straight line segments (See the figure 1 and 2).

When we apply the Voronoi partitioning technique to pattern classification problems, flexible choice of the representing point for each Voronoi region is significant. For this purpose we define a *weighted* α*-centroid* and a formula to calculate it. Given m points $\boldsymbol{p}_1, \cdots, \boldsymbol{p}_m$ on $\mathcal{S}^n$ and weights $w_k \geq 0, k = 1, \cdots, m$, the weighted α-centroid $\boldsymbol{c}_w^{(\alpha)}$ is defined by the minimizer of the following problem:

$$\min_{\boldsymbol{p} \in \mathcal{S}^n} \sum_{k=1}^{m} w_k D^{(\alpha)}(\boldsymbol{p}, \boldsymbol{p}_k).$$

By differentiating the above with θ^i and considering the optimality condition, we have the escort probabilities of $\boldsymbol{c}_w^{(\alpha)}$ as

$$P_i(\boldsymbol{c}_w^{(\alpha)}) = \frac{1}{\sum_{k=1}^m w_k Z_q(\boldsymbol{p}_k)} \sum_{k=1}^m w_k Z_q(\boldsymbol{p}_k) P_i(\boldsymbol{p}_k), \quad i = 1, \cdots, n+1.$$

Thus, the weighted α-centroid is represented as the usual weighted average in the escort probabilities.

While the α-Voronoi partition has a one-dimensional freedom in adjusting the parameter α (or equivalently q), the adjustment tends not to work well for large α (or $q \approx +\infty$) for distributions that have the largest probabilities for the same event. This can be understood by considering the corresponding escort distributions, i.e., they are concentrated in the same corner of the simplex in such a situation. Similarly, the classification tends not to work when $\alpha \approx -1$ (or $q \approx 0$) because all the corresponding escort distributions are concentrated near the uniform distribution.

To resolve this problem, we introduce the following projective transformation:

$$\Pi_{\boldsymbol{t}} : \mathcal{S}^n \ni (p_i) \mapsto (\tilde{p}_i) \in \mathcal{S}^n, \quad \text{where } \tilde{p}_i(\boldsymbol{p}) := \frac{t_i^{-1} p_i}{\sum_{j=1}^{n+1} t_j^{-1} p_j}$$

for $\boldsymbol{t} = (t_1, \cdots, t_{n+1})$ in the positive orthant.

Note that the inverse projective transformation is $\Pi_{\boldsymbol{t}^{-1}}$ where $\boldsymbol{t}^{-1} := (t_1^{-1}, \cdots, t_{n+1}^{-1})$, and $\Pi_{\boldsymbol{t}}$ for $\boldsymbol{t} \in \mathcal{S}^n$ maps $\boldsymbol{t}$ to the uniform distribution. Hence, if we use $\Pi_{\boldsymbol{t}}$ as a preconditioner for given data of discrete distributions before the α-Vononoi partitioning, we can expect the inprovement of classification performance.

Illustrative numerical examples

As an illustrative example we consider α-Voronoi partition of the the given four kinds of discrete distributions (the left one of Figure 1) into four classes. In spite of adjusting α (equivalently q) one of data denoted by the symbol $\bullet$ is classified into the region of data denoted by $\triangle$. The right one of Figure 1 is representation of the α-Voronoi partition in escort probabilities.

Executing projective transformation before the partitioning given data are classified successfully (Figure 2). In both figures the symbol $*$ denotes unweighted ($w_1 = \cdots = w_4$) α-centroids for the corresponding classes, and $\boldsymbol{t}$ for the projective transformation is the unweighted α-centroid of those of four data classes.

Concluding remarks

As is summarized in the preliminary section, introduction of the escort probabilities and the conformal divergence enables us to construct α-Voronoi partitions via the efficient standard algorithm involving a convex potential function. We apply this algorithm to pattern classification problems for data expressed by discrete probability distributions.

While the Voronoi partition technique might not be more efficient than the other naive methods in higher dimensional case, the underlying geometrical idea could be applied to other application such as likelihood ratio test.

Bibliography

[1] T. M. Cover and J. A. Thomas, Elements of information theory, Wiley (1991).

[2] H. Imai and M. Inaba, Divergence-Based Geometric Clustering and Its Underlying Discrete Proximity Structures *IEICE Trans. Inf. & Syst.*, **E83-D** (2000) 27.

[3] G. Lebanon, Metric Learning for Text Documents *IEEE Trans. on Pattern Analysis and Machine Intelligence*, **28** (2005) 497.

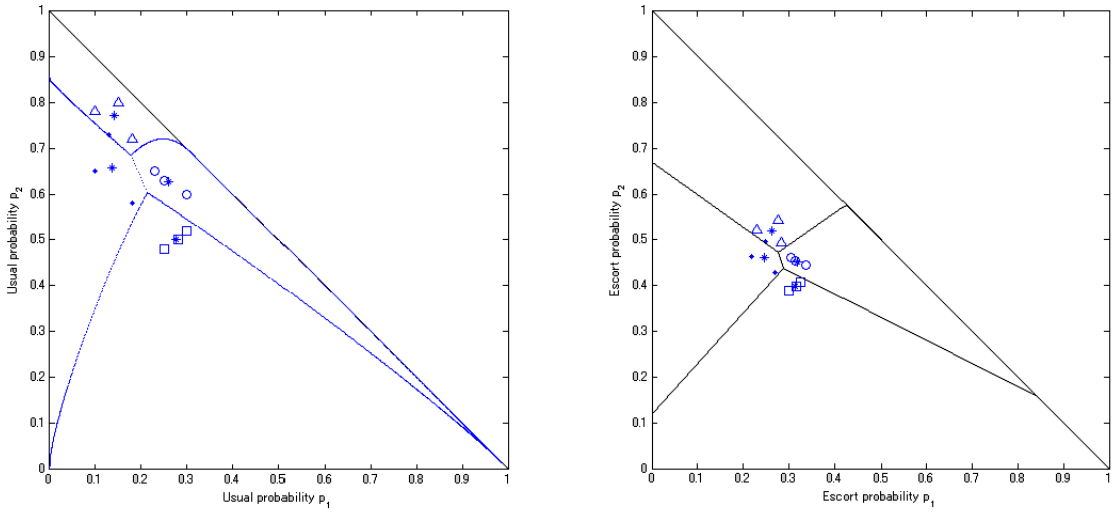

Figure 1: α-Voronoi diagram on $\mathcal{S}^2$ w.r.t. usual probabilities (left) and escort probabilities (right) for q=0.4

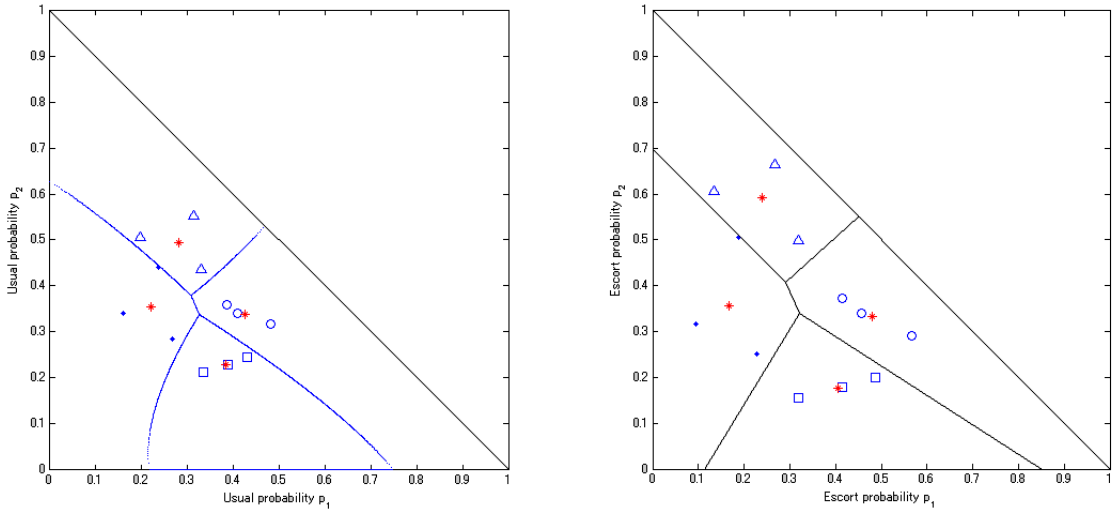

Figure 2: α-Voronoi diagram on $\mathcal{S}^2$ w.r.t. usual probabilities (left) and escort probabilities (right) for q=0.4 with projective transformation as preconditioning

[4] J.-D. Boissonnat, F. Nielsen and N. Nock, *Discrete Comput. Geom.*, **44** (2010) 281.

[5] S.-I. Amari, *Differential-Geometrical Methods in Statistics*, (Springer-Verlag, Berlin, 1985).

[6] S.-I. Amari and H. Nagaoka, *Methods of Information Geometry*, (AMS&Oxford, Rhode Island, 2000).

[7] A. Ohara, H. Matsuzoe and S.-I. Amari, Conformal geometry of escort probability and its applications, Modern Physics Letters B, Vol. 26, No. 10, 1250063, 2012

[8] A. Ohara, H. Matsuzoe and S.-I. Amari, A dually flat structure on the space of escort distributions, arXiv:1010.4965v1, 2010.

[9] C. Beck and F. Schlögl, *Thermodynamics of Chaotic Systems*, (Cambridge University Press, Cambridge, 1993).

[10] H. Edelsbrunner, *Algorithms in Combinatorial Geometry* (Springer-Verlag, 1987).

Authors' Information

Atsumi Ohara - *Department of Electrical and Electronics Engineering, University of Fukui, Bunkyo 3-9-1, Fukui 910-8507, Japan; e-mail: ohara@fuee.u-fukui.ac.jp*
Major Fields of Scientific Research: Information Geometry

Yuya Nagatani - *Department of Electrical and Electronics Engineering, University of Fukui, Bunkyo 3-9-1, Fukui 910-8507, Japan; e-mail: nagatani.hase@gmail.com*
Major Fields of Scientific Research: Pattern recognition

METRIC TENSOR AS DEGREE OF COHERENCE IN THE DYNAMICAL ORGANIZATION OF THE CENTRAL NERVOUS SYSTEM

Sisir Roy, Rodolfo Llinás

Abstract: *The mechanism by which neuronal networks dynamically organize and differentiate during development is a salient issue concerning neurogenesis. This central event reflects a topological order and its metrizability. One important parameter in this process concerns the role of tremor and intrinsic electrical properties of neurons [Llinàs 1988] from a different in the developmental organization of Central Nervous System (CNS), which we now would like to develop more formally. While tremor is usually considered an undesirable parameter in the generation of coordinated movement it is actually essential in efficient motor execution and reflects fundamental intrinsic neuronal electrophysiological oscillation. In addition, we propose, such intrinsic properties contribute to organize the neuronal connectivity that results in the development of internal coordinate reference systems. Thus the degree of coherence in the oscillatory activities of neuron can be interpreted as embodying a metric tensor of non-Euclidean space that produce topological order associated to CNS development.*

Keywords: *Degree of coherence, Metric tensor, Nervous System, Intrinsic Oscillation, Functional Geometry*

Introduction

Central Nervous System (CNS) activity has evolved to represent the external world into internal parameters that ultimately organize and modulate its interactivity with the surrounding environment. Such evolution forged neuronal ensembles, as interconnected groups (areas) capable of internally defining specific intrinsic parameters reflecting significant properties of the world addressable by motor commands. Intrinsic characters and internal trends fundamentally modulate the activity in such areas. Thus the parameters which internalize the world are fundamentally self reliant and internally consistent, and represent a secondary emission imbedded reality, but only on their own terms and parameters. Such intrinsically driven set of compartments internalize the specific sensory representations that support movement interaction with the external reality. Thus, sensors by acting in unison (co-variants) represented external properties to be transformed into guided action on the world (contra-variants), implementing appropriate motor specification. It was originally proposed [Pellionisz and Llinas 1982; Pellionisz and Llinas 1985] that such correspondences between covariant vectors (for sensory effects) and contravariant quantities (for motor preparation and effectuation) constituted structures of metric spaces, which provide the brain with internal models of the world. The dimension of time was added[Roy and Llinás 1988] to these metrics: in that work stochastic metrics represented chaos at local levels that stabilize smooth oscillations at greater scale [Leznik et al 2002] giving quanta of information at 40Hz. However, in this paper the main issue is what aspects of cell function serve as the linkage between single cell properties and the development of neuronal nets as it relates to the interaction with the external world.

The prevailing view at this time is that such organized structure is basically a product of genetic information unfolded in time and of epigenetic variables relating to (i) position, (ii) axonal growth, (iii) target location. Edelman [Edelman 1984] added one more step towards understanding the process of organization i.e. the specific regulation of cellular movement through gated adhesiveness followed by *selective stabilization* of synaptic convertibility [Changeux and Danchin 1976]. One of us [Llinàs 1984a] critically analyzed the situation and raised questions concerning (1) what further parameters other than biochemical are selective and (2) what mechanisms implement this selection. It was proposed, at that time a new hypothesis, relating these two aspects of network genesis to intrinsic neuronal auto-rhythmicity that could be considered as playing a central role in early organization of nerve nets [Llinàs 1984b]. Autorhythmicity and cell to cell communication, through electronic coupling, could in addition generate synchronicity of firing by entrainment of co-existing intrinsic oscillatory properties. These properties along

with the chemical synaptic transmission present in early embryos, were thus proposed as an essential electrical substrate of the organization of brain circuits [Llinàs 1984a]. From a different perspective it is known that controlled tremor can be considered the basis for motricity [Llinàs 1991]. The essential feature of tremor is a kind of activity that is sustained and regular. Tremor is usually considered as undesirable property in the organization of coordinated movement but, in fact, it is essential in the organization of the internal coordinate reference systems.

It is well-known that during development embryos go through distinct stages of tremor and rhythmic twitching. In Parkinson's disease mechanical oscillatory simulation of a finger by external device may induce tremor that irradiates progressively upwards along the limb. The tremor march phenomenon indicates that the different portions of CNS which control limb movement are coupled to each other by the ability to be phase-locked and to resonate with tremor occurring in one of its parts. The mechanism responsible for generating tremor may be considered to be associated to the oscillatory rhythm as coherent properties of CNS neurons. We propose that the degree of coherence depending on intrinsic neuronal oscillation produce topological order to the neuronal networks. This degree of coherence can be identified as Non-Euclidean metric tensor of this topological space associated to CNS. At first the role of tremor in the development of organization of nervous system will be briefly discussed in section II and then the topological order and the metric tensor for the topological space associated to the functional states of CNS will be constructed in section III. Possible implications will be discussed in section IV.

Tremor and Dynamic Organization of Central Nervous System

Coghill in his well known book Anatomy and the Problem of Behavior addressed the neuro-embryological basis of behavior for diverse vertebrates. He tried to find basic principles that would be valid for vertebrates in general. The development of behavior in vertebrates as proposed by Coghill [Coghill 1920] has been opposed by Windle1 [Windle 1940]which emphasizes that the local reflexes are the basic units of behavior. Hamburger [Hamburger 1963] in his comprehensive review critically analyzed the two approaches and the Spontaneous and reflexogenic motility are considered to be as two independent basic ingredients of embryonic behavior. It is also mentioned that the direct observations of motility in case of higher vertebrates the behavior is uncoordinated in the early stage. Bakeoff et al [Bekoff et al 1975] studied $7 - 7.5$-day chick embryo using electromyography since this stage of chick embryo is close to the inception of overt motility in immature leg. This effort was motivated to find whether or not the motor system is organized at this stage. Their study indicated sensory input is not required for the development of coordinated motor output. Their investigation also showed that embryos go through distinct stages of tremor and rhythmic twitching during development. The essential feature of tremor is that of an activity that is sustained and oscillatory motion of a body part. The early studies show that physiological tremor is related to the rhythmic neural activity of CNS where as pathological tremor be a distortion or amplifications of this rhythmic oscillations. Indeed, neuronal oscillation and resonance determine much of the active movement dynamics of limbs and thus provide, by feedback through the afferent systems, information about the dynamics of the body reference frames [Llinàs 1984a]. For example, in cases of Parkinson's disease, mechanical oscillatory stimulation of a finger by an external device may induce tremor that irradiates progressively upwards, along the limb, in a manner similar to the Jackson's march of motor seizures. It follows that the different portions of the CNS which control limb movement are coupled to each other by the ability to the phase-locked and to resonate with tremors occurring in one of its portions. This indicated the serious possibility that during development CNS may utilize the tremor in establishing an internal geometry of the coordination between the peripheral structures such as muscles and their sensory return to the CNS to establish the dynamics of movement control.

Indeed, since the tremor ultimately returns to the CNS by different afferent receptor connectivity, it may be used, during development, to establish some of the n-dimensional vectorial transformation (in frequency hyperspace) which underlie the implementation of sensory input into coordinated motor output. Thus, the tremor and twitching of a given muscle group and the ability it has to generate sensory feedback by the production of actual movement, by the direct activation of the sensory feedback or by corollary discharge, would ultimately serve to establish the physiologically meaningful connectivity between afferent input and motor output. The importance of this interaction becomes clearer when considering that it occurs very early in development prior to the generation of truly organized

movement and could thus serve as an epigenetic organizing influence in determining selective stabilization of neuronal networks [Changeux et al 1973]. This mechanism of central oscillation-giving rise to tremor- in turn generating a sensory stimulus which is feedback to the central oscillator, would ultimately result in the internal modulation of the sensorimotor transformation.

Functional Significance of Tremor

The functional significance of physiological tremor is one of the fascinating issues in neuroscience. Since the physiological tremor is a low amplitude and low frequency [Llinàs 1984a; Llinàs 1991; Coghill 1920; Windle 1940; Hamburger 1963] Hz range oscillation during the maintenance of steady body postures, it is considered a source of unwanted noise in the system, something to be controlled rather than exploited. Such a view was prevalent for a long period. Simultaneously with the development of the ideas described above concerning intrinsic neuronal oscillations and tremor, 1983 Goodman and Kelso [Goodman and Kelso 1983] also explored tremor critically and suggested it could have important functions rather than being just unwanted source of variability. Here, CNS in the process of minimizing this variability (tremor) by neuronal mechanisms capable of plasticity, especially during development, uses adaptive changes that establish the internal geometry required for the transformation of sensory input into a motor output which would be, de facto, in resonance with the bodyï£¡s coordinated dynamics. In addition to tremor organizing sensori-motor transform, oscillatory interaction between other portions of the neurons system must also be at work during development. During development, neurons are known to have auto-rhythmicity. This intrinsic auto-rhymicity is considered to be one of the central mechanism in the early organization of neuronal networks. Auto-rhymicity and cell-to-cell communication through electronic coupling, which characterizes embryonic tissue, can generate synchronicity of firings by entrainment of coexisting intrinsic oscillatory properties. In fact, the degree of coherence of the oscillations or rhythms associated to field potentials or spike trains is shown to be related to degree of communication between structures. These structures are nothing but large-scale network property. The degree of coherence determines the geometrical organization of nervous system.

Degree of Coherence and Metric Tensor

Theory of coherence of electromagnetic filed has been widely discussed both in case of classical and quantum paradigm. The diffraction and interference effects of electromagnetic waves are observed depending on the nature of coherent disturbances. The fully coherent disturbance is a mathematical idealization and in reality the disturbance is intermediate between fully coherent and incoherent to the extent that we can address them as partial coherence. The theory of partial coherence in classical theory has been developed based on Maxwell wave theory and is usually considered a component of the more general information theory concerning statistical dynamics a means to understand information transfer. The theory of coherence is closely connected with classical noise theory and with the theory of quantum fluctuations in the quantum mechanics field. At first we discuss some of the basic concepts useful in understanding the degree of coherence.

Mutual Coherence and Degree of Coherence

The mutual coherence function $\Gamma_{12}(\tau)$ can be defined as

$$\Gamma_{12}(\tau) =< V(\vec{x}_1, t)V*(\vec{x}_2, t+\tau) >$$

where$\vec{x}_1 \& \vec{x}_2$ denotes the position vector, the asterisk a complex conjugate and the bracket be the time average i.e.

$$< F >= lim_{T\to\infty} \frac{1}{2T} \int_T^T F dt$$

Above mutual coherence function the following crossing symmetry condition holds :

$$\Gamma_{12}^{*}(\tau) = \Gamma(-\tau)$$

due to the stationarity property of the disturbances. Considering the normalized mutual coherence, we define the degree of coherence as

$$\gamma_{12}(\tau) = \frac{\Gamma_{12}(\tau)}{\sqrt{\Gamma_{11}(0)}\sqrt{\Gamma_{22}(0)}}$$

where

$$0 \leq |\gamma_{12}(\tau)| \leq 1$$

. $\gamma_{12} = 1$ characterizes the complete coherence and for zero value the complete incoherence. Like the mutual coherence function, the degree of coherence is a function of seven variables : six position coordinates and the time delay coordinate τ. The theory of partial coherence is used to describe the phenomena in real world. Perina [Perina 1969; Perina 1969] investigated the matrix formulation of partial coherence using the Hilbert-Schmidt theory of linear integral equation and its functional theory of coherence. This is similar to Heisenberg matrix and Schrodinger wave formulations of quantum mechanics.The two formulations are shown to be equivalent due to the isomorphism of L_2 spaces(the space of square integrable functions in Lebesgue sense) and I_2 spaces (space of Fourier coefficients of functions from L_2 to a complete orthogonal system of functions). In the similar spirit a covariant formulation of partial coherence has been done using the *quantization* of the object and its image [Gabor 1956] to interpret the degree of coherence as metric tensor in non-Euclidian space called the optical space. This allows to study the partial coherence as a property of the optical space.The intensity can be written in quadratic form as

$$I = \sum_{i,j} \gamma_{ij} u^i u^j$$

where $u^i \equiv u(\xi_i)$, ξ_i are the points of quantization. Here, $\gamma_{ij} \equiv \gamma(u^i, u^j)$. Now one defines a non-Euclidian metric in the usual way[19] using the quadratic form

$$(ds)^2 = \sum_{i,j}^{n} \gamma_{ij} du^i du^j$$

. As $I \geq 0$ this quadratic form is semi positive definite. It is to be noted that the mutual coherence function and the degree of coherence are measurable quantities in contrast to the non-measurable vectors of Maxwell theory. In case of incoherent field, the metric tensor simply reduces to the Euclidian one i.e. $\gamma_{ij} = \delta_{ij}$.

Propagating waves in the cortex and internal geometry

Travelling waves of oscillatory behavior of the nervous system play crucial role in computation and communication between the various subsystems of the brain [Petrov 1961; Ermentrout 2001] including the olfactory system of vertebrates and invertebrates. These waves may take various spatio-temporal forms for example: the membrane voltage profile of neurons at different locations is essentially one-dimensional plane wave. Rubino et al [Rubino et al 2006] studied the information transfer in the motor cortex mediated by propagating waves for high frequency oscillations. They suggested that this information transfer is understood with respect to the spatiotemporal characteristics of the neuronal ensemble oscillatory behavior. The stimulus induced oscillations of the ensemble of neurons and resonances are widely studied in many sensory systems. The synchronization of the oscillatory networks have drawn large attention in various contexts especially the real world neuronal networks. Recently, Motter et al [Motter et al 2005] investigated the synchronization of those complex networks that are considered to have strong heterogeneity in the degree (connectivity) distribution. They have shown that the synchronization of such complex networks depend on the degree and the maximum synchronization is achieved when network is weighted and the overall cost involved in the coupling is minimum. Again here in the oscillatory networks the total

strengths of all in-links $k(1-\beta)$ with degree k_i at a node i can be interpreted as a property of the input function of the oscillators rather than the property of the links. We, thus suggest that the tremor in the input makes the overall cost in the coupling minimum so as to achieve maximum synchronicity. In fact, the emerging physical properties from in vitro network are the propagation speeds, synaptic transmission, information creation and capacity. The information speed is estimated based on the wave like associated to the oscillatory neuronal networks. Pathological brain states such as epilepsy are considered to be associated to activity waves. Generally, the neuronal waves are divided into three broad classes [Ermentrout and Pinto 2007]:

- Stationary waves
- Active waves
- Oscillation generated or Phase waves

The phase wave is generated via the intrinsically oscillatory properties where the local het- erogeneity, anisotropy or dynamic instabilities induce phase difference varying over space. The degree of coherence of the waves associated to oscillatory network of neurons is a physically measurable quantity. This degree of coherence can be interpreted as non- Euclidian metric tensor in a space called internal space similar to that described for optical space for electromagnetic waves. This internal space is similar to that proposed some years ago3 associated to CNS. It is to be noted that the optical space in case of electromagnetic waves help us to study the coherence properties of waves themselves in the spirit of Einsteinï£¡s geometric description of the gravitational field. Here, we like to emphasize that the coherence behavior of the oscillatory activity of ensemble of neurons can be studied as a property of the internal geometry as previously mentioned [Roy and Llinás 2011].

Discussions

Oscillations and tremor are generally considered as unwanted variability or noise, present in brains as an unwanted property. Moreover, the limitation put by physical laws in Thermodynamics and Quantum Theory forces us to think of noise as trouble when we try design electronic devices. On the other hand, in living systems, starting from unicellular object like Diatom -Bacteria to more complex ensembles such as neuronal networks noise, as defined in physics is a required component for its functionality. In fact it has been recently pointed out that the Central Nervous System (CNS) depends on noise, which carries no signal information, to enhance signal detection thus emphasizing the fundamental role of noise in information processing of brain. The emphasis of this paper, thus, is geared to underline the significance that intrinsic oscillation and its counterpart, tremor, plays in the development and basic functional organization of the central nervous system. Indeed those two variables play a fundamental role in the development of the actual topological structure associated functioning neuronal networks. Indeed, the degree of coherence associated with the oscillatory networks is centrally determined by the tremor and hence the metric tensor of this topological space. This justifies, in our eyes, our heuristic arguments regarding the role of oscillation in the organization of the nervous system.

Bibliography

[Bekoff et al 1975] Bekoff Anne et al (1975) Coordinated Motor Output in the Hindlimb of the $7-$Day Chick Embryo, Proc.Nat.Acad. Sci(USA) **72**:1245-1248.

[Changeux and Danchin 1976] Changeux, J.P. and Danchin, A. (1976) Selective stabilisation of developing synapses as a mechanism for the specification of neuronal networks, Nature **264**:705-711.

[Changeux et al 1973] Changeux Jean-Pierre et al (1973) A Theory of the Epigenesis of Neuronal Networks by the Selective Stabilization of Synapses; Proc.nat.Acad.Sci **70**:2974-2978.

[Coghill 1920] Coghill, G.E.(1920) Anatomy and the Problem of Behaviour, pp.113 (Cambridge, at the University Press).

[Goodman and Kelso 1983] Goodman D. and Kelso J.A.S (1983) Exploring the Functional Significance of Physiological Tremor : A Biospectroscopic Approach; Exp. Brain res. **49**:419-431.

[Edelman 1984] Edelman M. Gerald(1984) Cell adhesion and morphogenesis : The regulator hypothesis, Proc.Nat.Acad.Sci (USA) **81**:1460-1464.

[Ermentrout 2001] Ermentrout Bard G.(2001) Travelling Electrical Waves in Cortex : Insights from Phase Dynamics and Speculation on a Computational Role;Neuron **29**:33-44.

[Ermentrout and Pinto 2007] Ermentrout Bard G. and Pinto David (2007) Neurophysiology and Waves, SIAM News **40**, No.2.

[Gabor 1956] Gabor D.(1956) Astronomical Optics and Related Subjects Ed. by Z. Kopal, North Holland Pub.Co, Amsterdam pp.17.

[Hamburger 1963] Hamburger Viktor(1963) Some aspects of the embryology of behavior, The Quarterly Review of Biology **38**:342-365.

[Leznik et al 2002] Leznik, E., Makarenko and , Llinàs, R. (2002) Electrotonically mediated oscillatory patterns in neuronal ensembles: an in vitro voltage-dependent dye imaging study in the inferior olive. J. Neurosci., **22**: 2804-2815.

[Llinàs 1984a] Llinàs, R. Rodolfo(1984a) Oscillation and resonance as the basic mechanism for the dynamic organization of the CNS, Trab. Inst. Cajal (Madrid).

[Llinàs 1984b] Llinàs, R. Rodolfo (1984b) Possible role of tremor in the organisation of the nervous system; Movement Disorders: Tremor. Edt. by L.J.Findley and R.Capildeo, Macmillan, pp.475-4

[Llinàs 1988] Llinàs R. (1988) The intrinsic electrophysiological properties of mammalian neurons: insights into central nervous system function. Science, **242**: 1654-1664.

[Llinàs 1991] Llinás, R.(1991) The noncontinuous nature of movement execution. In: Motor Control: Concepts and Issues, eds. D.R. Humphrey and H.J. Freund, John Wiley & Sons Ltd., Dahlem Konferenzen pp 223-242. 77.

[Motter et al 2005] Motter E.Adilson et al (2005) Network Synchronization, Diffusion and the Paradox of Heterogeneity, Phys.Rev. E **71**:1-9.

[Pellionisz and Llinas 1982] Pellionisz, A. and Llinás R. (1982) Space-time representation in the brain: the cerebellum as a predictive space-time metric tensor. Neuroscience, **7**: 2949-2970.

[Pellionisz and Llinas 1985] Pellionisz, A. and Llinás, R. (1985) Tensor network theory of the metaorganization of functional geometries in the CNS. Neuroscience, **16**: 245-273.

[Perina 1969] Perina J.(1969) Theory of Coherence, Czech J.Phys. B **19**:151-193.

[Perina 1963] Perina J.(1963)Une théorie covariante générale des images optiques evec emploi des groupes de Lie ; Optica Acta **10**:333-335.

[Petrov 1961] Petrov A.Z.(1961)Prostranstva Einstejna, GIFML,Moskva, pp. 81.

[Roy and Llinás 1988] Roy S.and Llinás R.(1988)Dynamic geometry, brain function modeling, and consciousness Progress in Brain Research;R. Banerjee & B.K. Chakrabarti (Eds.), **168**:133-144.

[Roy and Llinás 2011] Roy S. and Llinás R.(2011)The role of Noise in Brain Function, Image in Action, Procd. data Analysis in Astronomy Ed. by Z.Bertrand et al (World Scientific Publsihers, Singapore)

[Rubino et al 2006] Rubino Doug et al (2006) Propagating waves mediate information tranfer in the motor cortex; Nature Neuroscience **9**:1549-1557.

[Windle 1940] Windle, W.F.(1940) Physiology of the Fetus, pp.249. W.B.Saunders, Philadelphia.

Authors' Information

Sisir Roy *- Physics and Applied Mathematics Unit, Indian Statistical Institute, 203 Barrackpore Trunk Road, Kolkata, 700108, India.*
e-mail: sisir@isical.ac.in

Rodolfo Llinás *- New York University School of Medicine, 530 First Avenue, New York, NY, 10016 USA.*
e-mail: llinar01@med.nyu.edu

HARDWARE IMPLEMENTATION OF RANK CODEC

Igor Sysoev, Ernst Gabidulin

Abstract: *The authors present a hardware implementation of the codec for rank codes. Parameters of rank code are (8,4,5). Algorithm was implemented on FPGA Spartan 3. Code rate is 1/2. The codec operates with elements from Galois field $GF(2^8)$. The device can process informational data stream up to 77 MiB/s. Proposed results should help understanding rank code structure and simplify the problem of its application.*

Keywords: *rank codes, codec, error correction code, weak self-orthogonal bases, rank metric, FPGA, key equation, Euclidean algorithm, fast computing.*

ACM Classification Keywords*: B.2.4 High-Speed Arithmetic*

MSC*: 12Y05, 65Y20, 68W35.*

Introduction

Rank codes were developed in 1985 [Gabidulin, 1985]. They are an analogue of Reed-Solomon codes. The key difference between them lies in the definition of the metric. Unlike Reed-Solomon codes, which use Hamming metric, rank codes use rank metric. A new technique of data transmission, called "Network coding" was proposed in 2000 [Ahlswede, 2000]. According to this technique several packets can be combined together by a node for transmission and the rank codes are the most suitable method of correcting errors in such systems. There are many theoretical papers dedicated to rank coding. However none of them consider hardware implementation.

In this work we will concentrate on our algorithms for rank codes and describe how we implemented them. Next part of the paper is organized as follows. At first it will be discussed coding procedure and its complexity. Secondly we are going to discuss our implementation of decoder block, talk about calculating the syndrome, solving key equation, computing error occured and correcting an informational vector. Thirdly we will give the information about resource requirements of the coder. And finally we are going to emphasize and discuss the main results.

Coding scheme

Coding scheme is implemented through multiplication informational vector u by generating matrix G. Coding scheme is similar to rank code syndrome calculating procedure. Entries of the matrix are the elements of the extended field $GF(q^N)$. Let rank code has such parameters – (n, k, d). Then we can write an informational vector

$$u = (u_1, u_1, \ldots .u_k), u_i \in GF(q^N). \tag{1}$$

We assume $n = N$ and $n = 2k$ unless otherwise stated. So current code rate equals $1/2$. Generating matrix G of rank code are

$$G_{(k\times n)} = \begin{Vmatrix} g_1 & g_2 & \cdots & g_n \\ g_1^{[1]} & g_2^{[1]} & \cdots & g_n^{[1]} \\ \vdots & \vdots & \ddots & \vdots \\ g_1^{[k-1]} & g_2^{[k-1]} & \cdots & g_n^{[k-1]} \end{Vmatrix}, \tag{2}$$

where $[i]$ means Frobenius power or q^i. Calculated code vector is equal to the product

$$g = u \cdot G = (g_1, g_2, \ldots, g_n), g_i \in GF(q^N). \tag{3}$$

Papers [Gabidulin, 2010] and [Sysoev, 2011] are describe how to perform similar operation using weak self-orthogonal bases [Gabidulin, 2006]. In this case asymptotic complexity of the operation can be evaluated as ($N = n$)

$$\mathcal{C}_{code} = \mathcal{O}\left((\log N)^2 N\right) + \mathcal{O}(N^{\log_2 3}). \tag{4}$$

Decoding scheme

Code vector g can be distorted during data transmission. So write

$$y = g + e, \tag{5}$$

where

$$e = (e_1, e_2, \ldots, e_n), e_i \in GF(q^N). \tag{6}$$

If there are no more information apart from received vector y then decoder will be able to correct this word if and only if

$$rank(e) \leq \frac{d-1}{2}. \tag{7}$$

Syndrome computing

There are some ways to decode rank codes. Decoding using syndrome (i.e. syndrome decoding) are best investigated. Syndrome is the product of received vector y and check matrix H

$$s = y \cdot H. \tag{8}$$

If all entries of the syndrome (8) are equal to zero elements then rank decoder makes a decision that there are no errors. It associates the received vector $c = y$ with an appropriated informational vector. The check matrix,

$$H_{(d-1\times n)} = \begin{Vmatrix} h_1 & h_2 & \cdots & h_n \\ h_1^{[1]} & h_2^{[1]} & \cdots & h_n^{[1]} \\ \vdots & \vdots & \ddots & \vdots \\ h_1^{[k-1]} & h_2^{[k-1]} & \cdots & h_n^{[k-1]} \end{Vmatrix}, \tag{9}$$

is connected to the generating matrix (2) and must fulfil next condition

$$GH^T = 0. \tag{10}$$

The complexity of the operation (8) may be estimated in similar way as the complexity of coding scheme. So we can use the evaluation (4).

Key equation solving

An important decoding step is the key equation solving. We shall denote the basis of an error space by b_E, that is

$$b_E = (E_1, E_2, \ldots, E_m), \tag{11}$$

where m – rank of the error occurred with $E_i \in GF(q^N)$. For next discussion we will need the definition

Definition 1: Polynomial $L(z)$ over $GF(q^N)$ called *linearized* if $L(z) = \sum_i L_i z^{p^i}$.

Let $\Delta(z)$ denotes a linearized polynomial which roots are superposition of the vectors from (11), so called *error span polynomial*,

$$\Delta(z) = \sum_{p=0}^{m} \Delta_p z^{[p]}. \tag{12}$$

Then

$$\Delta(E) = 0, \tag{13}$$

and E is any linear superposition of the basis vectors from (11)

$$E = \sum_{i=1}^{m} \beta_i E_i, E_i \in b_E, \forall \beta_i \in GF(q). \tag{14}$$

Then let us write the key equation for rank code

$$F(z) = \Delta(z) \cdot S(z) \mod z^{[d-1]}. \tag{15}$$

In (15) $F(z)$ are defined as

$$F(z) = \sum_{i=0}^{m-1} F_i z^{[i]}, \tag{16}$$

where

$$F_i = \sum_{p=0}^{i} \Delta_p s_{i-p}^{[p]}, i = 0, 1, \ldots, m-1 \tag{17}$$

and $S(z)$ denotes linearized syndrome polynomial

$$S(z) = \sum_{j=0}^{d-2} s_j z^{[j]}. \tag{18}$$

In paper [Gabidulin, 1985] the author showed that for solving the key equation it is sufficiently to divide $z^{[d-1]}$ by syndrome polynomial (18). One of the way is using the method of successive divisions (i.e. Euclidean algorithm). In papers [Sysoev, 2011] and [Gabidulin, 2011] it was proposed optimized Euclidean algorithm for linearized polynomials. This algorithm allow us to use recurrence scheme and are most suitable for hardware implementation. Its asymptotic complexity are evaluated as

$$\mathcal{C}_{euclid} = \mathcal{O}(N^{3.585}). \tag{19}$$

Finding roots of error span polynomial

After the last operation the decoder should find roots of key equation $\Delta(z) = 0$

$$\Delta(z) = \sum_{p=0}^{m} \Delta_p z^{[p]}. \tag{20}$$

Remember that this solution should satisfy (14). To solve key equation we can use the method, described in [Berlekamp, 1968]. For this, we will need the following theorem

Theorem 1: *Let $L(z)$ – linearized polynomial and $z = \sum_k Z_k \alpha^k$, where $Z_k \in GF(q)$, then $L(z) = \sum_k Z_k L(\alpha^k)$*

Proof. See [Berlekamp, 1968]. ■

From Theorem 1 it follows that for finding roots of error span polinomial 12, it is necessary to calculate value of this polynomial in certain points and express the results in standard basis

$$b_{std} = (\alpha^0, \alpha^1, \alpha^2, \ldots, \alpha^N), \alpha \in GF(q^N). \tag{21}$$

That is

$$\Delta(\alpha^k) = \sum_{i=0}^{m} \lambda_{ki} \cdot \alpha^i, k = 0, 1, \ldots, m, \lambda_{ki} \in GF(2^N). \tag{22}$$

After this calculation we can construct a matrix $(m+1) \times (m+1)$, which entries are from $GF(q)$

$$\Omega = \begin{Vmatrix} \lambda_{00} & \lambda_{01} & \cdots & \lambda_{0m} \\ \lambda_{10} & \lambda_{11} & \cdots & \lambda_{1m} \\ \cdots & \cdots & \cdots & \cdots \\ \lambda_{m0} & \lambda_{m1} & \cdots & \lambda_{mm} \end{Vmatrix}. \tag{23}$$

Then the problem of finding roots of error span polynomial is equivalent to the finding a solution for the next matrix equation:

$$Z \cdot \Omega = \begin{vmatrix} Z_0 & Z_1 & \ldots & Z_m \end{vmatrix} \cdot \begin{Vmatrix} \lambda_{00} & \lambda_{01} & \cdots & \lambda_{0m} \\ \lambda_{10} & \lambda_{11} & \cdots & \lambda_{1m} \\ \cdots & \cdots & \cdots & \cdots \\ \lambda_{m0} & \lambda_{m1} & \cdots & \lambda_{mm} \end{Vmatrix} = \begin{vmatrix} 0 & 0 & \cdots & 0 \end{vmatrix}. \tag{24}$$

The null vector is placed at the right side of the equation (24). This equation may be solved by the means of transformation of the matrix from current form into idempotent one (see example 2.57 in [Berlekamp, 1968]). Then the roots of error span polynomial, or (11), may be derived from matrix rows. Thus we will calculate error values (11).

Find error locator

After calculating (11) it is necessary to calculate error locator. At first step we need to solve a shortened set of equations [Gabidulin, 1985]:

$$\sum_{j=1}^{m} E_j x_j^{[p]} = s_p, p = 0, 1, \ldots, m-1. \tag{25}$$

All the equations transform in such way that at the end of operations we will got unknown variables of equal power, that is

$$\sum_{j=1}^{m} E_j^{[m-p]} x_j^{[m-1]} = s_p^{[m-p]}, p = 0, 1, \ldots, m-1. \tag{26}$$

Complexity of the operation (25) are evaluated as

$$\mathcal{C}_{conv} = \mathcal{C}_{mult} \left((m-1)^2 + \frac{(m-1)m}{2} \right), \tag{27}$$

where $\mathcal{C}_{mult}$ is the multiplication complexity for the pair of elements from the extended finite field $GF(q^N)$ in the current basis. In paper [Gabidulin, 2010] and [Sysoev, 2011] It was shown how we may optimize a set of base operations (multiplication, powering, inversion) using weak self-orthogonal bases. The set of equations (26) is the system of linear equations. It can be rewrited into the product of matrix by vector

$$\begin{Vmatrix} E_1^{[m-1]} & E_2^{[m-1]} & \cdots & E_m^{[m-1]} \\ E_1^{[m-2]} & E_2^{[m-2]} & \cdots & E_m^{[m-2]} \\ \vdots & \vdots & \ddots & \vdots \\ E_1^{[0]} & E_2^{[0]} & \cdots & E_m^{[0]} \end{Vmatrix} \begin{Vmatrix} x_1^{[m-1]} \\ x_2^{[m-1]} \\ \vdots \\ x_{m-1}^{[m-1]} \end{Vmatrix} = \begin{Vmatrix} s_0^{[m-1]} \\ s_1^{[m-2]} \\ \vdots \\ s_{m-1}^{[0]} \end{Vmatrix}. \tag{28}$$

To solve a system of equations (26) expressed in (28), we will use Gaussian elimination. So

$$\begin{Vmatrix} 1 & \tilde{E}_{12} & \cdots & \tilde{E}_{1m} \\ 0 & 1 & \cdots & \tilde{E}_{2m} \\ \vdots & \vdots & \ddots & \vdots \\ 0 & 0 & \cdots & 1 \end{Vmatrix} \begin{Vmatrix} x_1^{[m-1]} \\ x_2^{[m-1]} \\ \vdots \\ x_{m-1}^{[m-1]} \end{Vmatrix} = \begin{Vmatrix} \tilde{s}_0 \\ \tilde{s}_1 \\ \vdots \\ \tilde{s}_{m-1} \end{Vmatrix}. \tag{29}$$

Complexity of solving such the system (29) using Gaussian Elimination evaluated as

$$\mathcal{C}_{Gauss} = \mathcal{C}_{inv} \cdot m + \mathcal{C}_{mult} \left(\sum_{k=1}^{m} k^2 \right) + \mathcal{C}_{add} \left(\sum_{l=1}^{m} l(l-1) \right), \tag{30}$$

where $\mathcal{C}_{add}$ and $\mathcal{C}_{inv}$ are appropriated estimations of complexity for the sum of two elements from extended field and inversion of the element in current basis.
Complexity of the solution (reduction to Gaussian form) equals to

$$\mathcal{C}_{solveX} = (\mathcal{C}_{mult} + \mathcal{C}_{add}) \frac{m(m-1)}{2}. \tag{31}$$

After this operation we will got a set of independent equations

$$\sum_{i=1}^{m} x_p^{[m-1]} = \hat{s}_p, p = 0, 1, \ldots, m-1. \tag{32}$$

Each equation from (32) is solving by means of raising to power $[n-(m-1)]$. Complexity of the powering may be evaluated as

$$\mathcal{C}_{xPow} = \mathcal{C}_{mult} \cdot m(n-(m-1)). \tag{33}$$

After the calculating x_p we may form a system of equation which solution is a set of error locators [Gabidulin, 1985]

$$x_p = \sum_{j=1}^{n} Y_{pj} h_j, p = 1, 2, \ldots, m. \tag{34}$$

In equation (34) h_j are the entries of the first row in check matrix (9) with $h_j \in GF(q^N)$. Y_{pj} are elements of the error locators matrix $(m \times n)$, $Y_{pj} \in GF(q)$. It is worth noting that all the equations (34) are independent and have unique solution. The element $h_j \in GF(q^N)$ can be expressed in the form of vector which entries are the elements h_{ji} from $GF(q)$. Thus each equation (34) can be represented in the next form

$$X_p = \hat{H} \cdot Y_p = \begin{Vmatrix} x_{p1} \\ x_{p2} \\ \vdots \\ x_{pn} \end{Vmatrix} = \begin{Vmatrix} h_{11} & h_{21} & \cdots & h_{n1} \\ h_{12} & h_{22} & \cdots & h_{n2} \\ \vdots & \vdots & \ddots & \vdots \\ h_{1n} & \cdots & \cdots & h_{nn} \end{Vmatrix} \cdot \begin{Vmatrix} Y_{p1} \\ Y_{p2} \\ \vdots \\ Y_{pn} \end{Vmatrix}. \tag{35}$$

To find Y_p it is necessary to multiply X_p by the matrix $\hat{H}^{-1}$. This matrix is independent from input information and may be evaluated at the step of device development. Complexity of the operation should be not more than (upper-bound estimate)

$$\mathcal{C}_Y = \mathcal{C}_{add} \cdot (n-1)m. \tag{36}$$

Error finding and vector correction

Using known error locators matrix Y_{pj} (from (34)), and the obtained error span matrix E_i (11), it will be simple to got error values e_k for each entry from received corrupted code vector y

$$e = EY = \begin{Vmatrix} E_1 & E_2 & \cdots & E_m \end{Vmatrix} \cdot \begin{Vmatrix} Y_{11} & Y_{12} & \cdots & Y_{1n} \\ Y_{21} & Y_{22} & \cdots & Y_{2n} \\ \vdots & \vdots & \ddots & \vdots \\ Y_{m1} & Y_{m2} & \cdots & Y_{mn} \end{Vmatrix}. \tag{37}$$

Error correction operation is a simple subtraction

$$g = y - e. \tag{38}$$

A common complexity of the error calculation and code vector correction are evaluated as

$$\mathcal{C}_e = \mathcal{C}_{add} \cdot (nm). \tag{39}$$

After the correction of received vector we need to find informational vector

$$\tilde{u} = g \cdot D = u \cdot G \cdot D. \tag{40}$$

For equality $\tilde{u}$ and u it is necessary to satisfy the condition

$$G_{(k\times n)} \cdot D_{(n\times k)} = I_{(k\times k)}, \tag{41}$$

where I denotes the unity matrix with identity components from $GF(q^N)$ at the diagonal. Matrix D is defined unambiguously and calculates a priori. Complexity of multiplication vector g by matrix D may be estimated as

$$\mathcal{C}_u = \mathcal{C}_{mult} \cdot mn + \mathcal{C}_{add} \cdot (n-1)m. \tag{42}$$

Resource demanding

The authors have implemented described algorithm using hardware description language VHDL. Our goal was the developing a codec for rank code with the following parameters $(8, 4, 5)$. A base field was $GF(2)$. An extended field was $GF(2^8)$, i.e. $N = 8$. Decoder has no information about row and column erasures.

Codec was designed as IP-block with simple inputs and outputs. The rest of the world can use signal “LOAD” and “Y[7:0]” for data input. For outputs other blocks should use corrected vector “I[7:0]" with “VALID” and “FAIL" flags. Such way does not constrain data channel. So the codec can be used with any transmitter such as copper (i.e. RS-485/Ethernet), memory (i.e. NAND Flash) or radio (i.e. ZigBee/WiFi) channels.

For more objective results this rank codec does not depend on specialized FPGA blocks (such as multipliers, block ram, I/O blocks). The device may be used not only in FPGA but also in applications specific integrated circuit (ASIC). Block scheme of full decoder you can see at figures 1 and 2.

Figure 1 shows blocks for searching error basis and interconnection between them. One can see two state machines, for “Euclid” and “Error Span” stages (denoted as “SM”). Structure is purposefully pipelined. So next decoding operation starts can begin before previous operation finish. Syndrome block consist of four independent calculators for each transposed check matrix row. Euclid stage block performs operations on linearized polynomials. “Euclid main” block are more complex and more frequently used. It decreases current power at each step of Euclidian algorithm. “Euclid final” are used once per decoding. “Error Span” block is simpler. It performs calculate values of Δ linearized polynomial and outputs its roots.

Figure 2 shows block diagram of algorithm for calculating error locator. One can see state machines chain. These state machines share memory and computational resources between each other. The system also have pipelined structure. Final stage “Data correction" check syndrome value and can decode received vector if there are no errors occured. Otherwise, it performs errors searching and, after that, calculations for finding informational vector. The obtained structure and results may be optimized better. But they are initial point and will help us to more precise evaluate complex systems based upon rank codes.

We used Active-HDL 7.2 Student Edition from Aldec [Aldec inc., 2012] for simulation. Our project was developed for commercial FPGAs XC3S700AN-4FGG484C [Xilinx inc., 2008][Xilinx inc., 2012] and XC6SLX16-3CSG225 [Xilinx inc., 2012]. For generating the configuration bit file for FPGA we use software ISE WebPack by Xilinx inc. 13.1 [Xilinx inc., 2011].

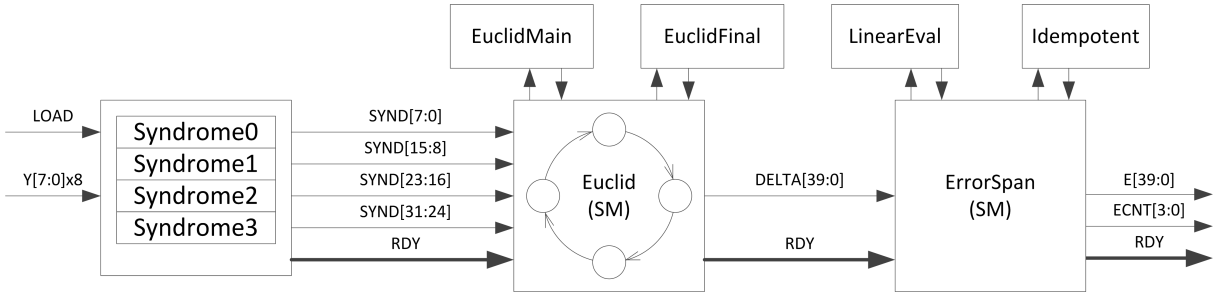

Figure 1: Searching error basis block diagram

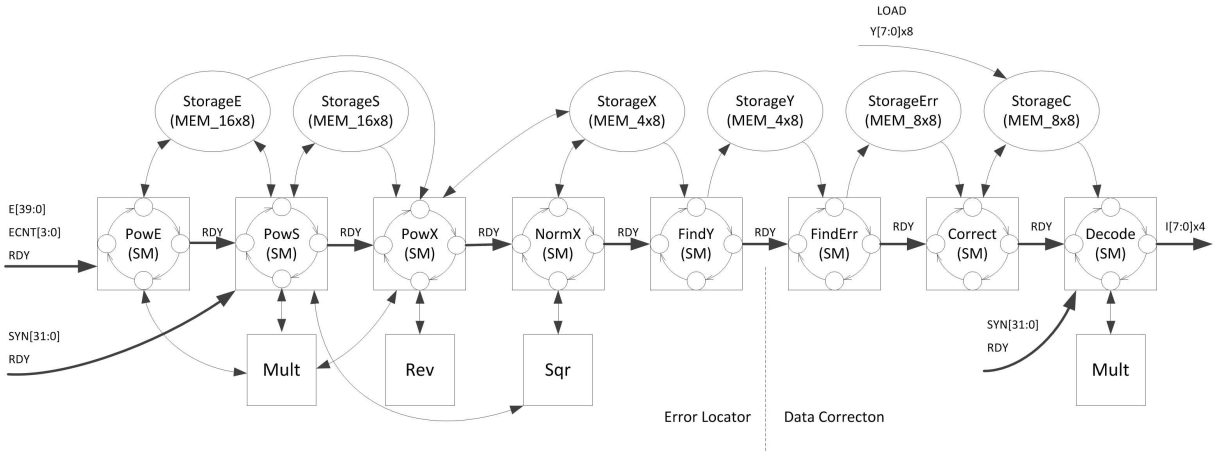

Figure 2: Block diagram searching error locator and decoding received vector

Synthesis, translation, mapping and routing were performed with default settings. One can see authors's results in table 1. The codec can be run at 155 MHz Spartan-6 and 86 MHz for Spartan-3. So if current code rate is 1/2 then codec can perform data processing with 77 MiB/s and 43 MiB/s speed accordingly. When this work started, the best chip for commertial devices was Spartan-3AN. Today FPGA Spartan-6 preferred for new budget designs. It is recent and more popular FPGA [Xilinx inc., 2012]. The key difference between two FPGAs is the using technology and architecture. The Spartan-3 (denotes as "S3") technology is 90 nm, while Spartan-6 (denoted as "S6") one is 45 nm. Such difference in technology impacts on achievable speed. Indeed, table 1 shows speed increasing.

Spartan 3A contain 4-input Look-Up table (LUT). Each LUT implements logic plus storage elements used as flip-flops or latches [Xilinx inc., 2012]. Each configurable logic block in Spartan-6 consists of two slices. Each slice in Spartan-6 contains four 6-input LUTs, eight flip-flops and miscellaneous logic. As one can see in table of results, in new architecture number of used slices has been dramatically decreased. Obtained results show this difference between two FPGAs.

So table describes not only resource demanding for the new device, but also for legacy one. One can see and how new architecture suits for the codec. The main conclusion from the results lies in idea that rank codes may be implemented for industrial and experimental purposes, even in small series-produced devices.

Table 1: Simulation and synthesize results

Operation	Delay,	Slices,		Flip-Flops,		4-input LUTs,		Max. freq,	
	cycles	number (%)		number (%)		number (%)		MHz	
		S3	S6	S3	S6	S3	S6	S3	S6
Full coder	14	850 (14)	209 (9)	921 (8)	630 (3)	1247 (11)	859 (9)	163	282
Syndrome stage	25	728 (12)	196 (9)	897 (8)	620 (3)	933 (8)	614 (7)	176	313
KES (Euclid) stage	2040	1837 (31)	826 (36)	1980 (17)	1956 (11)	2945 (25)	2045 (22)	87	156
Error span stage	977	489 (8)	156 (7)	321 (3)	302 (2)	859 (7)	422 (5)	130	174
Error locator stage	401	877 (15)	262 (12)	927 (8)	784 (4)	1214 (10)	545 (6)	143	202
Data correction stage	15	96 (2)	32 (1)	92 (1)	82 (0)	164 (1)	72 (1)	212	344
Full decoder	3458	3979 (68)	1380 (61)	4420 (38)	4027 (22)	6106 (54)	3564 (40)	86	155
Full codec	3472	4829 (82)	1583 (70)	5341 (45)	4657 (26)	7353 (62)	4423 (49)	86	155

Conclusion

Achieved results are important for further scientific research. They will help to estimate more carefully parameters of the systems based upon rank codes. Understanding the internal structure of the hardware codec should direct research efforts to the most important problems. Likewise, the results may be used to compare rank codes with Reed-Solomon codes from applied aspect.

In what follows one should consider more complex codecs, examine dependence of hardware implementation complexity on the main parameters and develope new algorithms for more efficient decoding.

Acknowledgements

The authors would like to thank Nina. I. Pilipchuk, Sergey M. Vladimirov, Alexander I. Kolybelnikov, Alexey V. Ourivsky and Alexander L. Shishkin for constructive critique and valuable advices.

Bibliography

[Gabidulin, 1985] E.M. Gabidulin, Theory of Codes with Maximum Rank Distance, Problems of Information Transmisson, Moscow, Vol. 21, No 1, 1985, pp. 3–16.

[Gabidulin, 2010] E.M. Gabidulin and I.Y. Sysoev Rank Codes Using Weak Self-Orthogonal Bases, Computational Technologies in Electrical and Electronics Engineering (SIBIRCON-2010), Irkutsk, July 2010, pp. 70–71.

[Ahlswede, 2000] R. Ahlswede E.,N. Cai S.-Y. R. Li and R.W.Yeung, Network information flow, IEEE Trans. Inform. Theory, Vol. IT-46, pp. 1204-1216, July 2000.

[Sysoev, 2011] I.Y. Sysoev, Fast Algorithm for Computing Rank Code Syndrome Using Weak Self-Orthogonal Basis in $GF(2^{2^N})$, Proceedings of the 13-th International Conference "Digital signal processing and its applications", Moscow, 2011, Vol.1, pp. 78–81.

[Gabidulin, 2006] E.M. Gabidulin and N.I. Pilipchuk, Symmetric matrices and codes correcting rank errors beyond the $\lfloor (d-1)/2 \rfloor$ bound, Discrete Appl. Math., Feb. 2006, Vol. 154, I. 2, pp. 305–312.

[Gabidulin, 2011] E.M. Gabidulin and I.Y. Sysoev, Modified Algorithm for Decoding Rank Codes (in russian), *Proc. of 54th MIPT Scientific Conference*, 2011, Vol. 2, pp. 55-57.

[Sysoev, 2011] I.Y. Sysoev, Efficient Euclidian Algorithm for Linearized Polynomials (in russian), Proc. of the IX International Scientific Conference "Perspective technologies in the Information Transfer Means 2011", Vladimir, 2011, Vol. 3, pp. 40–45.

[Berlekamp, 1968] E.R. Berlekamp, Algebraic Coding Theory, New-York: McGraw-Hill Book Company, 1968.

[Aldec inc., 2012] Aldec inc., Active-HDL Manual, www.aldec.com, Aldec Web-cite, 2012.

[Xilinx inc., 2008] Xilinx inc, Spartan-3AN FPGA Family Datasheet, www.xilinx.com, 2008, P. 108.

[Xilinx inc., 2012] Xilinx inc., Spartan-3AN FPGA User Guides, www.xilinx.com, 2012.

[Xilinx inc., 2012] Xilinx inc., Spartan-6 Family Overview, www.xilinx.com, 2012.

[Xilinx inc., 2011] Xilinx inc., ISE Design Suite, http://www.xilinx.com/support/download/index.htm, 2011.

Authors' Information

Igor Y. Sysoev *– Post-graduate student, Moscow Institute of Physics and Technology (State University), P.O. Box: 141700, Dept. of Radio Engineering and Telecommunications, Dolgoprudny, Russia; e-mail: Igor.Sisoev@gmail.com*
Major Fields of Scientific Research: Rank Codes, ECC, Complexity, Digital Systems.

Ernst M. Gabidulin *– Doctor of Engineering, Professor, Moscow Institute of Physics and Technology (State University), P.O. Box: 141700, Dept. of Radio Engineering and Telecommunications, Dolgoprudny, Moscow Region, Russia; e-mail: ernst_gabidulin@yahoo.com*
Major Fields of Scientific Research: Coding Techniques, Coding Theory, Cryptography, Complexity, Shannon Theory.